NSF/RA-780085
PB 283 705

A Report on Research Sponsored by
NATIONAL SCIENCE FOUNDATION
(RANN)
Grant No. ENV74-14766

STRUCTURAL WALLS IN EARTHQUAKE-RESISTANT BUILDINGS

Dynamic Analysis of Isolated Structural Walls PARAMETRIC STUDIES

by

Arnaldo T. Derecho
Satyendra K. Ghosh
Mohammad Iqbal
George N. Freskakis
Mark Fintel

Submitted by
RESEARCH AND DEVELOPMENT
CONSTRUCTION TECHNOLOGY LABORATORIES
PORTLAND CEMENT ASSOCIATION
5420 Old Orchard Road
Skokie, Illinois 60077

March 1978

50272-101

REPORT DOCUMENTATION PAGE	1. REPORT NO. NSF/RA-780085	2.	3. Recipient's Accession No. PB283705

4. Title and Subtitle
Structural Walls in Earthquake-Resistant Buildings: Dynamic Analysis of Isolated Structural Walls-PARAMETRIC STUDIES (Final Report 1974-1978)

5. Report Date
March 1978

6.

7. Author(s)
A.T. Derecho, S.K. Ghosh, M. Iqbal et al

8. Performing Organization Rept. No.
PCA Ser. 1587

9. Performing Organization Name and Address
Portland Cement Association
5420 Old Orchard Road
Skokie, Illinois 60077

10. Project/Task/Work Unit No.

11. Contract(C) or Grant(G) No.
(C) ENV7414766
(G)

12. Sponsoring Organization Name and Address
Applied Science and Research Applications (ASRA)
National Science Foundation
1800 G Street, N.W.
Washington, D.C. 20550

13. Type of Report & Period Covered
(1974-1978)
Final

14.

15. Supplementary Notes
This is the second of a series of four reports on the Analytical Investigation on Earthquake-Resistant Structural Walls and Wall Systems

16. Abstract (Limit: 200 words)
The results of a parametric study to identify the most significant structural and ground motions parameters, as these affect the dynamic inelastic response of isolated structural walls, is presented. The parameters examined include intensity, duration and frequency content of the ground motion and the following variables relating to the structure: fundamental period, yield level in flexure, yield stiffness ratio, unloading and reloading parameters characterizing the decreasing stiffness hysteretic loop assumed for the model, damping, stiffness and strength taper along height of structure, and base fixity condition. Results are presented in the form of maximum response envelopes for horizontal and interstory displacements, bending moment, shear, rotational ductility and cumulative plastic hinge rotations as well as time-history plots of response. Results of the study indicate that the most important parameters are the fundamental period, yield load, and the earthquake intensity.

17. Document Analysis a. Descriptors

Earthquakes
Seismic waves
Critical frequencies
Intensity
Dynamic structural analysis
Dynamic response
Earthquake resistant structures
Design criteria

b. Identifiers/Open-Ended Terms

c. COSATI Field/Group

18. Availability Statement	19. Security Class (This Report)	21. No. of Pages
NTIS.		233
	20. Security Class (This Page)	22. Price PC A11 MF A01

(See ANSI-Z39.18) See Instructions on Reverse

OPTIONAL FORM 272 (4-77)
(Formerly NTIS-35)
Department of Commerce

CAPITAL SYSTEMS GROUP, INC.
6110 EXECUTIVE BOULEVARD
SUITE 250
ROCKVILLE, MARYLAND 20852

TABLE OF CONTENTS

SYNOPSIS

Although structural walls have a long history of satisfactory use in stiffening buildings against wind, there is insufficient information on their behavior under strong earthquakes. Observations of the performance of buildings during recent earthquakes have demonstrated excellent behavior of buildings stiffened by properly proportioned and designed structural walls. Both safety and damage control can be obtained economically with structural walls.

The primary objective of the analytical investigation, of which the work reported here is a part, is the estimation of maximum forces and deformations that can reasonably be expected in critical regions of structural walls in buildings subjected to strong ground motion. The results of the analytical investigation, when correlated with data from the concurrent experimental program, will form the basis for a design procedure to be developed as the ultimate objective of the overall investigation.

This is the second part of a comprehensive report on the analytical investigation. It discusses the results of parametric studies of various structural and ground motion parameters. These parameters are examined in terms of their effects on the dynamic inelastic response of isolated structural walls. Among the structural parameters considered are fundamental period, yield level, yield stiffness ratio, character of the hysteretic force-displacement loop (reloading and unloading stiffnesses) damping, stiffness and strength taper, and degree of base fixity. Also considered are the three parameters characterizing stong-motion accelerograms: duration, intensity, and frequency content.

Dynamic Analysis of Isolated Structural Walls

PARAMETRIC STUDIES

by

A. T. Derecho[1], S. K. Ghosh[2], M. Iqbal[3],
G. N. Freskakis[4] and M. Fintel[5]

BACKGROUND

Although structural walls (shear walls)* have a long history of satisfactory use in stiffening multistory buildings against wind, not enough information is available on the behavior of such elements under strong earthquake conditions.

Observations of the performance of buildings subjected to earthquakes during the past decade have focused attention on the need to minimize damage in addition to ensuring the general safety of buildings during strong earthquakes. The need to control damage to structural and nonstructural components during earthquakes becomes particularly important in hosptials and other facilities that must continue operation following a major disaster. Damage control, in addition to life safety, is also economically desirable in tall buildings designed for residential and commercial occupancy, since the nonstructural components in such buildings usually account for 60 to 80 percent of the total cost.

There is little doubt that structural walls offer an efficient way to stiffen a building against lateral loads. When

[1]Manager, and [3]Structural Engineer, Structural Analytical Section, Engineering Development Department; [2]Senior Structural Engineer, and [5]Director, Advanced Engineering Services Department; and [4]Formerly, Senior Structural Engineer, Design Development Section, Portland Cement Association, Skokie, Illinois.

*In conformity with the nomenclature adopted by the Applied Technology Council(1) and in the forthcoming revised edition of Appendix A to ACI 318-71, "Building Code Requirements for Reinforced Concrete", the term "structural wall" is used in place of "shear wall".

proportioned so that they possess adequate lateral stiffness to reduce interstory distortions due to earthquake-induced motions, walls effectively reduce the likelihood of damage to the non-structural elements in a building. When used with rigid frames, walls form a structural system that combines the gravity-load-carrying efficiency of the rigid frame with the lateral-load-resisting efficiency of the structural wall.

Observations of the comparative performance of rigid frame buildings and buildings stiffened by structural walls during recent earthquakes,[3,4,5] have clearly demonstrated the superior performance of buildings stiffened by properly proportioned structural walls. Performance of structural wall buildings was better both from the point of view of safety as well as damage control.

The need to minimize damage during strong earthquakes, in addition to the primary requirement of life safety (i.e., no collapse), clearly imposes more stringent requirements on the design of structures. This provided the impetus for a closer examination of the structural wall as an earthquake-resisting element. Among the more immediate questions to be answered before a design procedure can be developed are:

1. What magnitude of deformation and associated forces can reasonably be expected at critical regions of structural walls corresponding to specific combinations of structural and ground motion parameters? How many cycles of large deformations can be expected in critical regions of walls under earthquakes of average duration?
2. What stiffness and strength should structural walls, in representative building configurations, have relative to the expected ground motion in order to limit the deformations to acceptable levels?
3. What design and detailing requirements must be met to provide walls with the strength and deformation capacities indicated by analysis?

The combined analytical and experimental investigation, of which this study is a part, was undertaken to provide answers to the above questions. The objective of the overall investigation is to develop practical and reliable design procedures for earthquake-resistant structural walls and wall systems.

The analytical program to accomplish part of the desired objective consists of the following steps:

a. Characterization of input motions in terms of the significant parameters to enable the calculation of critical or "near-maximum" response using a minimum number of input motions[6].

b. Determination of the relative influence of the various structural and ground motion parameters on dynamic structural response through parametric studies[7]. The purpose of these studies is to identify the most significant variables.

c. Calculation of estimates of strength and deformation demands in critical regions of structural walls as affected by the significant parameters determined in Step (b). A number of input accelerograms chosen on the basis of information developed in Steps (a) and (b) are used[8].

d. Development of procedure for determining design force levels[8] by correlating the stiffness, strength and deformation demands obtained in Step (c) with the corresponding capacities determined from the concurrent experimental program[9].

Another important result of the analytical investigation is the determination of a representative loading history that can be used in testing laboratory specimens under slowly reversing loads[10].

The first phase of this investigation deals mainly with isolated structural walls. A detailed consideration of the dynamic response of frame-wall and coupled wall structures is planned for subsequent phases of the investigation.

This is the second part of the report on the analytical investigation. It discusses the results of parametric studies of structural and ground motion parameters as they affect the dynamic inelastic response of isolated structural walls. The evaluation of the relative influence of these parameters on dynamic inelastic response represents a major step towards developing a design procedure for earthquake-resistant structural walls. By comparing the effects of different variables on the relevant response quantities, the parametric studies serve to identify the most significant variables. The subsequent development can then be formulated in terms of these major variables. The material presented here is based on Part B of Ref. 7 and corresponds to Step (b) listed above.

The first part of the report dealt mainly with the characterization of input motions in terms of duration, intensity and frequency content, particularly as they related to dynamic inelastic response.

The investigation has been supported in major part by Grant No. ENV74-14766 from the National Science Foundation, RANN Program. Any opinions, findings and conclusions expressed in this report are those of the authors and do not necessarily reflect the views of the National Science Foundation.

OBJECTIVES

Dynamic Inelastic Response Analysis

The major objective of the parametric studies is to evaluate the relative influence of the various structural and ground motion parameters on the dynamic inelastic response of structural walls and wall systems. Effects of selected variables on response quantities such as maximum total and interstory displacements are examined. Particular attention is placed on the effects of the parameters studied on the maximum forces (especially shear) and deformations in critical regions of structural walls.

The parametric study is necessary in view of the many variables that affect dynamic structural response to ground motions. Because of the need to develop a simple design procedure, only the most significant parameters can be considered in formulating the design methodology. By identifying the most important variables, the parametric study allows the subsequent effort, i.e., the determination of estimates of force and deformation demands in critical regions of structural walls, to concentrate on a manageable few of the most significant parameters. These can then form the basis for developing the design procedure.

During the first phase of the program, dynamic analyses were carried out on isolated structural walls, with only exploratory runs made for frame-wall and coupled wall systems. Isolated walls were analyzed not only to obtain dynamic response data on this basic element, but also to establish a reference with which results for the more complex structural wall systems can be compared.

In certain cases, the frame in a frame-wall structure or the coupling beams in a coupled wall structure are relatively flexible compared to the structural wall. In these cases, the wall can be considered to act essentially as an isolated structural element.

Sectional Analysis Under Combined Flexure and Axial Load

In addition to the parametric study dealing with dynamic response of isolated walls, a start was made on a parametric study of wall sections subjected to combined flexure and axial load. The objective of this analysis was to evaluate the relative effects of selected design variables on ductility and other characteristics of the primary moment-curvature ($M-\phi$) curve for representative structural wall sections. For the primary $M-\phi$ curve, the loading applied is an essentially static, monotonically increasing flexure with constant axial load.

Among the more important input to the dynamic response analysis is the force-deformation relationship of members, in addition to structure dimensions and geometry. The effects of design variables on dynamic response can thus be examined in terms of their influence on the primary $M-\phi$ curve of critical sections -- at least to the extent that the primary $M-\phi$ curve affects dynamic response. Among the design variables considered were:

a. shape of structural wall cross-section
b. percentage of longitudinal reinforcement
c. level of axial load
d. degree of confinement of compression zone concrete

Results of the study of the effects of sectional shape on the behavior of wall sections under combined bending and axial load were included in the Progress Report of August 1975[11].

An initial effort also was made toward developing charts (interaction diagrams) to serve as a basis for proportioning wall sections in earthquake-resistant structures. Preliminary charts based on sectional analyses under combined bending and axial load, covering a wide range of selected parameters, were presented in Supplement 3[12] to the Progress Report of August 1975.

Because any recommendations on the detailed proportioning of structural wall sections will have to await final reduction

and evaluation of experimental data, it was decided to defer this work until adequate test data became available. Of major concern here is the effect of shear and cyclic loading on the behavior of structural walls.

The subsequent discussion is concerned mainly with the analysis of inelastic dynamic response of structures.

ANALYSIS PROCEDURE - AN OVERVIEW

It was recognized early in the study that if the design procedure to be developed is to be put in practical form, it will have to involve only the most important parameters affecting the behavior of structural walls under seismic conditions. A parametric study considering reasonable variations in what are thought to be significant structural and ground motion variables was carried out as a preliminary step to the compilation of data for the design procedure. Once the most significant variables are identified, the design procedure can be based on these few major parameters.

The general procedure followed in the parametric study is described below.

1. Structural Model. A reference 20-story isolated structural wall, representing a typical element in a structural wall or "cross-wall" structure, was designed on the basis of the 1973 Uniform Building Code (UBC)[13], Zone 3 requirements.*

   A number of other designs were also considered to determine the practical range of variation of the required strength (yield level) corresponding to different stiffnesses and wall cross sections. Based on this study, the ranges of variation of the different structural parameters were established.

   Among the more important structural parameters considered were the fundamental period, T_1, and the flexural yield level, M_y, i.e., the force required to produce first yield in bending. For the purpose of defining the "first yield", a bilinear idealization was used to replace the actual curvilinear force-

*It is pointed out that the use of UBC requirements to establish the dimensions (mainly relating to strength) of the reference structure has little bearing on the results of the analysis. The principal reason for the use of the UBC provisions (or of any code provisions for that matter) is to establish the practical range of variation of certain design parameters.

deformation relationship of structural members. For the 20-story structure studied, an initial fundamental period ranging from 0.8 sec. to 2.4 sec., and a yield level for the base of the wall ranging from 500,000 in.-kips (56,500 kN·m), to 1,500,000 in.-kips (169,500 kN·m) were considered.

2. Input Ground Motions. For input motions, a small number of accelerograms were selected from among the recorded and artificially generated accelerograms catalogued in Ref. 6. These were chosen so that the ranges of dominant frequencies for the "peaking accelerograms"[6] more or less covered the period range of interest, i.e., between 0.80 sec. and 3.0 sec.

   In studying input motions, the following three characteristics affecting dynamic structural response were recognized[6]:

   a. intensity - used here as a measure of the amplitude of the large acceleration pulses;
   b. duration of the large-amplitude pulses;
   c. frequency characteristics.

   Except where duration was the parameter of interest, all the structures analyzed were subjected to 10 seconds of ground motion. The input motions were normalized with respect to intensity by multiplying the as-recorded or as-generated acceleration ordinates by a factor calculated to yield a "spectrum intensity"* equal to some percentage of a reference spectrum intensity, SI_{ref}. The reference spectrum intensity used in this study is that corresponding to the first 10 seconds of the NS component of the 1940 El Centro record. Factors designed to yield 1.5 SI_{ref} were used to normalize most of the input accelerograms.

3. Response Parameters of Interest. A major requirement of the analysis for the dynamic response study was

*Defined here as the area under the 5%-damped relative velocity response spectrum between periods of 0.1 and 3.0 seconds.

consideration of inelastic deformations at critical regions of structural members. Economic considerations in design generally result in structural dimensions that allow inelasticity to develop when a structure is subjected to a major earthquake. Consequently, the magnitude of the inelastic deformations (or the ductility requirement) becomes the principal response parameter of interest. In addition to the ductility requirement, especially at the base of the wall, the maximum horizontal and interstory displacements and associated maximum forces, i.e., moments and shears, were noted.

4. Computer Program for Dynamic Analysis. A number of dynamic inelastic analysis computer programs were examined and the availability of support for modifications deemed essential for the planned investigation were considered. On the basis of these considerations, the program DRAIN-2D[14] was chosen for this work. The program has been implemented on the CDC 6400 at Northwestern University. The present version of the program, used in the analysis of isolated structural walls, includes a capability for considering a 'degrading stiffness' model for reinforced concrete beams, developed by R. W. Litton and G. H. Powell. Also included is an option to output compact time histories of response. Further modifications were introduced into the program by S. K. Ghosh and A. T. Derecho[15] at the Portland Cement Association. These allow plotting of response data. Modifications to Program DRAIN-2D, done by I. Buckle and G. H. Powell (August 1976) at the request of PCA, include a model for a shear-shear slip mechanism at plastic hinges, in addition to the flexural hinge. An option to consider a third, descending branch of the primary $M-\theta$ and $V-\gamma$ curves is also included in this latest modification.

5. Preliminary Analysis. To permit extensive evaluation of selected parameters, an effort was made to minimize the cost per analysis without sacrificing accuracy in the relevant data. To do this, a preliminary series of analyses was done to examine the possibility of using a lumped-mass model of an isolated wall with a lesser number of concentrated masses than floor levels. Also, the maximum permissible length of time step for use in numerical integration was evaluated. The question of the most appropriate model for the hinging region at the base of the wall also was considered.

6. Basic Approach to Analysis. The dynamic analyses assumed structural elements with unlimited deformation capacity (or ductility). This was done since a major objective of these analyses is the determination of the magnitude of deformation requirements corresponding to specific combinations of parameter values.

To isolate the effect of individual variables on response, only the particular parameter under study was varied in the reference structure at any one time. It is recognized that the process of modifying only one basic parameter of a structure while suppressing any change in other parameters* is artificial and may sometimes result in unrealistic structures. However, this was found necessary to avoid uncertainties in evaluating the effect of each variable.

The frequency content of the input motion was considered first because of the significant effect it can have on the dynamic response of a structure. It was necessary to identify early in the investigation the frequency content distribution that would produce near-maximum response in structures with specific

*For instance, increasing the stiffness (and hence the frequency) of a structural wall by increasing its overall dimensions or its depth will ordinarily be accompanied by an increase in its strength or yield level.

periods and yield levels. This would allow use of the appropriate input motion in subsequent analyses where other parameters were varied.

7. Presentation of Results. The results of the parameter study are presented mainly in the form of envelopes of selected response quantities, i.e., the maximum horizontal displacements, interstory displacements, moments, shears, ductility ratios and cumulative plastic hinge rotations along the height of the structure.

Time history plots of a number of response quantities were also obtained and are presented where they help in understanding the observed behavior. In addition, moment-rotation curves are shown for some cases.

Plots summarizing the results of the parametric studies are presented. An attempt is then made to assess the relative importance of the different structural parameters. This is done by comparing the effects of these parameters on selected response quantities, the effect of each parameter being normalized with respect to its corresponding practical range of variation to allow comparison.

COMPUTER PROGRAMS

General features of the computer programs used in the analytical investigation are described briefly below. Most of these programs have been implemented on the CDC 6400 at the Vogelback Computing Center of Northwestern University.

Dynamic Inelastic Analysis of Structures - Program DRAIN-2D

The dynamic response analyses were done using program DRAIN-2D, developed at the University of California at Berkeley. A number of modifications, intended to allow more efficient extraction and plotting of output data, have been introduced into the program at PCA. Detailed information concerning the program is given in Refs. 14 and 15.

The essential features of the program, as implemented at Northwestern University, are as follows:

1. The program considers only plane structures.
2. A structure may consist of a combination of beam or beam-column elements, truss elements or infill panel elements. The moment-rotation characteristics for the beam elements can be defined as a bilinear relationship that may be stable hysteretic or may exhibit the "degrading stiffness" characteristic for deformation cycles subsequent to yielding. More recent modifications to the program relating to force-displacement characteristics are discussed in a subsequent paragraph.
3. The mass of the structure is assumed to be concentrated at nodal points.
4. Horizontal and vertical components of the input (base) acceleration may be considered simultaneously. The input motions are assumed to be applied directly to the base of the structure (no soil-structure interaction effects are considered).
5. Several types of damping may be specified, including mass-proportional and stiffness-proportional damping.

6. Elastic shear deformation and the P- effect in frame elements can be taken into account.
7. Output options include printouts of response quantities (e.g., displacement components and forces at node points and plastic rotations at member ends) corresponding to specified nodes and response envelopes at given time intervals. Envelopes of basic response quantities are automatically printed at the end of each computer run. Time histories of specified response quantities presented in compact form also can be obtained.

For structures consisting of beam elements, (including columns under constant axial load) plots of a variety of response quantities can be obtained during each run.

The structural stiffness matrix is formulated by the direct stiffness method, with the nodal displacements as unknowns. Dynamic response is determined using step-by-step integration by assuming a constant response acceleration during each time step.

Elements of particular interest in this study are beams and beam-columns, and especially beams characterized by a progressive decrease in reloading stiffness with cycles of loading subsequent to yield. In DRAIN-2D, both flexural and axial stiffnesses of these elements are considered. Variable cross sections may be taken into account by specifying the appropriate stiffness coefficients. Inelasticity is allowed in the form of concentrated plastic hinges at the element ends. For beam-column elements, interaction between axial force and moment in causing yielding is taken into account in an approximate manner.

The primary moment-rotation curves for the inelastic hinges at the ends of beam and beam-column elements are specified in terms of an initial stiffness, k, and a post-yield stiffness, $k_y = r_y k$ as shown in Fig. 1. The ratio $r_y = k_y/k$ will be referred to as the yield stiffness ratio.

Two types of hysteresis loops can be specified for the moment-rotation curve characterizing the inelastic point hinges at element ends. The first is the more common stable loop, shown in Fig. 2a. For this case, the unloading and reloading stiffnesses are both equal to the initial stiffness. The program accounts for the inelastic behavior of this type of element by assuming an equivalent element consisting of two parallel components, one elastic and the other elasto-plastic.

The second type of hysteresis loop is one that exhibits a decreasing stiffness for reloading cycles subsequent to yield. The basic or primary moment-rotation curve for the beam element with decreasing stiffness is defined in Fig. 1. After yielding occurs, however, the reloading branch, and to a minor degree the unloading branch, of the curve exhibits a decrease in slope (i.e., stiffness). This decrease in stiffness is assumed to be a function of the maximum rotation reached during any previous cycle. The detailed behavior of an inelastic point hinge, such as unloading and reloading from intermediate points within the primary envelope, is determined by a set of rules that are an extended version of those proposed by Takeda and Sozen[16]. A single element is used for this case.

Modifications Introduced into DRAIN-2D: Early runs using DRAIN-2D indicated the desirability of certain changes in the program. At the request of the Portland Cement Association, G. H. Powell and R. W. Litton at the University of California, Berkeley, introduced changes into the program to enable it to consider modifications of the basic Takeda model for the decreasing stiffness beam element. The unloading and reloading parameters α and β shown in Fig. 2b allow the basic decreasing stiffness model to be varied to correspond more closely to experimental results. These have been incorporated into the program. Powell and Litton also provided options for printing and storing on file the time histories of most response quantities in a compact and convenient form.

In addition to the above modifications, a major effort was made at the Portland Cement Association to incorporate plotting capabilities into the program. Plots of time histories of forces and deformations, as well as response envelopes, can be obtained automatically with each run. Options to punch cards for both envelopes and time histories of response have also been incorporated. These can be used to plot curves in comparative studies.

All modifications to the program DRAIN-2D as used in the study of isolated walls, have been documented and are discussed in detail in Ref. 15.

A more recent (August 1976) modification to DRAIN-2D, undertaken by I. Buckle and G. H. Powell at the request of PCA, allows the modelling of the hinging region in a beam element in the form of a flexural 'point hinge' and a shear-shear slip mechanism. The latter is designed to simulate the transverse relative displacement that can occur between the ends of a hinging region. The force-displacement relationships for both of these mechanisms can be specified in terms of a three-segment curve. The third segment represents the loss in strength accompanying displacements beyond the point of maximum resistance.

Behavior of the hysteresis loops under cyclic reversed loading with the modified program can range from the 'stable loop' to Clough's model for degrading stiffness[17]. Plotting routines developed for earlier versions of the program have already been adapted to the subroutines for this latest modification. These latest options added to DRAIN-2D have not been used in the study of isolated walls reported here. However, it is intended to use these options in the study of coupled walls and frame-wall systems.

Sectional Analysis Under Combined Flexure and Axial Load

As a first step in the parametric study of sections under combined flexure and axial compression, a computer program was developed for the analysis of typical wall cross sections. This program allows a wide range of geometric and material pro-

perties to be specified. Sections of all commonly encountered shapes, containing a large number of reinforcement layers, can be considered.

Stress-strain properties of steel and concrete are represented by realistic analytical relationships built into the program, or may be in the form of experimental data defined at discrete points. Output for each section analyzed is obtained as a set of bending moment and curvature values, corresponding to a given magnitude of axial load applied to the section. Detailed documentation for this program is given in Ref. 18.

This program was used also to determine the ranges of variation of the yield level and yield stiffness ratio corresponding to practical wall cross sections used in the dynamic response parametric studies.

Other Programs

Two dynamic analysis computer programs, DYMFR[19] and DYCAN[20], developed at the Portland Cement Association, were used primarily to determine the undamped natural frequencies and mode shapes of the buildings considered in the parametric study. DYMFR is a program for dynamic analysis of plane frame-wall systems, while DYCAN is designed specifically for dynamic analysis of inelastic isolated cantilevers. Both these programs are implemented on the META4-1130 computing system at the Portland Cement Association.

Another PCA-developed program, DYSDF[21], for the dynamic analysis of single-degree-of-freedom systems (both linear and nonlinear) was used to calculate and plot response spectra for various input motions considered in connection with this investigation.

A number of other independent programs have been developed for specific purposes. Among these is a program, AREAMR[22], that utilizes the punched data from DRAIN-2D to compute the cumulative areas under moment-rotation diagrams, and the cumulative rotational ductilities. Results can be plotted as functions of elapsed time.

Another useful program is ANYDATA[23]. Given a number of input arrays, this program can produce plots according to various specified arrangements. A number of smaller programs have been developed for preparing composite plots of response envelopes and time histories. A separate class of small programs has also been prepared for processing punched data from the sectional analysis program.

PRELIMINARY STUDIES

Before the parametric studies could be undertaken, several questions relating to modelling had to be answered. For this purpose, preliminary analyses were carried out. These analyses were made to:

a. explore the possibility of using a lesser number of lumped masses in the model than the number of floors in the prototype;
b. examine alternative techniques for modelling the hinging region at the base of the wall and determine the most appropriate feasible model; and
c. determine the proper integration time step to be used in the analysis.

Questions (a) and (c) were considered in an effort to reduce the computer time required for each analysis. Question (b) assumed importance in this particular study because of the need to obtain reliable estimates of the expected deformations in the hinging region and to correlate these with experimental data.

Exploratory analyses were also carried out to assess the significance of the so-called P-Δ effect on dynamic response.

The basic structure considered in the parametric studies was also used in the preliminary analyses. This is a hypothetical 20-story building consisting mainly of a series of parallel structural walls, as shown in Fig. 3. The building is 60 ft x 144 ft in plan and rises some 178 ft above the ground. All story heights are 8 ft-9 in. except the first story, which is 12 ft.

Number of Lumped Masses in Model

Effect of the number of lumped masses on the accuracy of the results was investigated using the models shown in Fig. 4. The 20-mass model represents a full model of the 20-story building shown in Fig. 3. The reduced models of five and eight

masses have nodes spaced at closer intervals near the base for a more accurate determination of the behavior of the hinging region.

Results of dynamic analyses for the 8-mass model compared very closely to those for the full model. In both cases, the structure had a fundamental period of 1.4 sec. The 5-mass model yielded the same maximum top displacement, but somewhat different moments, shears and plastic rotations in the lower part of the wall.

Based on these results and considering the desired accuracy for relative story displacements, it was decided to lump the masses at alternate floor levels in the upper portion of the wall. In the lower portion, the masses were lumped at each floor level. The resulting 12-mass model is shown in Fig. 5. A comparison of results obtained with this model and the full 20-mass model showed excellent agreement.

Modelling of the Plastic Hinge Region

Proper modelling of the region of potential hinging at and near the base of the wall is important if a reliable assessment of the deformation requirements in this critical region is expected. The model of the plastic hinging region should not only be realistic but also allow meaningful interpretation of the dynamic analysis results in terms that relate to measurable quantities in the experimental investigation.

As previously explained, program DRAIN-2D[12] accounts for inelastic effects by allowing the formation of concentrated "point hinges" at the ends of elements when the moments at these points equal the specified yield moment. The moment-rotation characteristics of these point hinges can be defined in terms of a basic bilinear relationship. This relationship develops into either a stable hysteretic loop or exhibits a decrease in reloading stiffness with loading cycles subsequent to yield. Since the latter model represents more closely the behavior of reinforced concrete members under reversed inelastic loading, it was used throughout this investigation.

In modelling an element with bilinear moment-rotation characteristics using DRAIN-2D, a major problem is the determination of the properties to be assigned to the hinge. These properties can be derived by considering the program model and relating its properties to a real member subjected to the same set of forces as shown in Fig. 6. The initial hinge stiffness, K_s, can then be taken as a very large number so that the two systems are identical up to the point when yielding occurs. In the post-elastic range, hinge properties can be derived by imposing the condition that total rotation in the model, θ_2, be equal to the total rotation in the real element, θ_1. This yields the following expression for the yield stiffness ratio of the point hinge, r_2, (i.e., the ratio of the slope of the post-yield branch to the slope of the initial branch of the bilinear moment-rotation curve):

$$r_2 = \left[\frac{r_1}{K_s(1 - r_1)(1 - \gamma)}\right] \frac{2EI}{\ell} \qquad (1)$$

where:

r_1 = yield stiffness ratio for the cantilever element

K_s = rotational stiffness of the point hinge in the model before yielding

= ratio of the tip moment to the moment at the fixed end

The main difficulty in using the above expression is that the ratio of the end moments, γ, is not known beforehand and, in fact, varies throughout the analysis. In addition, if the bending moment in the element is not uniform, the moment-rotation relationship for the element or a segment of it does not have the same shape as the sectional moment-curvature relationship. Thus, the yield stiffness ratio, r_1, and the yield moment, M_y, corresponding to the moment-rotation relationship of the element, are unknowns. One way to overcome these problems is to divide each member into short elements so that the moments at the two ends are approximately equal and thus $\gamma \sim 1$.

For this case, the moment-rotation relationship is proportional to the moment-curvature relationship so that the desired properties can be obtained easily.

In this investigation it was found desirable to use the minimum number of nodal points consistent with an accurate determination of deformations in the hinging region. This was done to economize on the cost of each run and thus allow examination of a wider range of parameter values. Preliminary studies indicated that if nodal points were established at every story level near the base of the wall (where hinging is expected), the ratio of end moments for each segment could be taken approximately equal to 0.9. For the model with nodal points as shown in Fig. 7a, (the same as those shown in Fig. 5) this ratio was used to determine r_1 and M_y from the moment-curvature relationship and r_2 using Eq. (1). Analyses were then made using this model and one where the lower region of the wall was divided into much shorter elements as shown in Fig. 7b. The curvature is approximately uniform over the shorter elements.

Results of the dynamic analyses were almost identical for rotations and forces in the hinging region. The displacements in the upper stories also compared very well although some discrepancies occurred in the displacements of the lower stories. Thus, it was decided that for the parametric studies, it would be sufficiently accurate to use element lengths equal to the height of a story near the base of the wall and to assume a ratio equal to 0.9 for the end moments in a segment.

Integration Time Step

The time step, Δt, to be used in the dynamic analysis is of primary concern since it affects both the accuracy of the results and the cost of computer runs. Some preliminary analyses using simple models indicated that an integration step as long as 0.02 sec. would result in sufficiently accurate results.

Using the final 12-mass model for a structure with fundamental period T_1 = 1.4 sec., a comparison of results was made

using values of $\Delta t = 0.02$ sec. and $\Delta t = 0.005$ sec. The results showed very good agreement. Plastic deformations were within one percent and the top displacements within 2.5 percent of each other. Based on these results, an integration time step $\Delta t = 0.02$ sec. was used for structures with initial fundamental periods of 1.4 sec. or longer.

In using a time step of 0.02 sec., irregularities in the solution were noticed in two cases -- in walls with significant discontinuities in stiffness, etc., and in input accelerograms where large changes in acceleration values occurred in one time step. For both these cases, the analyses were carried out using $\Delta t = 0.005$ sec. For structures with initial fundamental period, $T_1 = 0.8$ sec., a time step of 0.02 sec. appeared to be too large, even when extensive yielding occurred. For these cases, values of $\Delta t = 0.01$ and $\Delta t = 0.005$ yielded almost identical results.

The P-Δ Effect

The nonlinear effect of gravity loads on deformations was examined for a structure with $T_1 = 1.4$ sec., and yield level, $M_y = 500{,}000$ in.-kips. Although extensive yielding took place in the structure and the lateral displacements were significant, gravity load appeared to have no appreciable effect on the response. Because of this, the P-Δ effect was not considered in the subsequent analyses.

PARAMETRIC STUDIES

Once the basic elements of the dynamic analysis model have been established, the parametric studies could proceed to evaluate the relative influence of selected structural and ground motion parameters on dynamic response. As mentioned, The major purpose of the parametric studies is to identify the most significant variables needed in formulation of the design procedure.

Parameters Considered

Behavior of a building subjected to earthquake motions is affected by a number of variables related to its dynamic and structural properties and the characteristics of the ground motion. In this study those variables expected to have a significant effect on the response of the structure, particularly the force and deformation requirements in individual members as well as the entire structure are investigated. The variables considered are:

a. Structure characteristics:
    1. fundamental period of vibration, as affected by stiffness,
    2. strength or yield level,
    3. stiffness in post-yield range,
    4. character of the moment-rotation relationship of hinging regions,
    5. viscous damping,
    6. variations in stiffness and strength along the height,
    7. degree of fixity at the base of the structure,
    8. height variations (number of stories).

b. Ground motion parameters:
    1. intensity,
    2. frequency characteristics,
    3. duration.

Effects of these parameters on the seismic response of isolated structural walls were investigated by dynamic inelastic

analyses of suitable mathematical models. The structural models were obtained by changing values of selected parameters in a basic reference structure. Properties of the reference structure and the range of variation in the individual parameters are discussed in the following sections.

Basic Building Properties

The basic structure considered is a hypothetical 20-story building consisting mainly of a series of parallel structural walls, as shown in Fig. 3. The building is 60 ft x 144 ft in plan and about 178 feet high. All story heights are 8 ft-9 in. except the first story, which is 12 ft.

For the dynamic analysis, the mass of the structure was calculated to include the dead weight and 40 percent of the live load specified for apartment buildings by the Uniform Building Code[13]. This percentage of live load was deemed reasonable and is consistent with the current specifications for the design of columns in the lower stories of buildings. However, in calculating the design lateral forces (UBC Zone 3) for the purpose of proportioning the wall, only the dead weight of the building was used, as specified by UBC.

Stiffness of the structural wall in the basic building was assumed uniform along its height since this provides a better reference for evaluating the effect of stiffness taper.

The reference structure, here denoted by ISW 1.4, has an initial fundamental period of 1.4 sec. and a corresponding drift index (i.e., the ratio of lateral deflection at top to total height) of approximately 1/950 under the design seismic forces. Yield moment at the base was assumed equal to 500,000 in.-kips (56,490 kN·m).*

*The design moment at the base of the wall, on the basis of UBC Zone 3 requirements, was calculated as 350,000 in.-kips. This corresponds to a yield moment of approximately 500,000 in.-kips when allowance is made for load factors, capacity reduction factors and the difference between the yield moment and the maximum moment capacity of typical reinforced concrete sections. (1 in.-kip = 0.113 kN·m)

A constant wall cross section was assumed throughout the height of the basic structure. However, a reduction in yield level of sections above the base was included to reflect the effect of axial load on the moment capacity. This, in effect, produced a moderate taper in strength. The taper in strength used in the basic structure represents about the maximum that can be expected due to axial load only. It was obtained by examining the interaction diagrams for several types of structural wall sections with different percentages of longitudinal steel.

Variation of Structural Parameters

The effects of the different structural and ground motion parameters on selected response quantities, were determined by a controlled variation of each parameter in the reference structure. In particular, shear and rotational ductility demand at the base of the wall and the interstory distortions were considered. In most cases, only a single parameter was varied in the basic structure with the others held constant. Although this process sometimes resulted in unrealistic combinations of structural properties, it was considered essential to a proper evaluation of the effect of each variable on dynamic response.

The range of variation in the values of a given parameter is important if the results of the parametric study are to have practical application. In the present study, the values of each parameter were chosen to represent a reasonable range of values commonly encountered in practice.

To examine the effect of the fundamental period of vibration, three other values were assumed in addition to the basic value of 1.4 sec. These were 0.8, 2.0 and 2.4 sec. The stiffness of the reference structure was modified - while keeping the stiffness distribution and the mass constant - to change the period. As an aid in selecting the appropriate stiffness, Fig. 8 was prepared. This figure relates the stiffness with the fundamental period and the drift ratio corresponding to the

code-specified forces. The period values covered represent a relatively wide range of structural wall buildings.

To arrive at a reasonable range of values for the other major structural parameter, the yield level, an examination of selected structural wall sections was undertaken. Yield strengths corresponding to selected combinations of rectangular and flanged wall sections of practical proportions and varying longitudinal steel percentages (0.5 to 4.0 percent) were determined for f_y = 60 ksi (414 X 10^6 N/m^2) and f'_c = 4,000 psi (28 X 10^6 N/m^2). Based on the results of these calculations and considering current design practice, it was decided to use yield level values ranging from the 500,000 in.-kips (56,490 kN.m) of the reference structure to 1,500,000 in.-kips (169,570 kN·m). Intermediate values of 750,000 in.-kips (84,740 kN· m) and 1,000,000 in.-kips (112,980 kN·m) were also considered.

Similar considerations were used in arriving at the ranges of values for the other structural parameters.

Ground Motion Parameters

As suggested in Ref. 6, a ground motion duration of 10 seconds was used for all analyses except when the effect of duration was investigated. The effect of intensity of the ground motion was investigated by normalizing each input in terms of the 5%-damped spectrum intensity corresponding to the first 10 seconds of the N-S component of the 1940 El Centro record, i.e., the "reference intensity", SI_{ref}. Intensities of 0.75, 1.0 and 1.5 relative to the 1940 El Centro (N-S) were considered.

With the duration of the ground motion fixed and the intensity normalized, the only other ground motion parameter that could significantly affect the results is frequency content. A basis for the broad classification of earthquake accelerograms according to frequency characteristics was proposed in Ref. 6. Using this system of classification, a number of records were chosen early in the study to evaluate the effect of the frequency content of input motions on dynamic structural response.

Once the effect of this particular parameter on response was determined, the number of input motions used for investigating the other parameters could be reduced to one or two. This procedure was necessary to limit the total number of analyses while still retaining a reasonable assurance that the calculated responses would provide a good estimate of structural requirements under a likely combination of unfavorable conditions.

A complete list of the parameter variations considered is given in Tables 1a through 1d. The list is divided according to the fundamental period of the structure. Thus, structures with a fundamental period of 0.8 sec. are listed under a basic structure denoted by ISW 0.8, and so on. The third column in the table shows the variations in the basic value used in the parametric study.

Dynamic analyses were carried out for each combination of parameters shown in Table 1. Throughout these analyses it was assumed that structural elements possess unlimited inelastic deformation capacity (ductility) since a major objective of the study is the determination of the deformation requirements corresponding to particular values of a parameter.

DISCUSSION OF RESULTS

Data from the dynamic analyses consist of plots of response quantities directly relating to the specific objectives of this study. In selecting the response quantities to be plotted, primary importance was given to the behavior of the hinging region at the base of the wall. Generally, the base of the wall represents the most critical region from the standpoint of expected deformations and its importance to the behavior of the wall and other structures which may be attached to the wall.

In addition to quantities characterizing the response of the hinging region, the horizontal interstory distortions along the height of the wall have also been recorded. Here, a distinction is drawn between two measures of interstory distortion. In isolated structural walls, which exhibit predominantly cantilever flexure-type behavior, the interstory "tangential deviation", (i.e., the deviation or horizontal displacement of a point on the axis of the wall at a given floor level measured from the tangent to the wall axis at the floor immediately below it - see Fig. 9), rather than the "interstory displacement", provides a better measure of the distortion that the wall suffers. In fact, the tangential deviations vary in the same manner as, and are directly reflected in, the bending moments that are induced by the lateral deflection of the wall.

For open frame structures characterized by a 'shearing type' deformation (resulting from the flexural action of the individual columns of the frame), the interstory displacement varies in about the same manner along the height of the structure as the tangential deviation and has been used as a convenient index of the potential damage to both structural and nonstructural components of this type of building[24]. Figure 10 shows the typical variation with height of these two quantities for a statically-loaded cantilever wall.

Selected Results of Analysis

The results of a typical analysis are presented as envelopes of maximum displacements, forces and ductility requirements along the height of the structure. In addition, response history plots of a variety of quantities, including moment-plastic hinge rotation, moment-nodal hinge rotation and moment versus shear values have been obtained. To allow convenient comparison of responses for the parametric study, composite plots of envelopes and composite response history plots were prepared from punched cards of each run.

Figures 11 through 21 have been included to give an indication of the types of results obtained from each analysis through the plotting options introduced into Program DRAIN-2D[15]. Figure 11a, for instance, shows the time history of horizontal displacement of the top of the reference structure ISW 1.4 (with fundamental period, T_1 = 1.4 sec. and yield level, M_y = 500,000 in.-kips). The structure was subjected to the E-W component of the 1940 El Centro record, normalized to yield a 5%-damped spectrum intensity equal to 1.5 times the spectrum intensity of the N-S component of the same record. Figure 11b shows the same type plots for the intermediate floor levels of the same structure. Figures 12a and 12b are time history plots of the interstory displacements between the different floor levels of the same reference structure.

Rotation time histories are of particular interest in the lower part of the wall. Figure 13 shows the variations with time of the total rotations from the base of the wall to floor levels 1 and 2. Figure 14 shows the time history of the plastic hinge rotation in the first story. Plots of moment and shear at the base vs. time are shown in Figs. 15 and 16. It is worth noting the relatively more rapid fluctuation with time of the shear force when compared to the moment at the base of the wall. This is an indication of the greater sensitivity of the shear force to higher modes of response.

Sample plots of two types of moment-rotation curves are shown in Figs. 17 and 18 for the same reference structure.

Plots of moment versus total rotation were used to determine the required rotational ductility at the base of the wall.

The change with time in the cumulative nodal rotation at the first floor level (split into primary and secondary components as illustrated in Fig. 33) is shown in Fig. 19. The nodal rotation at the first floor level represents the total rotation in the wall segment between the base and the first floor level and serves as a convenient measure of the deformation within this region.

Figure 20 shows the variation with time of the cumulative area under the base moment-nodal rotation hysteresis loop for the basic structure ISW 1.4. In calculating the areas for Fig. 20, the base moment was nondimensionalized by dividing by the corresponding value of the base moment at first yield.

To study the variation of the ratio of moment to shear, as well as the absolute values of these quantities, moment versus shear plots were obtained with each analysis. Figure 21 shows an example of such a plot.

The results of the analyses are presented mainly as envelopes of maximum values of horizontal story displacements, interstory displacements, bending moments, horizontal shears, rotational ductility requirements, and cumulative plastic hinge rotations over the entire height of the structure.

The rotational ductility requirement for a member as plotted in these response envelopes is defined as:

$$\mu_r = \frac{\theta_{max}}{\theta_y} \tag{2a}$$

where θ_{max} is the maximum rotation at the base of the wall and θ_y is the rotation corresponding to yield. In terms of moments, this definition becomes:

$$\mu_r = 1 + \frac{(M_{max} - M_y)}{r_y M_y} \tag{2b}$$

where the yield stiffness ratio, r_y, is the ratio of the slope of the second, post-yield branch to the slope of the initial or elastic branch of the primary bilinear moment-rotation curve of the member.

To compare response histories for different values of a particular parameter, histories of normalized forces and deformations were obtained by dividing the value of the particular response quantity at any time by the corresponding value at first yield. Figure 25, for example, shows the time variation of the normalized nodal rotation at the first floor level. The dotted, horizontal lines through ordinates +1.0 and -1.0 correspond to first yield in each case.

Ground Motion Parameters

Effect of Frequency Characteristics

It was considered desirable to investigate the effect of the frequency characteristics of the input motion on dynamic response early in the study in order to select the record(s) for use in analyzing the other parameters. This question is basic to the problem of determining the critical input motion in relation to the properties of a given structure. For this purpose, and to confirm the qualitative observations made in connection with response spectra of single-degree-of-freedom systems in Ref. 6, three separate sets of analyses were made. These are listed in Table 2.

The first set of analyses corresponds to the reference structure with fundamental period, T_1 = 1.4 sec. and consists of the four accelerograms listed under Set (a) in Table 2. All the accelerograms were normalized to 1.5 times the 5%-damped spectrum intensity (SI) of the N-S component of the 1940 El Centro record;* the normalization factors are listed in Table 2. The normalized accelerograms are shown in Fig. 22, and the corresponding 5%-damped velocity spectra are shown in Fig. 23. Also shown for comparison is the velocity spectrum for the N-S component of the 1940 El Centro record. The artificial accel-

*In the following discussion, the 5%-damped spectrum intensity (SI) of the first 10 seconds of the N-S component of the 1940 El Centro record, for the period range 0.1 sec. to 3.0 sec., will be denoted by "$SI_{ref.}$" (which has a value of 70.15 in. = 1781.8 mm).

erogram S1 was designed to have a broad-band spectrum and was generated using the program SIMQKE developed by Gasparini[25].

Entries in the fourth column of Table 2 indicate the accelerogram classification in terms of the general features of its velocity spectra relative to the initial fundamental period of the structure, as discussed in Ref. 6. Thus, a "peaking (0)" classification indicates that the 5%-damped velocity response spectrum for this accelerogram shows a pronounced peak at or close to the fundamental period of the structure considered (in this case, T_1 = 1.4 sec.). A "peaking (+)" classification indicates that the peak in the velocity spectrum occurs at a period value greater than that of the fundamental period of the structure.

A "broad-band" classification, as discussed in Ref. 6, refers to an accelerogram with a 5%-damped velocity spectrum which remains more or less flat over a region extending from the fundamental period of the structure to at least one second greater. A "broad-band ascending" classification is similar to a broad-band accelerogram, except that the velocity spectrum exhibits increasing spectral values for periods greater than the initial fundamental period.

The second and third sets of analyses undertaken to study the effects of frequency characteristics of the input motion include two and three accelerograms, respectively. These are also listed in Table 2. These sets correspond to structures with fundamental periods of 0.8 sec. and 2.0 sec.

In addition to the above three sets, a set of two analyses was made using an input motion intensity equal to 0.75 ($SI_{ref.}$) to illustrate the interaction between the intensity of the input motion and the yield level of a structure in determining the critical frequency characteristics of the input motion.

(a) T_1 = 1.4 sec., M_y = 500,000* in.-kips

Envelopes of response values for the structure with period of 1.4 sec. and yield level, M_y = 500,000

*500,000 in.-kips = 56,490 kN·m.

500,000 in.-kips, are shown in Fig. 24.* Figures 24a, 24b, and 24c indicate that the E-W component of the 1940 El Centro record, classified as "broad-band ascending" with respect to frequency characteristics, produces relatively greater maximum displacements, interstory displacements and ductility requirements than the other three input motions considered. However, the same record produces the lowest value of the maximum horizontal shear. The artificial accelerogram S1 produces the largest shear, as shown in Fig. 24d. Because all structures yielded and the slope of the second, post-yield branch of the assumed moment-rotation curve is relatively flat, the moment envelopes shown in Fig. 24c do not show any significant differences among the four input motions used.

An idea of the variation with time of the flexural deformation at the base of the wall under each of the four input motions of Set (a) of Table 2 is given in Fig. 25. This figure shows the normalized rotations of the node at floor level "1", which represent the total rotations occurring in the first story. To plot the curves in Fig. 25, the absolute values of the rotations in each case were divided by the corresponding rotation when yielding first occurred. The two dotted lines on each side of the zero axis (at ordinates +1.0 and -1.0) thus represent the initial yield level for all cases. The actual location of the 'state point' describing the deformation of the first story segment relative to its moment-rotation curve at each instant of time is indicated in Fig. 26, for the structure subjected to the 1940 El Centro, E-W motion.

It is interesting to note in Fig. 25 that although the intense motion starts relatively early under the

*In the envelopes for rotational ductility requirements, values less than 1.0 represent ratios of the calculated maximum moments to the yield moment, M_y.

artificial accelerogram S1 (Fig. 22), yielding occurs first under the 1940 El Centro E-W motion. The relative magnitude of the rotation at first yielding, however, is greater under both S1 and the Pacoima Dam S16E record, a "peaking (0)" accelerogram.

As expected, the 1971 Holiday Orion record,* a "peaking (+)" accelerogram, produced a much lower response during the first few seconds, since the velocity spectrum for this motion (Fig. 23) peaks at a period greater than the initial fundamental period (T_1 = 1.4 sec.) of the structure. As the structure yields and the effective period increases, however, the response under this excitation increases gradually.

It is significant to note in Fig. 25 that as yielding progresses and the effective period increases, it is the "broad band ascending" type of accelerogram (in this case, the 1940 El Centro E-W component) that excites the structure most severely. Response to the other types of accelerograms - particularly the peaking accelerograms - tend to diminish.

An indication of the change in fundamental period of a structure, as the hinging (or yielded) region progresses from the first story upward, is given by Fig. 27, for different values of the yield stiffness ratio, $r_y = EI_2/EI_1$ or $(EI)_{yield}/(EI)_{elastic}$. The figure is based on the properties of the reference structure with initial fundamental period, T_1 = 1.4 sec. It is pointed out that since the structure goes through unloading and reloading stages as it oscillates in response to the ground motion (Fig. 17), the general behavior reflects the effects of the "elastic" or unloading stiffness, as well as its yield or reloading stiffness. The effect of each stiffness will

*The record obtained at the first floor of the Holiday Inn on 8244 Orion Boulevard, Los Angeles, during the San Fernando earthquake of February 9, 1971.

depend on the duration of the response under each stiffness value, as governed by the character of the input motion. When yielding occurs early, it seems reasonable to assume that both elastic and yield stiffnesses play about equal roles in influencing the "effective period" of the structure. This is particularly true for the type of structure considered here since the condition at the critical section (i.e., the base of the wall) determines to a large degree the response of the structure. In the Takeda model[16] of the hysteretic loop, the initial portions of the reloading branches of the moment-rotation loops (Fig. 17) have stiffness values intermediate between the initial elastic and yield stiffnesses of the primary curve.

Figure 24f shows the cumulative plastic hinge rotations, i.e., the sum of the absolute values of the inelastic hinge rotations over the 10-second response period. This parameter reflects the combined effect of both the number and amplitude of inelastic cycles and provides another measure of the severity of the response. The fact that the artificial accelerogram S1 produces a slightly greater cumulative plastic hinge rotation at the base of the wall than does the 1940 El Centro E-W component, in spite of the lesser amplitude of the associated maximum rotation (Fig. 24e), indicates that the response to S1 is characterized by a relatively greater number of cycles of inelastic oscillation than the response to El Centro E-W. This is indicated in the more jagged character of the response history curve corresponding to S1, shown in Fig. 25. It is a reflection of the considerably greater number of acceleration pulses over the 10-second duration in S1 than in any of the recorded accelerograms shown in Fig. 22.

It can be seen in Fig. 24b that the relative effect of the parameter considered (in this case, the frequency characteristics of the input motion) is similar on both interstory displacements and tangential deviations, the main difference between the two quantities being in their distribution along the height of the structure. For the subsequent cases, only the horizontal interstory displacement envelopes are shown. In considering these figures, the significance of the interstory displacement relative to the distortion in an isolated wall, and particularly its distribution along the height as compared to the corresponding tangential deviations, must be borne in mind.

(b) $T_1 = 0.8$ sec., $M_y = 1{,}500{,}000$* in.-kips

To study the effects of frequency characteristics for the case of short-period structures with relatively high yield levels, a "peaking (0)" accelerogram (N-S component of the 1940 El Centro) and a "broad-band ascending" type (E-W component of the 1940 El Centro) were considered.

Figure 28 shows response envelopes of displacement, moments, etc. This figure indicates that the peaking accelerogram consistently produces a greater response in the structure than does a broad-band record. A comparison of Fig. 28e with Fig. 24e, shows that the ductility requirements are not only significantly less for this structure with a high yield level, but that yielding has not progressed as high up the structure as in the case of the structure considered under (a), with period $T_1 = 1.4$ sec. and a low yield level. For the type of structure considered here, where the displacements of the lower floors are generally in phase (fundamental mode predominating), the magnitude of the ductility requirements at the

*1,500,000 in.-kips = 169,570 kN·m.

base of the wall is a direct function of the extent to which yielding has progressed up the height of the wall.

The greater response of the structure under the N-S component of the 1940 El Centro (peaking) follows from the fact that the dominant frequency components for this motion occur in the vicinity of the period of the structure, (Fig. 23). In this region, the E-W component has relatively low-power components. Also, because of the high yield level of the structure, yielding was not extensive, particularly under the E-W component and apparently did not cause the period of the yielded structure to shift into the range where the higher-powered components of the E-W motion occur. On the other hand, Fig. 28e indicates that under the N-S component of 1940 El Centro, yielding in the structure extended up to the 4th floor level, as against the 2nd floor level under the E-W component. The greater extent of this yielding and the accompanying increase in the effective period of the structure could easily have put the structure within the next peaking range of the El Centro N-S component (Fig. 23).

(c) T_1 = 2.0 sec., M_y = 500,000* in.-kips

For this structure, the peaking accelerogram used was the E-W component of the record taken at the first floor of the Holiday Inn on Orion Boulevard, Los Angeles, during the 1971 San Fernando earthquake. The record has a 5%-damped velocity spectrum that actually peaks at about 1.75 sec. and can thus be classified as a "peaking (-)" accelerogram relative to the structure. The other input motion considered is the E-W component of the 1940 El Centro record ("broad-band ascending").

The response envelopes of Fig. 29 indicate, as in Set (a) with a structure period T_1 = 1.4 sec. and

*500,000 in.-kips = 56,490 kN·m.

M_y = 500,000* in.-kips, that where yielding is significant, the horizontal and interstory displacements, as well as the bending moments and ductility requirements near the base, are greater for the broad band accelerogram than for the peaking motion. Also, as in Set (a), the extensive yielding which occurs near the base results in a reduction of the maximum horizontal shears. Thus, Fig. 29d, like Fig. 24d, shows the maximum shears corresponding to the E-W component of the 1940 El Centro to be less than those for the other input motions. The greater base shears associated with these other input motions can be partially attributed to the higher (effective) modes of vibration. As pointed out earlier, a comparison of Fig. 15 with Fig. 16 clearly indicates the greater sensitivity of the horizontal shears, as compared to bending moments (and displacements), to higher mode response. Figure 23 shows that most of the other input motions considered have spectral ordinates in the low-period range that are generally greater than those of the 1940 El Centro E-W record.

The results of the preceding analyses serve to confirm the observations made in Ref. 6 relative to the velocity spectrum. Thus, for structures where extensive yielding occurs, resulting in a significant increase in the effective period of vibration, the "broad band ascending" type of accelerogram can be expected to produce greater deformations than a "peaking" accelerogram of the same intensity. Where the expected yielding is of limited extent so that the increase in effective period is minor, a peaking accelerogram is more likely to produce greater deformations than a broad band accelerogram of the same intensity. Since the extent of yielding is a function of the earthquake intensity, the yield level of the structure, and the frequency characteristics of the input motion, these factors must be considered in selecting an input motion for a given structure to obtain a reasonable estimate of the maximum response.

Interaction Between Intensity and Yield Level

To verify the observation concerning the relationship of the input motion intensity and the structure yield level, the reference structure ISW 1.4 (T_1 = 1.4 sec., M_y = 500,000 in.-kips) was subjected to two input motions with an intensity equal to 0.75 ($SI_{ref.}$). The two motions used were the S16E component of the 1971 Pacoima Dam record and the E-W component of the 1940 El Centro record. As indicated in Table 2, the Pacoima Dam record is a "peaking (0)" accelerogram relative to the initial fundamental period of the structure, while the El Centro motion is of the "broad band ascending" type.

The resulting envelopes of response, shown in Fig. 30, serve to further confirm the observation made earlier that when yielding in the structure is not extensive enough to cause a significant increase in the effective period of the structure, the peaking accelerogram is likely to produce the more critical response. Figure 30e shows that in this case, yielding in the structure has not extended far above the base when compared to Set (a) where the input motion was twice as intense (Fig. 24e).

Note that in Set (a) considered earlier, the 1940 El Centro, E-W record (a "broad-band" accelerogram), with intensity equal to 1.5 ($SI_{ref.}$), represents the critical motion, while the Pacoima Dam record (a "peaking" motion) produces a relatively lower response. By reducing the intensity of the motions by one-half so that yielding in this structure is significantly reduced, the Pacoima Dam record becomes the more critical motion, as Fig. 30 shows.

To summarize, it is pointed out that because the extent of yielding in a structure is influenced by the yield level of the structure, M_y, as well as the intensity of the input motion, both parameters must be considered when selecting the appropriate input motion, with particular reference to its frequency characteristics.

In selecting an input motion for use in the analysis of a structure at a particular site, the probable epicentral distance

and intervening geology should be considered. These considerations, which affect the frequency content of the ground motion at the site, may logically rule out the possibility of dominant components occurring in certain frequency ranges. Because the high-frequency components in seismic waves tend to attenuate more rapidly with distance than the low-frequency components, it is reasonable to expect that beyond certain distances, depending on the geology, most of the high-frequency components are damped out so that only the low-frequency (long-period) components need be considered.

Effect of Duration of Earthquake Motion

In studying the effect of duration of the earthquake motion, the response of the reference structure, with period T_1 = 1.4 sec. and M_y = 500,000 in.-kips, to the first 10 seconds of the E-W component of the 1940 El Centro record was compared with its response to an accelerogram with a 20-second duration. Both accelerograms were normalized to yield a spectrum intensity equal to 1.5 ($SI_{ref.}$).

The 20-second accelerogram consists of the first 12.48 seconds of the E-W component of the 1940 El Centro record followed by that portion of the same record between 0.98 sec. and 8.5 sec. The intent in putting together this composite accelerogram was to subject the structure to essentially the same first 10 seconds of input motion but to extend the period of excitation using acceleration pulses of about the same intensity as those occurring in the first 10 seconds. Because the 1940 El Centro, E-W component has its peak acceleration at about 11.5 seconds, it was decided to include this peak in the composite record and add a segment from the more intense portion of the first 10 seconds to make a 20-second record. The inclusion of the peak acceleration at 11.5 sec. and the addition of the extra 7.5 sec. of fairly intense pulses, however, sufficiently altered the velocity response spectrum. Because of this change, a normalizing factor smaller than that used for the 10-sec. input motion was indicated to obtain a spectrum intensity equal to

1.5 times that of the 1940 El Centro, N-S component. Thus, a normalizing factor of 1.54 was calculated for the 20-second composite accelerogram, compared to a factor of 1.88 used for the 10-second input record. This means that the amplitude of the pulses in the 10-second input was larger than in the first 10 seconds of the 20-second composite accelerogram by a factor of 1.88/1.54 or 1.22. A plot of the unnormalized 20-sec. composite accelerogram is shown in Fig. 31a. The corresponding relative velocity response spectra are given in Fig. 31b.

In the response envelopes of Fig. 32, the curves corresponding to the 20-sec. composite accelerogram described above are marked "20 sec.-(a)". This figure shows that the displacements, interstory displacements, moments, shears and ductility requirements are greater for the 10-sec. record than for the 20-sec. composite record having the same spectrum intensity. In spite of this, the cumulative ductility, i.e., the sum of the absolute values of the plastic rotations in the hinging region, is greater for the 20-sec. long record, as shown in Fig. 32f. This follows from the fact that the structure goes through a greater number of inelastic oscillations when subjected to longer excitation. The cumulative plastic hinge rotation plotted in Fig. 32f represents the sum of the "primary" and the "secondary" plastic rotations illustrated in Fig. 33. Because it is a measure of the number and extent of the excursions into the inelastic region which the critical segment in a member undergoes, the cumulative plastic hinge rotation represents an important index of the severity of deformation associated with dynamic response. This is particularly true for members which tend to deteriorate in strength with repeated cycles of inelastic deformation, i.e., with relatively short low-cycle-fatigue lives.

The time history of rotation of the node at the first floor level of the wall when subjected to the two input motions discussed above is shown in Fig. 34. The curve marked "10 sec." actually corresponds to the first 20 seconds of the 1940 El Centro, E-W record, normalized so that the spectrum intensity

for the first 10 seconds equals 1.5 times $SI_{ref.}$. As might be expected, the response of the structure during the second 10 secs. of the normalized 1940 El Centro E-W record (marked "10-sec." in Fig. 34) decays after 12 seconds. In comparison, the structure continues to oscillate through several cycles of relatively large amplitude during the same time interval of the 20-sec. composite accelerogram.

The third curve in Figs. 32 and 34, marked "20 sec.-(b)", represents the response of the structure to the 20-sec. composite accelerogram when scaled by the same factor used in normalizing the 10-sec. record. Note that the curves marked "10-sec." and "20 sec.-(b)" in Fig. 34 coincide over the first 10 seconds.

Both Figs. 32f and 34 indicate that the major effect of increasing the duration of the large-amplitude pulses in the input accelerogram is to increase the number of cycles of large-amplitude deformations which a structure will undergo. This conclusion assumes that the intensity and frequency characteristics of the additional motion do not differ significantly from those of the shorter duration input.

Effect of Earthquake Intensity

To examine the effect of earthquake intensity, three sets of analyses were run corresponding to different combinations of the fundamental period, T_1 and the yield level, M_y. In all cases, the input motion used was the first 10 seconds of the E-W component of the 1940 El Centro record, normalized to different intensity levels in terms of $SI_{ref.}$.

Table 3 shows the values of the periods and yield levels assumed for the structure, together with the different intensity levels of input motion used for each set. The response envelopes for all these cases are shown in Figs. 35, 36 and 37. In all cases, there is a consistent increase in the response with increasing intensity, a behavior also observed by other investigators.

Figure 35 shows that the displacements, interstory displacements and ductility requirements increase almost proportionally with increasing intensity. The maximum moments and shears, however, do not show a proportional increase to reflect the increase in intensity. Thus, Figs. 35c and 35d show that an increase in intensity level from 1.0 to 1.5 produces about the same increase in the maximum moments and shears as an increase from 0.75 to 1.0 in intensity level.

Figure 36e indicates that with a yield level, M_y = 1,000,000* in.-kips, the yielding, even under a 1.5 intensity level input motion, does not extend too high up the structure. For this case, the N-S component of the 1940 El Centro record, which has a velocity spectrum that peaks at about 0.8 sec. produces a greater response--for the same intensity (see Set (b) of "Effect of Frequency Characteristics").

Structural Parameters

The combinations of significant structural parameters used in investigating the effect of each parameter on dynamic response have been summarized in Table 4. In almost all cases, the parameter values in each set have been chosen so that only the parameter of interest is varied while the other variables remain constant.

The fundamental period, T_1, and the yield level, M_y, (the basic parameters characterizing the primary force-deformation curve of the structure), were extensively studied using different combinations of structural parameters. The slope of the post-yield branch of the primary bilinear moment-rotation curve, as defined by the yield stiffness ratio, r_y, was also considered in detail. Also studied was the sensitivity of the dynamic response to varying degrees of stiffness degradation in the hinging region of the wall. The effect of the shape of hysteretic loop was examined by assuming different values parameters α and β which define the slopes of the unloading and reloading branches, respectively, of the M-θ loop of potential

*1,000,000 in.-kips = 112,900 kN.m.

inelastic hinges (Fig. 3). Other parameters investigated included viscous damping, taper in stiffness and strength along the height of the structure, the fixity condition at the base, and the number of stories.

Based on the study of the effects of the frequency characteristics of input motions, it was decided to use the first 10 seconds of the E-W component of the 1940 El Centro record, as input motion for the analyses of the effects of all the structural parameters on dynamic response. An intensity equal to 1.5 ($SI_{ref.}$) was used throughout.

Effect of Fundamental Period, T_1

The effect of the initial fundamental period of the structure, T_1, was investigated by using four sets of data as shown in Table 4, each corresponding to a different yield level, M_y. Because of the close interrelationship between these two major structural parameters, it was deemed necessary to study the effects of the structure period under varying values of the yield level.

(a) Yield Level, M_y = 500,000 in.-kips

Corresponding to this yield level, four values of the fundamental period were used, namely, 0.8, 1.4, 2.0 and 2.4 secs. Even though the stiffness associated with a period, T_1, of 0.8 sec. is rather high for a structural wall section having a yield level of 500,000 in.-kips, this parameter combination was considered in order to provide some indication of the behavior of structures which might fall in this range.

Figure 38 shows envelopes of response quantities for this set. In Fig. 38a and 38b, the maximum horizontal and interstory displacements show a consistent increase with increasing fundamental period (or decreasing stiffness) of the structure. The rotational ductility requirements, expressed as a ratio of the maximum rotation to the rotation at first yield, how-

ever, become greater with decreasing fundamental period, a trend also observed by Ruiz and Penzien[26]. Figure 38e indicates, as do similar plots shown earlier, that the greater the ductility requirements at the base, the higher the yielding generally extends above the base.

Because all structures considered in Fig. 38 have the same yield level, and have a relatively flat slope for the post-yield branch of the M-θ curve (r_y = 0.05), the maximum moments and shears shown in Figs. 38c and 38d do not differ significantly for all four cases considered. The shorter-period structures show only slightly greater moments at the base. Figure 38e also indicates that for structures with relatively low yield levels, where yielding is significant, ductility requirements do not decrease significantly with an increase in period beyond a certain value of the fundamental period. Thus, the ductility requirements for structures with periods of 2.0 and 2.4 sec. are about the same.

It is worth noting that although Fig. 38e shows the rotational ductility requirements as increasing with decreasing period of the structure, the absolute value of the maximum rotation for the stiff structure is less than that for the more flexible structure. The distinction between these two measures of the deformation requirement is illustrated in Fig. 39, for the case of structures with M_y = 500,000 in.-kips. Figure 38f, for instance, shows the cumulative plastic hinge rotation, i.e., the sum of the absolute values of the inelastic hinge rotations, as increasing with increasing period of the structure. This trend follows directly from the larger deformations of the more flexible structures.

Variation with time of the flexural deformation in the first story for the four structures considered

in this set is shown in Figs. 40a and 40b. In Fig. 40a, the rotations have been normalized by the respective yield levels of each structure. For instance, the rotations for the structure with T_1 = 0.8 sec. have been divided by its yield rotation value of 0.00014 radians and those for the structure with T_1 = 2.0 sec., by 0.00070 radians. Thus, the absolute magnitude of the rotations for the latter structure are actually 0.00070/0.00014 or 5.0 times those of the former on the basis of the ordinates shown in this figure. The variation with time of the actual magnitude of the rotations (in radians) for the four cases considered are shown in Fig. 40b.

(b), (c) and (d) Yield Level, M_y = 750,000,* 1,000,000 and 1,500,000 in.-kips, respectively

The same general trends observed in Set (a) above with respect to displacements, moments and ductility requirements are also apparent in Figs. 41 through 43 for the higher values of the yield level, M_y. Thus, as in Set (a), an increase in period results in an increase in the horizontal and interstory displacements and a decrease in the moments and the ductility requirements (expressed as a ratio). Although the horizontal shears do not change much with changing period for a given yield level, no clear trend can be observed insofar as the effect of period variation on the base shear is concerned. Generally, though, the shears tend to be slightly higher for shorter-period structures.

A comparison of Figs. 40f and 41f with Figs. 42f and 43f shows that while for structures with relatively low yield levels (i.e., M_y = 500,000 and 750,000 in.-kips) the cumulative plastic hinge rotation tends to decrease with decreasing period of the

*750,000 in.-kips = 84,740 kN·m.

the reverse trend appears to hold as M_y increases beyond a certain value. As noted earlier, the ratio of the maximum rotation to the yield rotation diminishes with increasing period of the structure, for a given yield level, M_y. This means that the relative extent of yielding diminishes with increasing period of a structure. Also, as the yield level increases, the degree of inelastic action generally diminishes, as might be expected and as indicated by a comparison of Figs. 38e, 41e, 42e and 43e. Thus, an increase in both yield level and fundamental period would combine to reduce the amount of inelastic action in a structure; and where this combined effect is such as to make yielding in a structure insignificant, the cumulative plastic rotation becomes less for the long-period structure than for the short-period structure. Figure 42e shows that for the structure with M_y = 1,000,000 in.-kips and T_1 = 2.0 sec., yielding is not too significant. Figure 43e indicates that the structure with M_y = 1,500,000 in.-kips and T_1 = 2.4 sec. remains essentially elastic under a base motion with intensity SI = 1.5 ($SI_{ref.}$).

Effect of Yield Level, M_y

Three sets of yield level values were considered corresponding to fundamental period values of 0.8, 1.4, and 2.0 sec. The different values included in each set are listed in Table 4.

Envelopes of maximum response values showing the effect of yield level are given in Figs. 44, 46 and 47 corresponding to the three values of the fundamental period assumed.

The following general comments apply to all cases shown in these figures. For the same fundamental period, the horizontal and interstory displacements decrease sharply as the yield level increases from 500,000 in.-kips to a value associated with nominal yielding at the base (a value which tends to decrease

with increasing value of the fundamental period). This is evident from a comparison of Figs. 44a and 44b with Figs. 47a and 47b. Above this value, the trend is reversed and an increase in yield level is accompanied by an increase in horizontal and interstory displacements. Maximum moments and shears increase almost proportionally with the yield level, as shown in plots (c) and (d) of Figs. 44, 46, 47. As observed earlier under "Effect of Fundamental Period", rotational ductility requirements increase significantly as the yield level decreases. This qualitative trend has also been observed in connection with the response of single-degree-of-freedom systems[27]. Figure 44f shows that the cumulative plastic hinge rotations also increase as the yield level decreases. A normalized time history plot of the total rotation in the first story is shown in Fig. 45 for the four structures with fundamental period, T_1 = 1.4 sec.

Fundamental Period and Yield Level Effects - Summary

The interrelationship between the effects of the initial fundamental period, T_1, and the yield level, M_y, on the dynamic response of 20-story isolated structural walls is summarized in Fig. 48. The plots in the figure correspond to only one input motion, i.e., the E-W component of the 1940 El Centro record, with the acceleration amplitude adjusted to yield a 5%-damped spectrum intensity equal to 1.5 ($SI_{ref.}$). Properties of the structures considered are those for the basic structures listed in Table 1.

Figure 48 shows the effects of both T_1 and M_y on the maximum horizontal displacement of the top of the structure, the maximum interstory displacement along the height of the wall and the maximum moment, (in terms of the yield moment, M_y), the maximum shear, rotational ductility (expressed as a ratio of the maximum rotation to the corresponding yield rotation) and the cumulative plastic hinge rotation at the base of the wall. The maximum values of the response parameters are also listed in Table 5.

The following significant points, noted earlier in relation to the study of the separate effects of the fundamental period and the yield level, are summarized below for convenience in considering the curves shown in Fig. 48.

(a) Maximum Top Displacement and Maximum Interstory Displacement

For a particular value of the yield level, M_y, an increase in the fundamental period (indicating a decrease in the stiffness of the structure) results in an increase in horizontal and interstory displacements.

For a given fundamental period and for relatively low yield level values, the maximum displacements decrease with increasing yield level. Beyond a certain value of the yield level (which tends to decrease with increasing value of the fundamental period) associated with nominal yielding, the above trend is reversed, i.e., the maximum displacements increase with increasing yield level.

Figure 48a shows a dotted curve representing the top displacement resulting from the distributed design base shear, V_b, as specified in the Uniform Building Code (1976 Edition)--with the factors Z, S and I set equal to 1.0.

(b) Maximum Moment and Rotational Ductility at Base

For a particular yield level value, the ratios M_{max}/M_{yield} and $\theta_{max}/\theta_{yield}$ as measures of the maximum moment and rotational ductility at the base, respectively, generally decrease with increasing fundamental period, the decrease being more rapid for lower yield levels. For a constant fundamental period, the above ratios consistently increase with decreasing yield level.

It should be pointed out that the yield level of 500,000 in.-kips is not too realistic for structural walls having stiffnesses associated with fundamental period values less than 1.4 sec.

(c) Maximum Base Shear

For a particular yield level, M_y, the maximum base shear decreases as the fundamental period increases from 0.8 sec. to a certain value, which value increases with increasing yield level. Beyond this value of the fundamental period, the maximum base shear increases with increasing period of the structure.

(d) Cumulative Plastic Hinge Rotation at Base

Figure 48f indicates, as noted earlier, that for structures with relatively low yield levels (i.e., M_y = 500,000 and 750,000 in.-kips) in which significant yielding occurs, the cumulative plastic hinge rotation at the base increases with increasing fundamental period over the entire period range (0.8 - 2.4 sec.) considered. For higher values of the yield level, the cumulative plastic hinge rotation increases with increasing period up to a point where the combination of high yield level and long period results in only nominal yielding. Beyond this value of the fundamental period (which decreases with increasing yield level) the trend reverses and the cumulative plastic hinge rotation decreases with increasing fundamental period until the point where no yielding occurs.

Curves corresponding to the design base shear as specified in the Uniform Building Code (UBC-76), multiplied by load factors of 1.4 and 2.0 are shown in Fig. 48d for comparison with the results of the dynamic analysis.

Effect of Yield Stiffness Ratio, r_y

The effect of the slope of the second, post-yield branch of the primary bilinear moment-rotation curve of the members that make up the structural wall was investigated. This was accomplished by considering a value of the yield stiffness ratio, r_y, (i.e., the ratio of the slope of the second, post-yield

branch to the slope of the initial, elastic branch of the M-curve), equal to 15%, in addition to the value of 5% used for most cases. As indicated in Table 4, these two values of the yield stiffness ratio were used with three combinations of the fundamental period and yield level. In addition, a value of r_y = 0.01 was considered for the case of structures with T_1 = 1.4 sec. and M_y = 500,000 in.-kips.

Response envelopes for the three sets are given in Figs. 49, 50 and 51. These figures show that even with significant yielding at the base, as indicated by the plots for rotational ductility, an increase in the value of the yield stiffness ratio from 5% to 15% generally does not produce any significant effect of the response. As might be expected, the effect of a change in the value of the yield stiffness ratio, r_y, is more apparent in structures with relatively low yield levels (M_y = 500,000 in.-kips). There is a substantial (50%) reduction in the rotational ductility requirement at the base for the long-period (T_1 = 2.0 sec.) structures and a 20% reduction in the horizontal and interstory displacements for the moderately-long period (T_1 = 1.4 sec.) structures accompanying an increase in the yield-stiffness ratio from 5% to 15%. The effect of increasing the yield stiffness ratio is less apparent in structures with relatively high yield levels, as shown by Fig. 50.

A decrease in the yield stiffness ratio from 5% to 1% results in an increase in the rotational ductility requirement at the base by a factor of 1.85 (Fig. 49e). There is a lesser increase in the cumulative plastic hinge rotation. Except for these, the effect of r_y on the response is relatively minor for the range of values considered. An increase in the slope of the post-yield branch of the M-θ curve tends to reduce the horizontal and interstory displacements as well as the ductility requirements at the base while increasing the moments and shears slightly.

It will be noted that for the Takeda model of the hysteretic M-θ loop, the effective stiffness of an element during most of the response after yielding may be governed not so much by the primary M-θ curve as by the rules governing the slope of the reloading stiffness associated with this model. The effect of r_y becomes significant only when the motion of the structure proceeds in a particular direction long enough for the primary curve to govern. However, because the post-yield slope in the bilinear M-θ curve represents the least value of stiffness of the structure, it can be expected to have a greater effect on the maximum displacement and rotations than the subsequent "reduced" stiffnesses. The effect becomes most pronounced for structures with low yield levels (relative to the intensity of the input motion). Significant displacements and ductility requirements can then be expected particularly for low values of r_y. An idea of the percentage of the total response time, during which the post-yield branch of the primary curve governs the effective stiffness of the structure, can be obtained from Fig. 52, which shows the moment-rotation loop for the base of the structure with T_1 = 1.4 sec., M_y = 500,000 in.-kips and r_y = 15%.

Effect of Character of M-θ Hysteretic Loop

To investigate the effects of other parameters, the quantities α and β defining the slopes of the unloading and reloading branches of the Takeda model hysteretic loop (Fig. 53) were assigned values of 0.10 and 0.0, respectively. The sensitivity of the calculated response to variations in the values of these two parameters was examined by analyzing structures using different values of α and β.

A value of 0.30 was considered for the unloading parameter α in addition to the basic value of 0.10 (with β = 0), for a structure with T_1 = 1.4 sec. and M_y = 500,000 in.-kips. For the reloading parameter β, values of 0.4 and 1.0 were assumed in addition to the basic value of 0 (with α = 0.10).

Furthermore, results for a model with a stable bilinear hysteretic loop (Fig. 53) were obtained for comparison with the response of structures with different values of β. The effect of the reloading parameter β was investigated for two sets of structures, one set representing low yield levels (M_y = 500,000 in.-kips, T_1 = 1.4 sec.) and the other relatively higher yield levels (M_y = 1,000,000 in.-kips, T_1 = 0.8 sec.). The various combinations used in this study are listed also in Table 4.

Figure 54, which shows response envelopes for cases where the parameter α is allowed values of 0.10 and 0.30 (with β = 0) indicates practically no difference in the maximum response values corresponding to the two assumed values of α.

Figures 55 and 56 show the response envelopes for cases when the reloading parameter β is varied. Both figures indicate that the effect of this parameter on dynamic response is not significant.

For structures with low yield level (M_y = 500,000 in.-kips, Fig. 55), an increase in the slope of the reloading curve--corresponding to increasing values of β--results in slight reductions in horizontal and interstory displacements and cumulative plastic hinge rotations. Where yielding is not as extensive, as in structures with M_y = 1,000,000 in.-kips (compare Fig. 56e with 55e), the effect of variations in β is even less significant. For this case, the trend with respect to maximum horizontal displacements is reversed, so that the structure with the stable bilinear hysteretic loop exhibits slightly greater displacements than any of the structures with decreasing-stiffness loops. The cumulative plastic hinge rotations, however, still increase as β decreases (Fig. 56f). Note that this same trend in the maximum response values was observed in the study of the effect of the yield level, M_y (Fig. 44).

In each of the two sets of analyses where the reloading parameter β was varied, the maximum moments, shears and rotational ductility requirements at the base are practically the

same in spite of the significant difference in the slopes of the reloading curves.

The variation with time of the nodal rotations at the first story level for the structures with T_1 = 1.4 sec. and M_y = 500,000 in.-kips are shown in Fig. 57. For all cases, the figure shows that the maximum response to the particular input motion used occurs very early, during which time the primary bilinear curve (identical for all cases) governs; the envelopes of maximum response values do not differ significantly from each other. However, after the first major inelastic cycle of response occurs and the rules assumed for the reloading stiffness in each case take effect, the responses reflect the differences in the M-θ hysteresis loops. Thus, after first yield, the rotations tend to be greater for the lower values of β (corresponding to reloading branches with flatter slopes or lesser stiffness).

Moment vs. nodal rotation plots for the structure with a stable hysteretic loop and that with β = 0.40 are shown in Fig. 58. The corresponding plot for the structure with β = 0 is shown in Fig. 18.

Effect of Damping

Viscous damping assumed for the structures in this investigation consists of a linear combination of stiffness-proportional and mass-proportional damping. The damping distribution among the initial component modes is defined in terms of the percentage of the critical damping for the first and second modes, which are assumed to be equal. For most of the analyses, a damping coefficient of 0.05 was assumed.

To evaluate the effect of damping, a second value of the damping coefficient, equal to 0.10, was considered. The responses corresponding to these two values of damping were compared for two combinations of the fundamental period, T_1, and the yield level, M_y, as shown in Table 4.

Envelopes of response corresponding to structures with intermediate period and low yield level (i.e., T_1 = 1.4 sec.,

M_y = 500,000 in.-kips) are shown in Fig. 59. As observed in other studies, the general effect of increasing damping in a structure is to reduce the response. For the structures considered in this particular set, increasing the damping coefficient from 0.05 to 0.10 produced only a relatively small (about 12% in the maximum top displacement) reduction in response.

Figure 60 shows the response envelopes of structures with low period and relatively high yield level, i.e., T_1 = 0.8 sec., M_y = 1,000,000 in.-kips. The effect of increasing the damping coefficient from 0.05 to 0.10 for this set is likewise insignificant. When compared with results for the first set of structures with low yield level, Fig. 60 indicates that an increase in the viscous damping coefficient from 5% to 10% produces a slightly lower reduction (9%) in the maximum top displacement. However, in terms of deformation requirements, the increase in damping produces a relatively greater percentage reduction in the high-yield-level (M_y = 1,000,000 in.-kips) structure than the structure where extensive yielding occurs (M_y = 500,00 in.-kips): 19% as against 8% for the rotational ductility requirements and 41% as compared to 13% for the cumulative plastic hinge rotation. This increase in the energy dissipated through damping as the extent of inelasticity diminishes, and vice versa, was also noted by Ruiz and Penzien[26].

Effect of Stiffness Taper

In examining the effect of other parameters the structures considered have uniform stiffness throughout their entire height. To study the effect of a taper in stiffness, the response of a structure with the stiffness variation shown in Fig. 61 was compared to that of a structure with uniform stiffness. A ratio of $(EI)_{base}$ to $(EI)_{top}$ equal to 2.8 was used (corresponding to A/B = 4.0, Fig. 59), the absolute value of the stiffness being adjusted to yield a fundamental period of 1.4 sec.

Figure 60, which shows the corresponding response envelopes, indicates that for the period and yield level the horizontal

and interstory displacements as well as the cumulative plastic rotations at the base are less for the tapered than for the uniform structure. However, the moments, shears and rotational ductility requirements at and near the base are greater for the tapered structure than for the wall with uniform stiffness.

Effect of Strength Taper

To evaluate the effect of a taper in the strength (yield level) of the wall, the following three cases were considered:

(a) A taper ratio (i.e., the ratio of the yield level at the base to that at the top of the wall) of 2.0, with equal changes in strength occurring regularly at every story level. This is the taper used in the reference structure, which reflects the effects of axial loads on the moment capacity.

(b) A taper ratio of 3.8, with equal changes in strength occurring at every fourth story level, in a manner similar to the stiffness taper shown in Fig. 61. In addition, changes reflecting the effect of the axial load occur at every story level.

(c) A taper ratio of 1.0, representing uniform strength throughout the height of the wall.

Response envelopes for this set are shown in Fig. 63. Except for the increased rotational ductility requirement in the intermediate stories of the structure with a taper ratio of 3.8 as shown in Fig. 63e, the effect of strength taper for the particular period and yield level considered appears to be negligible.

Effect of Fixity Condition at Base

The effect of yielding of the foundation at the base of the wall was considered by introducing a rotational spring (with linear M-θ characteristic) at the base of the analytical model. If the base fixity factor, F, is defined as the ratio of the moment developed at the base to that which would be developed

if the base were fully fixed, under the same deformation, the spring stiffness, K_s, for the model shown in Fig. 64 is given by

$$K_s = \left(\frac{F}{1 - F}\right) \frac{3EI}{\ell} \qquad (3)$$

In the analysis, the (linear) spring representing the rotational restraint of the foundation was modelled by an extension of the wall below the base having the appropriate flexural stiffness. This is shown in Fig. 65. The stiffness of the element used to simulate foundation restraint corresponding to each degree of base fixity assumed is also shown in the figure for the two sets considered.

Figure 66 shows a comparison of response envelopes for the first set, in which the reference structure (T_1 = 1.4 sec., M_y = 500,000 in.-kips) has a fully fixed base (i.e., F = 1.0), with cases in which the base fixity factor was assigned values of 0.75 and 0.50. Note that the initial fundamental period of 1.4 sec. applies only to the fully fixed-base structure. The calculated fundamental period for the structure with F = 0.75 was 1.43 sec. and for the structure with F = 0.50, 1.52 sec.

Increases in the maximum horizontal and interstory displacements, in almost the same proportion as the increase in the fundamental period, accompany the decrease in the base fixity factor, F, from the fully fixed value of 1.0 to 0.75 (20% increase in the maximum top displacement) and then to 0.50 (80% increase). It is interesting to note that for this group of low-yield-level structures where significant yielding occurs, relaxation in the base fixity results in increases (though slight) in maximum moment and shears and in rotational ductility requirement at the base. In the case of the rotational ductility requirement, there is a 20% increase accompanying a decrease in the base fixity factor from 1.0 (fully fixed) to 0.50.

Figure 66f indicates that even though the ductility requirement at the base increases with decreasing base fixity as

shown in Fig. 66e, the cumulative plastic hinge rotation decreases with decreasing base fixity. Since the yield rotation is the same for all three structures in each set and the periods do not differ significantly from each other, this reversal in trend for these two measures of deformation may at first appear contrary to expectation. Figure 67, which shows the variation with time of the plastic hinge rotation at the bases of the walls, provides some explanation for this reversal in trend. The figure shows that although the maximum plastic hinge rotation increases with decreasing base fixity, the number of oscillations and hence the cumulative plastic hinge rotation tends to increase as the base fixity increases (and the period decreases).

To examine the effect of the base fixity condition on structures with high yield levels, a second set of analyses was undertaken for a basic structure with T_1 = 0.8 sec. and M_y = 1,500,000 in.-kips. Values of the base fixity factor equal to 0.75 (T_1 = 0.83 sec.) and 0.50 (T_1 = 0.88 sec.) were considered in addition to the fully fixed case.

Figure 68 shows response envelopes for this set. As in Set (a), Figs. 68a and 68b show the expected increase in maximum displacements due to a relaxation of the base fixity. However, for the structures in this set in which yielding was relatively small (compare Fig. 68e with Fig. 66e), the maximum moments and shears, as well as the rotational ductility and the cumulative plastic hinge rotation at the base, tend to decrease with a reduction in the base fixity factor. A 60% decrease in the rotational ductility requirement at the base accompanies a reduction in the base fixity factor from 1.0 to 0.50.

Effect of Number of Stories

The effect of the number of stories or the height of the structure on dynamic response was investigated by considering 10-, 30- and 40-story variations of the basic 20-story reference structure. The stiffness of the structure in each case was adjusted to yield the same fundamental period (T_1 = 1.4 sec.)

as the basic structure. Two sets of analyses were made, as listed in Table 4. In the first set, a common value of the yield level, M_y, equal to 1,000,000 in.-kips, was assumed for all four structures. The purpose here was to isolate the effect of the number of stories on the response. In practice, however, the strength of walls would normally be expected to increase with the height of the building. In view of this, a second set of analyses was made with the yield level in each case adjusted to result in a ductility ratio of about 4 to 6 at the base of the wall.

A 12-mass model was used for both the 10- and 40-story walls, with the masses spaced at every half-story in the lower two stories of the 10-story wall and at every other floor in the lower eight stories of the 40-story structure. For the 30-story structure, a 14-mass model was used, with the lumped masses spaced at every floor in the lower five floors.

Figure 69 shows response envelopes corresponding to the first set, i.e., with a constant yield level, M_y = 1,000,000 in.-kips, assumed for all four structures. As indicated in Fig. 69e, all structures except the 10-story wall yielded at the bases in varying degrees, the extent of yielding increasing with increasing height of structure. In the case of the 40-story structure, yielding extended above mid-height.

Except for the 10-story structure which responded elastically, the maximum displacements and interstory displacements for the 20-, 30- and 40-story structures were essentially the same at corresponding floors above the base. For the same yield level, the maximum bending moments, shears and ductility requirements (expressed as ratios of maximum to yield rotations) generally increase with increasing height of the structure. The cumulative plastic hinge rotations, however, tend to decrease with increasing height of structure. This behavior follows from the fact that in order to obtain the same fundamental period of 1.4 sec., the 40-story wall had to be relatively much stiffer than, say, the 20-story wall. In this case, the sectional stiffness of the 40-story wall had to be

15.8 times that of the 20-story wall in order to obtain the same period, and for the same yield moment had a correspondingly lesser yield rotation. Thus, for about the same maximum rotation (Fig. 69a), the ductility ratio for the 40-story structure is greater than that for the 20-story structure. Figure 70 shows a time history plot of the nodal rotations at a point corresponding to the 2nd floor above the base in each of the four structures considered under Set (a), as listed in Table 4.

Response envelopes for the second set of analyses--with the fundamental period, T_1, still equal to 1.4 sec. but with the yield level, M_y, adjusted so that the resulting ductility ratios at the base for all structures fall in the range of 4 to 6--are shown in Fig. 71. The yield level assumed in each case and the corresponding ductility ratios at the base are listed below, see also Fig. 71e.

No. of Stories	Assumed Yield Level, M_y (in.-kips)	Ductility Ratio at Base
10	200,000	5.4
20	750,000	4.9
30	1,500,000	6.0
40	2,500,000	5.9

For the conditions assumed in this set, the maximum displacements at the top of all four structures are about the same, as shown in Fig. 71a; the slight differences reflect the relative magnitudes of the base ductility ratio. The equal maximum deflection at the top for different heights of structure implies increasing interstory distortions with decreasing height. This is shown in Fig. 71b. The increase in the yield level with height of structure leads to a very regular increase in the maximum bending moment and shear with the number of stories. Figure 71f, however, indicates that the cumulative plastic hinge rotations at the base tend to increase with decreasing yield level and structure height, the effect of the former apparently predominating.

SUMMARY

Figures 72 through 83 provide a convenient summary of the effects of the structural and ground motion parameters considered on five response quantities. The five response quantities are the maximum values of the top displacement, interstory displacement, bending moment, shear force and rotational ductility at the base of the wall. Only in considering the effect of ground motion duration is the cumulative plastic rotation at the base shown. It has not been possible to conveniently summarize the effect of the frequency characteristics of input motions on structural response. However, this parameter has been adequately covered in the text.

In all of the summary figures (Figs. 72-83), the particular parameter considered is shown as the abscissa. The response quantities, plotted as ordinates, have all been non dimensionalized by using appropriate factors. In these figures, "H" is the total height of the wall and "h" is the story height.

Intensity and Duration of Ground Motion

Figure 72 shows that the response generally increases with increasing intensity of the input motion. The magnitude of response as well as the increase in response with increasing intensity is greater for long-period structures with low yield levels than for stiff, strong (i.e., short-period, high yield level) structures.

As mentioned earlier and shown in Fig. 73, the effect of duration of the input motion on response is not too significant, except on the cumulative plastic rotations.

Structural Parameters

The effect of the fundamental period of the structure on dynamic inelastic response of isolated walls is summarized in Fig. 74. This figure indicates the significant increase in horizontal and interstory displacements with increasing period (reflecting decreasing stiffness) of a structure. Note that

there is very little difference in displacements between walls having different yield levels. The effect of yield level is more apparent in the maximum moments, shears and rotational ductility. For these response quantities, the fundamental period does not have too significant an effect, except for structures with low yield levels.

The relationship between period and yield level indicated in Fig. 74 is again apparent in Fig. 75, which shows the effect of yield level on structural response. Thus, although the absolute value of the displacements increase with increasing period, the displacement for any particular fundamental period changes very little with increasing yield level. On the other hand, the maximum moment and shear, expressed in terms of the corresponding yield moment, as well as the rotational ductility, decrease with increasing yield level.

Figure 76 shows the effect on response of the yield stiffness ratio, r_y, i.e., the ratio of the slope of the second, post-yield branch of the bilinear primary moment-rotation curve to the slope of the initial branch. The major effect of this parameter is on the maximum moment and rotational ductility, although it is not too significant. As may be expected, an increase in r_y results in an increase in the maximum moment and a decrease in the rotational ductility demand.

The effect of the parameters α and β defining the slopes of the unloading and reloading branches of the hysteretic $M-\theta$ loop (Fig. 2b), and viscous damping are shown in Figs. 77 through 79. These figures indicate that for the range of values assumed for these parameters, their effects on the dynamic response of isolated walls are negligible.

Figures 80 and 81 show the effect of stepwise reductions in stiffness and strength along the height of the wall. A taper in stiffness, when compared to a uniform stiffness throughout the height of the wall, results in a slight decrease in maximum displacements and an increase in the maximum moments, shears and rotational ductility required. The effect of a taper in strength, for the range of values examined, is negligible.

The effect of the degree of base fixity, shown in Fig. 82, is most evident in the maximum displacements, which increase with decreasing base fixity. The effect of this parameter on the maximum moments, shears and rotational ductility demand is not too significant.

The solid curves in Fig. 83 represent the maximum responses of walls of different height, with their yield levels adjusted to give a rotational ductility demand at the base of from 4 to 6. For structures so proportioned, the effect of varying height on the normalized maximum moments and shears (expressed as ratios to the corresponding M_y and M_y/H, respectively) does not appear to be significant. The maximum displacement, expressed as a ratio to the corresponding total height, H, tends to diminish with increasing height of wall. The dashed curves in Fig. 83 correspond to walls with varying height but the same yield level at the base. As mentioned, this set does not represent a realistic condition.

Comparison of Different Parameters

To evaluate the relative importance of the different parameters examined in this study, Figs. 84 through 86 were prepared. To compare the effects of the different parameters on response, it was necessary to assume a practical range of values for each parameter. The ranges of values assumed for the various parameters are shown in the second column of Table 6 and also in Figs. 84 through 86. These values were based on current design practice as well as on judgment.

Figure 84 indicates the relative effects of the various parameters on the maximum displacement at the top of the wall. Curves corresponding to different values of the yield level, M_y, are shown in the figure. The ordinates in the figure represent the change in response corresponding to a change in the value of the particular parameter. The change in response is expressed as a ratio of the calculated response to the response associated with the value of the parameter at the lower end of its assumed practical range. The change in a parameter's

value is expressed as a percentage of its assumed practical range. A zero percent change in the value of a parameter corresponds to the lower end of its range. Thus, if the values of a parameter at the lower and upper ends of its assumed practical range of values are denoted by P_o and P_t, respectively, and P_i is a particular value of the parameter within the range,

$$\text{Value of Parameter Relative to Practical Range (abscissa in Figs. 84-86)} = \frac{|P_i - P_o|}{|P_t - P_o|} .$$

Similarly, if the calculated response corresponding to P_o is denoted by R_o and R_i is the response associated with the parameter value P_i, then,

$$\text{Relative Change in Response (ordinate in Figs. 84-86)} = \frac{|R_i - R_o|}{|R_o|} .$$

The quantities plotted in Figs. 84 through 86 are listed also in Table 6.

Figure 84 shows that as far as top displacement is concerned, the most significant structural parameter is the fundamental period of vibration, particularly as this is affected by the stiffness of the structure. The second most significant structural parameter affecting top displacement is the degree of base fixity. The most significant ground motion parameter is the earthquake intensity.

Relative effects of the various parameters on the maximum base shear is shown in Fig. 85, while Fig. 86 shows the effects on the rotational ductility demand at the base of the wall. Both of these figures show that with respect to shear and ductility demand, the most significant structural parameter is the yield level, M_y. The fundamental period, T_1, exhibits an important influence for the intermediate range of values. As in the case of top displacements, earthquake intensity has a significant influence on both the base shear and the ductility demand.

Since the maximum interstory displacement follows the same trend as the maximum top displacement, the remarks made with respect to the effects of the different parameters on the latter also apply to the former. The same relationship holds between the maximum moment and the rotational ductility demand at the base.

The above comparison indicates that the two most important structural variables affecting inelastic response are the fundamental period and the yield level. Inelastic response is also significantly affected by the intensity of the ground motion.

CONCLUSIONS

This study of the effects of selected structural and ground motion parameters is aimed at establishing the relative importance of these parameters with respect to the inelastic dynamic response of reinforced concrete structural walls. A total of 60 analyses are included in this study, covering variations in eleven parameters. The response quantities considered are those which experience and tests have indicated to be significant to the behavior of these walls. By identifying the most significant parameters affecting behavior, these parametric studies allow the formulation of the design procedure to be developed in the subsequent effort[8] based on these few significant variables.

The major considerations involved in assessing the relative importance of the various parameters are the magnitude of the deformation requirements and the accompanying forces. At the base of the wall, the critical region, the major concerns are amplitude and number of deformation cycles as well as the associated moments and shears. Along the height of the structure, magnitude of the maximum interstory distortions and the maximum horizontal displacements are of major interest. Interstory distortions,* and in a less direct manner, horizontal displacements, provide a good index of potential damage in a building. These response quantities also affect the stability of the structure.

The following conclusions and general observations can be made on the basis of the results of this study:

1. The most important structural parameters affecting inelastic dynamic response of isolated walls are the fundamental period, T_1, and the yield level, M_y. Intensity of the input motion is the principal ground motion parameter.

*Expressed appropriately as 'interstory tangential deviations' for isolated walls and as 'horizontal interstory displacements' for frame-wall systems.

2. For the same fundamental period and yield level, significant increases in horizontal displacements can result from a decrease in the degree of fixity at the base of the wall.

3. For the same intensity and duration of the ground motion, significant increases in response can result from an input motion having the appropriate frequency characteristics relative to the period and yield level of the structure.

   Where significant yielding can be expected in a structure, i.e., yielding that would appreciably alter the effective period of vibration, an input motion with a velocity spectrum of the "broad band ascending" type is likely to produce more severe deformation demands than other types of motion of the same intensity and duration. For cases where only nominal yielding is expected, "peaking" accelerograms tend to produce more severe deformations.

   The above considerations are important in determining near-maximum or critical response values for design purposes, or in specifying input motions for use in the analysis of particular types of structures.

4. Shear at the base of an isolated structural wall is more sensitive to higher mode response and generally undergoes a greater number of reversals than the moments or deformations. Because of this, the maximum base shear can be appreciably lower for input motions that produce extensive yielding and that are critical with respect to moments and displacements than for motions which produce lesser displacements. The criticality of response with respect to shear will depend on the relationship of the frequency characteristics of the input motion to the significant higher effective mode frequencies of the yielded structure.

The magnitude of shear forces is of particular interest because of the significant influence that these can have on the deformation capacity of the hinging region.

5. The major effect of the duration of ground motion is to increase the cumulative plastic rotations in hinging regions. The cumulative plastic rotation is another useful index of the severity of the deformation demand in critical regions of a structure and reflects both the magnitude and the number of cycles of loading associated with dynamic inelastic response.

6. Deformation requirements increase almost proportionally with an increase in the intensity of the ground motion.

   Determination of the appropriate intensity to use in a particular case will depend on such factors as earthquake magnitude, epicentral distance and site geology, all of which are beyond the scope of this report. As a matter of fact, the selection of the proper intensity, duration and frequency characteristics of the input motion for use in the analysis of a particular case will be determined to a large degree by factors not considered in this report. The observations based on this study, however, can aid in selecting input motion parameters by providing information concerning the effect of a particular parameter on structural response.

7. A direct result of increasing the stiffness of a structure and thus decreasing its fundamental period (assuming essentially the same mass) is the reduction in the maximum horizontal displacements and the interstory distortions along the height of the structure.

   The ductility requirement, expressed as a ratio of the maximum rotation to the rotation at first

yield, generally increases with decreasing fundamental period (or increasing stiffness) of a structure. This trend is mainly a reflection of the smaller absolute magnitude of the rotations for the stiffer structures. In structures with relatively low yield levels where significant yielding occurs, however, the cumulative plastic rotation in hinging regions tends to decrease with decreasing period. When the yield level is high enough so that only insignificant yielding results, the cumulative plastic hinge rotation tends to decrease with increasing period.

8. The magnitude of deformation requirements in hinging regions--in terms of ductility ratios and cumulative plastic hinge rotations--generally decreases with increasing values of the yield level. Maximum horizontal displacements and interstory distortions also tend to diminish with increasing yield levels, as long as significant yielding occurs. Within a narrow range, where only nominal yielding occurs, the maximum displacements--particularly in the upper stories of the structure--tend to increase with increasing yield level, until a value is reached when no yielding occurs, i.e., linear elastic response.

   Although the yield level in a structure usually does not vary independently of the fundamental period (an increase in stiffness is generally accompanied by an increase in the yield level), the effect of this major variable is worth noting, because of its inter action with the initial fundamental period and also because it affects the dominant or effective period of a yielding structure. The latter has important bearing on the type of ground motion that is likely to produce near-maximum or critical response.

- - - - - - - - - - -

By making possible an assessment of the relative importance of the different parameters affecting structural response, these parametric studies allow the subsequent effort, i.e., the determination of estimates of critical force and deformation requirements in hinging regions of structural walls, to concentrate on a manageable few of the more significant parameters as basis for the design procedure to be developed.

ACKNOWLEDGEMENTS

This investigation was carried out in the Engineering Services Department of the Portland Cement Association, Skokie, Illinois. Mr. Mark Fintel, then Director of Engineering Services, now Director of Advanced Engineering Services, served as overall Project Director of the combined analytical and experimental program. The help extended by Dr. W. G. Corley, Director, Engineering Development Department, in reviewing the draft of this report is gratefully acknowledged.

The project was sponsored in major part by the National Science Foundation, RANN Program, through Grant No. ENV74-14766.

Any opinions, findings and conclusions expressed in this report are those of the authors and do not necessarily reflect the views of the National Science Foundation.

REFERENCES

1. Applied Technology Council, Recommended Comprehensive Seismic Design Provisions for Buildings, Final Review Draft, ATC-3-05, Applied Technology Council, Palo Alto, California, January 7, 1977.

2. Appendix A, Building Code Requirements for Reinforced Concrete (ACI 318-77), American Concrete Institute, P.O. Box 19150, Redford Station, Detroit, Michigan 48219.

3. The Behavior of Reinforced Concrete Buildings Subjected to the Chilean Earthquakes of May 1960," Advance Engineering Bulletin No. 6, Portland Cement Association, Skokie, Illinois, 1963.

4. Fintel, M., "Quake Lesson from Managua: Revise Concrete Building Design?" Civil Engineering, ASCE, August 1973, pp. 60-63.

5. Anonymous, "Managua, If Rebuilt on Same Site, Could Survive Temblor," Engineering News Record, December 6, 1973, p. 16.

6. Derecho, A.T., Fugelso, L.E. and Fintel, M., "Structural Walls in Earthquake-Resistant Buildings - Analytical Investigations, Dynamic ananlysis of Isolated Structural Walls - INPUT MOTIONS," Final Report to the National Science Foundation, RANN, under Grant No. ENV74-14766, Portland Cement Association, January 1978.

7. Derecho, A.T., Ghosh, S.K., Iqbal, M., Freskakis, G.N., Fugelso, L.E., and Fintel, M., "Structural Walls in Earthquake-Resistant Buildings - Analytical Investigation, Dynamic Analysis of Isolated Structural Walls (Part A: Input Motions and Part B: Parametric Studies)," Report to the National Science Foundation, RANN, under Grant No. GI-43880, Portland Cement Association, October 1976.

8. Derecho, A.T., Iqbal, M., Ghosh, S.K. and Fintel, M., "Structural Walls in Earthquake-Resistant Buildings - Analytical Investigation, Dynamic Analysis of Isolated Structural Walls - DEVELOPMENT OF DESIGN PROCEDURE - DESIGN FORCE LEVELS," Final Report to the National Science Foundation, RANN, under Grant No. ENV74-14766, Portland Cement Association, March 1978.

9. Oesterle, R.G., Fiorato, A.E., Johal, L.S., Carpenter, J.E., Russell, H.G. and Corley, W.G., "Earthquake-Resistant Structural Walls - Tests of Isolated Walls," Report to the National Science Foundation, Portland Cement Association, 1976, 44 pp. (Appendix A, 38 pp.; Appendix B, 233 pp.).

10. Derecho, A.T., Iqbal, M., Ghosh, S.K., Fintel, M. and Corley, W.G., "Structural Walls in Earthquake-Resistant Buildings - Analytical Investigation, Dynamic Analysis of Isolated Structural Walls - REPRESENTATIVE LOADING HISTORY," Final Report to the National Science Foundation, RANN, under Grant No. ENV74-14766, Portland Cement Association, March 1978.

11. Derecho, A.T., Freskakis, G.N., Fugelso, L.E., Ghosh, S.K. and Fintel, M., "Structural Walls in Earthquake-Resistant Structures - Analytical Investigation, Progress Report," Report to the National Science Foundation, RANN, under Grant No. GI-43880, Portland Cement Association, August 1975.

12. Ghosh, S.K., Derecho, A.T. and Fintel, M., "Preliminary Design Aids for Sections of Slender Structural Walls," Supplement No. 3 to the Progress Report on the PCA Analytical Investigation, "Structural Walls in Earthquake-Resistant Structures," NSF-RANN Grant No. GI-43880, Portland Cement Association, August 1975.

13. International Conference of Building Officials, Uniform Building Code, 1973 Edition, 5360 South Workman Mill Road, Whittier, California, 90601. (The latest edition of the Code is the 1976 Edition.)

14. Kanaan, A.E. and Powell, G.H., "General Purpose Computer Program for Dynamic Analysis of Plane Inelastic Structures," (DRAIN-2D), Report No. EERC 73-6, Earthquake Engineering Research Center, University of California, Berkeley, April 1973.

15. Ghosh, S.K. and Derecho, A.T., "Supplementary Output Package for DRAIN-2D, General Purpose Computer Program for Dynamic Analysis of Plane Inelastic Structures," Supplement No. 1 to an Interim Report on the PCA Investigation, "Structural Walls in Earthquake-Resistant Structures," NSF-RANN Grant No. GI-43880, Portland Cement Association, Skokie, Illinois, August 1975.

16. Takeda, T., Sozen, M.A. and Nielsen, N.N., "Reinforced Concrete Response to Simulated Earthquakes," Journal of the Structural Division, ASCE, Proceedings, Vol. 96, No. ST12, December 1970.

17. Clough, R.W. and Johnston, S.B., "Effect of Stiffness Degradation on Earthquake Ductility Requirements," Proceedings, Japan Earthquake Engineering Symposium, Tokyo, October 1966.

18. Ghosh, S.K., "A Computer Program for the Analysis of Slender Structural Wall Sections under Monotonic Loading," Supplement No. 2 to an Interim Report on an Investigation

of Structural Walls in Earthquake Resistant Structures NSF-RANN Grant No. GI-43880, Portland Cement Association, Skokie, Illinois, August 1975.

19. Derecho, A.T., "Program DYMFR - IBM 1130 Program for the Dynamic Analysis of Plane Multistory Frames," Portland Cement Association, 1971 (unpublished).

20. Derecho, A.T., "Program DYCAN - IBM 1130 Program for the Dynamic Analysis of Isolated Cantilevers," Portland Cement Association, 1974 (unpublished).

21. Derecho, A.T. and Fugelso, L.E., "Program DYSDF - for the Dynamic Analysis of Inelastic Single-Degree-of-Freedom Systems," Portland Cement Association, 1975 (unpublished).

22. Ghosh, S.K., "Program AREAMR - for the Computation of Cumulative Areas under Moment-Rotation Curves and Cumulative Ductilities," Portland Cement Association, 1976 (unpublished).

23. Ghosh, S.K., "Program ANYDATA - A General Purpose Plotting Routine," Portland Cement Association, 1976 (unpublished).

24. Czernecki, R.M., "Earthquake Damage to Tall Buildings," Structures Publication No. 359, Department of Civil Engineering, Massachusetts Institute of Technology, January 1973.

25. Gasparini, D., "SIMQKE: A Program for Artificial Motion Generation," Internal Study Report No. 3, Department of Civil Engineering, Massachusetts Institute of Technology, January 1975.

26. Ruiz, P. and Renzien, J., "Probabilistic Study of the Behavior of Structures During Earthquakes," Earthquake Engineering Research Center Report No. EERC 69-3, University of California, Berkeley, March 1969.

27. Blume, J.A., Newmark, N.M. and Corning, L.H., Design of Multistory Reinforced Concrete Buildings for Earthquake Motions, Portland Cement Association, Skokie, Illinois, 1961.

TABLES AND FIGURES

Table 1a - Basic Structure Properties and Variations
Structure ISW 0.8

PROPERTIES	BASIC VALUE OR CHARACTERISTIC	VARIATIONS
STRUCTURAL		
Fundamental period	0.8 seconds	
Number of stories	20	
Height	178.25 ft.	
Weight (for mass computation)	4370 k/wall	
Stiffness parameter EI	6.346×10^{11} k-in^2	
Yield level, M_y	1,000,000 in-k	500,000 750,000 1,000,000 1,500,000 in-k
Yield stiffness ratio, r_y	0.05	0.15
Character of M-θ curve	Decreasing stiffness $\alpha = .10$, $\beta = 0$	
Damping	5% of critical	10% of critical
Stiffness taper $\frac{(EI)\ \text{base}}{(EI)\ \text{top}}$	1.0	
Strength taper $\frac{(M_y)\ \text{base}}{(M_y)\ \text{top}}$	2.0	
Basic fixity condition	Fully fixed	
INPUT MOTION		
Intensity	SI = 1.5 ($SI_{ref.}$)*	1.0 ($SI_{ref.}$)
Frequency characteristics	1940 El Centro, E-W	1940 El Centro, N-S 1952 Taft, S69E Artificial Acc. S1
Duration	10 seconds	

* $SI_{ref.}$ = 5%-damped spectrum intensity - between 0.1 and 3.0 seconds - corresponding to the first 10 seconds of the N-S component of the 1940 El Centro record.

Table 1b - Basic Structure Properties and Variations
Structure ISW 1.4

PROPERTIES	BASIC VALUE OR CHARACTERISTIC	VARIATIONS
STRUCTURAL		
Fundamental period	1.4 seconds	
Number of stories	20	10.40
Height	178.25 ft.	
Weight (for mass computation)	4370 k/wall	
Stiffness parameter EI	2.052×10^{11} k-in^{2*}	
Yield level, M_y	500,000 in-k	750,000 1,000,000 1,500,000 in-k, and elastic
Yield stiffness ratio, r_y	0.05	0.01, 0.15
Character of M-θ curve	Decreasing stiffness $\alpha = .10$, $\beta = 0$	$\alpha = .30$, $\beta = 0.4$, 1.0 and stable loop
Damping	5% of critical	10% of critical
Stiffness taper $\frac{(EI)\ \text{base}}{(EI)\ \text{top}}$	1.0	2.8
Strength taper $\frac{(M_y)\ \text{base}}{(M_y)\ \text{top}}$	2.0	1.0, 3.8
Basic fixity condition	Fully fixed	50% and 75% of fully fixed condition**
INPUT MOTION		
Intensity	$SI = 1.5\ (SI_{ref.})$	0.75 and 1.0 x $(SI_{ref.})$
Frequency characteristics	1940 El Centro, E-W	1971 Holiday Orion, E-W 1971 Pacoima Dam, S16E, Artificial Acc. S1
Duration	10 seconds	20 seconds

* EI = 5.004×10^{11} k-in for stiffness taper 2.8

** Period of 1.4 sec. corresponds to fully fixed condition.

Table 1c - Basic Structure Properties and Variations
Structure ISW 2.0

PROPERTIES	BASIC VALUE OR CHARACTERISTIC	VARIATIONS
STRUCTURAL		
Fundamental period	2.0 seconds	
Number of stories	20	
Height	178.25 ft.	
Weight (for mass computation	4370 k/wall	
Stiffness parameter EI	0.990×10^{11} k-in^2	
Yield level, M_y	500,000 in-k	750,000 1,000,000 in-k and elastic
Yield stiffness ratio, r_y	0.05	0.15
Character of M-θ curve	Decreasing stiffness $\alpha = .10$, $\beta = 0$	
Stiffness taper $\frac{(EI)\ \text{base}}{(EI)\ \text{top}}$	1.0	
Strength taper $\frac{(M_y)\ \text{base}}{(M_y)\ \text{top}}$	2.0	
Basic fixity condition	Fully fixed	
INPUT MOTION		
Intensity	SI = 1.5 ($SI_{ref.}$)	1.0 x ($SI_{ref.}$)
Frequency characteristics	1940 El Centro, E-W	1971 Holiday Orion, E-W
Duration	10 seconds	

Table 1d - Basic Structure Properties and Variations
Structure ISW 2.4

PROPERTIES	BASIC VALUE OR CHARACTERISTIC	VARIATIONS
STRUCTURAL		
Fundamental period	2.4 seconds	
Number of stories	20	
Height	178.25 ft.	
Weight (for mass computation)	4370 k/wall	
Stiffness parameter EI	0.684×10^{11} k-in^2	
Yield level, M_y	500,000 in-k	750,000 1,000,000 1,500,000 in-k
Yield stiffness ratio, r_y	0.05	
Character of M-θ curve	Decreasing stiffness $\alpha = .10$, $\beta = 0$	
Damping	5% of critical	10% of critical
Stiffness taper $\frac{(EI)\ \text{base}}{(EI)\ \text{top}}$	1.0	
Strength taper $\frac{(M_y)\ \text{base}}{(M_y)\ \text{top}}$	2.0	
Basic fixity condition	Fully fixed	
INPUT MOTION		
Intensity	$SI = 1.5\ (SI_{ref.})$	
Frequency characteristics	1940 El Centro, E-W	
Duration	10 seconds	

Table 2 - Summary of Input Motions Considered in Study of Frequency Characteristics

Set	Structure Period, T_1 (and M_y)	Input Motion	Frequency Content Characterization#	Intensity Normalization Factor*
a	1.4 sec. (500,000 in-k)	1971 Pacoima Dam, S16E component	Peaking (0)	0.59
		1971 Holiday Inn Orion, E-W component	Peaking (+)	3.22
		Artificial Accelerogram, S1	Broad band	1.65
		1940 El Centro, E-W component	Broad band, ascending	1.88
b	0.8 sec. (1,500,000 in-k)	1940 El Centro, N-S component	Peaking (0)	1.50
		1940 El Centro, E-W component	Broad band, ascending	1.88
c	2.0 sec. (500,000 in-k)	1971 Holiday Inn, Orion, E-W component	Peaking (-)	3.22
		1940 El Centro, E-W component	Broad band, ascending	1.88
		Artificial Accelerogram, S1	Broad band	1.65

* Calculated to yield a 5%-damped spectrum intensity (for the range 0.1 to 3.0 sec.) equal to 1.5 times the reference spectrum intensity, $SI_{ref.}$, i.e., the 5%-damped spectrum intensity of the N-S component of the 1940 El Centro record. ($SI_{ref.}$ = 70.15 in.) In all cases, only a 10-second duration of each accelerogram was considered.

\# Relative to the initial fundamental period, T_1, of the structure considered.

Table 3 - Structure Properties and Earthquake Intensity Levels Considered

Set	Fundamental Period, T_1	Yield Level, M_y	Levels of Intensity Used*
a	1.4 sec.	500,000 in-k	0.75, 1.0, 1.5
b	0.8 sec.	1,000,000 in-k	1.0, 1.5
c	2.0 sec.	500,000 in-k	1.0, 1.5

*In terms of $SI_{ref.}$

Table 4 - Summary of Structural Parameters

PARAMETER	VALUES OF PARAMETER CONSIDERED	REMARKS
Fundamental period, T_1 (sec.)	(a) 0.8, 1.4, 2.0, 2.4	M_y = 500,000 in-k
	(b) 0.8, 1.4, 2.0, 2.4	M_y = 750,000 in-k
	(c) 0.8, 1.4, 2.0	M_y = 1,000,000 in-k
	(d) 0.8, 1.4, 2.4	M_y = 1,500,000 in-k (r_y = 0.05)
Yield level, M_y (in-k)	(a) 500,000, 1,000,000, 1,500,000	T_1 = 0.8 sec.
	(b) 500,000, 750,000, 1,000,000 1,500,000 (Elastic)	T_1 = 1.4 sec.
	(c) 500,000, 750,000, 1,000,000	T_1 = 2.0 sec.
Yield Stiffness ratio, r_y	(a) 0.05, 0.15	T_1 = 0.8 sec.; M_y = 1,000,000 in-k
	(b) 0.01, 0.05, 0.15	T_1 = 1.4 sec.; M_y = 500,000 in-k
	(c) 0.05, 0.15	T_1 = 2.0 sec.; M_y = 500,000 in-k

Table 4 (cont'd.) - Summary of Structural Parameters

PARAMETER	VALUES OF PARAMETER CONSIDERED	REMARKS
Parameters characterizing shape of M-θ hysteretic loop: Takeda model parameters α and β	(a) α = 0.10, 0.30	T_1 = 1.4 sec. M_y = 500,000 in-k β = 0
	(b) β = 0, 0.4, 1.0 & stable loop	T_1 = 1.4 sec. M_y = 500,000 in-k α = 0.10
	(c) β = 0, 0.4, 1.0 & stable loop	T_1 = 0.8 sec. M_y = 1,000,000 in-k α = 0.10
Viscous damping (percent of critical)	(a) 5, 10	T_1 = 1.4 sec. M_y = 500,000 in-k
	(b) 5, 10	T_1 = 0.8 sec. M_y = 1,000,000 in-k
Stiffness taper $\frac{EI\ (base)}{EI\ (top)}$	(a) 1.0, 2.8	T_1 = 1.4 sec. M_y = 500,000 in-k
Strength taper $\frac{M_y\ (base)}{M_y\ (top)}$	(a) 1.0, 2.0, 3.8	T_1 = 1.4 sec. M_y (base) = 500,000 in-k

Table 4 (cont'd.) - Summary of Structural Parameters

PARAMETER	VALUES OF PARAMETER CONSIDERED	REMARKS
Base Fixity condition (percent of full fixity)	(a) 50, 75, 100	T_1 = 1.4 sec.* M_y = 500,000 in-k
	(b) 50, 75, 100	T_1 = 0.8 sec.* M_y = 1,500,000 in-k
Number of stories	(a) 10, 20, 30, 40	T_1 = 1.4 sec. M_y = 1,500,000 in-k
	(b) 10, 20, 30, 40	T_1 = 1.4 sec. M_y adjusted to yield ductility ratios $\sim$ 4 - 6

*Refers to the fully-fixed condition.

Table 5 - Effect of Fundamental Period and Yield Level on Dynamic Response of 20-Story Isolated Structural Walls

Earthquake Input: 1940 El Centro, E-W Component (10 sec., SI = 1.5 $SI_{ref.}$)

Yield Level, M_y (in-kips)	Initial Fundamental Period, T_1 (sec.) 0.8	1.4	2.0	2.4
Max. Top Displacement (in.)				
500,000	8.3	15.0	20.5	25.1
750,000	4.7	10.9	17.0	23.7
1,000,000	4.0	9.2	20.0	22.4
1,500,000	4.5	11.0	23.1	24.5 (E)*
Elastic	5.2	11.0	23.2	24.5
Max. Interstory Displacement (in.)				
500,000	0.47	0.86	1.24	1.56
750,000	0.28	0.65	1.12	1.51
1,000,000	0.24	0.58	1.25	1.51
1,500,000	0.29	0.75	1.57	1.76 (E)
Elastic	0.35	0.76	1.57	1.76
Max. Horizontal Shear at Base (kips)				
500,000	1030	830	1050	1060
750,000	1190	950	1070	1179
1,000,000	1330	1190	1120	1240
1,500,000	1610	1300	1150	1300 (E)
Elastic	1700	1420	1240	1300

*Elastic, i.e., structure did not yield.

Table 5 (cont'd.) - Effect of Fundamental Period and Yield Level on Dynamic Response of 20-Story Isolated Structural Walls

Earthquake Input: 1940 El Centro, E-W Component (10 sec., SI = 1.5 $SI_{ref.}$)

Yield Level, M_y (in-k)	Initial Fundamental Period, T_1 (sec.)			
	0.8	1.4	2.0	2.4
Moment at Base (in-k)				
500,000	813,000	711,000	651,000	648,000
750,000	996,000	941,000	862,000	903,000
1,000,000	1,214,000	1,149,000	1,126,000	1,107,000
1,500,000	1,701,000	1,583,000	1,609,000	1,519,000 (E)
Elastic	2,419,000	1,677,000	1,782,000	1,519,000
Rotational Ductility Ratio				
500,000	13.6	8.1	6.2	5.7
750,000	6.3	4.9	2.9	3.92
1,000,000	4.1	2.9	2.5	2.1
1,500,000	2.6	1.1	1.4	1.0
Cum. Plastic Hinge Rotation at Base (radians)				
500,000	1.06×10^{-2}	1.50×10^{-2}	1.76×10^{-2}	2.31×10^{-2}
750,000	$.92\times10^{-2}$	1.01×10^{-2}	1.13×10^{-2}	1.69×10^{-2}
1,000,000	0.73×10^{-2}	0.89×10^{-2}	$.66\times10^{-2}$	1.02×10^{-2}
1,500,000	$.50\times10^{-2}$	0.04×10^{-2}	$.09\times10^{-2}$	0.

Table 6 - Relative Changes in Response Quantities Due to Changes in Selected Parameters

Parameter	Practical Range	Parameter Values		Normalized Change in Response			
		Considered	% of Range	Top dis-placement	Base Shear	Rotational Ductility	Remarks
Fundamental period, T_1 (sec.)	0.8 - 2.4 sec.	0.8	0	0	0	0	M_y = 500,000 in-k
		1.4	38	0.79	0.14	0.32	
		2.0	75	1.46	0.01	0.48	
		2.4	100	2.01	0.02	0.52	
		0.8	0	0	0	0	M_y = 750,000 in-k
		1.4	38	1.29	0.18	0.22	
		2.0	75	3.58	0.10	0.54	
		2.4	100	5.00	0	0.37	
		0.8	0	0	0	0	M_y = 1,000,000 in-k
		1.4	38	1.28	0.11	0.3	
		2.0	75	3.94	0.16	0.4	
		2.4	100	4.55	0.07	0.5	
		0.8	0	0	0	0	M_y = 1,500,000 in-k
		1.4	0.38	1.45	0.19	0.58	
		2.0	75	4.13	0.28	0.46	
		2.4	100	4.45	0.19	0.63	
Yield moment M_y	.75 - 1.5 (10^6 in-k)	0.75	0	0	0	0	T_1 = 0.8 sec.
		1.00	33	0.15	0.16	0.34	
		1.50	100	0.11	0.32	0.59	
		0.75	0	0	0.16	0	T_1 = 1.4 sec.
		1.00	33	0.16	0.08	0.41	
		1.50	100	0.01	0.33	0.77	
	0.5-1.5 (10^6 in-k)	0.5	0	0	0	0	T_1 = 2.0 sec.
		0.75	25	0.17	0.32	0.53	
		1.0	50	0.03	0.47	0.60	
		1.5	100	0.13	0.63	0.77	
	0.5-1.0 (10^6 in-k)	0.5	0	0	0	0	T_1 = 2.4 sec.
		0.75	50	0.06	0.25	0.31	
		1.00	100	0.11	0.41	0.63	

Table 6 (cont'd.) - Relative Changes in Response Quantities Due to Changes in Selected Parameters

Yield stiffness ratio, r_y	0.01-0.20	0.01	0	0	0	0	T_1 = 1.4 sec. M_y = 500,000 in-k
		0.05	21	0.06	0.04	0.44	
		0.15	74	0.24	0.08	0.65	
Damping	0.02-0.15 of the critical	0.02	0	0	0	0	
		0.05	23	0.07	0.04	0.04	
		0.10	62	0.17	0.11	0.11	
Stiffness taper	1.0-2.8	1.0	0	0	0	0	
		2.8	100	0.25	0.22	0.62	
Strength taper	1.0-3.76	1.00	0	0	0	0	
		2.05	28	0.03	0.03	0.05	
		3.76	100	0.04	0	0.07	
Base fixity	75% - 100%	75	0	0	0	0	T_1 = 1.4 sec. M = 500,000 in-k
		100	100	0.18	0.03	0.05	
		75	0	0	0	0	T_1 = 0.8 sec. M_y = 1,500,000 in-k
		100	100	0.45	0.02	0.31	
Unloading parameter, α	0.1-0.3	0.1	0	0	0	0	T_1 = 1.4 sec. M_y = 500,000 in-k
		0.3	100	0.02	0	0.01	
Reloading parameter, β	0.0-1.0	0	0	0	0	0	
		0.4	40	0.02	0	0.10	
		1.0	100	0.12	0	0	
Ground motion duration	10 - 20 sec.	10	0	0	0	0	T_1 = 1.4 sec. M_y = 500,000 in-k
		20	100	0.21	0.07	0.22	
Ground motion intensity	0.75-1.5 $(SI)_{ref}$	0.75	0	0	0	0	T_1 = 1.4 sec. M_y = 500,000 in-k
		1.00	33	0.58	0.09	0.7	
		1.50	100	2.25	0.40	1.11	
		1.00	33	0.21	0.22	0.41	T_1 = 0.8 sec. M_y = 1,000,000 in-k
		1.50	100	0.63	0.67	1.24	

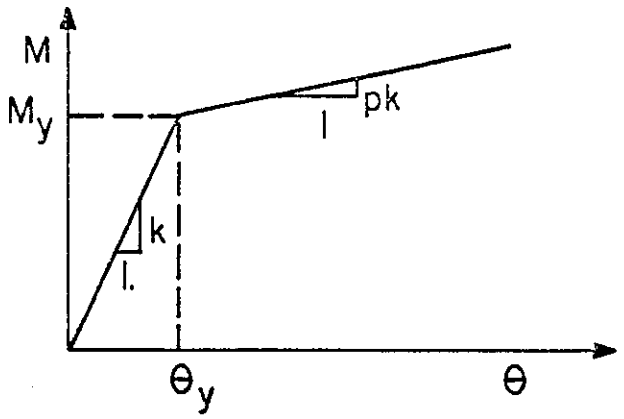

Fig. 1 Moment - Rotation Relationship

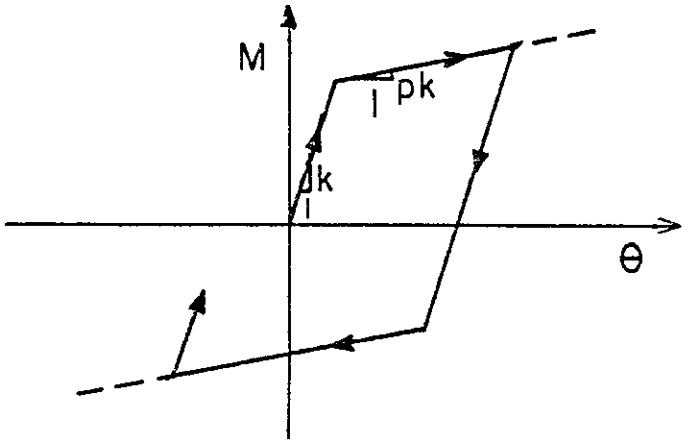

Fig. 2a Stable Hysteretic Loop

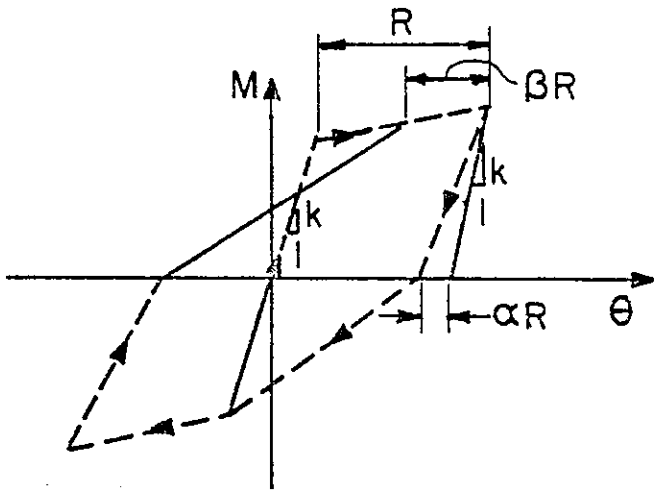

Fig. 2b Decreasing Stiffness Hysteretic Loop

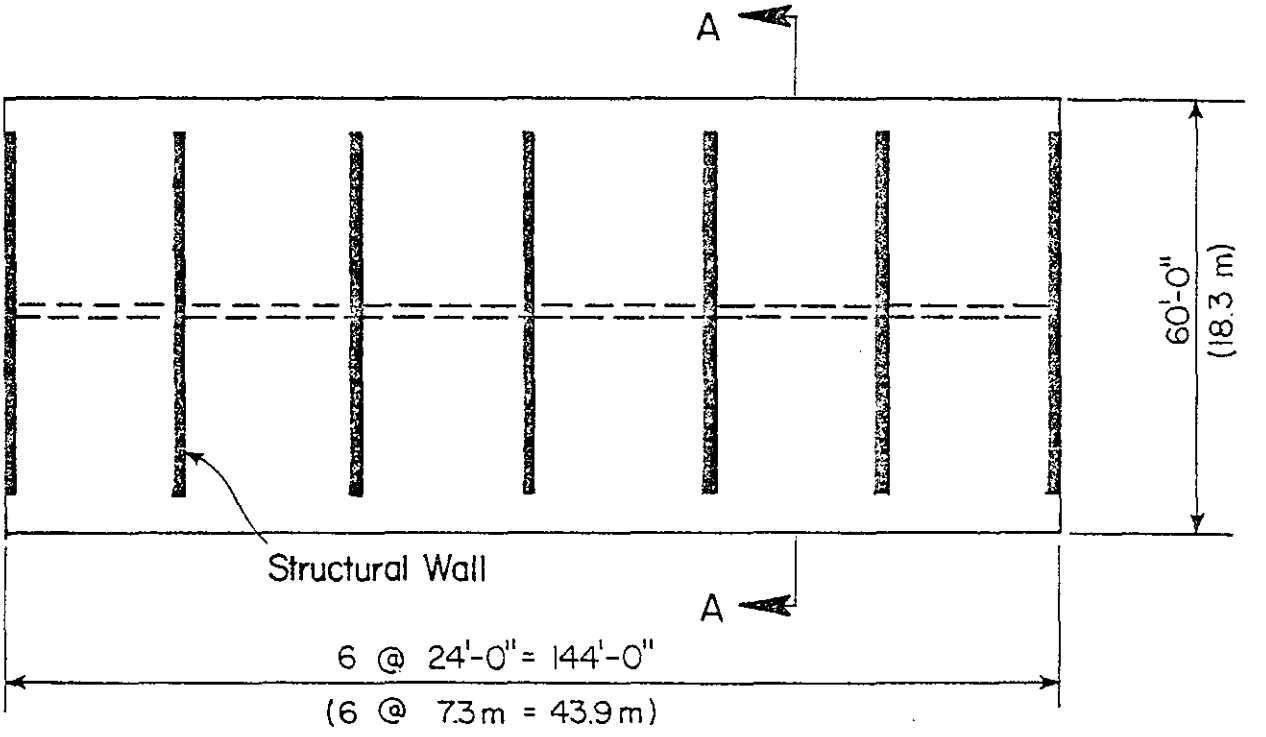

PLAN

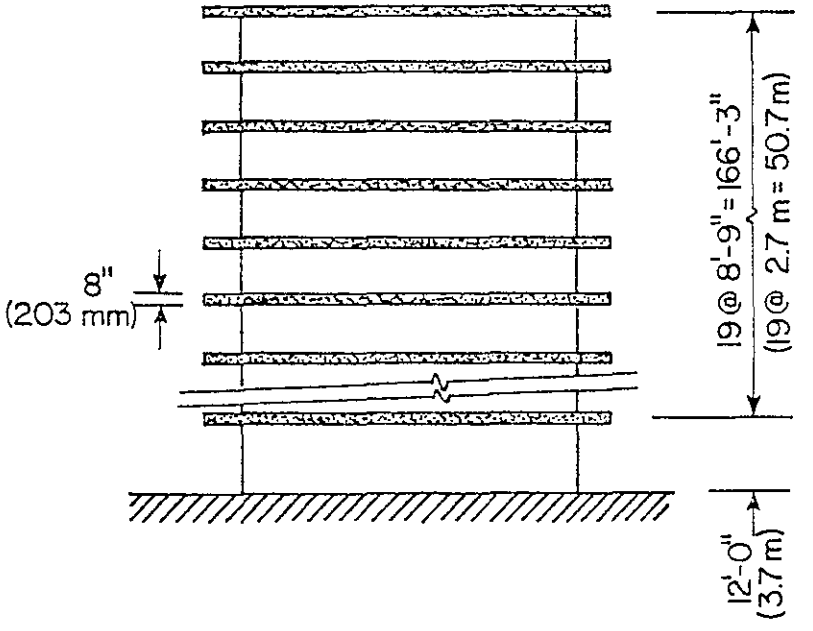

SECTION A-A

Fig. 3 Twenty Story Building with Isolated Structural Walls

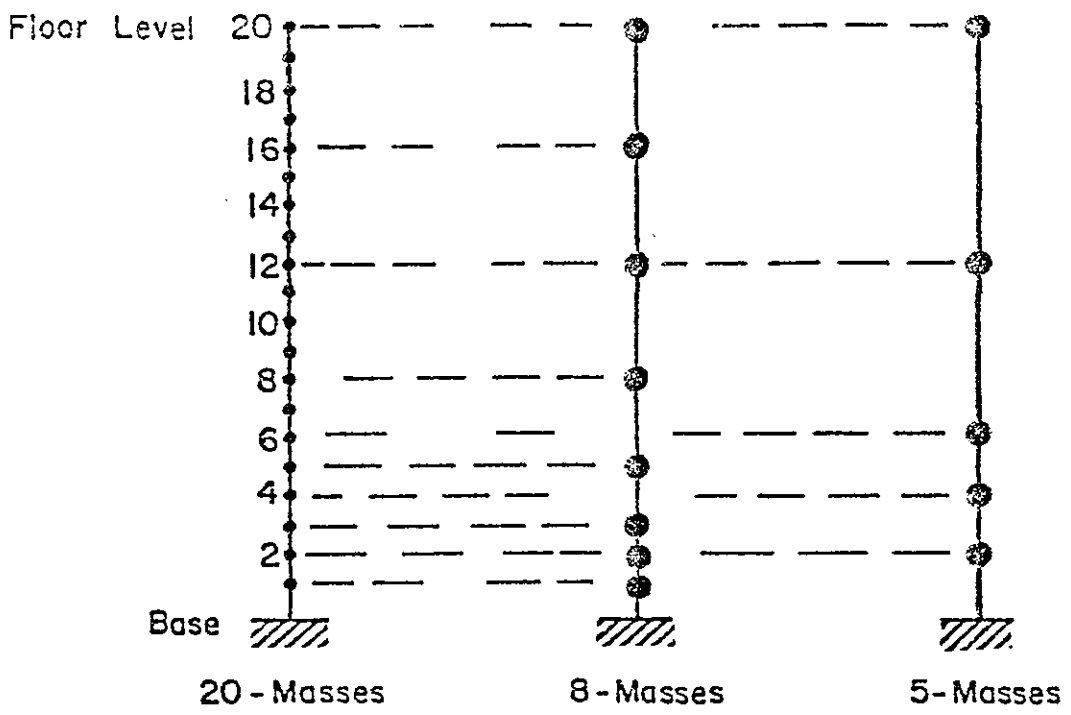

Fig. 4 Preliminary Models for 20 Story Building

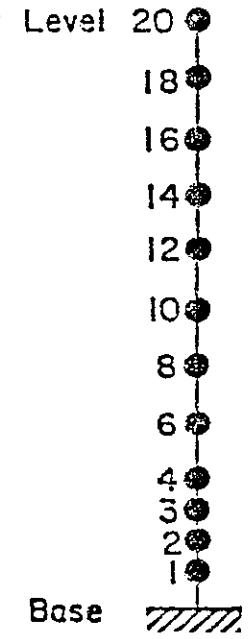

Fig. 5 Final Model - 12 Masses

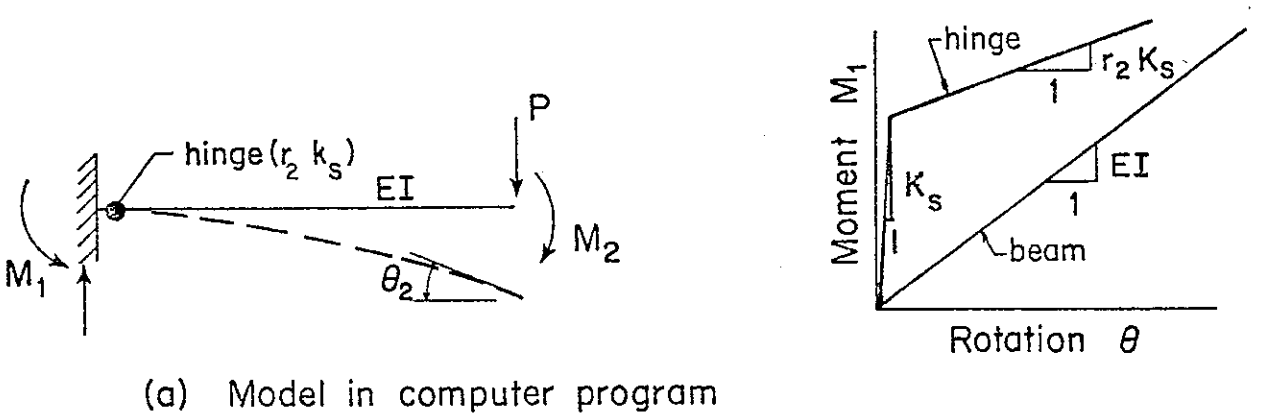

(a) Model in computer program

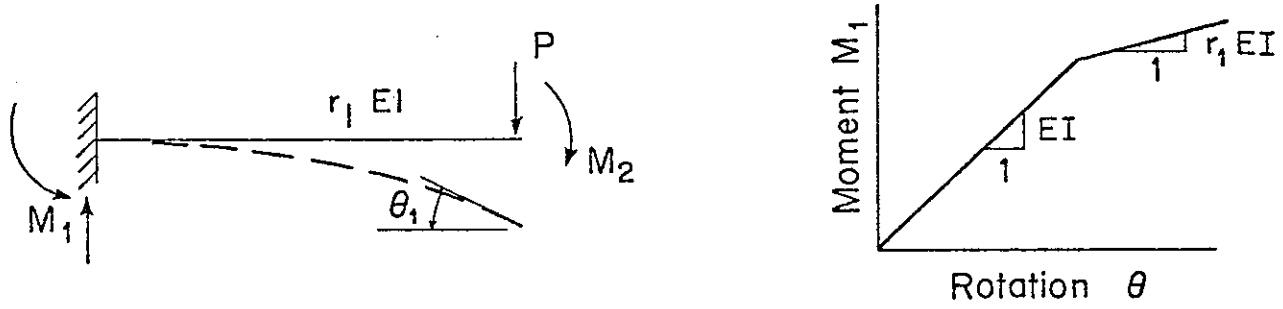

(b) Bilinear element

Fig. 6 Computer Model of Bilinear Element (After Yield)

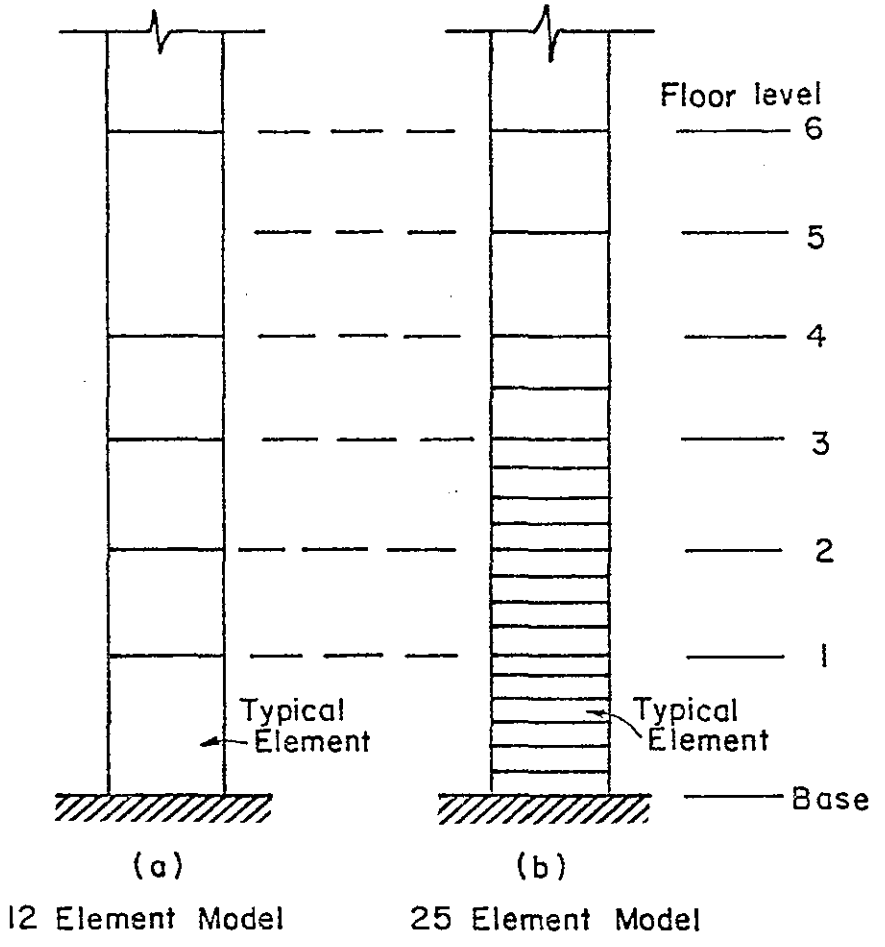

Fig. 7 Models for Lower Portion of Structural Wall

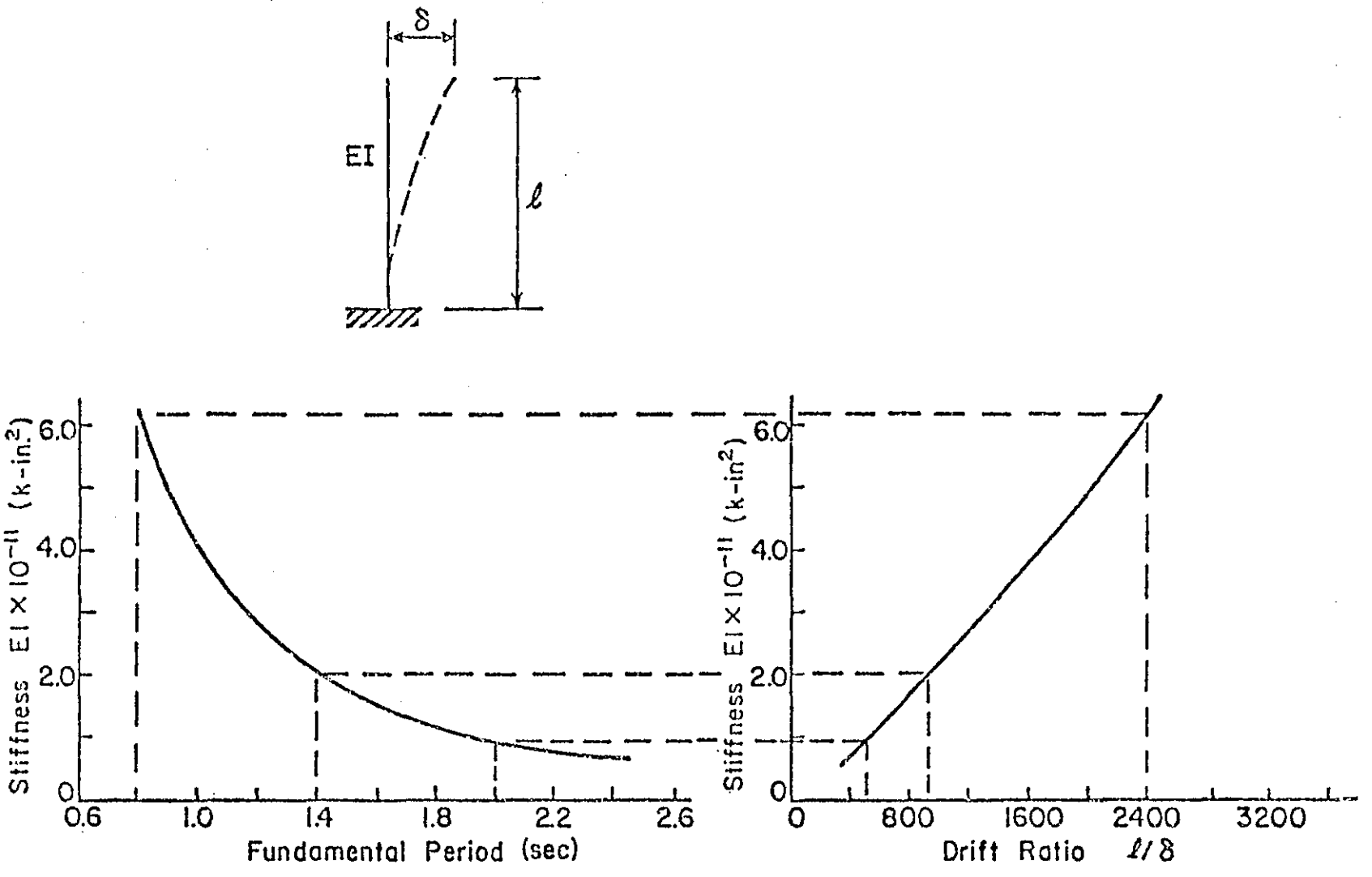

Fig. 8 Fundamental Period - Stiffness - Drift Relationship

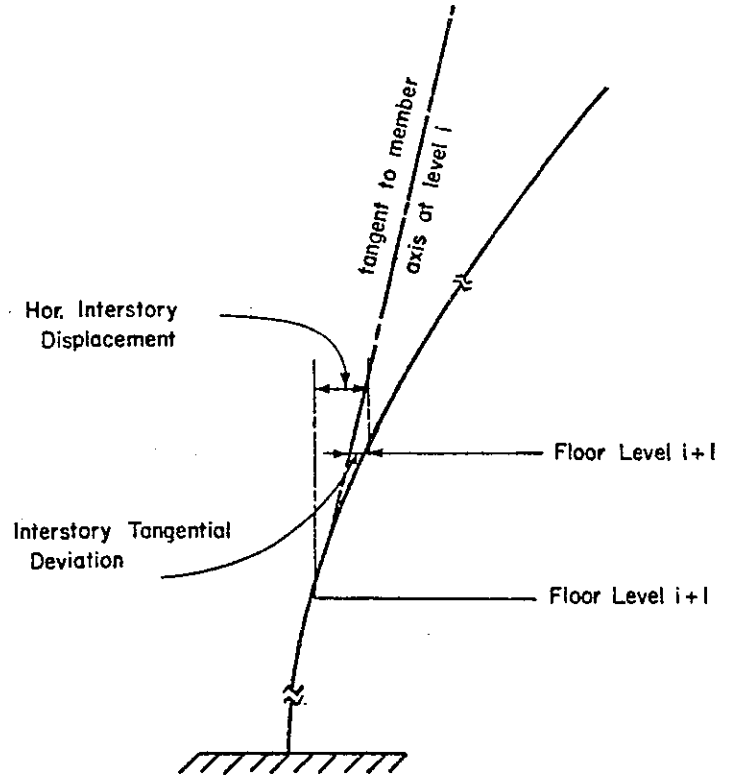

Fig. 9 Illustrating Tangential Deviation

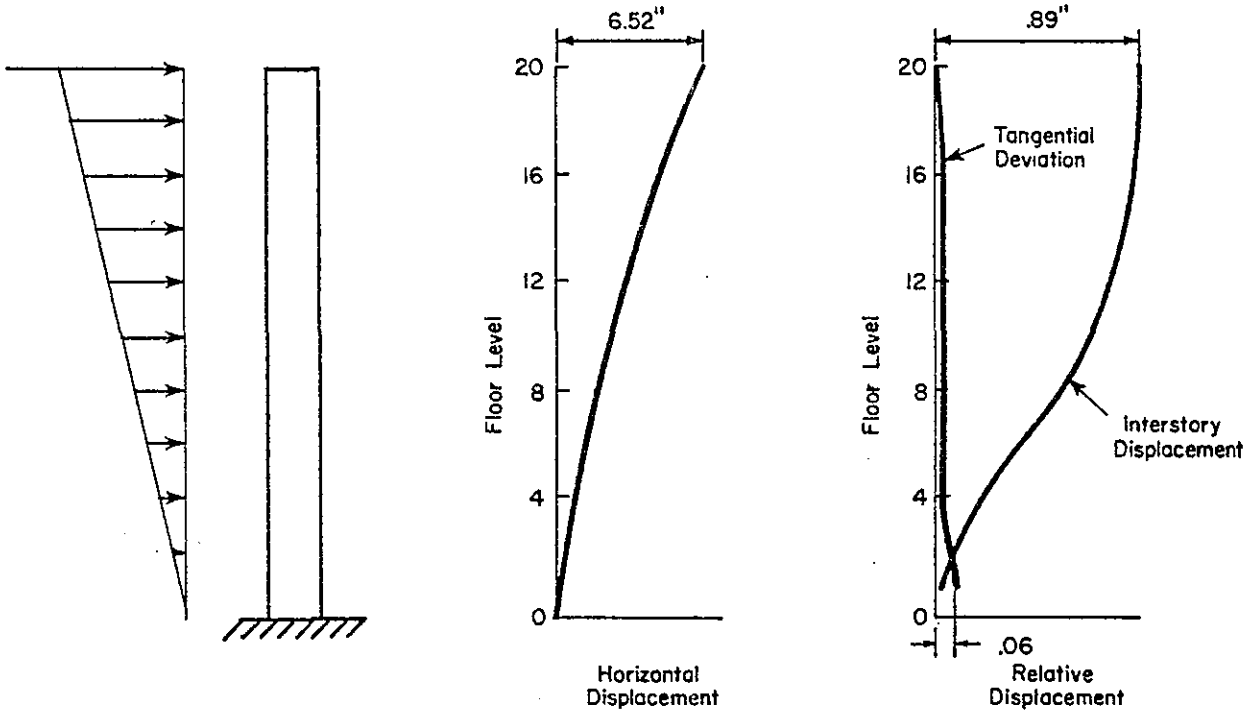

Fig. 10 Tengential Deviations versus Interstory Displacement

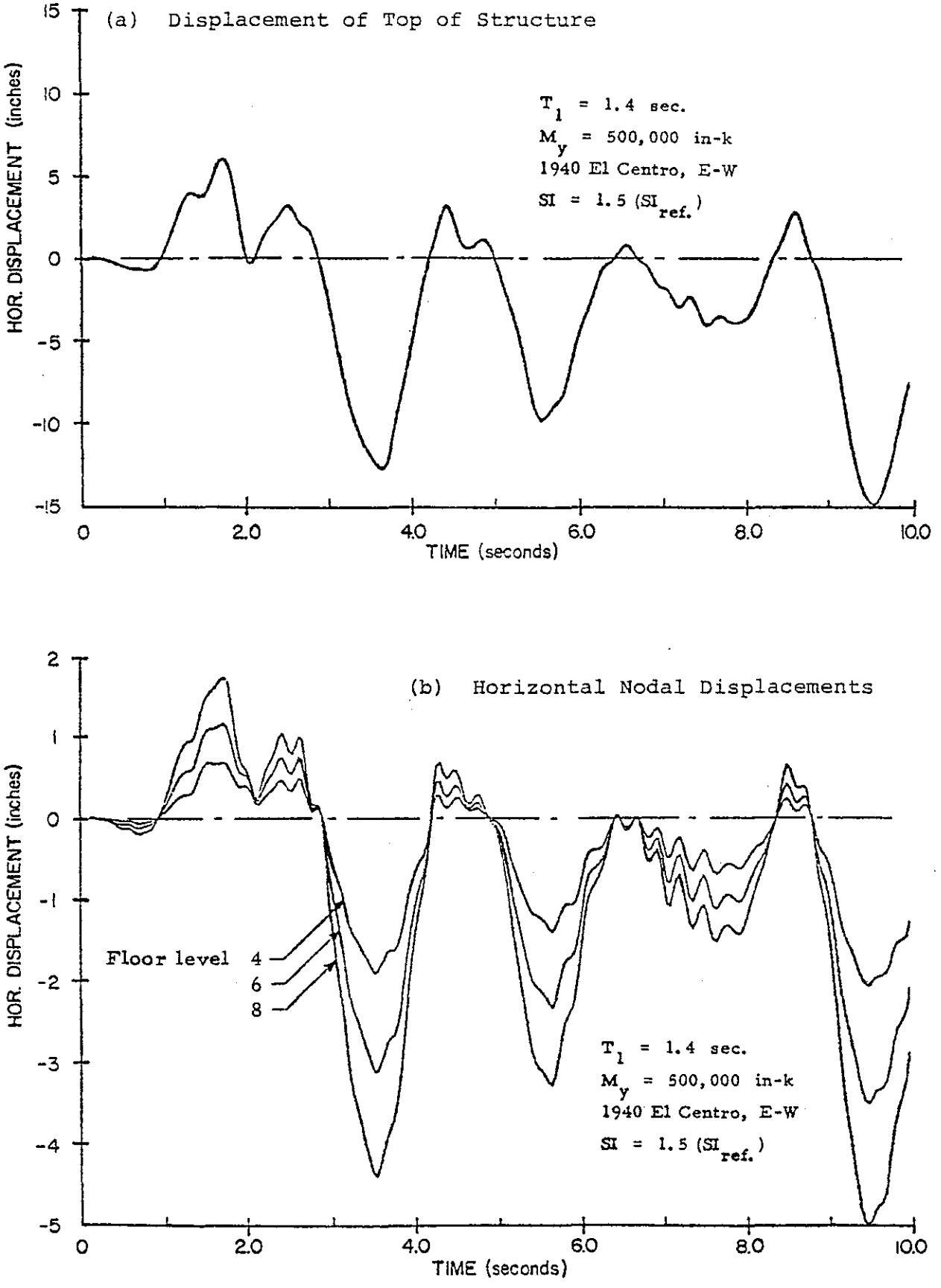

Fig. 11 Time Histories of Horizontal Displacements - Bldg. ISW 1.4

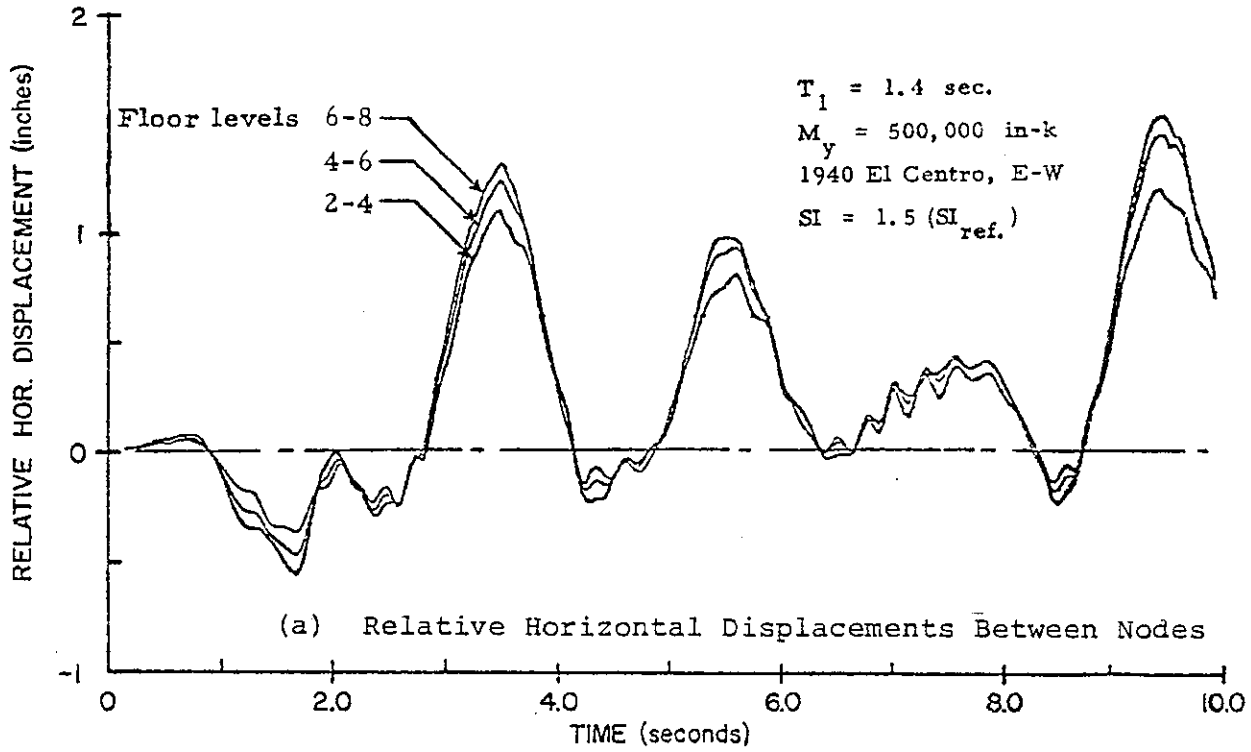

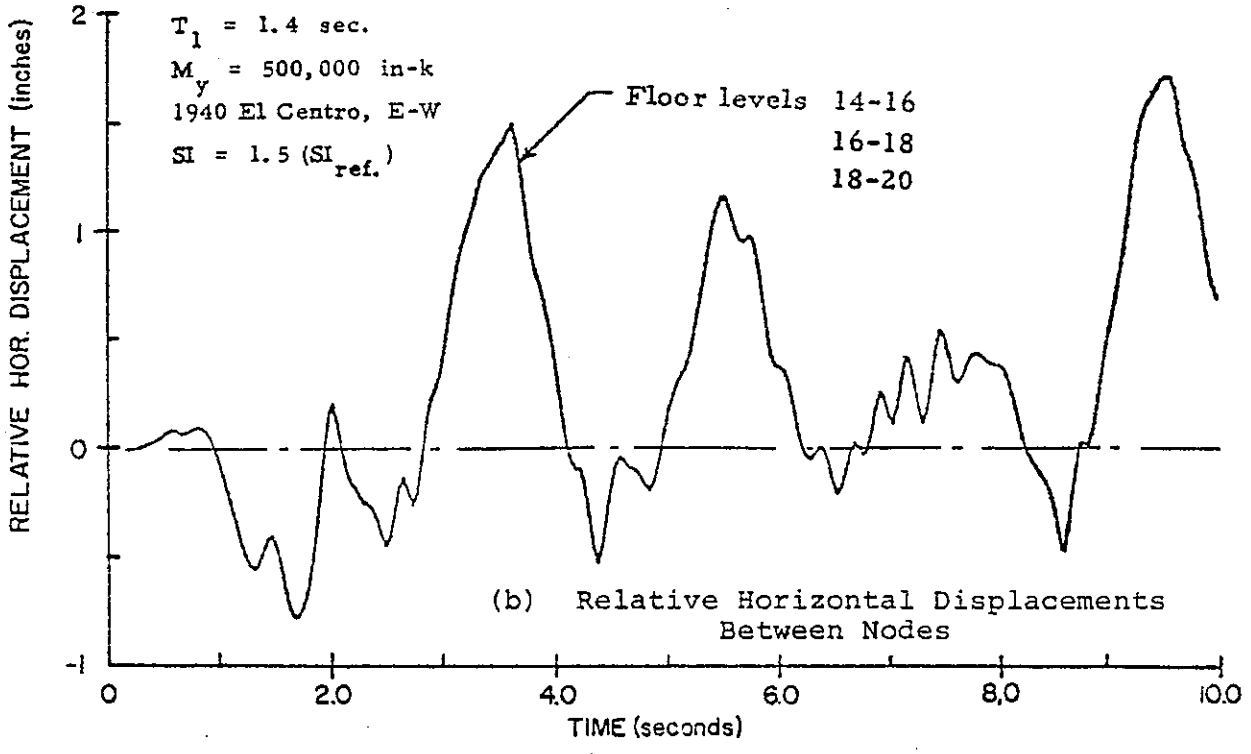

Fig. 12 Time Histories of Relative Horizontal Displacement -- Bldg. ISW 1.4

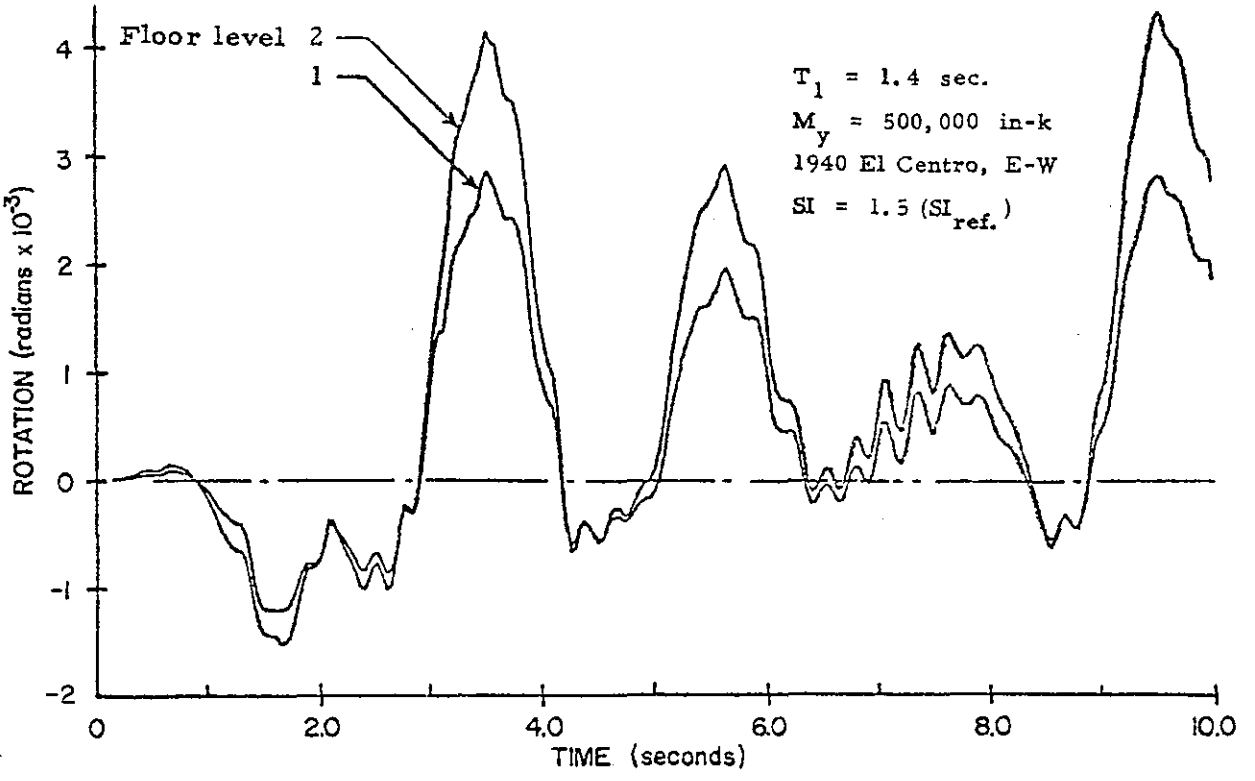

Fig. 13 Time Histories of Nodal Rotations - Bldg. ISW 1.4

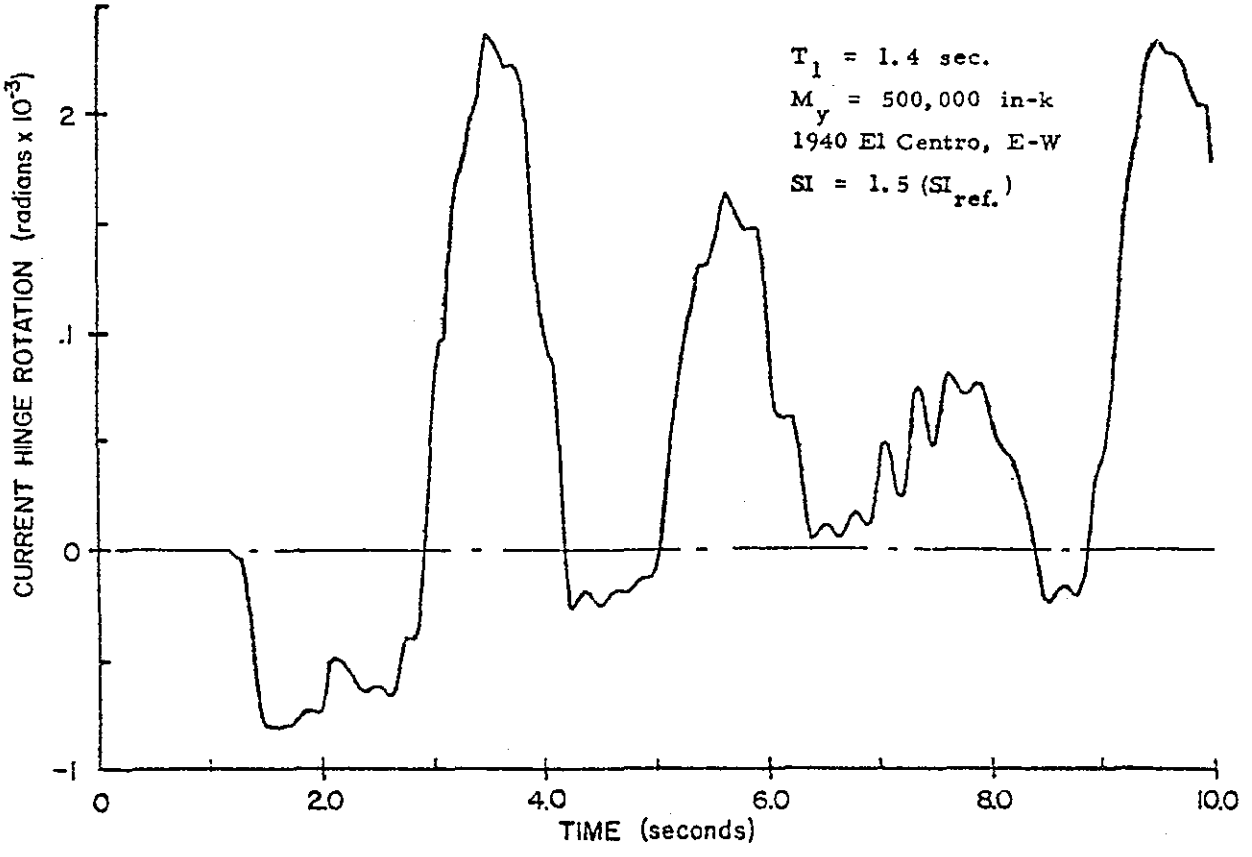

Fig. 14 Time History of Plastic Hinge Rotation at Base - Bldg. ISW 1.4

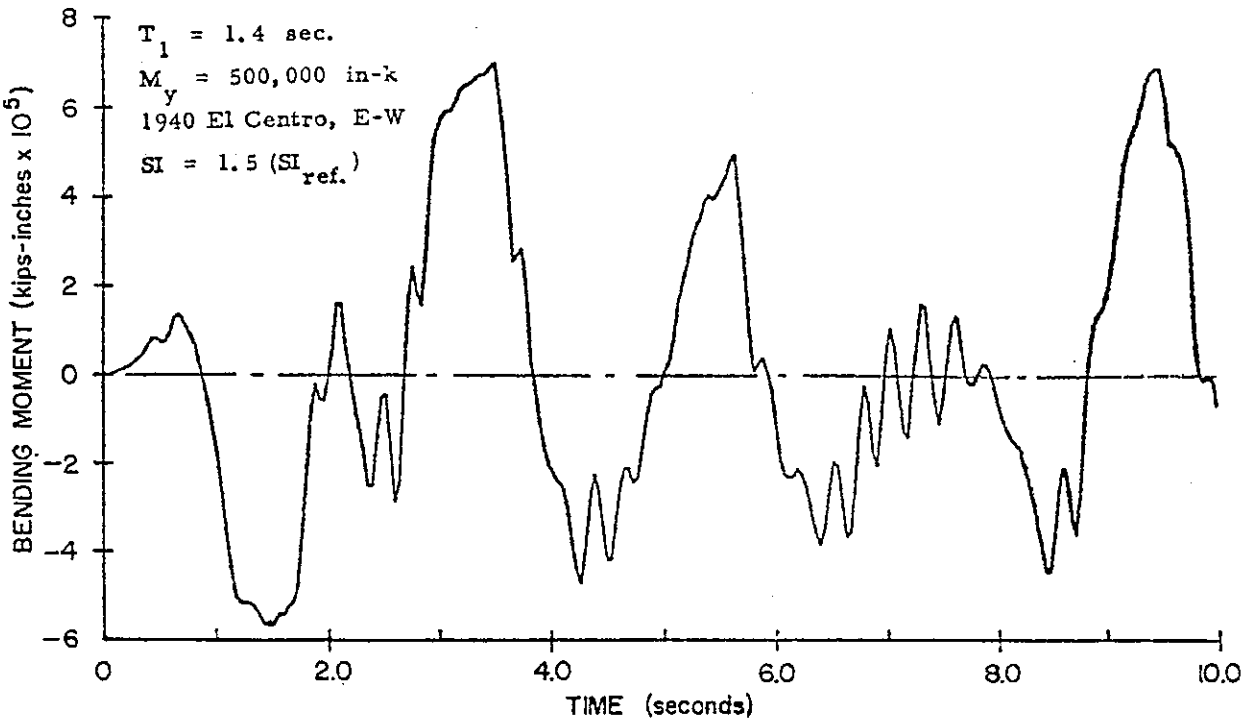

Fig. 15 Time History of Bending Moment at Base - Bldg. ISW 1.4

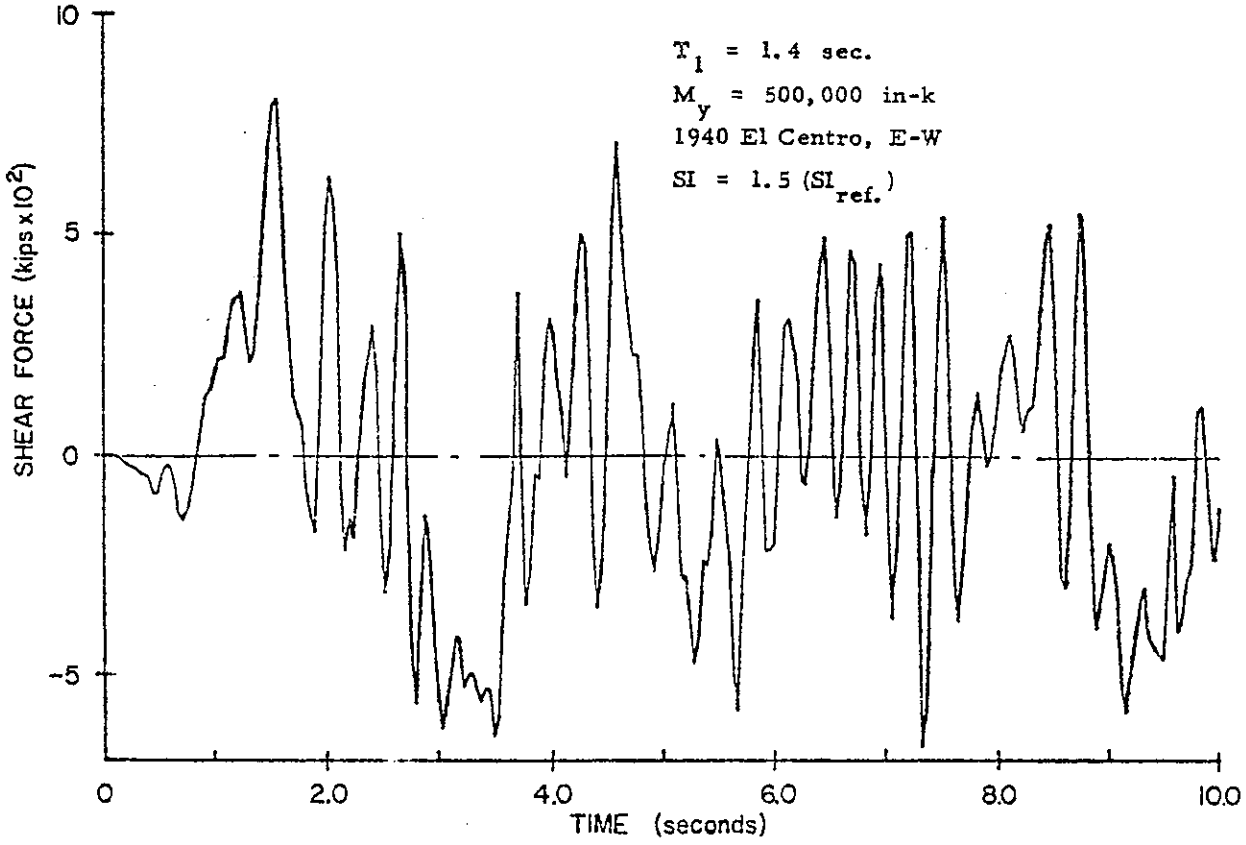

Fig. 16 Time History of Horizontal Shear at Base - Bldg. ISW 1.4

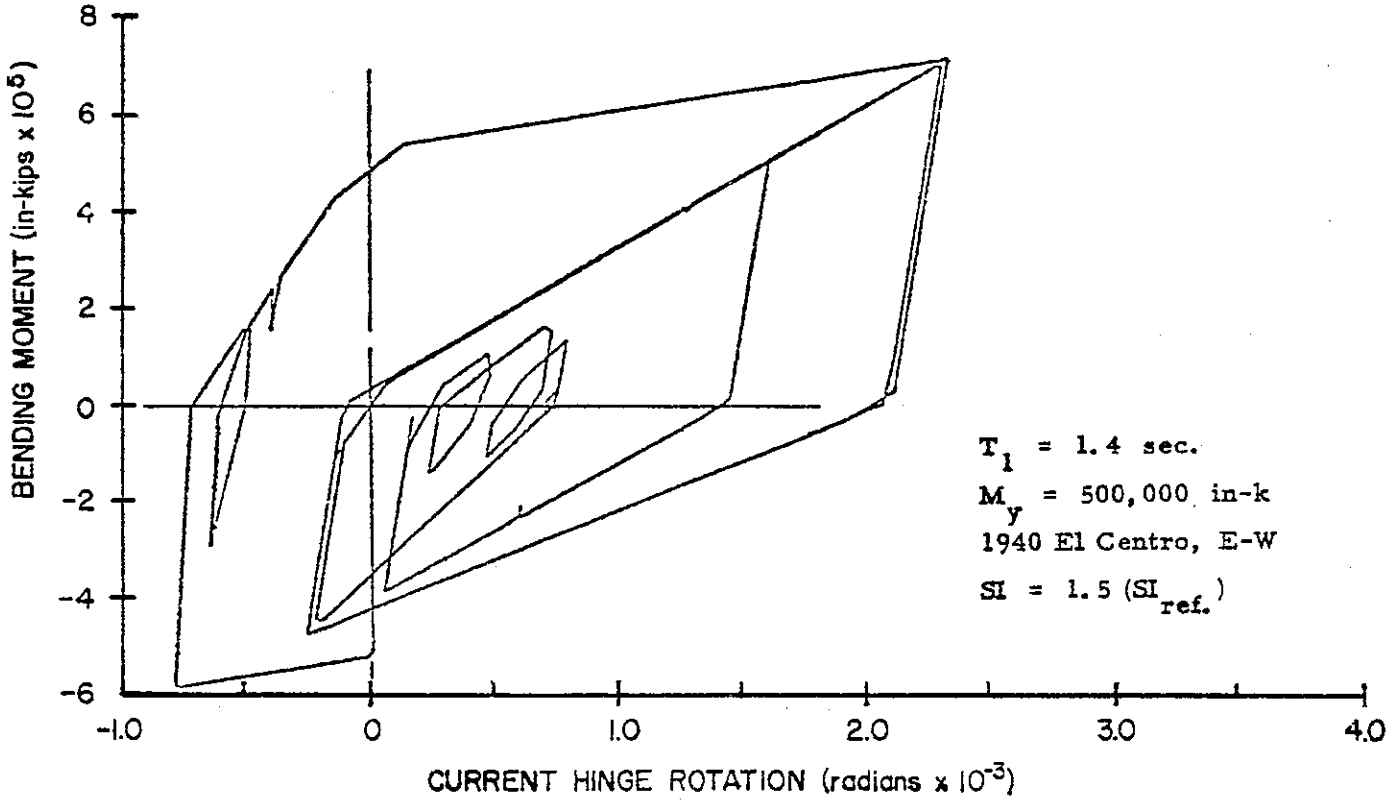

Fig. 17 Moment-Plastic Hinge Rotation Relationship - Bldg. ISW 1.4

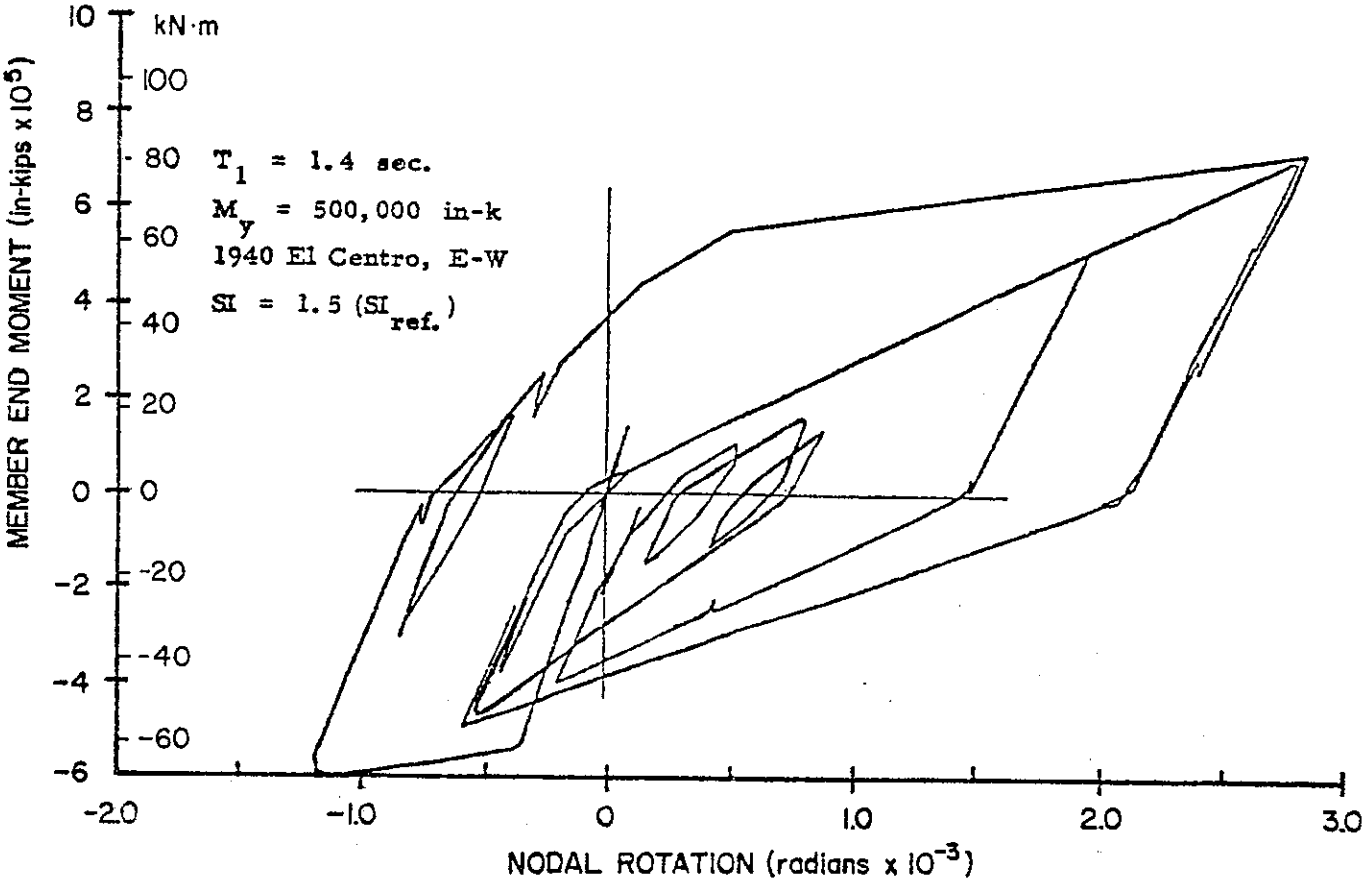

Fig. 18 Moment-Nodal Rotation Relationship - Bldg. ISW 1.4

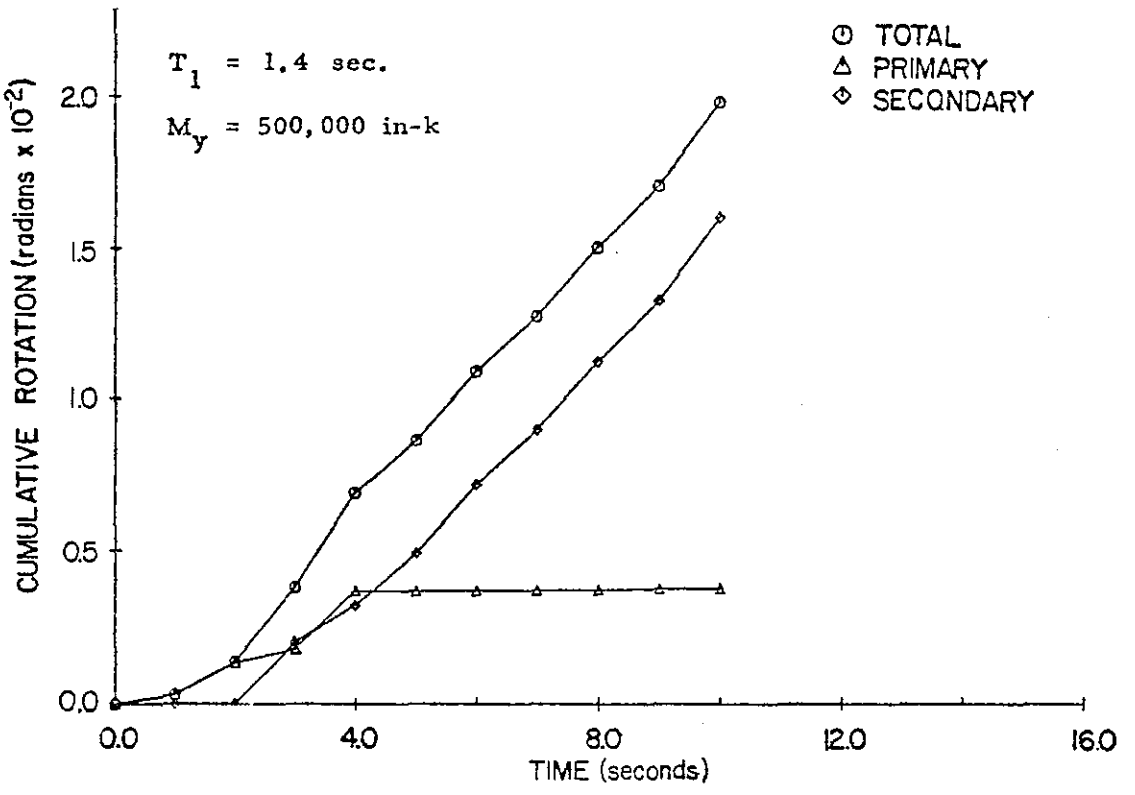

Fig. 19 Cumulative Nodal Rotations versus Time for Node at First Story Level - Bldg. ISW 1.4

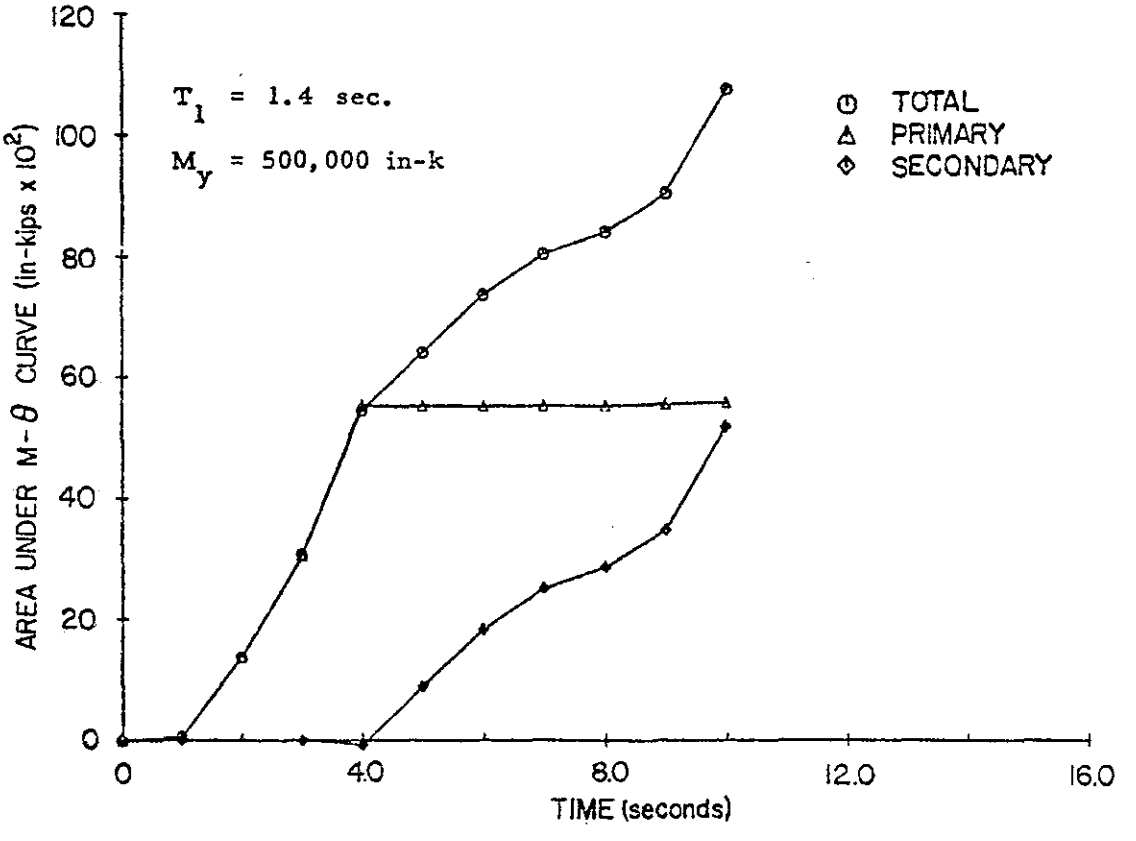

Fig. 20 Cumulative Rotational Energy versus Time for Node at First Floor Level - Structure ISW 1.4

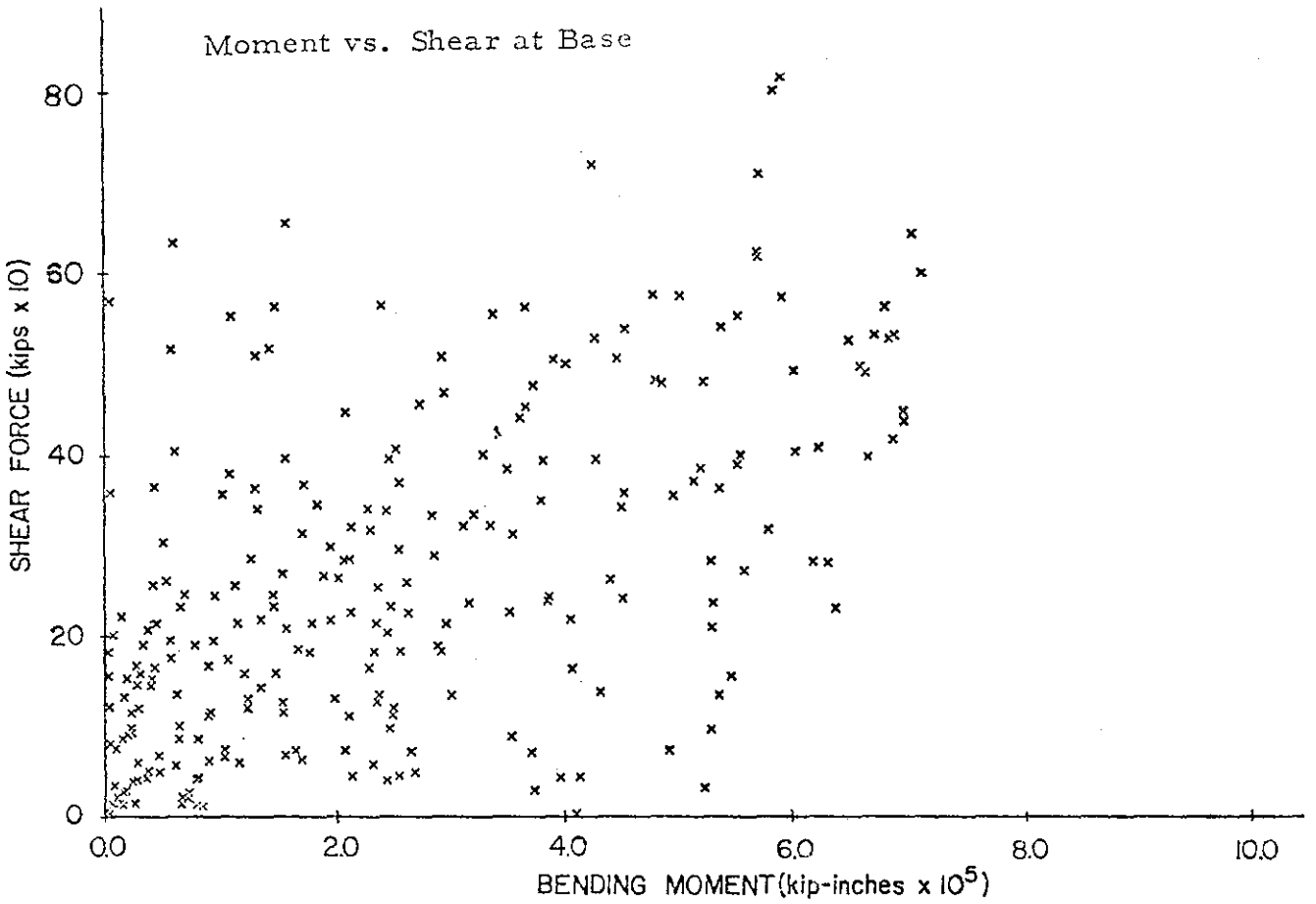

Fig. 21 Simultaneous Moment and Shear Values at Base at Each Time Interval During Response Bldg. ISW 1.4

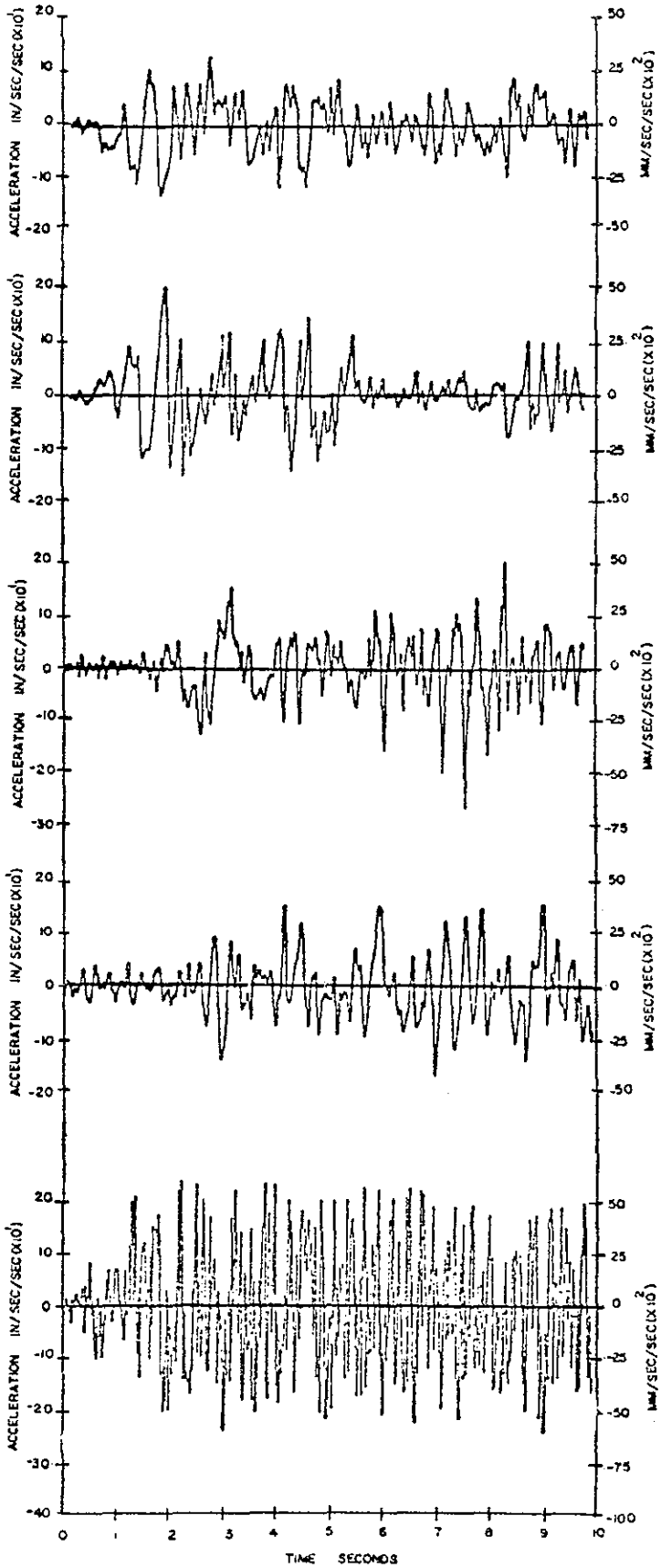

1940 El Centro, E-W
x 1.88

1940 El Centro, N-S
x 1.50

1971 Pacoima Dam, S16E
x 0.594

1971 Holiday Orion, E-W
x 3.22

Artificial Accelerogram, SI
x 1.66

Fig. 22 Ten-Second Duration Normalized Accelerograms

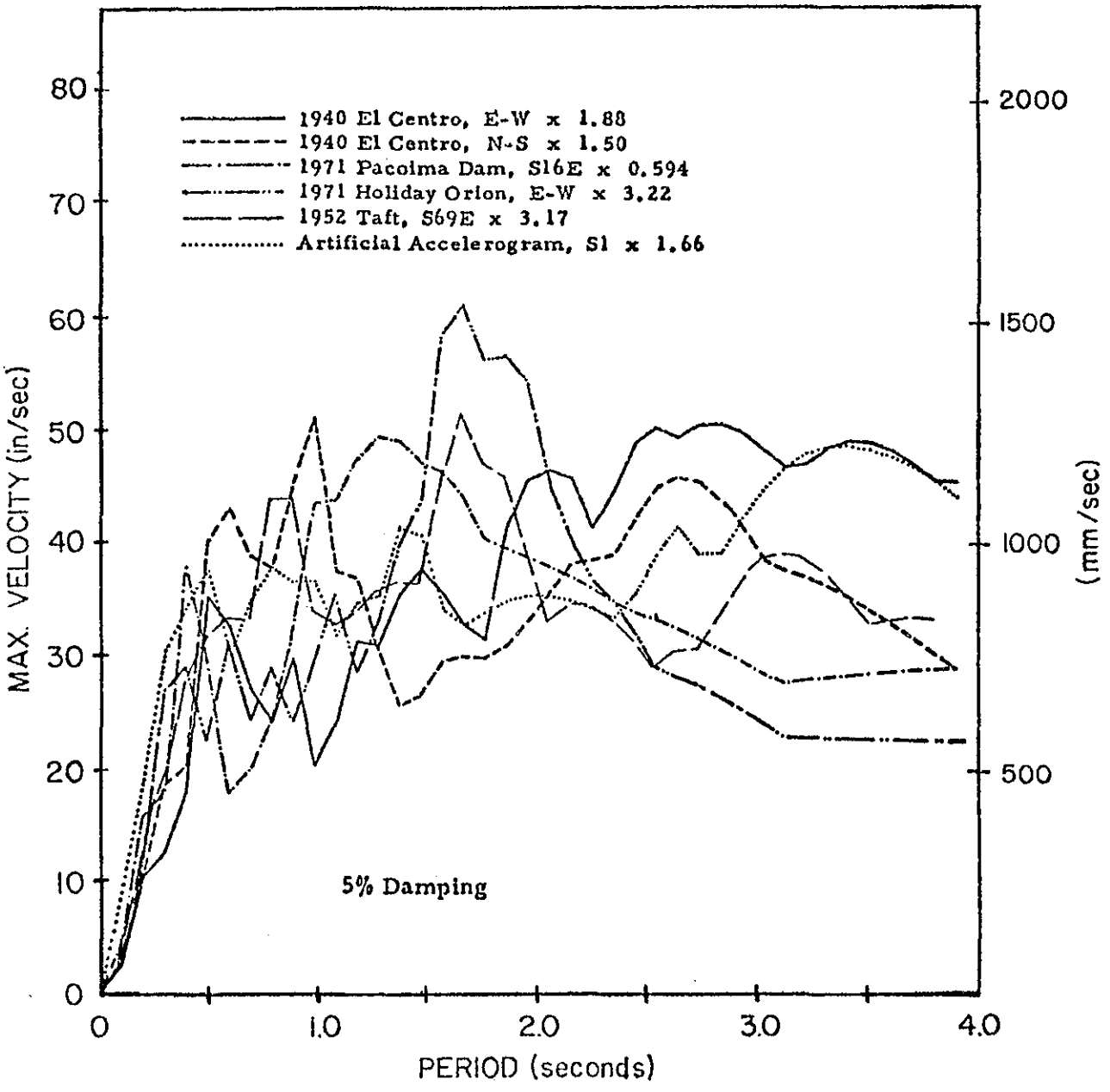

Fig. 23 Relative Velocity Response Spectra for First Ten-Seconds of Normalized Input Motions

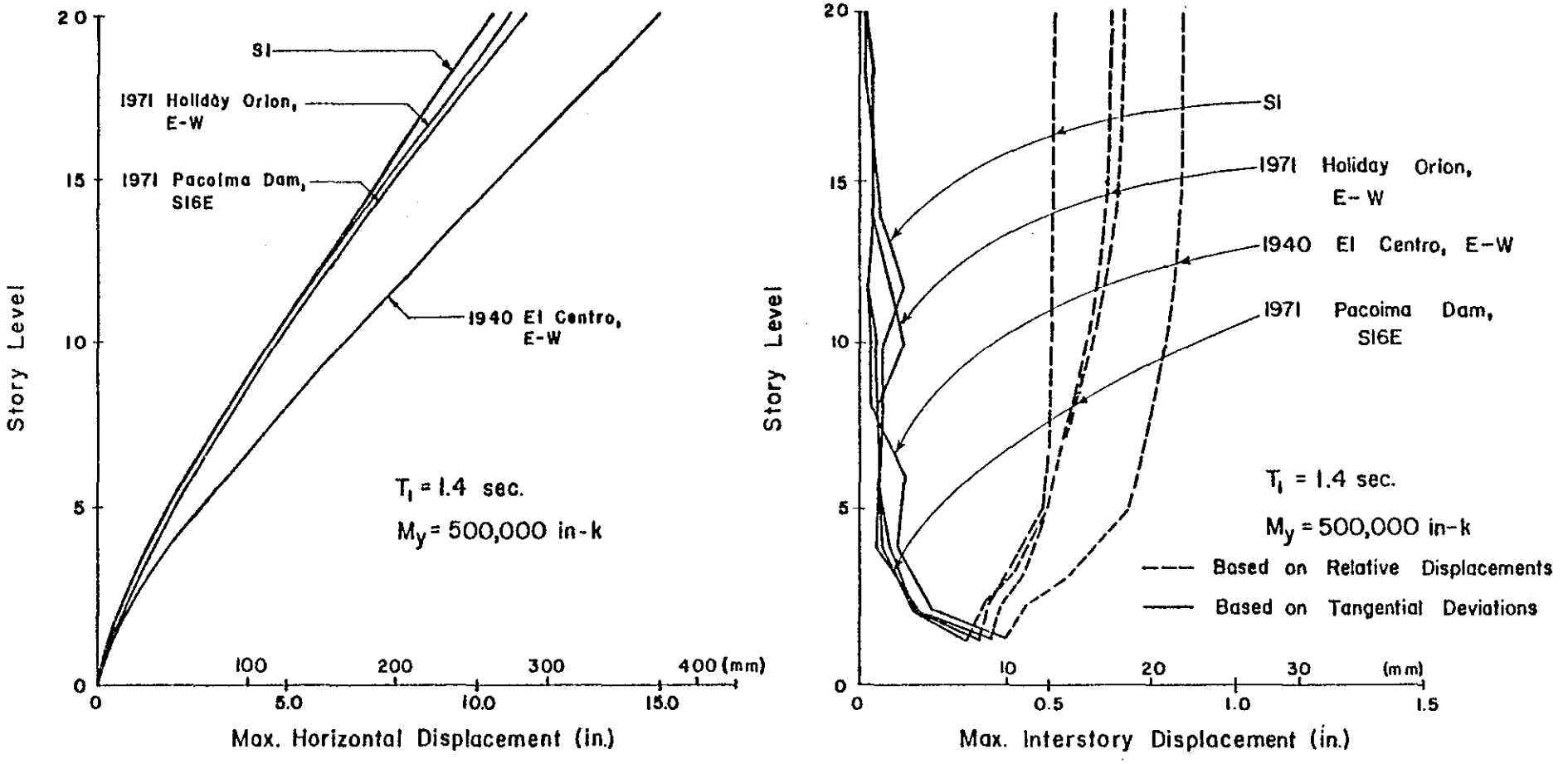

Fig. 24 Effect of Frequency Characteristics of Ground Motion

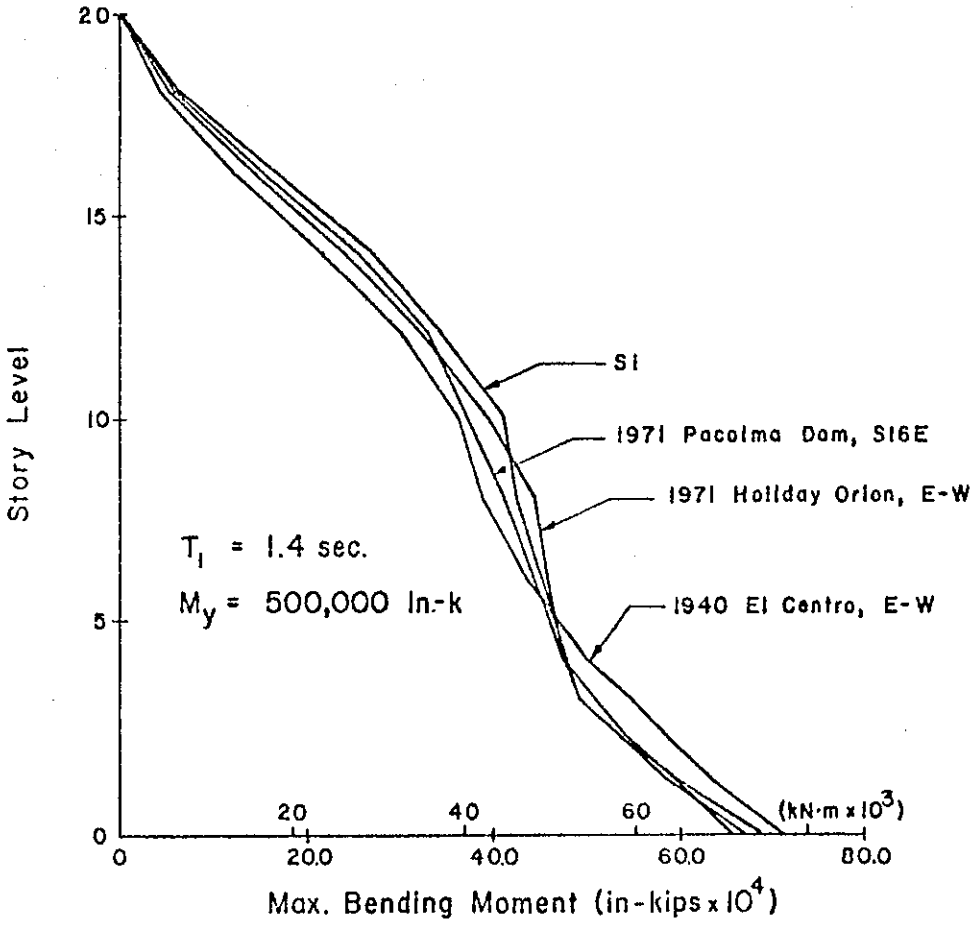

(c)

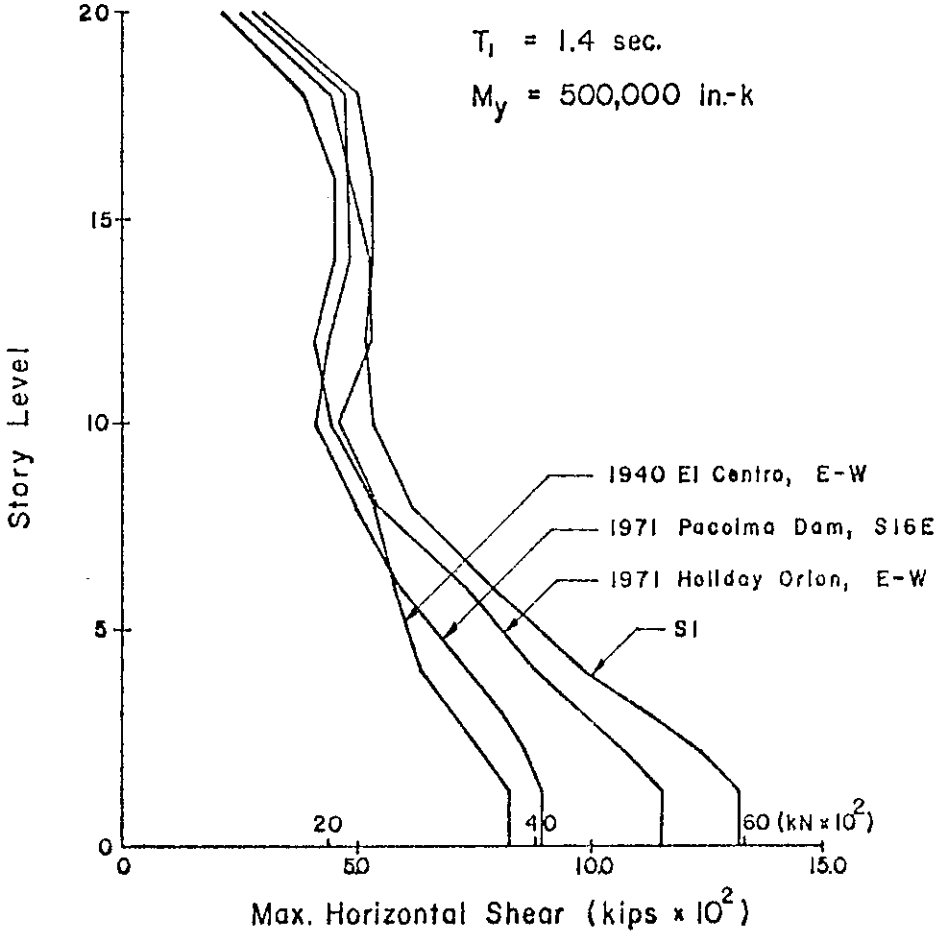

(d)

Fig. 24 (cont'd.) Effect of Frequency Characteristics of Ground Motion

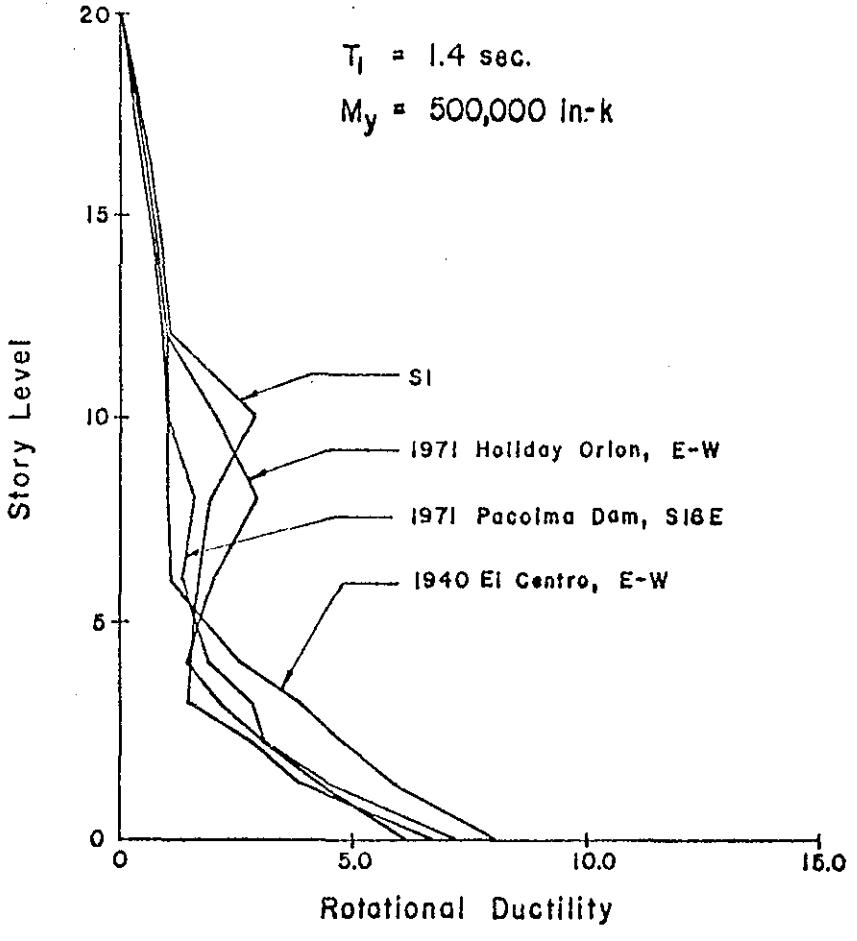

(e)

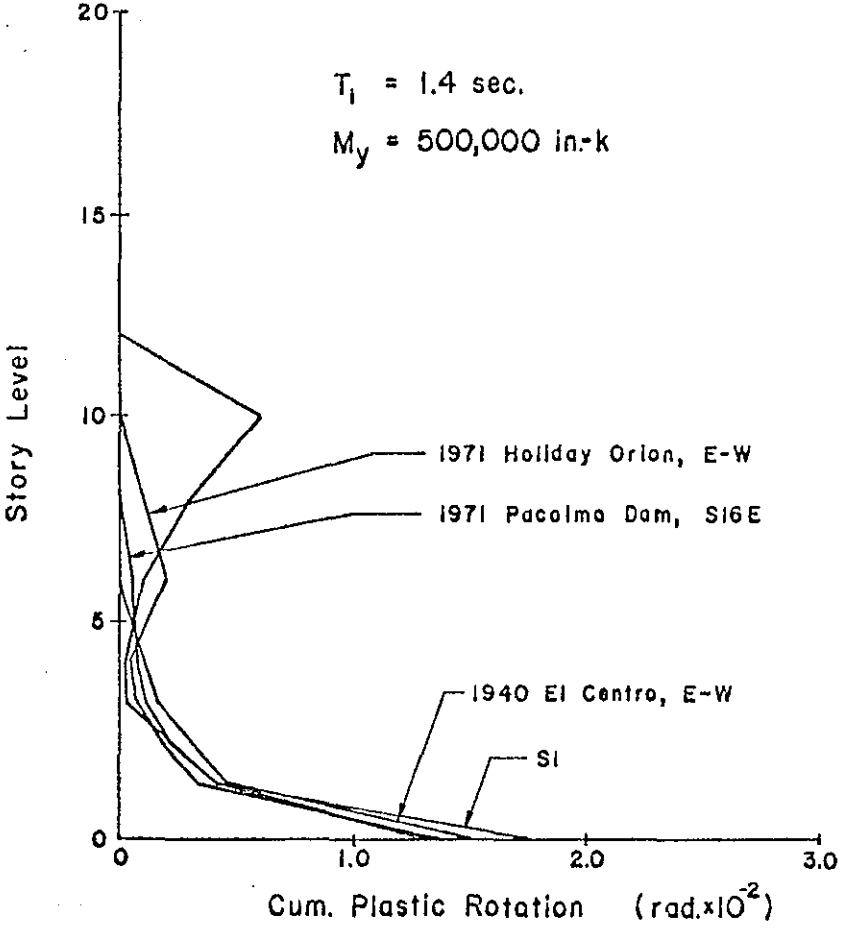

(f)

Fig. 24 (cont'd.) Effect of Frequency Characteristics of Ground Motion

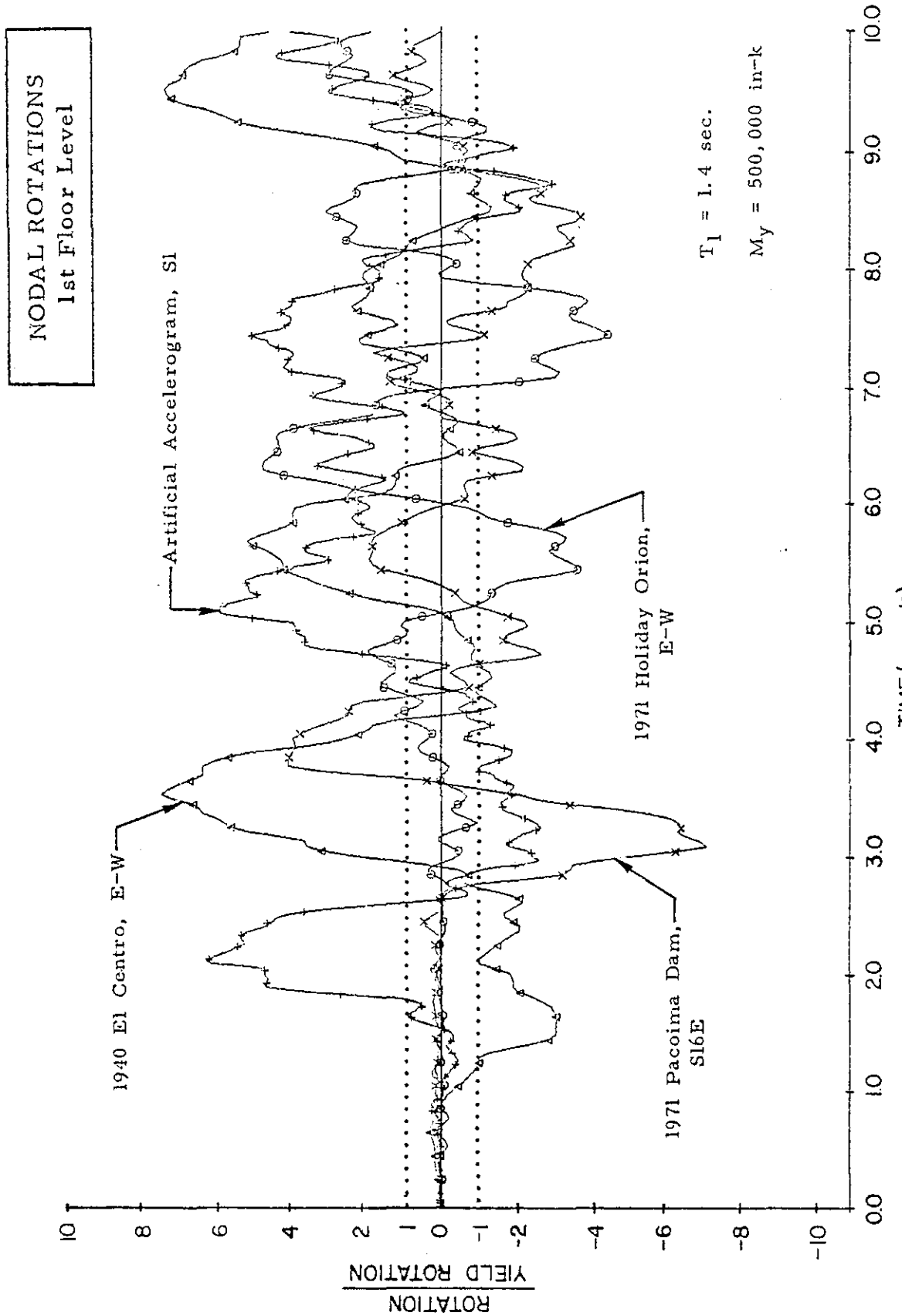

Fig. 25 Normalized Rotations in First Story versus Time for Ground Motions with Different Frequency Characteristics

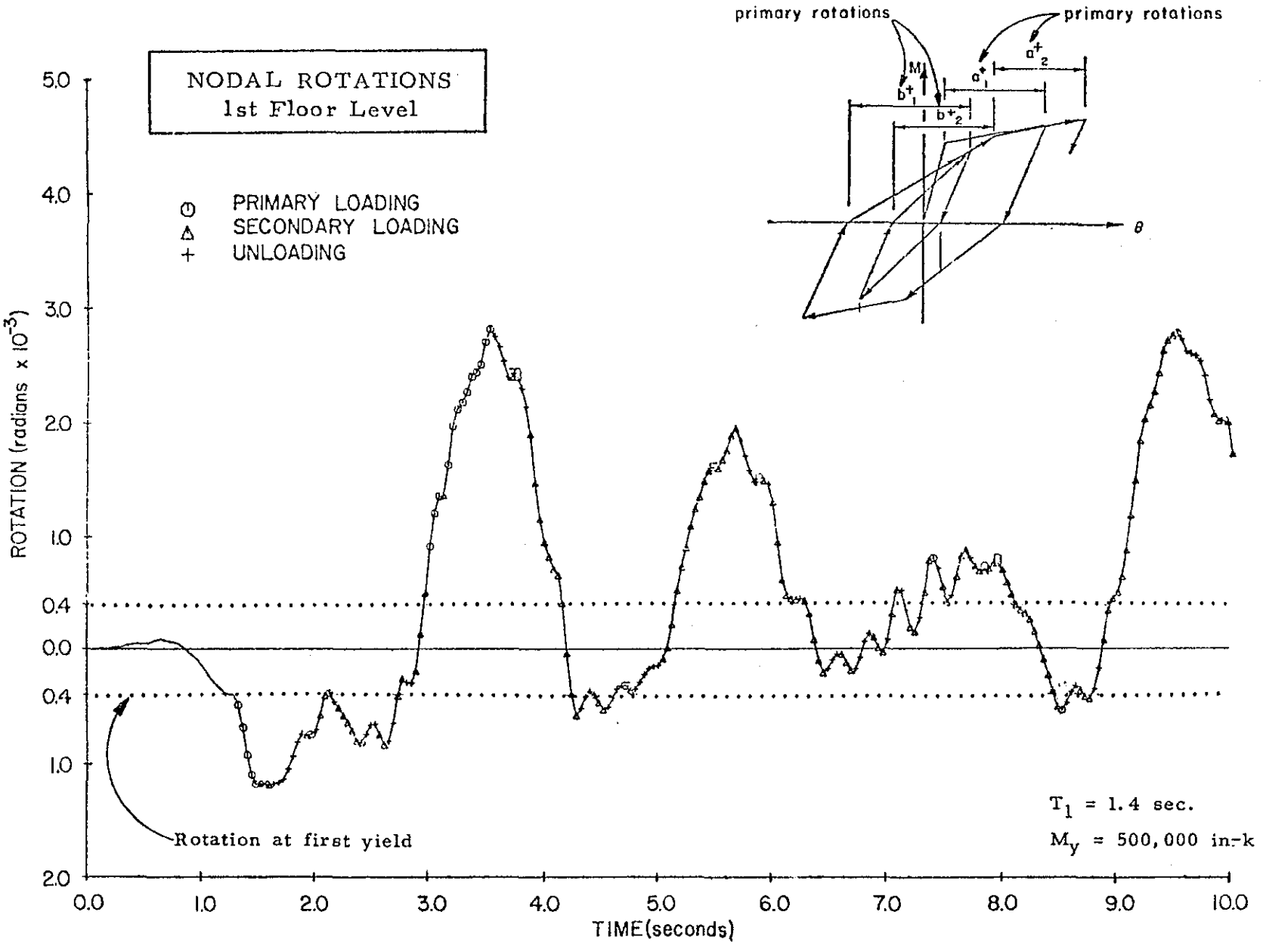

Fig. 26 Nodal Rotation History for Structure Subjected to 1940 El Centro, E-W Component

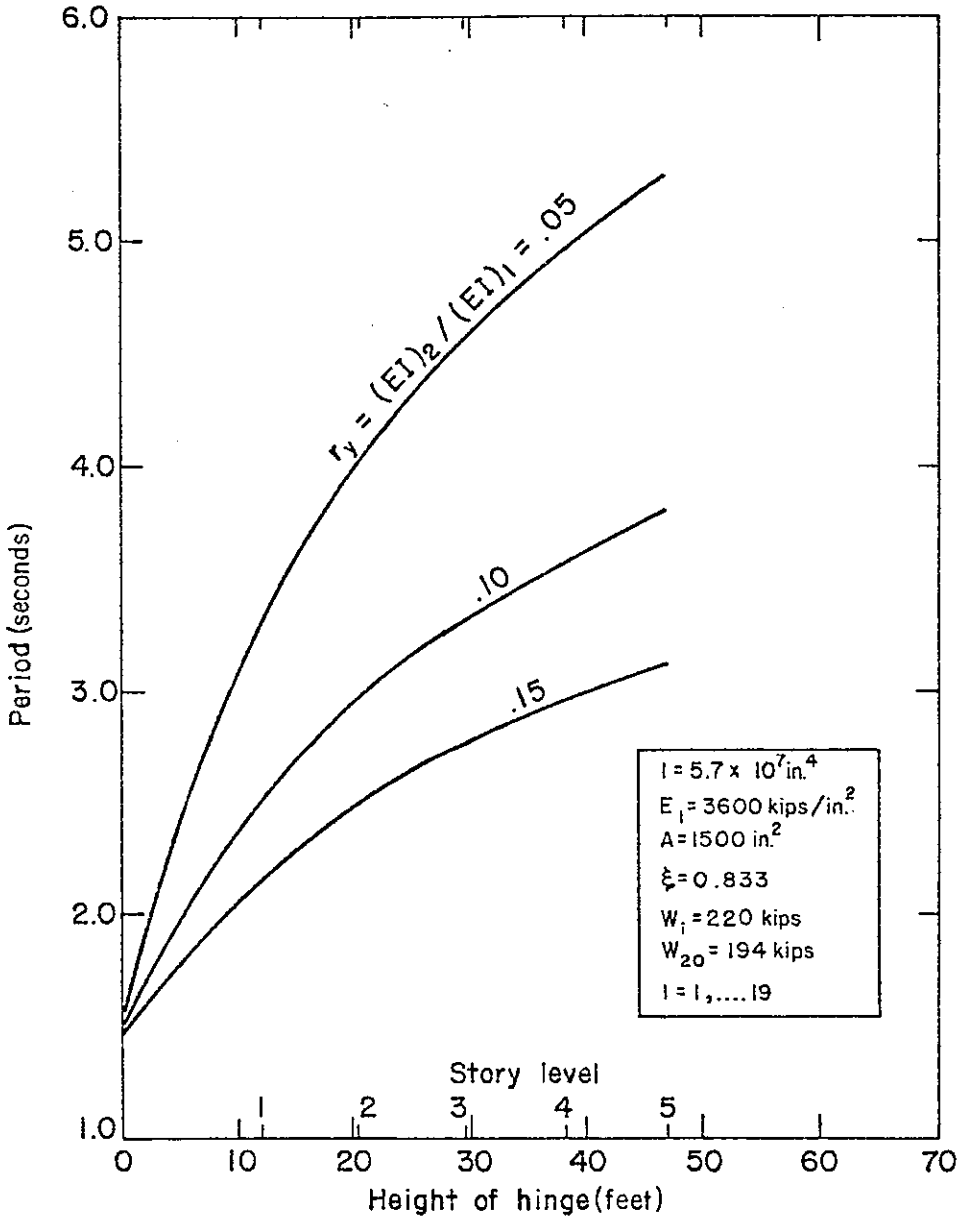

Fig. 27 Fundamental Period versus Height of Yield Hinge, 20-Mass Cantilever

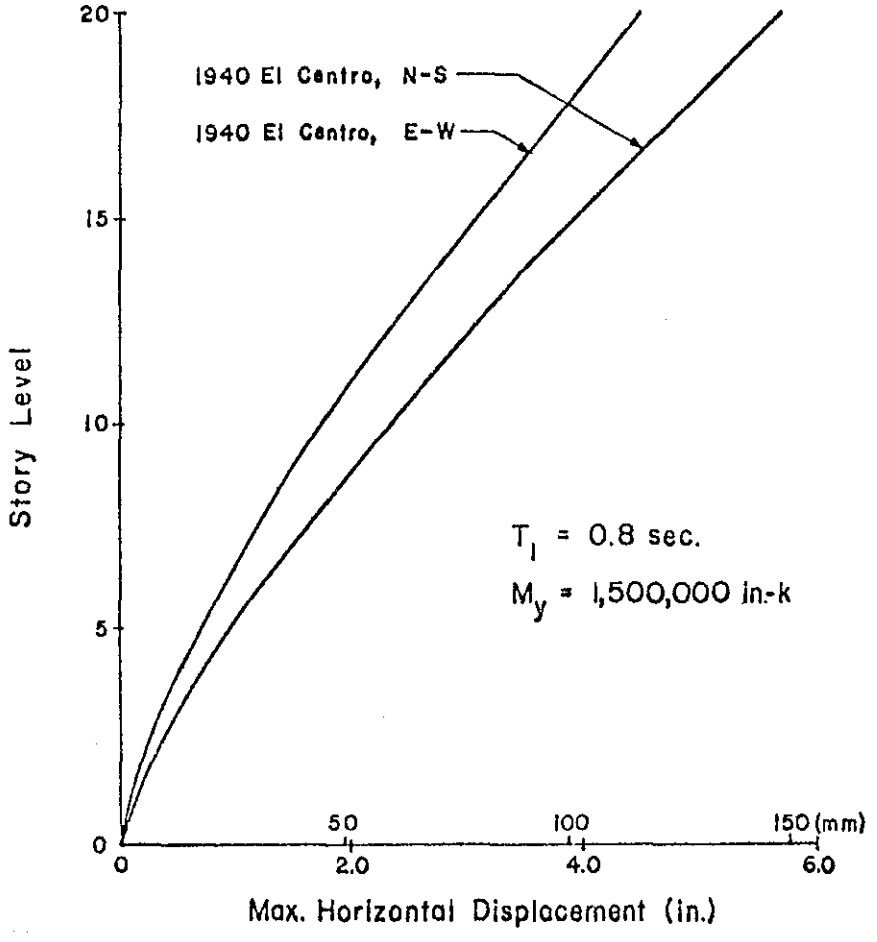

(a)

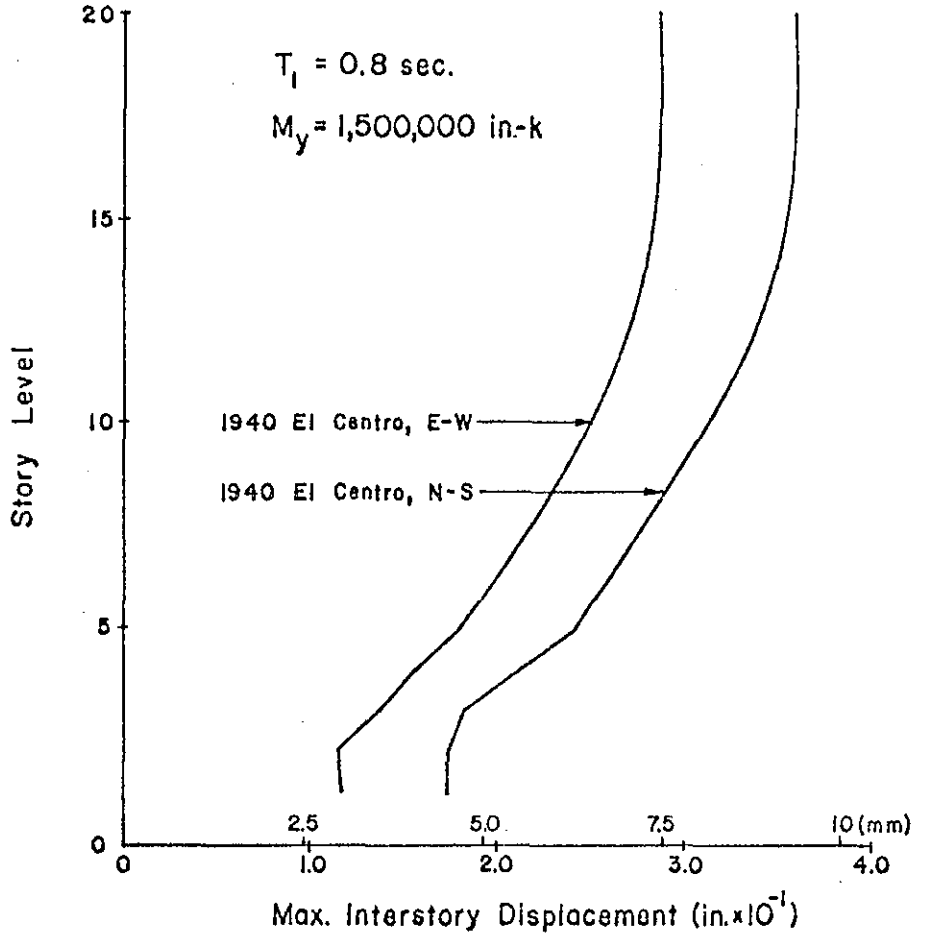

(b)

Fig. 28 Effect of Frequency Characteristics of Ground Motion

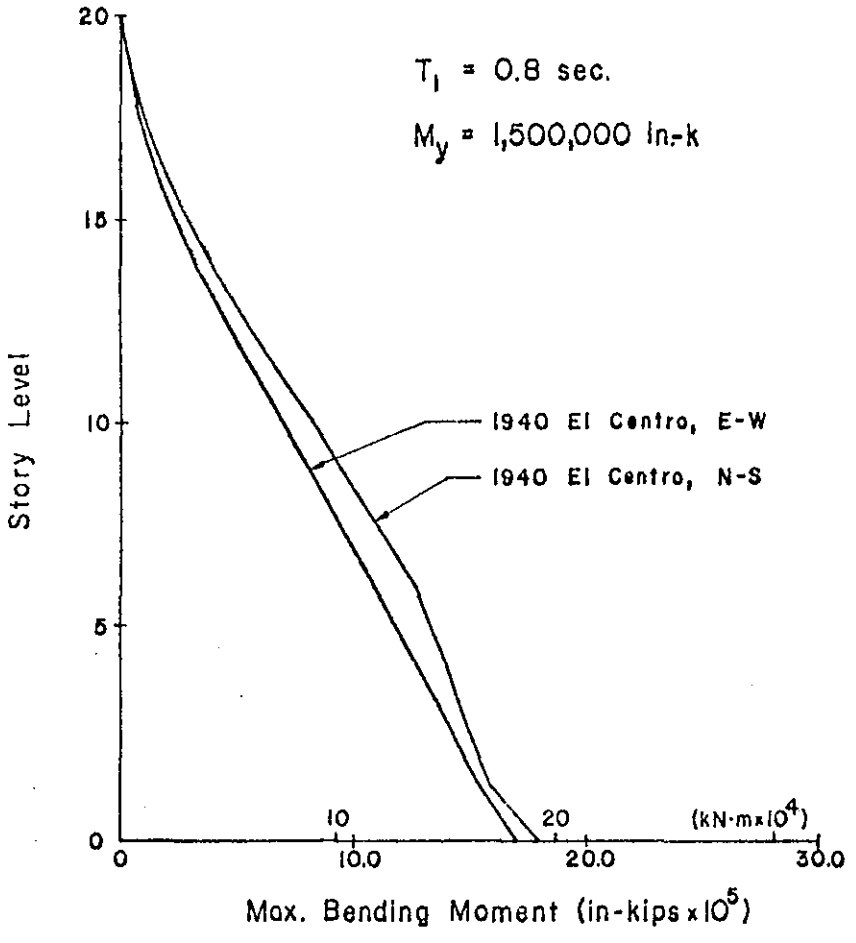

(c)

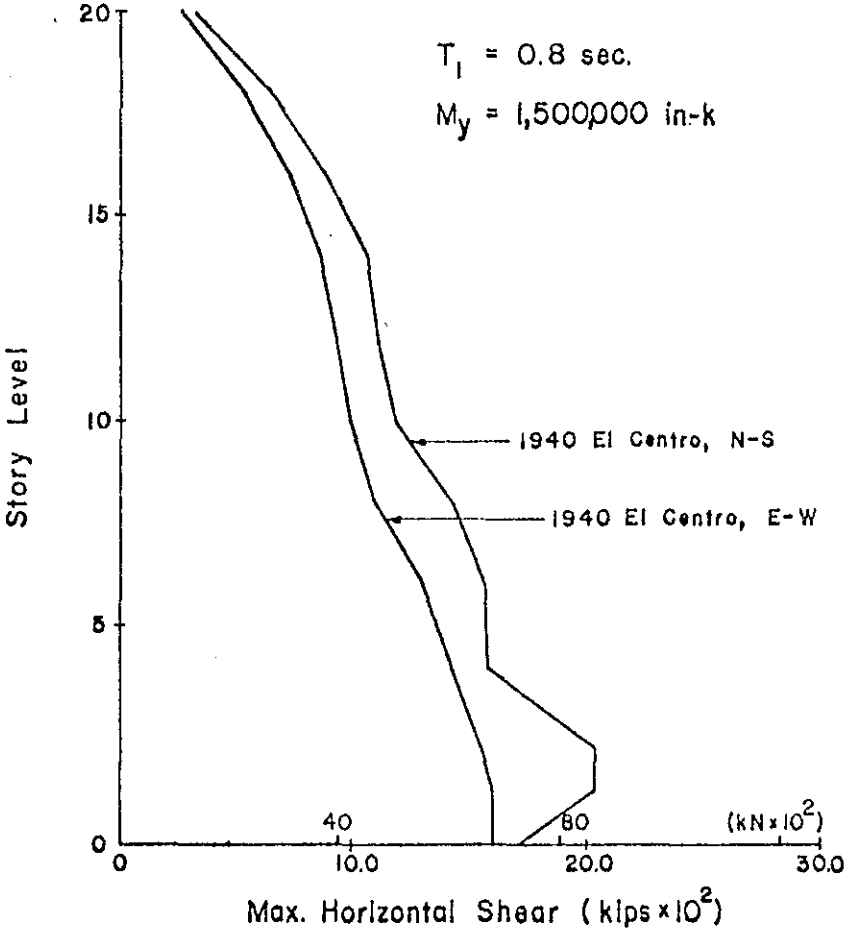

(d)

Fig. 28 (cont'd.) Effect of Frequency Characteristics of Ground Motion

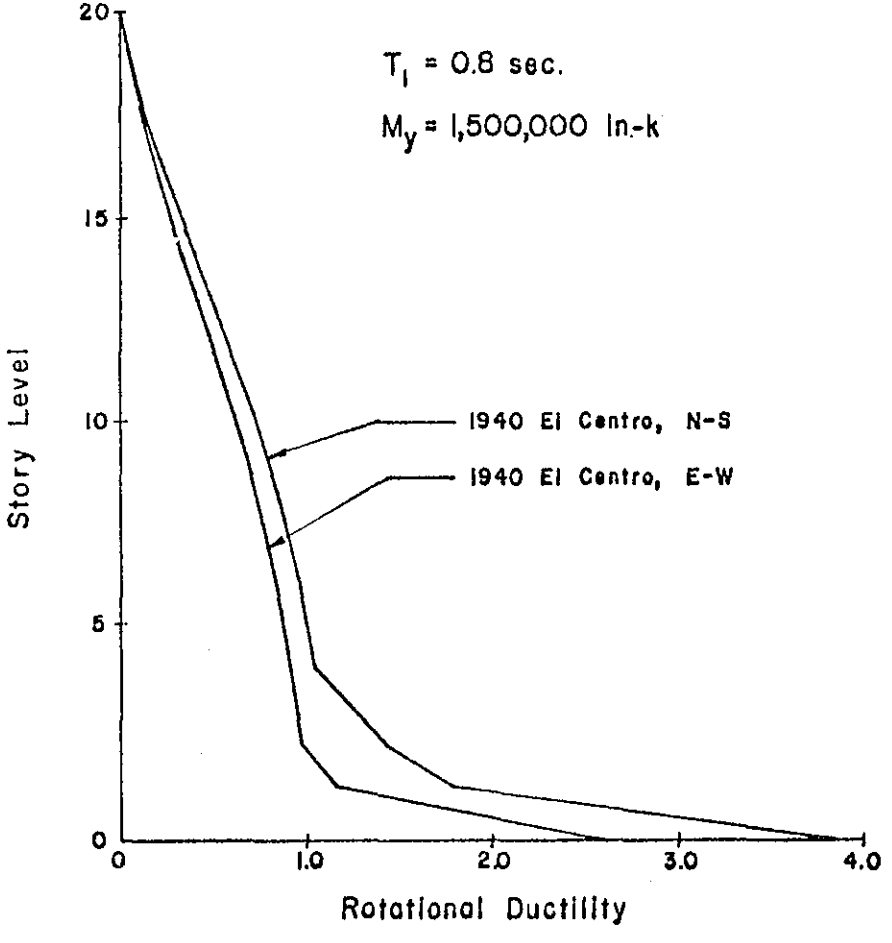

(e)

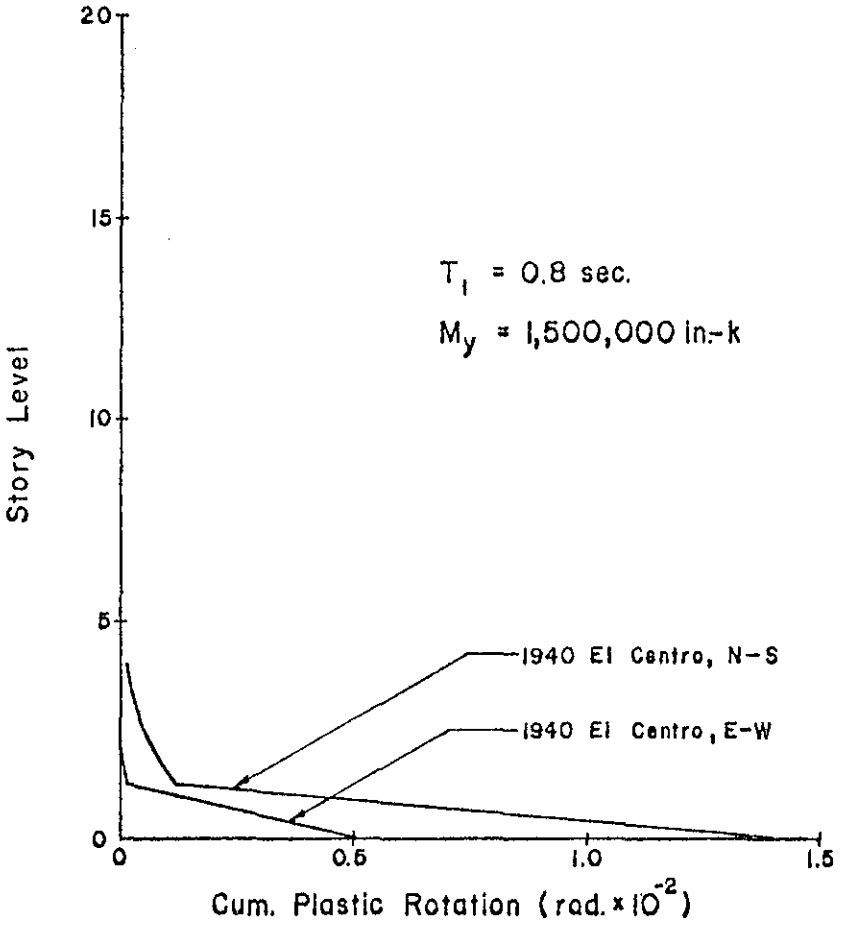

(f)

Fig. 28 (cont'd.) Effect of Frequency Characteristics of Ground Motion

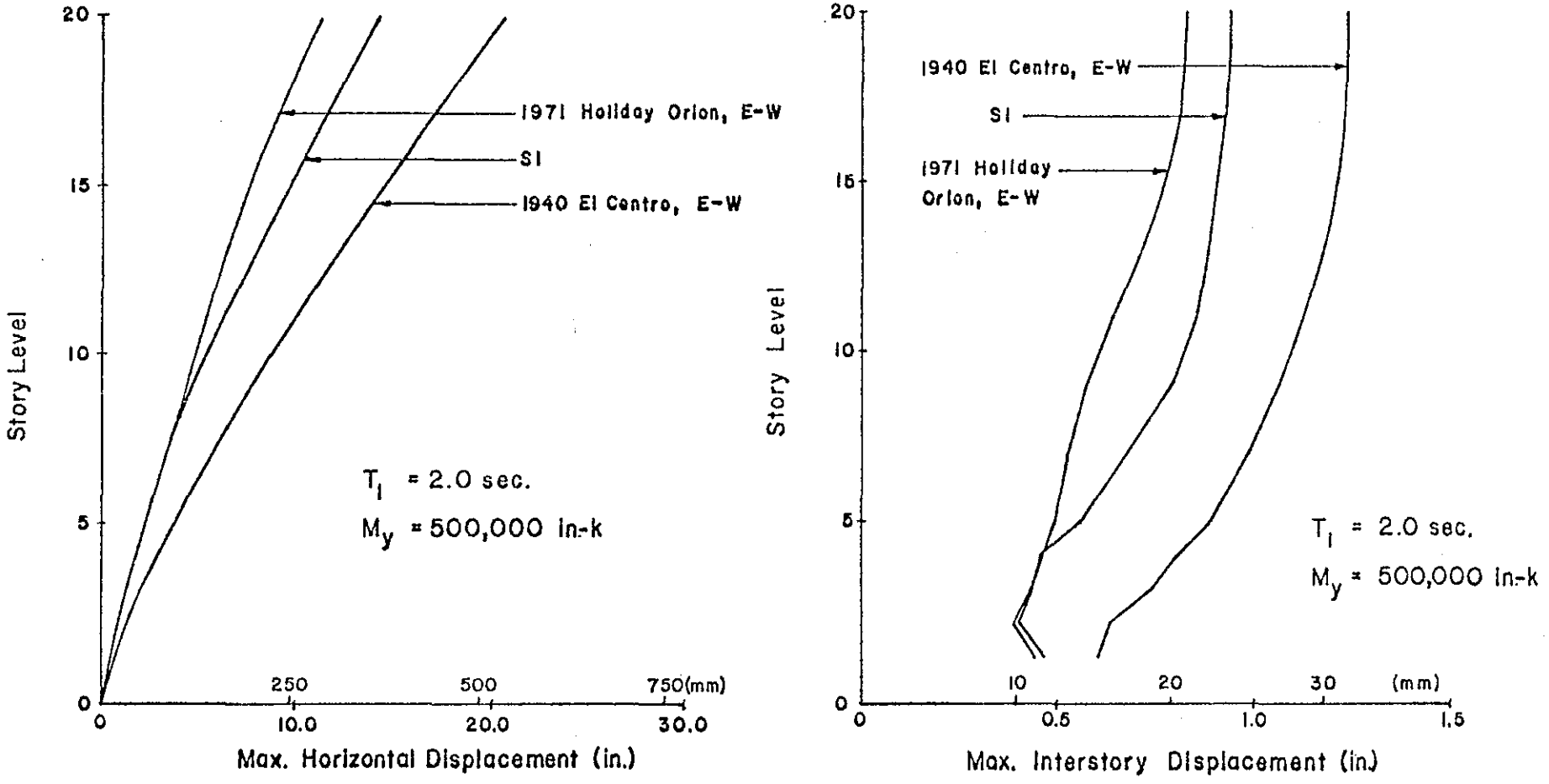

Fig. 29 Effect of Frequency Characteristics of Ground Motion

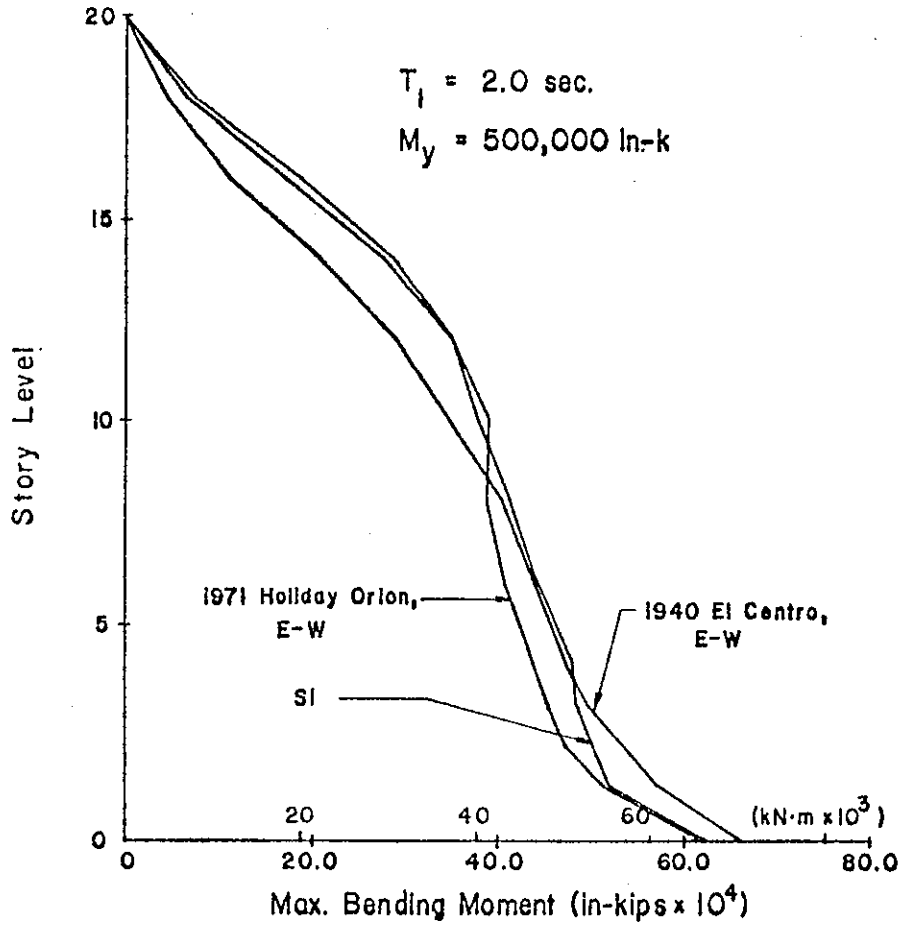

(c)

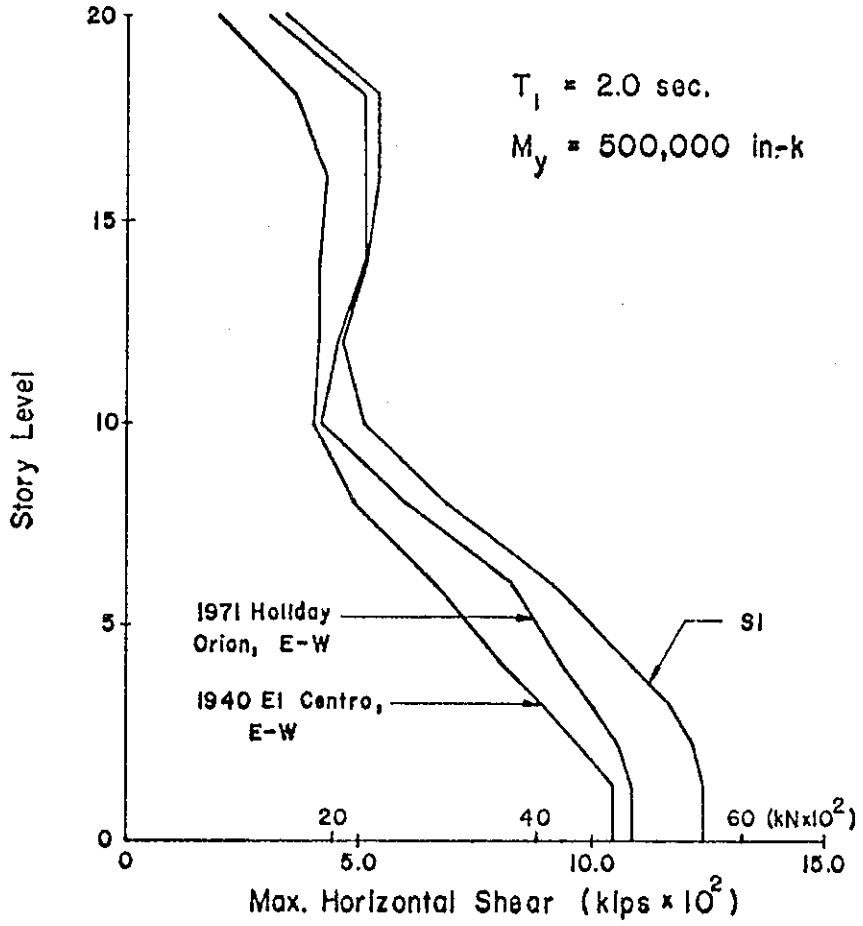

(d)

Fig. 29 (cont'd.) Effect of Frequency Characteristics of Ground Motion

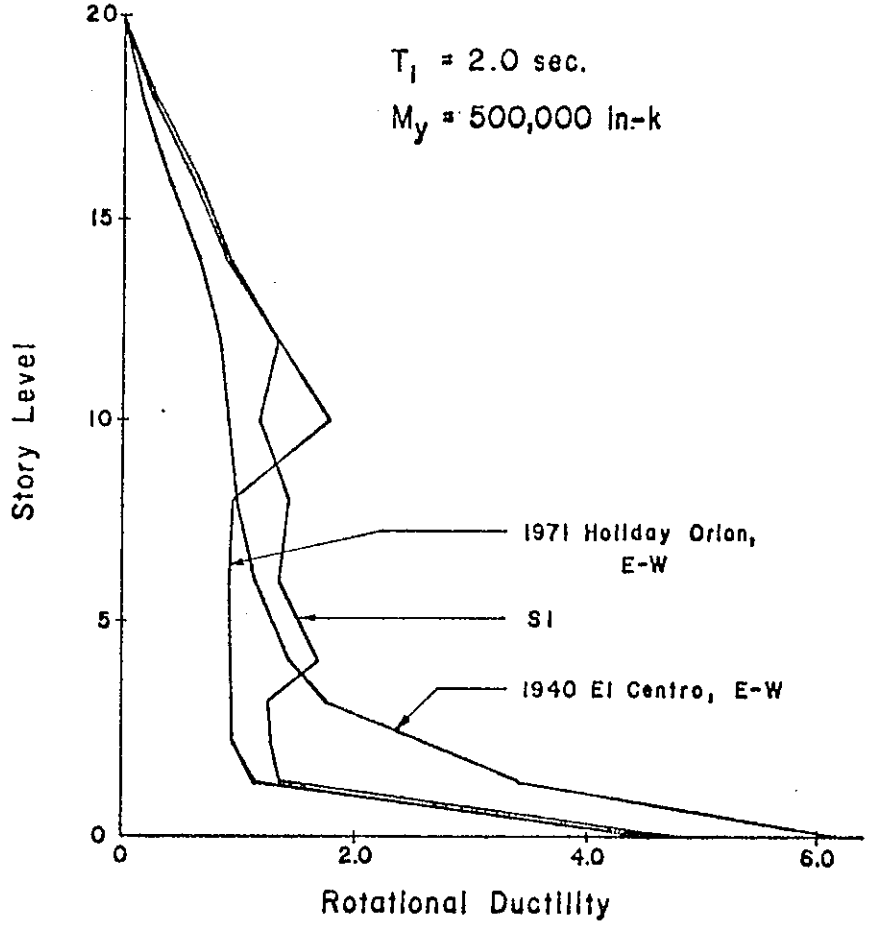

(e)

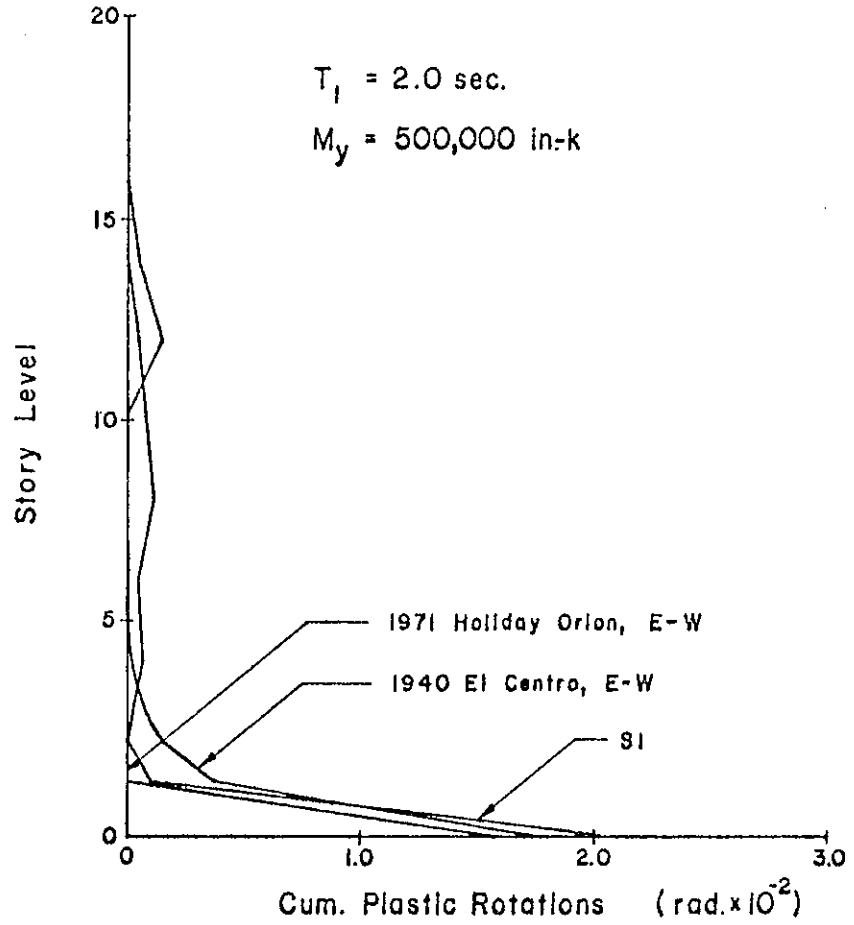

(f)

Fig. 29 (cont'd.) Effect of Frequency Characteristics of Ground Motion

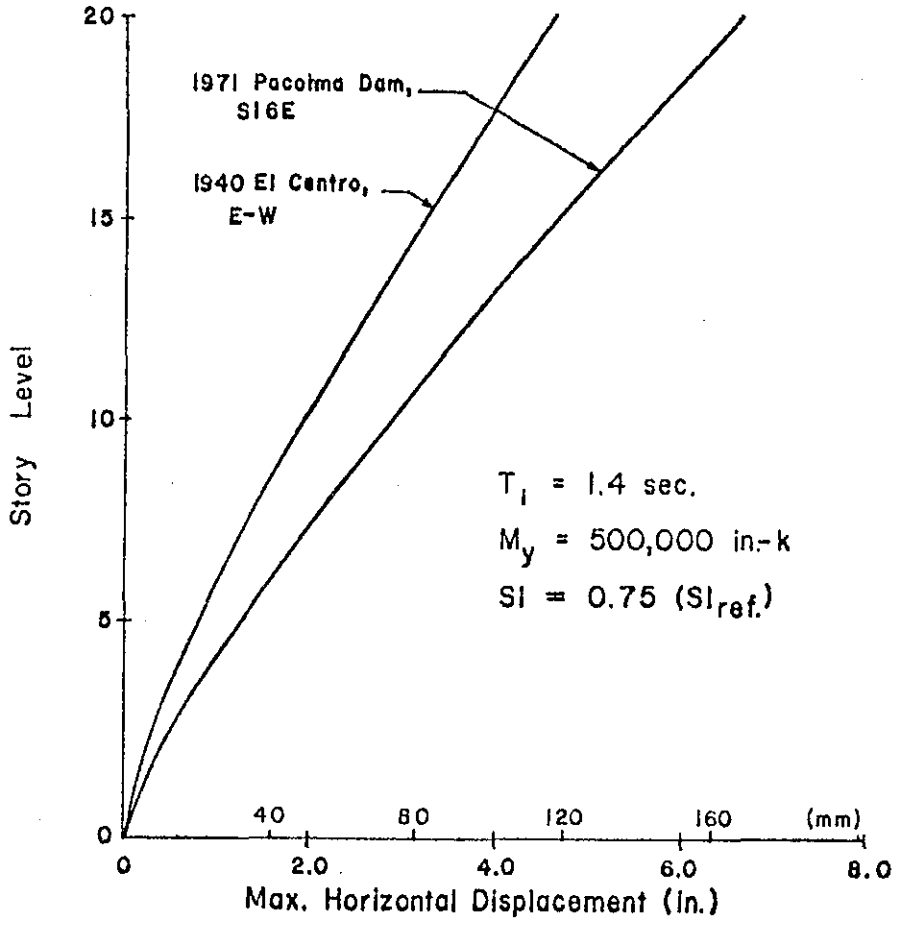

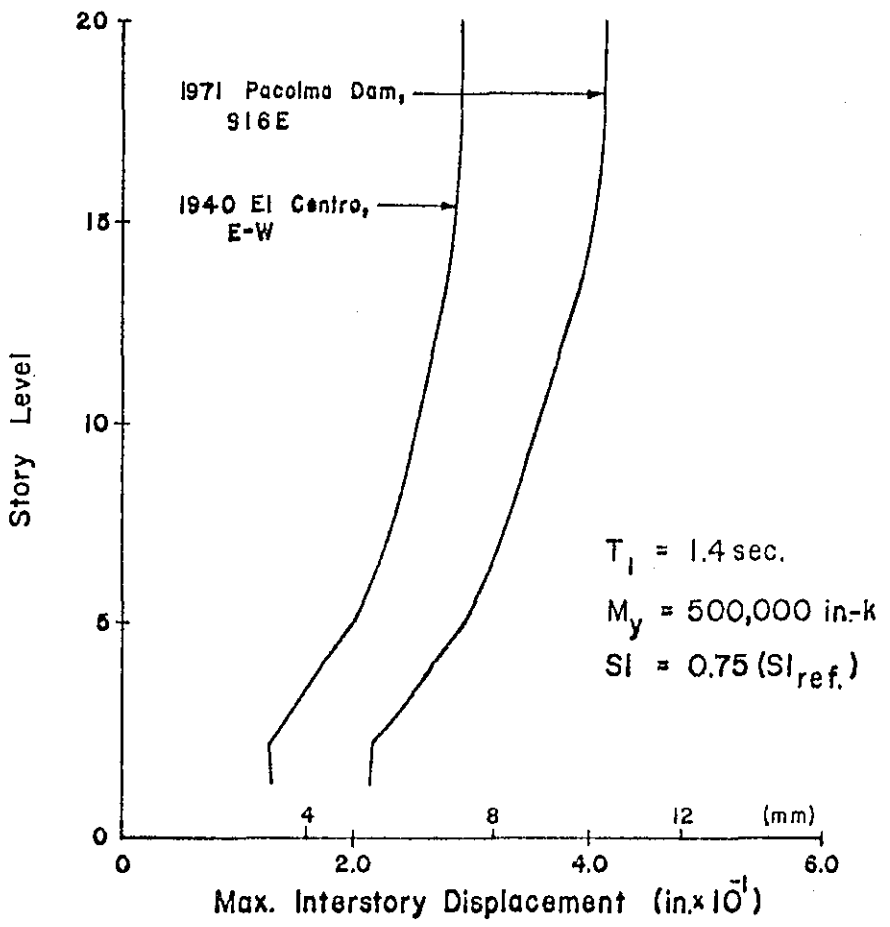

Fig. 30 Interacting Effects of Frequency Characteristics and Intensity of Ground Motion

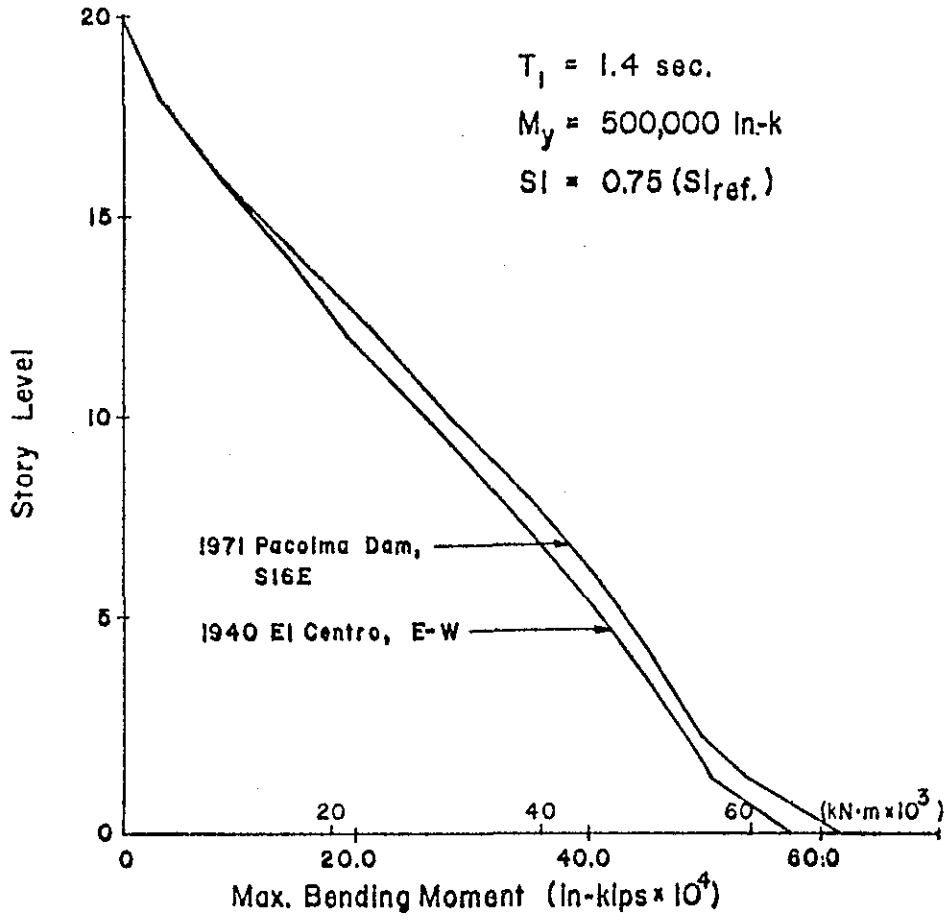

(c)

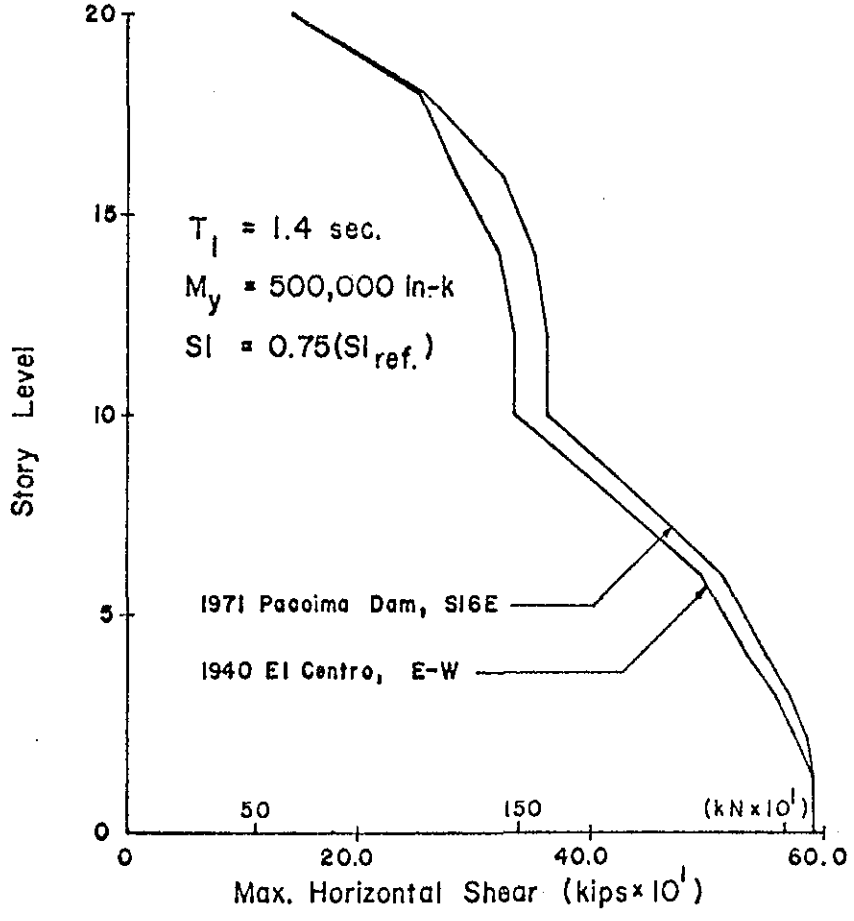

(d)

Fig. 30 (cont'd.) Interacting Effects of Frequency Characteristics and Intensity of Ground Motion

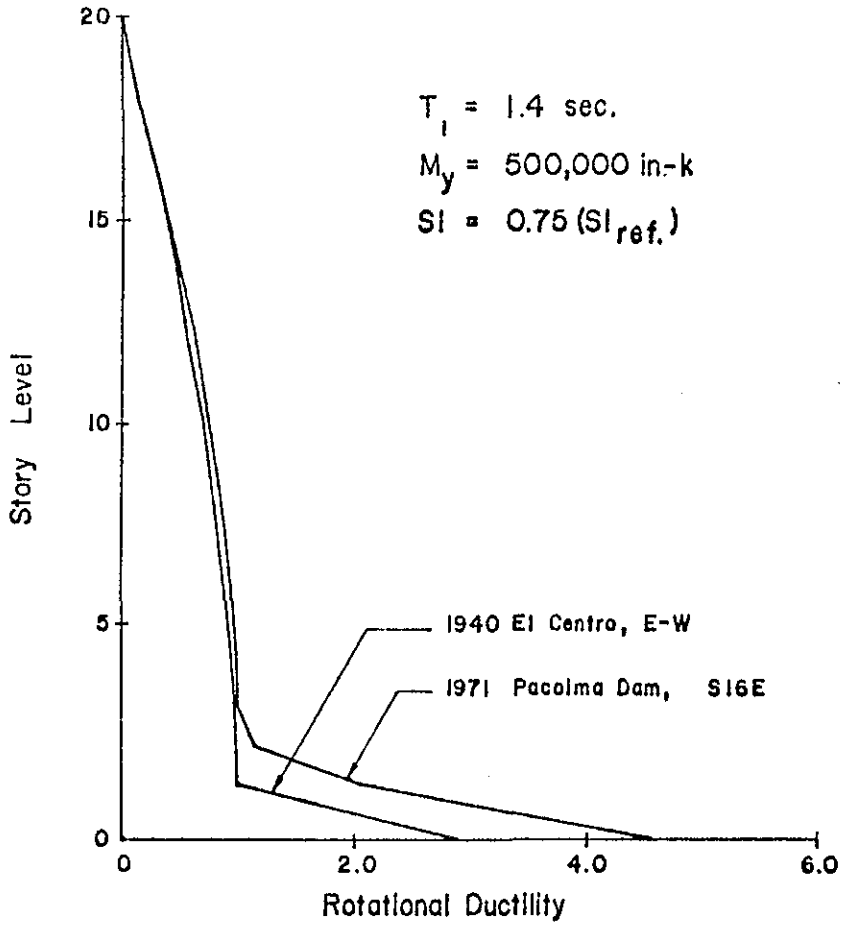

(e)

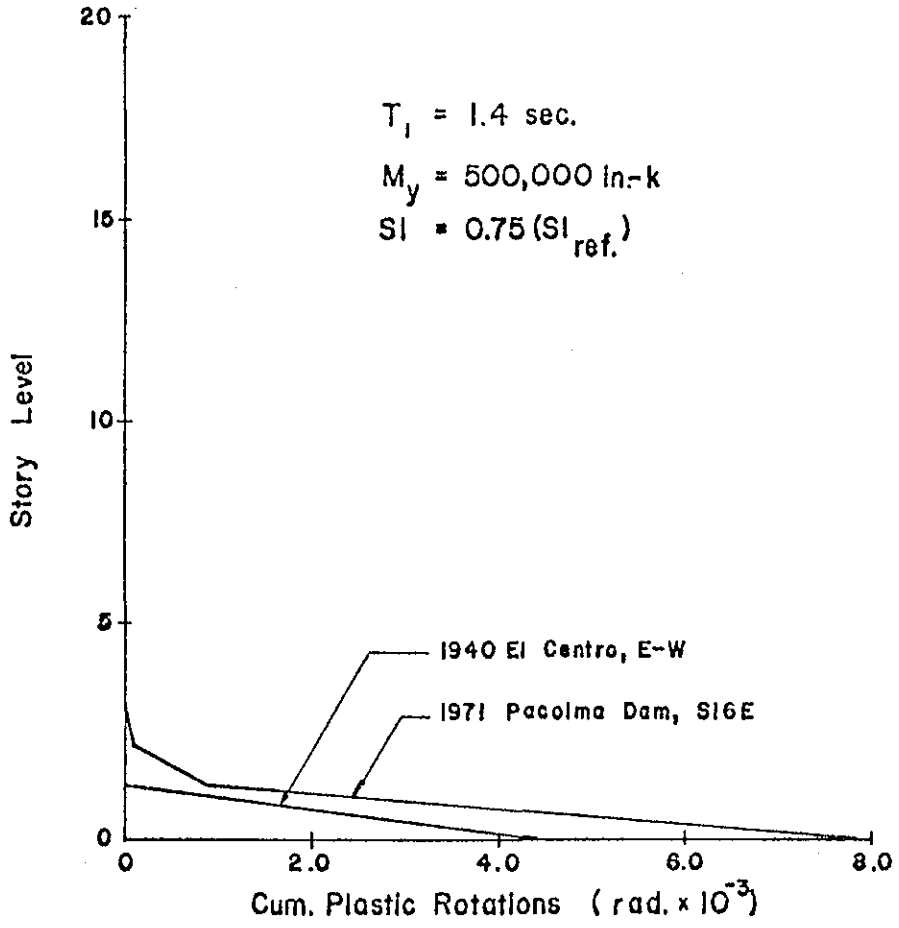

(f)

Fig. 30 (cont'd.) Interacting Effects of Frequency Characteristics and Intensity of Ground Motion

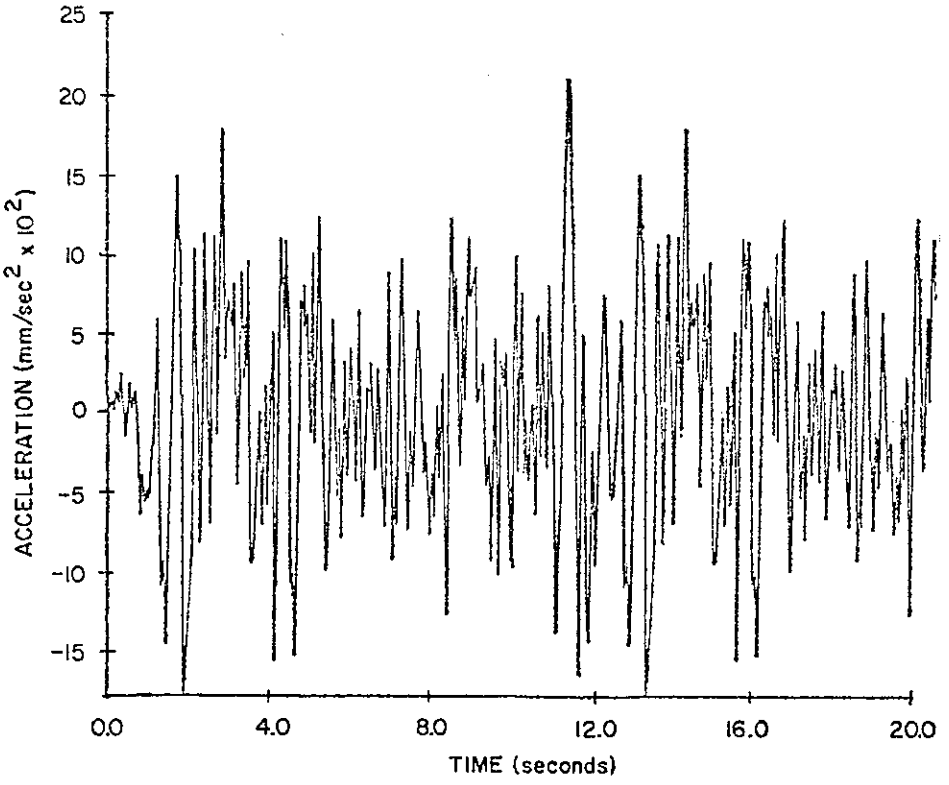

Fig. 31a Twenty-Second Composite Accelerogram

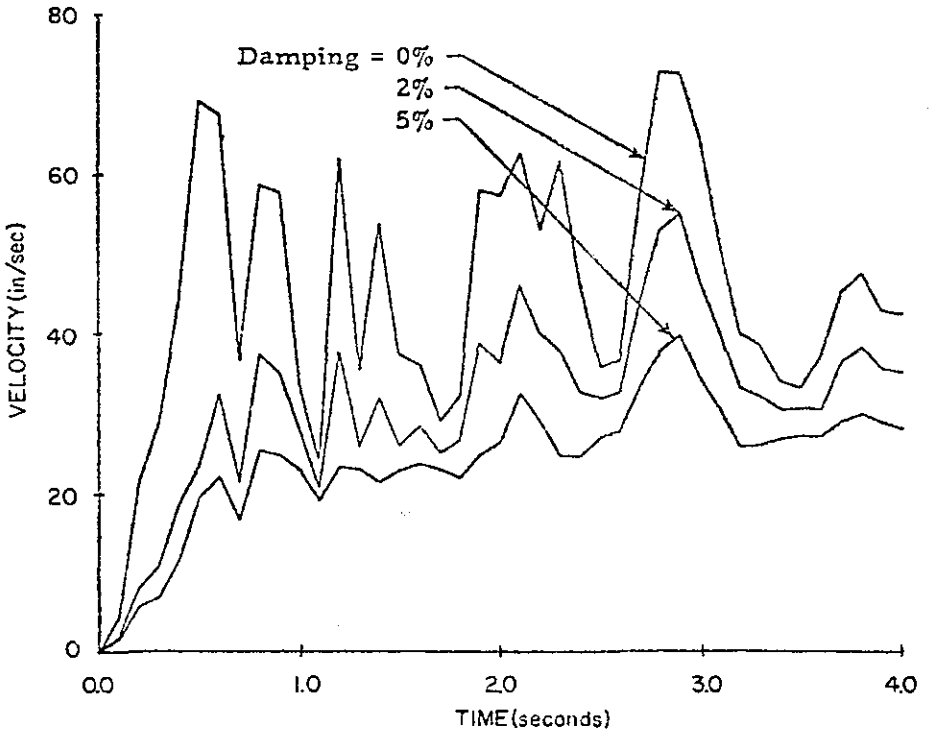

Fig. 31b Velocity Response Spectra for 20-Second Composite Accelerogram

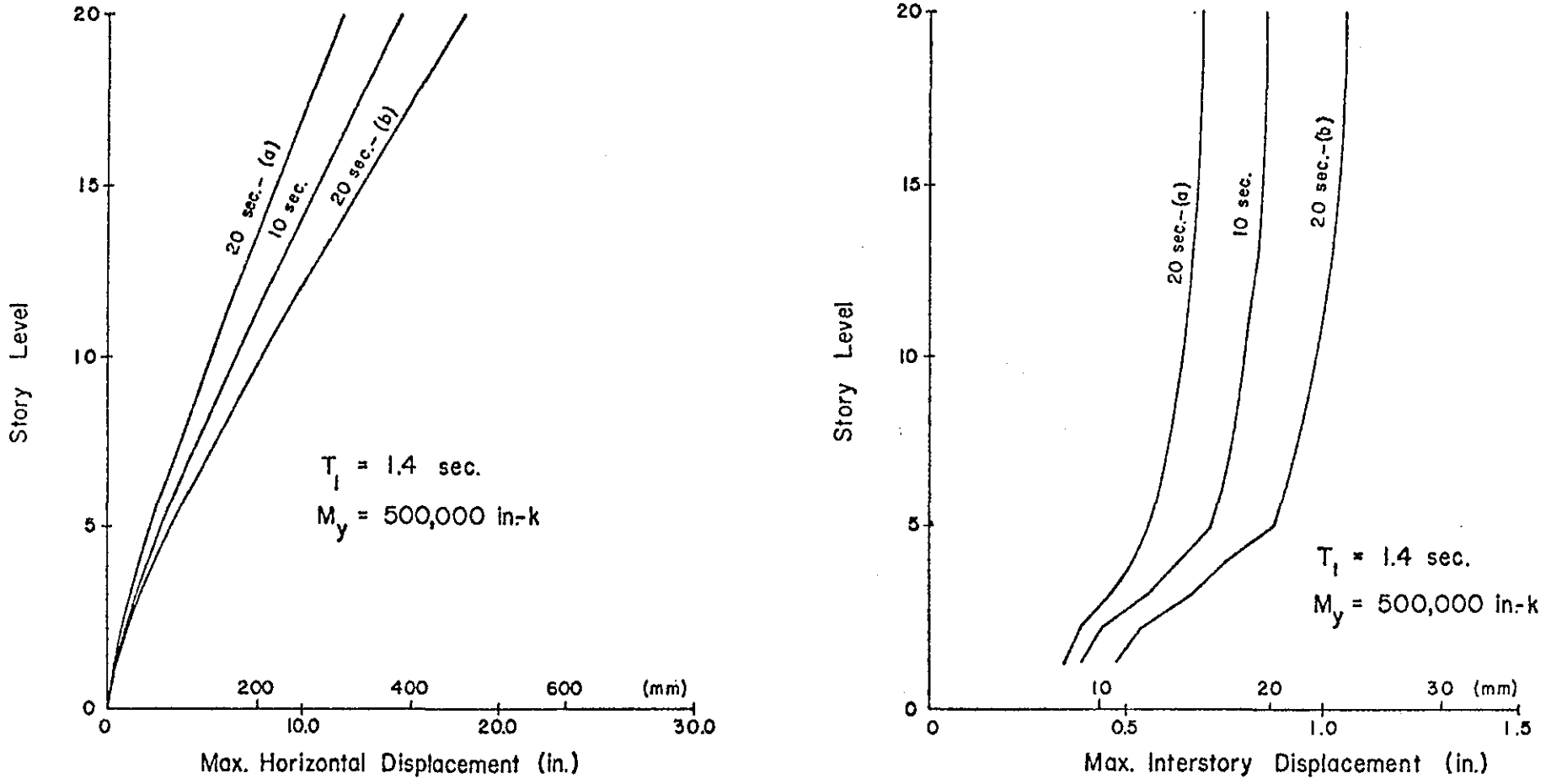

Fig. 32 Effect of Duration of Ground Motion

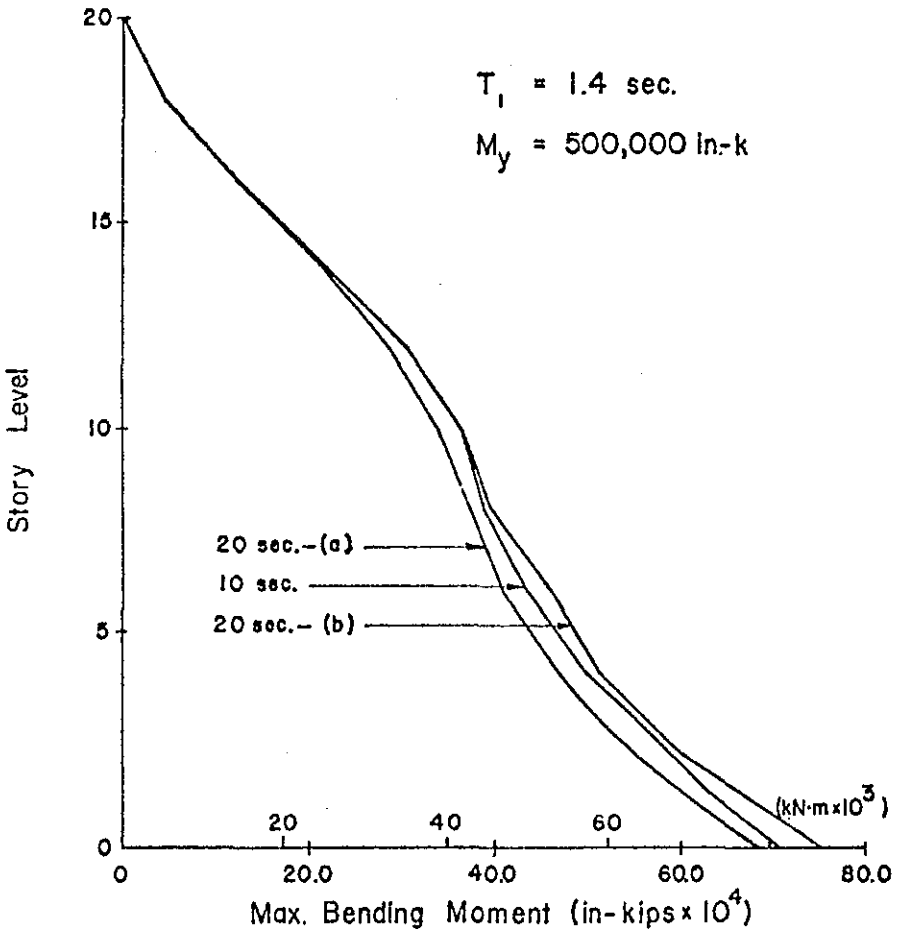

(c)

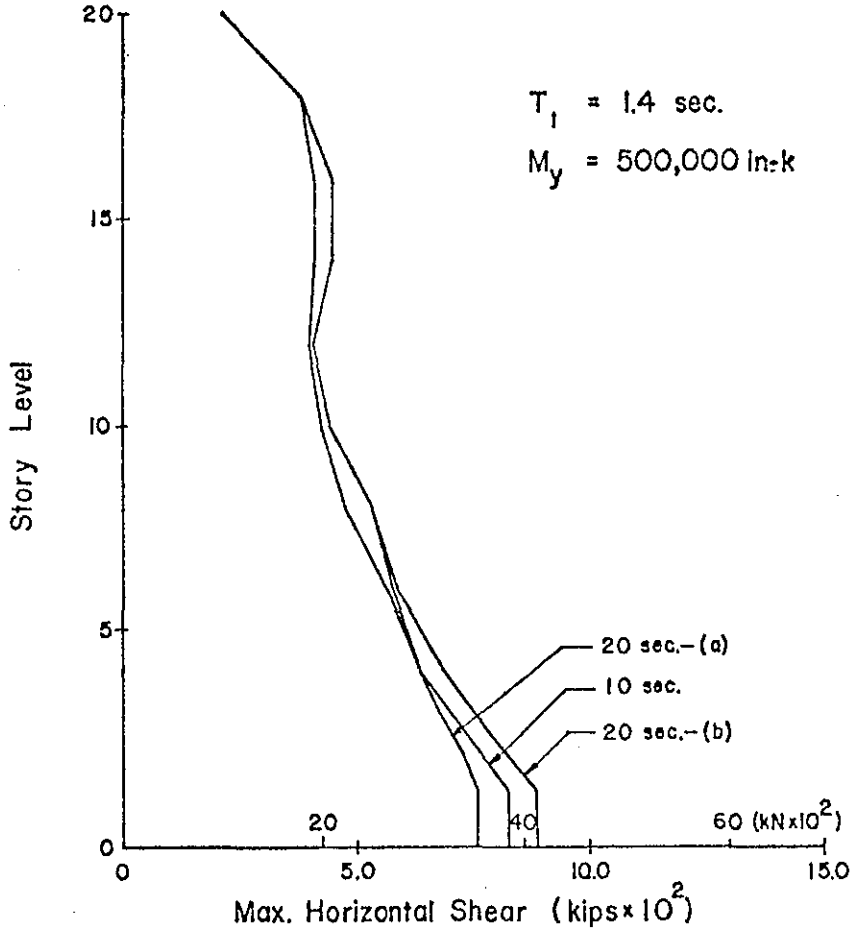

(d)

Fig. 32 (cont'd.) Effect of Duration of Ground Motion

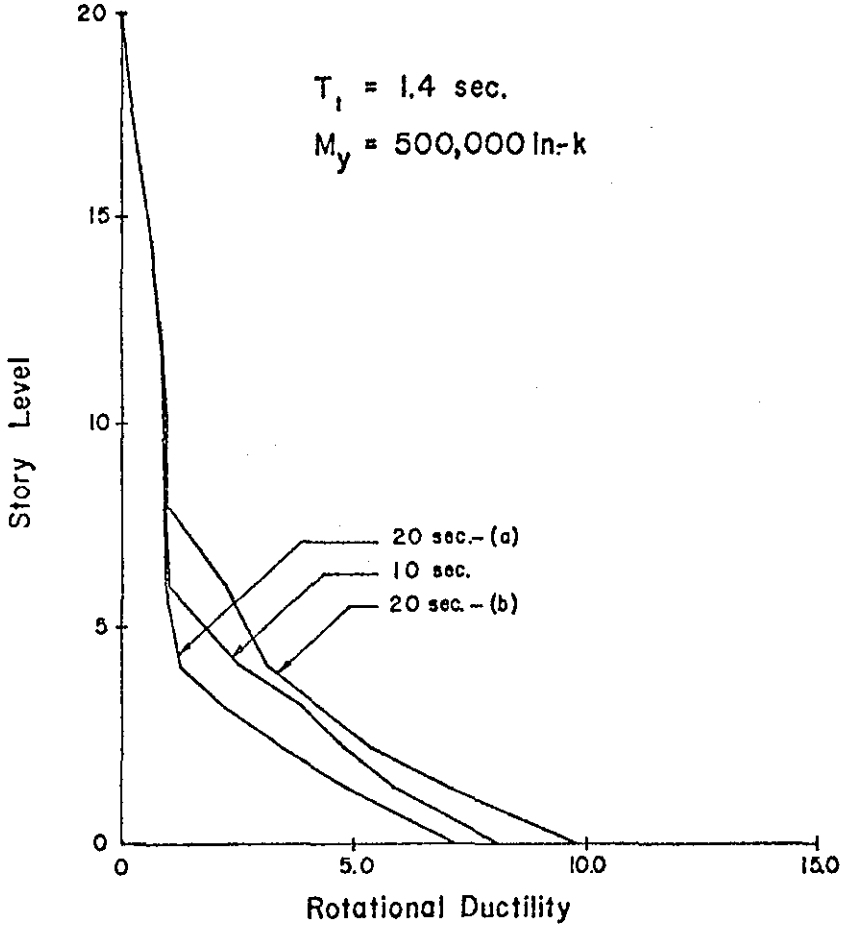

(e)

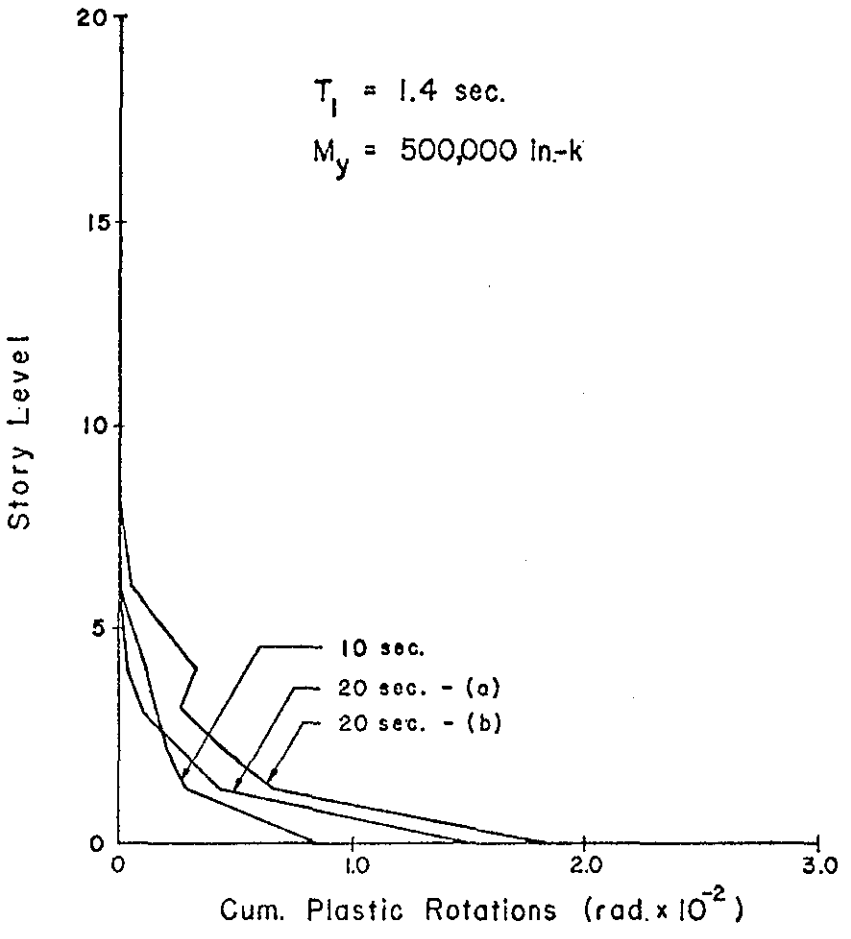

(f)

Fig. 32 (cont'd.) Effect of Duration of Ground Motion

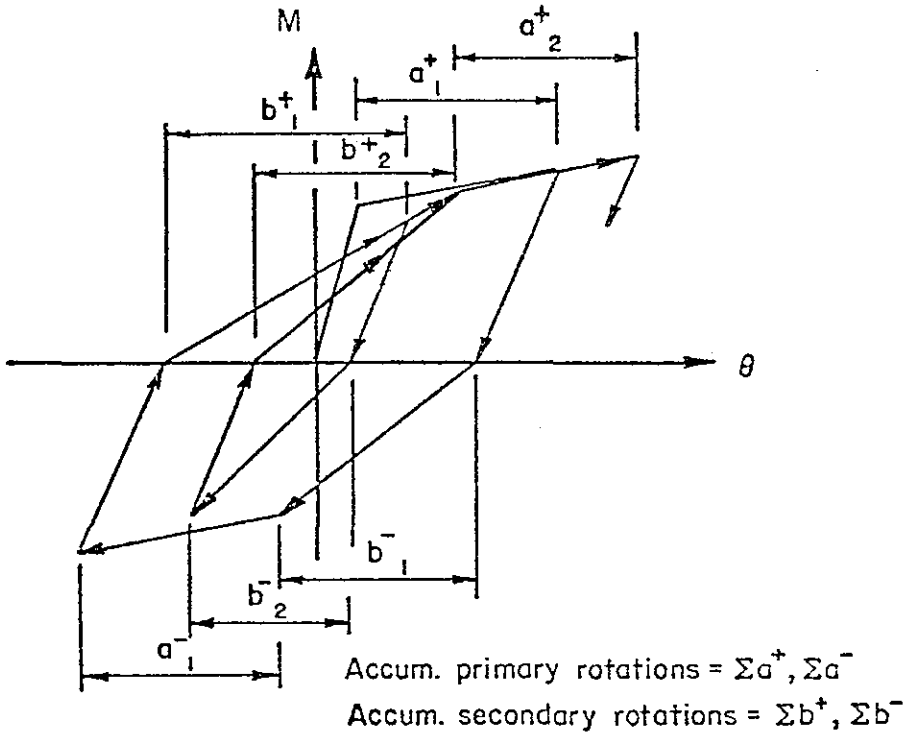

Fig. 33 Components of Cumulative Plastic Rotations for Takeda Stiffness Degrading Model

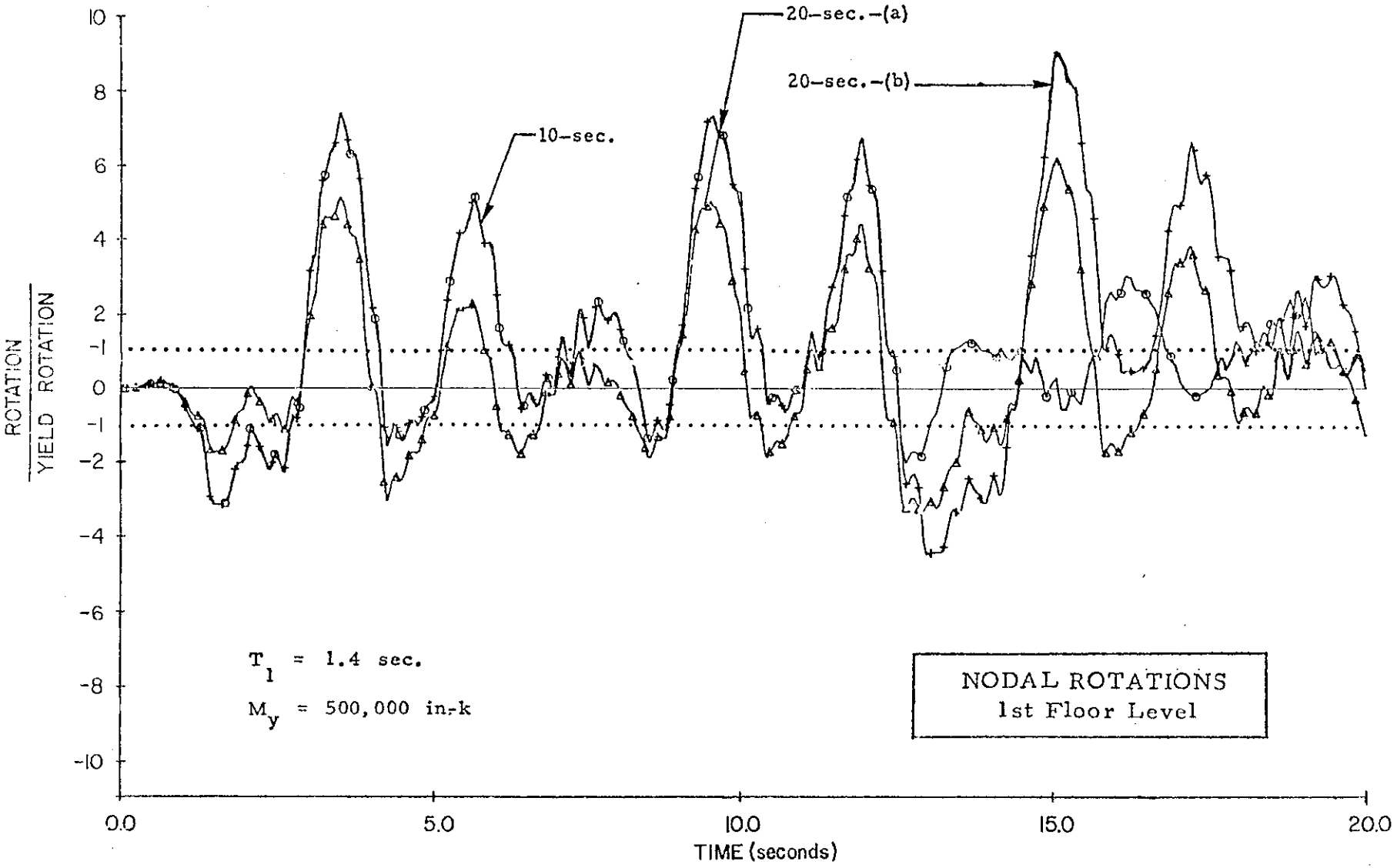

Fig. 34 Rotation in First Story versus Time for Different Durations of Ground Motion

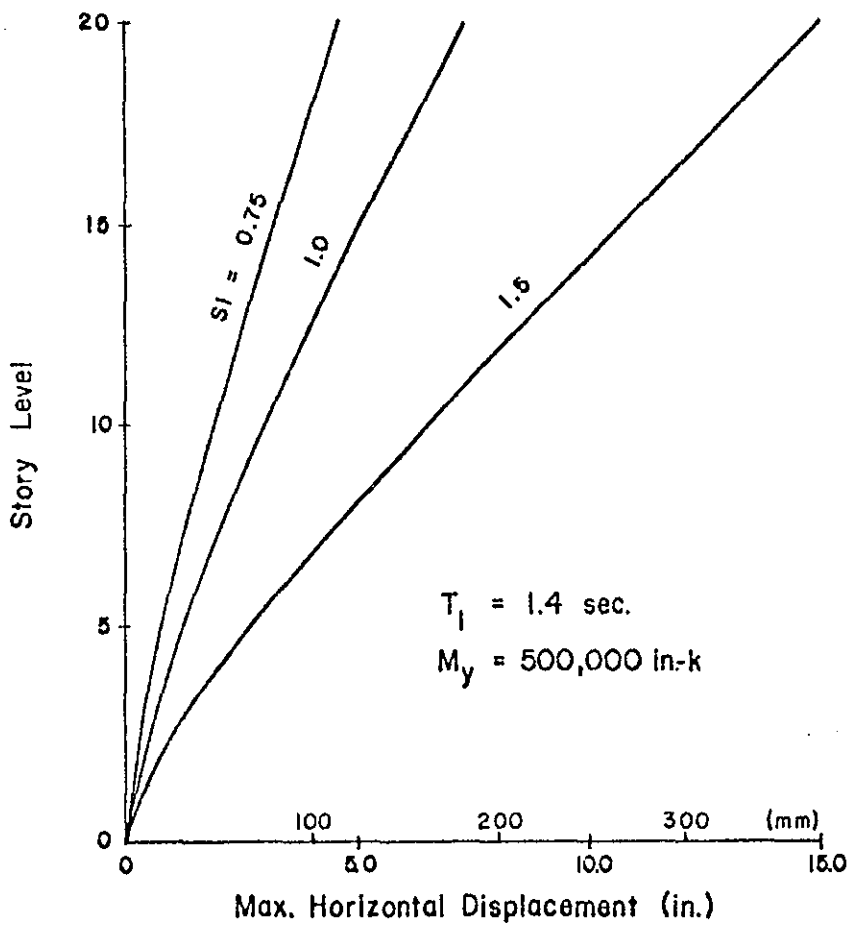

(a)

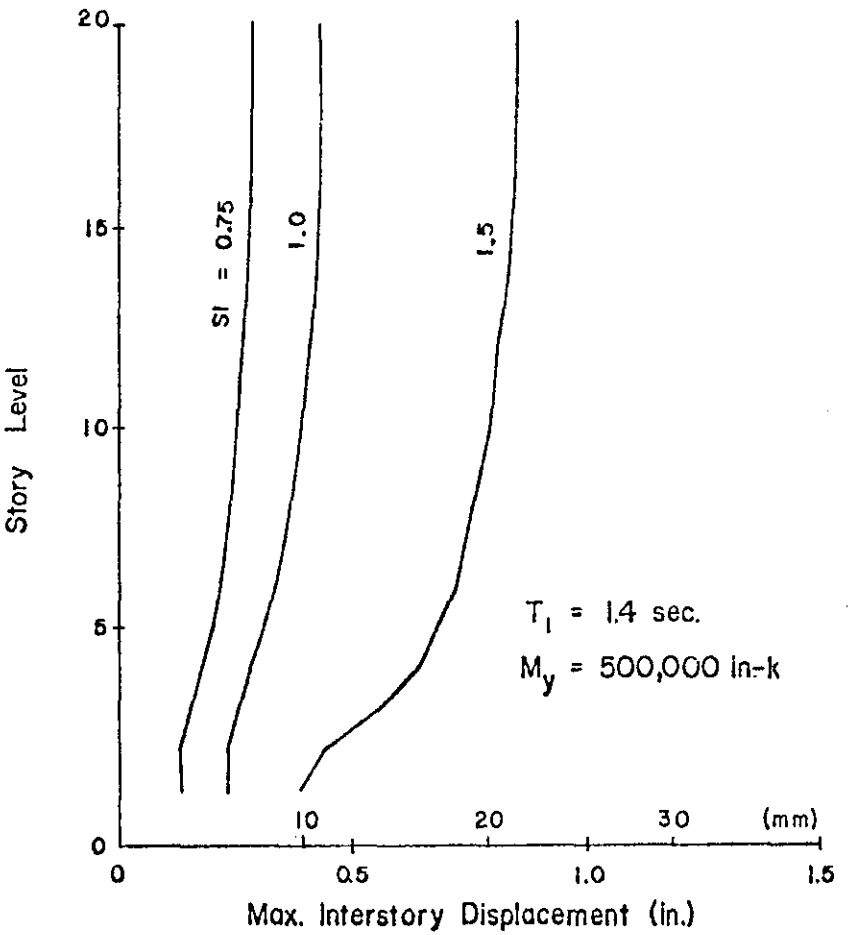

(b)

Fig. 35 Effect of Intensity of Ground Motion

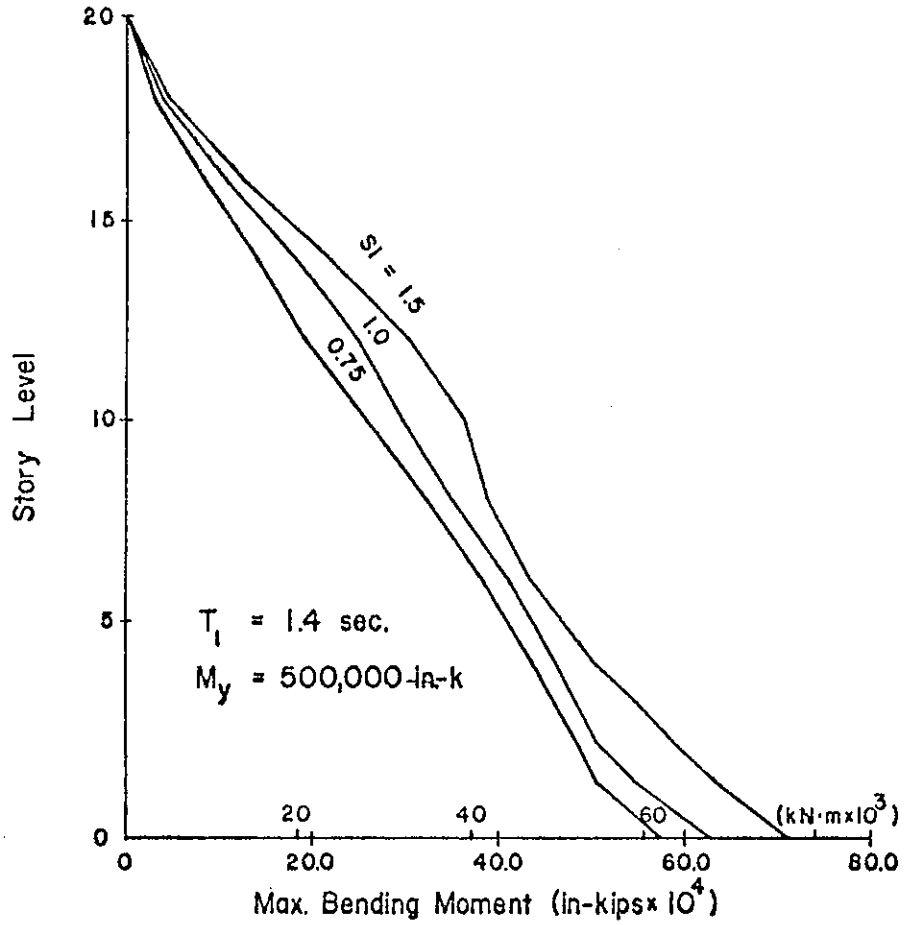

(c)

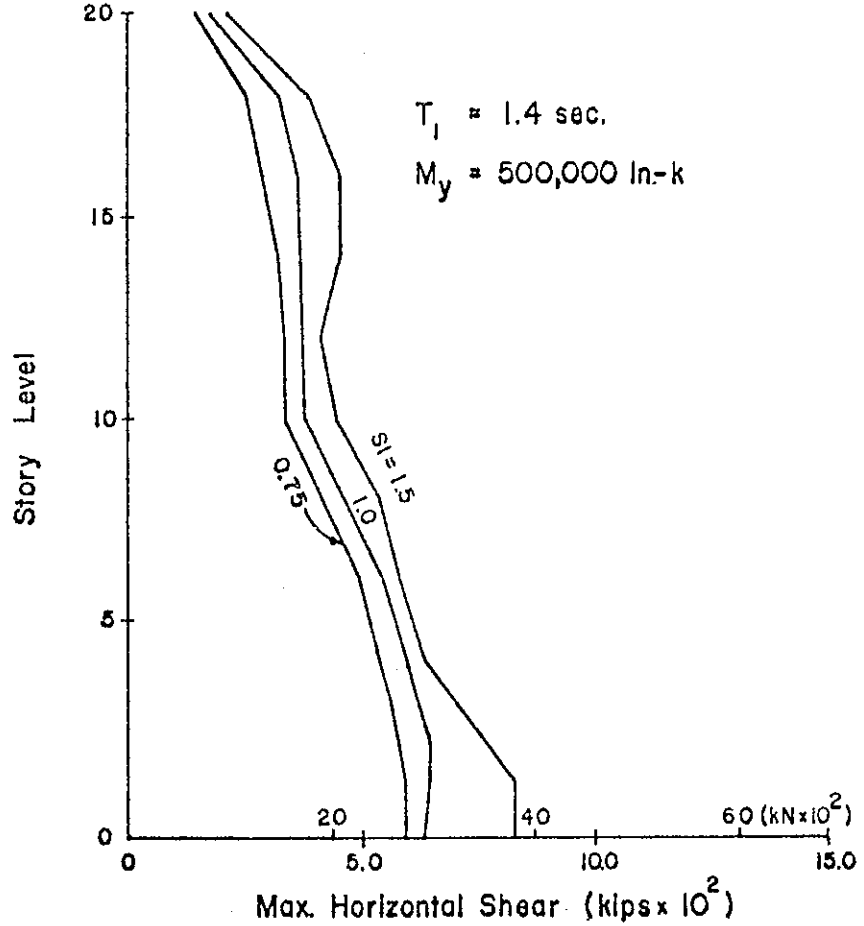

(d)

Fig. 35 (cont'd.) Effect of Intensity of Ground Motion

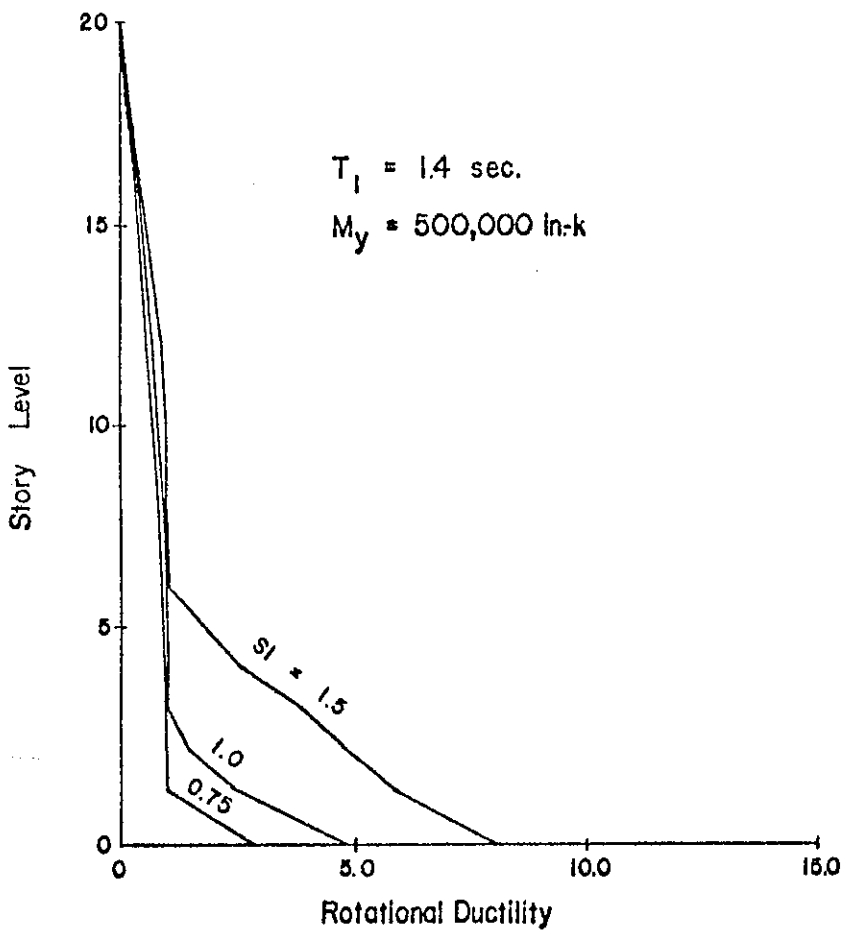

(e)

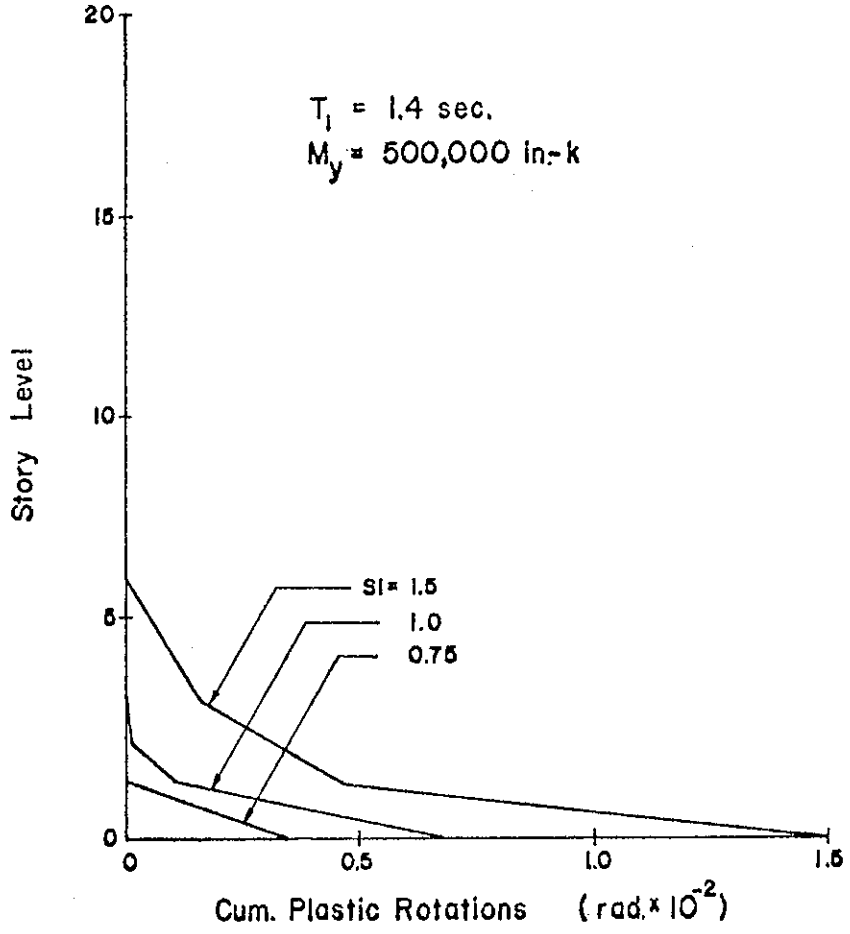

(f)

Fig. 35 (cont'd.) Effect of Intensity of Ground Motion

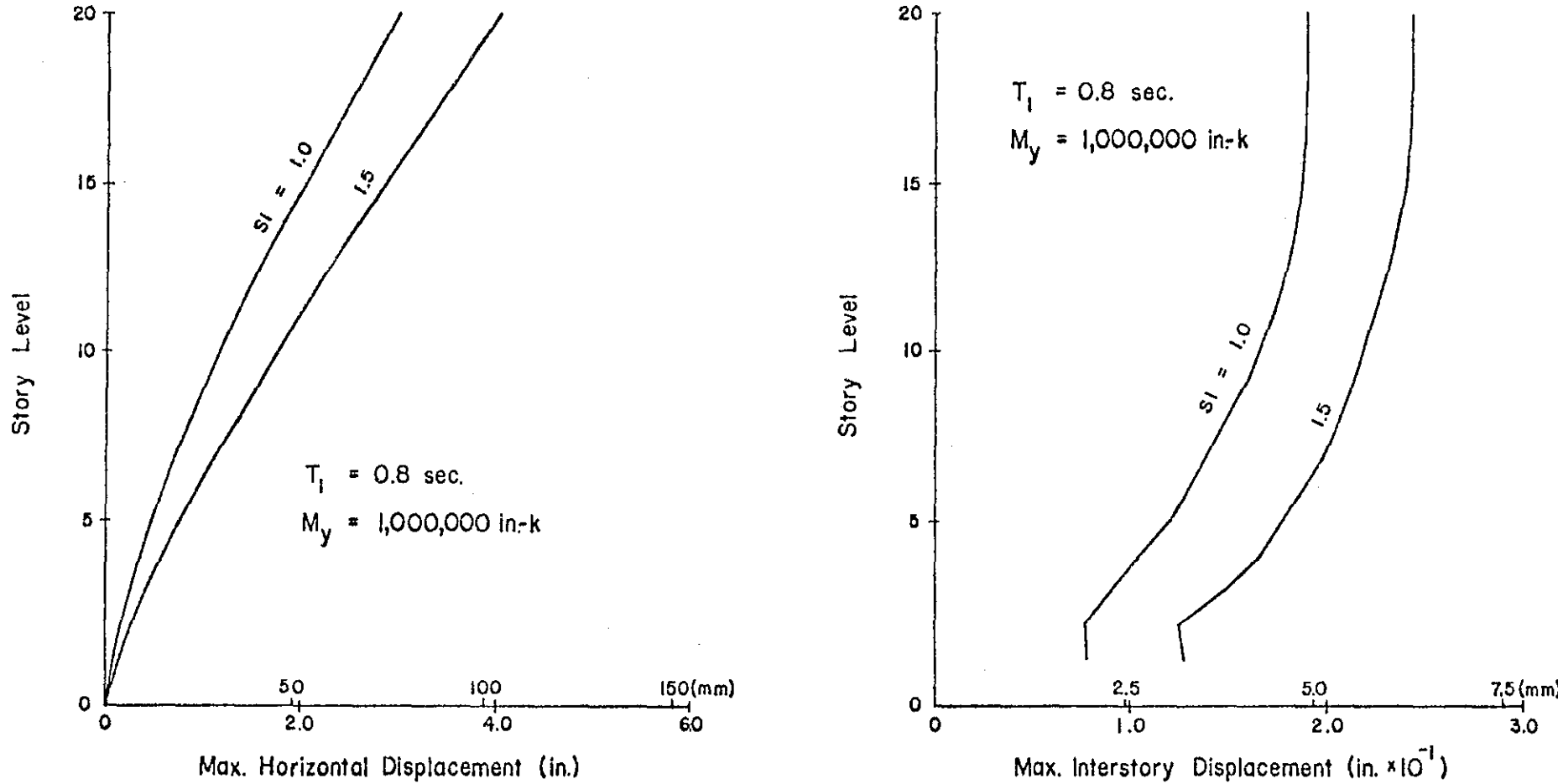

Fig. 36 Effect of Intensity of Ground Motion

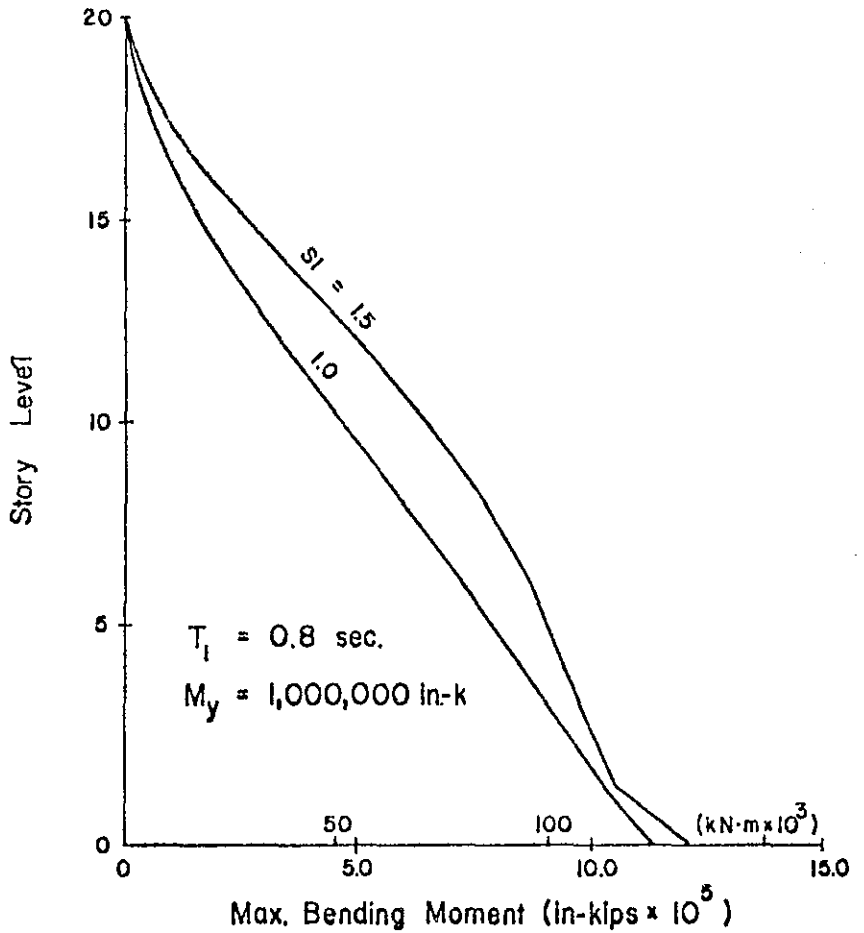

(c)

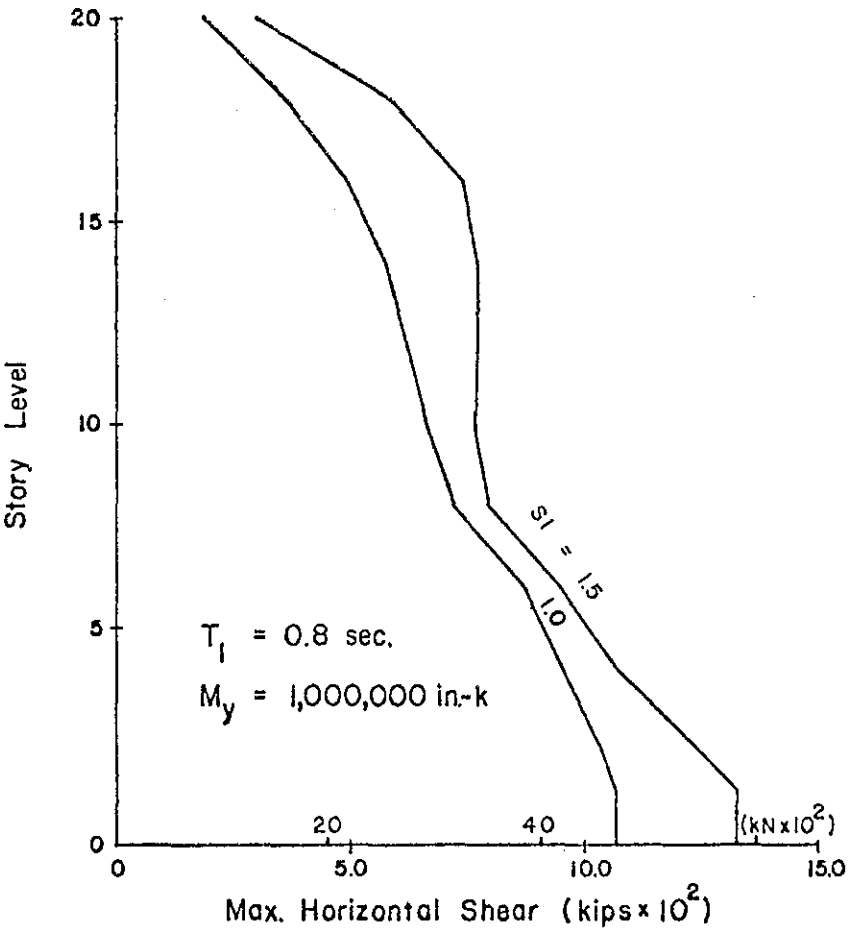

(d)

Fig. 36 (cont'd.) Effect of Intensity of Ground Motion

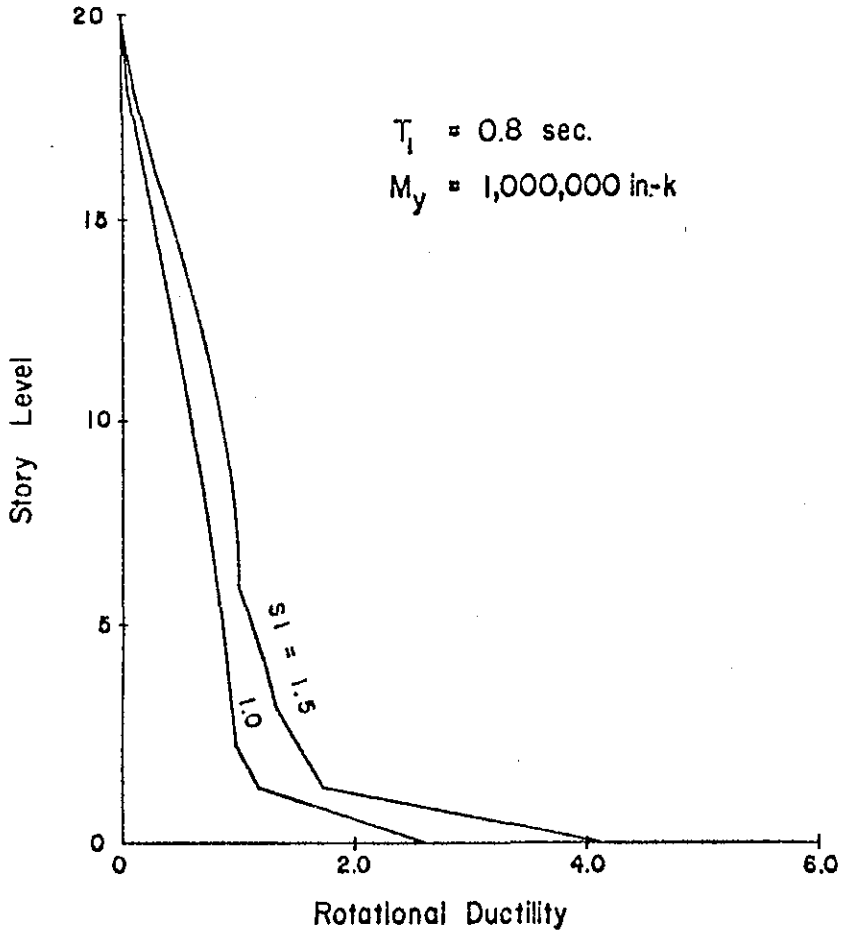

(e)

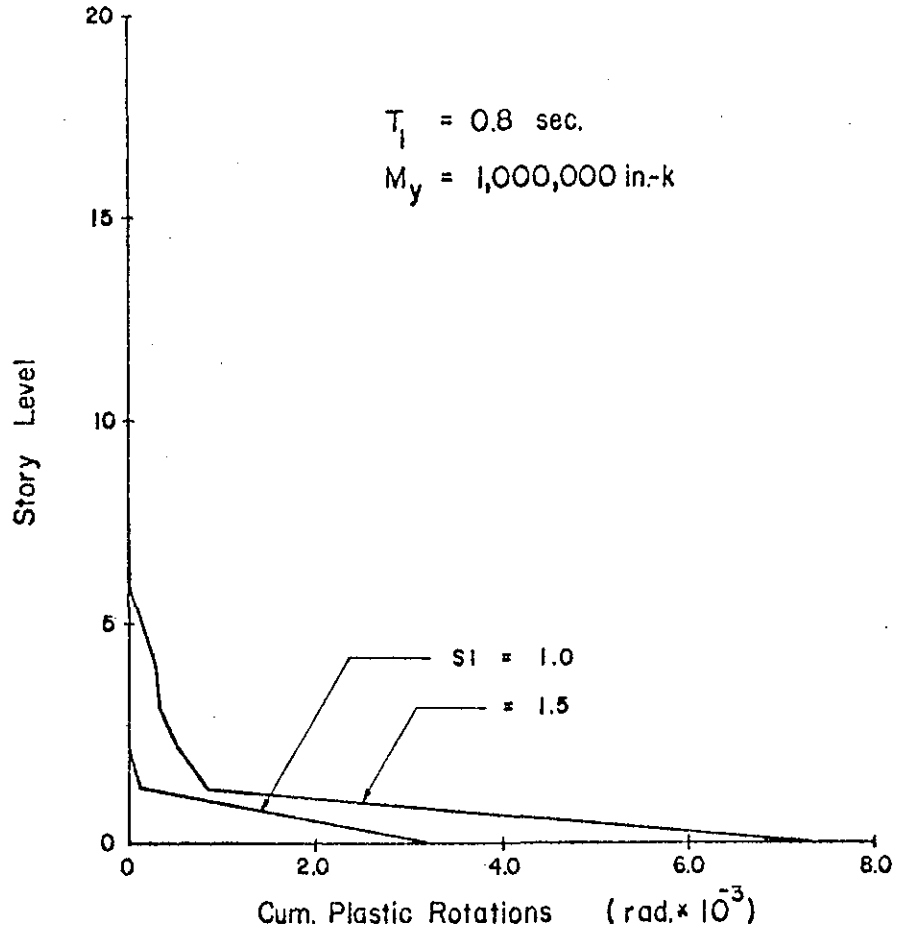

(f)

Fig. 36 (cont'd.) Effect of Intensity of Ground Motion

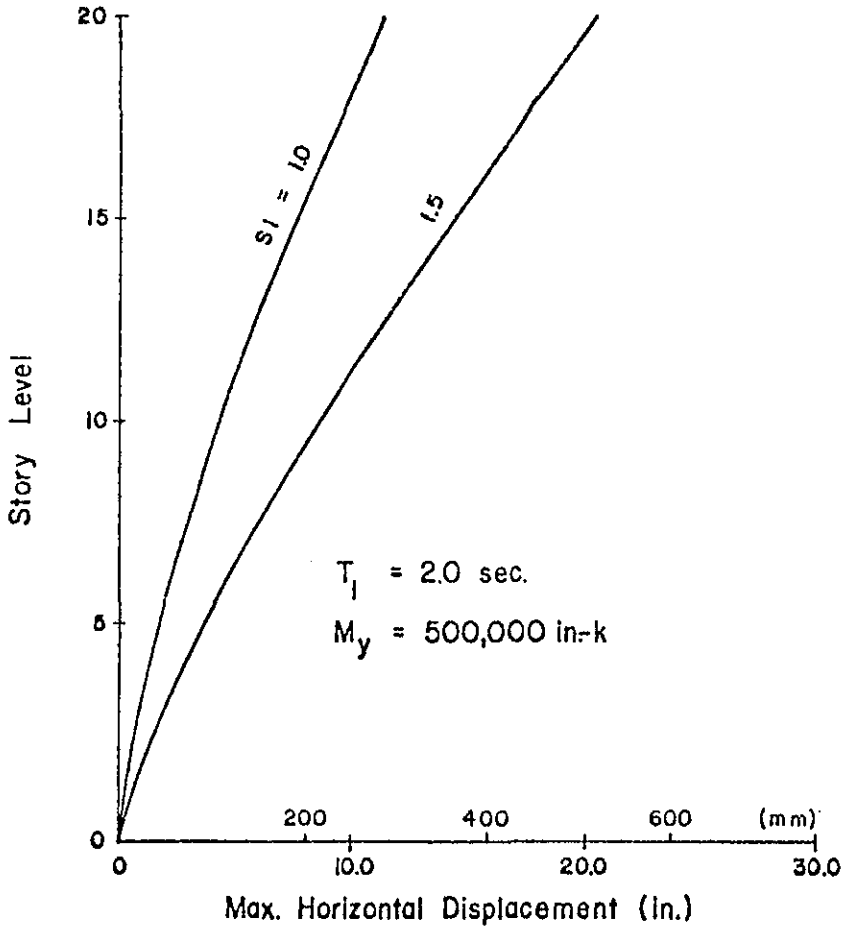

(a)

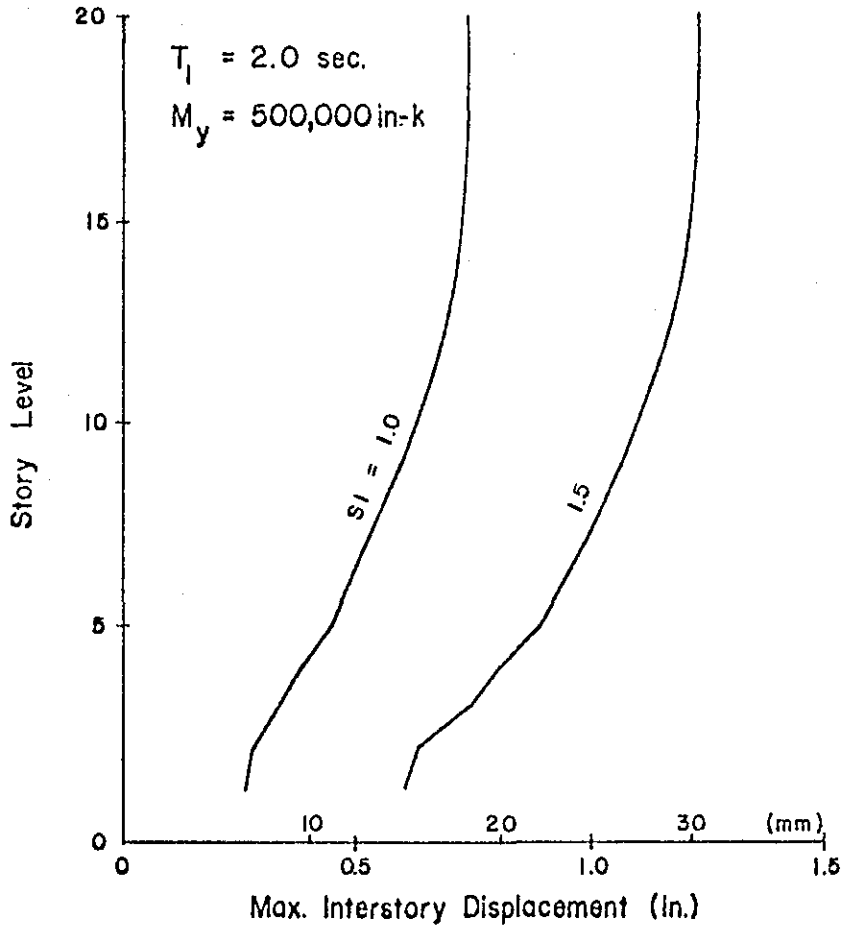

(b)

Fig. 37 Effect of Intensity of Ground Motion

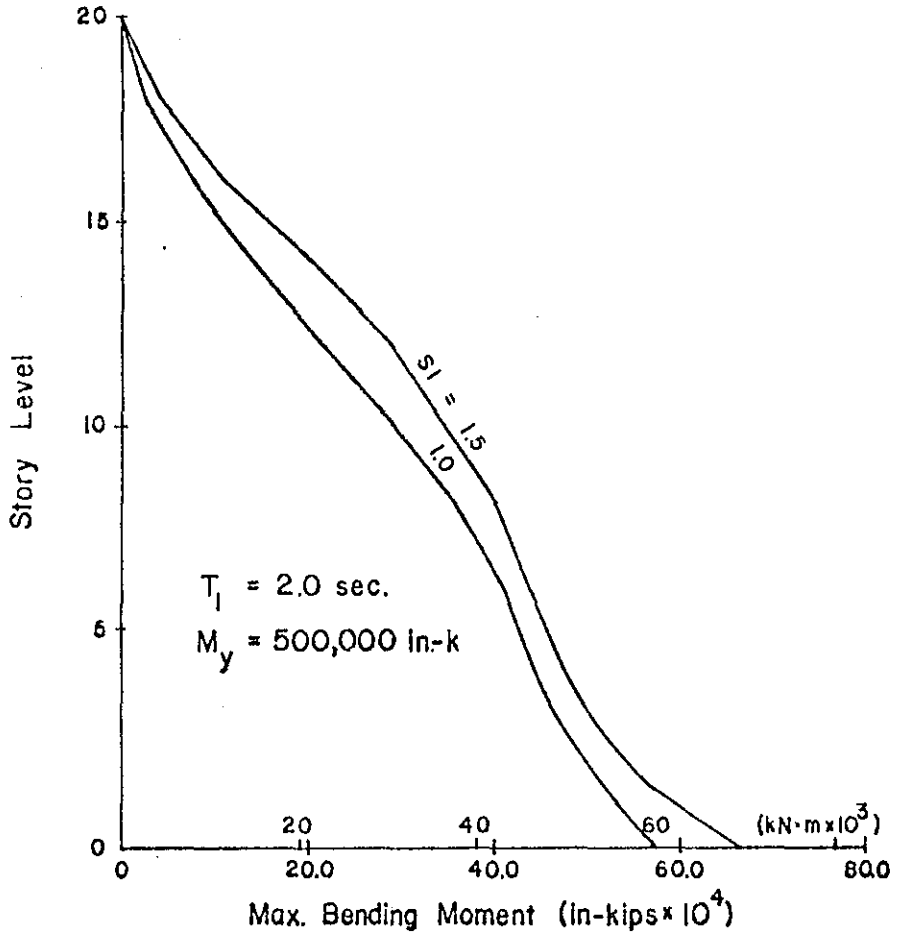

(c)

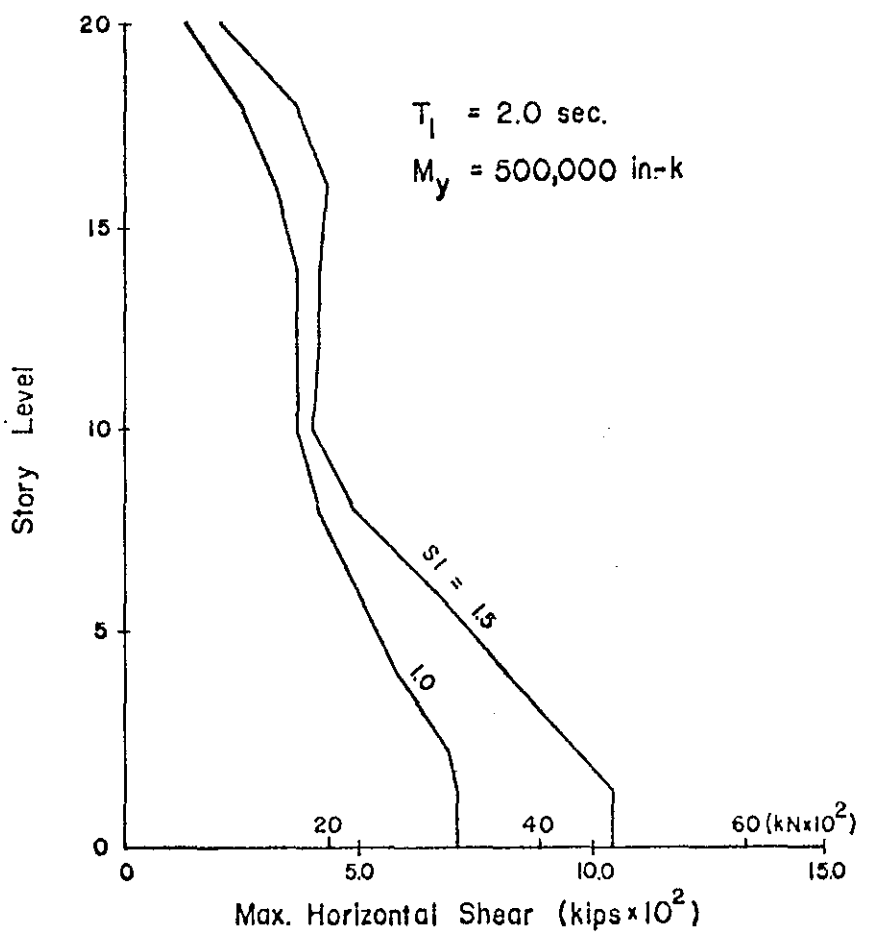

(d)

Fig. 37 (cont'd.) Effect of Intensity of Ground Motion

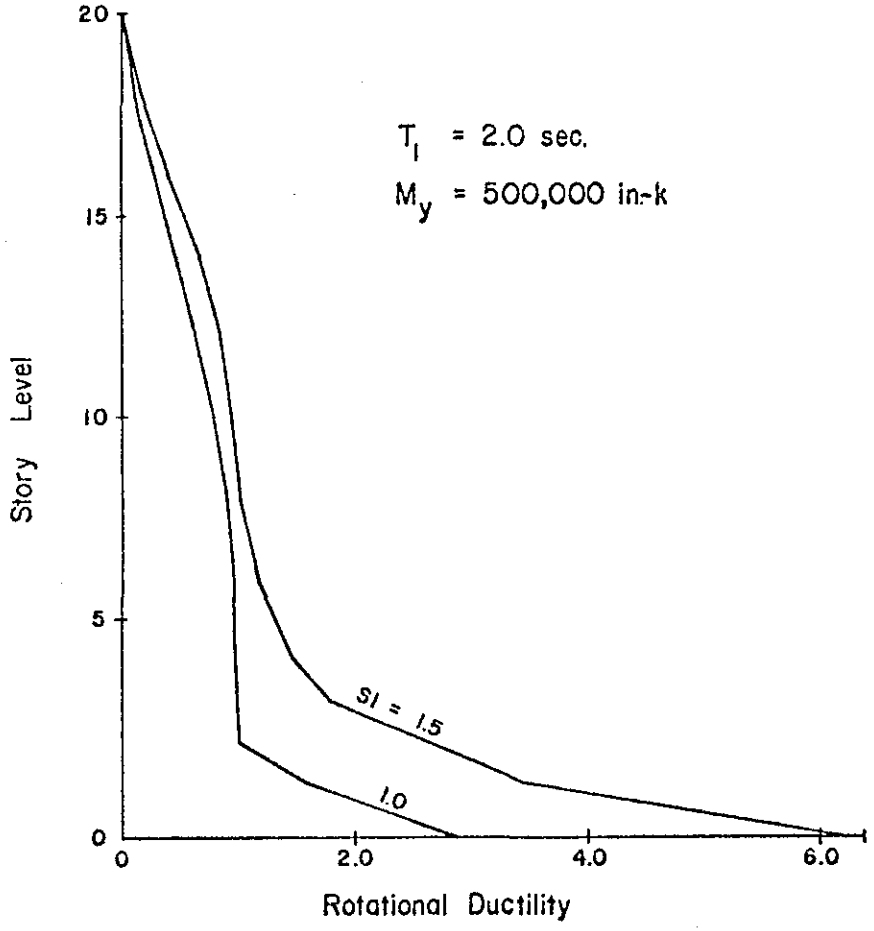

(e)

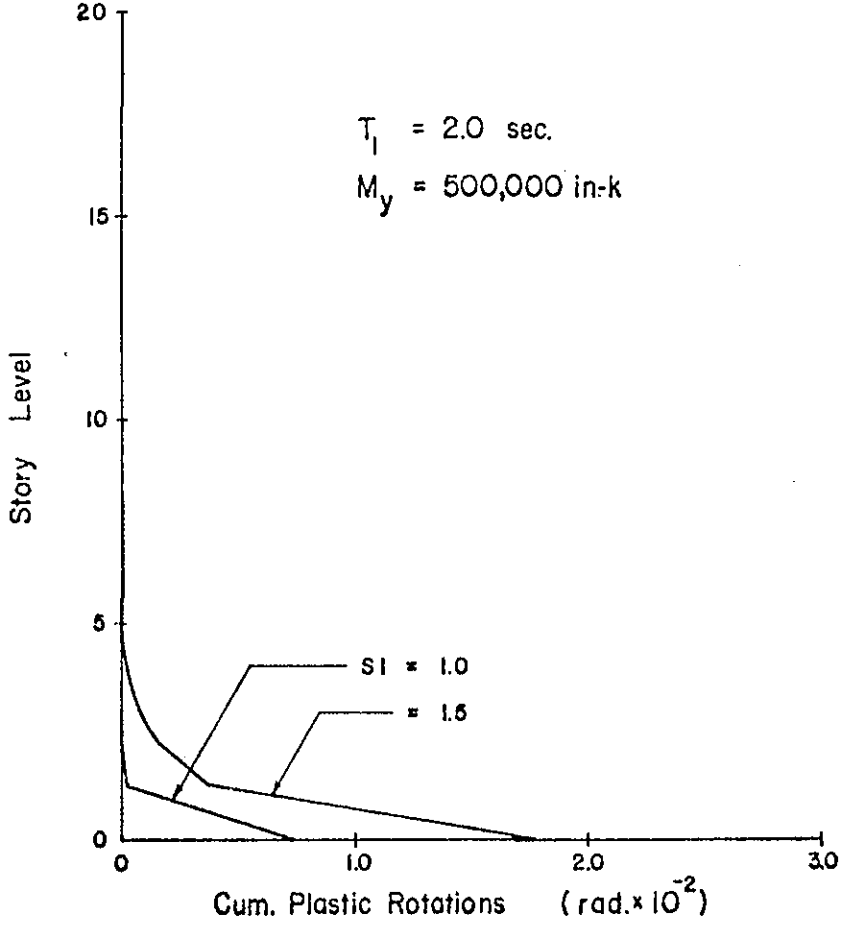

(f)

Fig. 37 (cont'd.) Effect of Intensity of Ground Motion

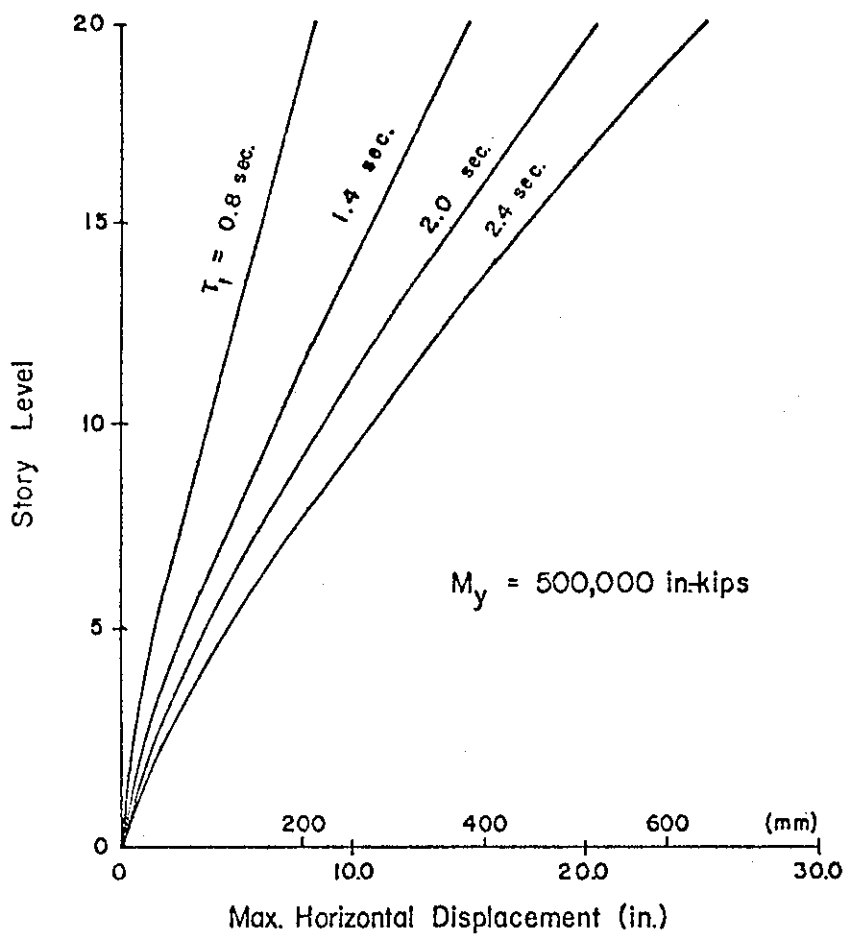

(a)

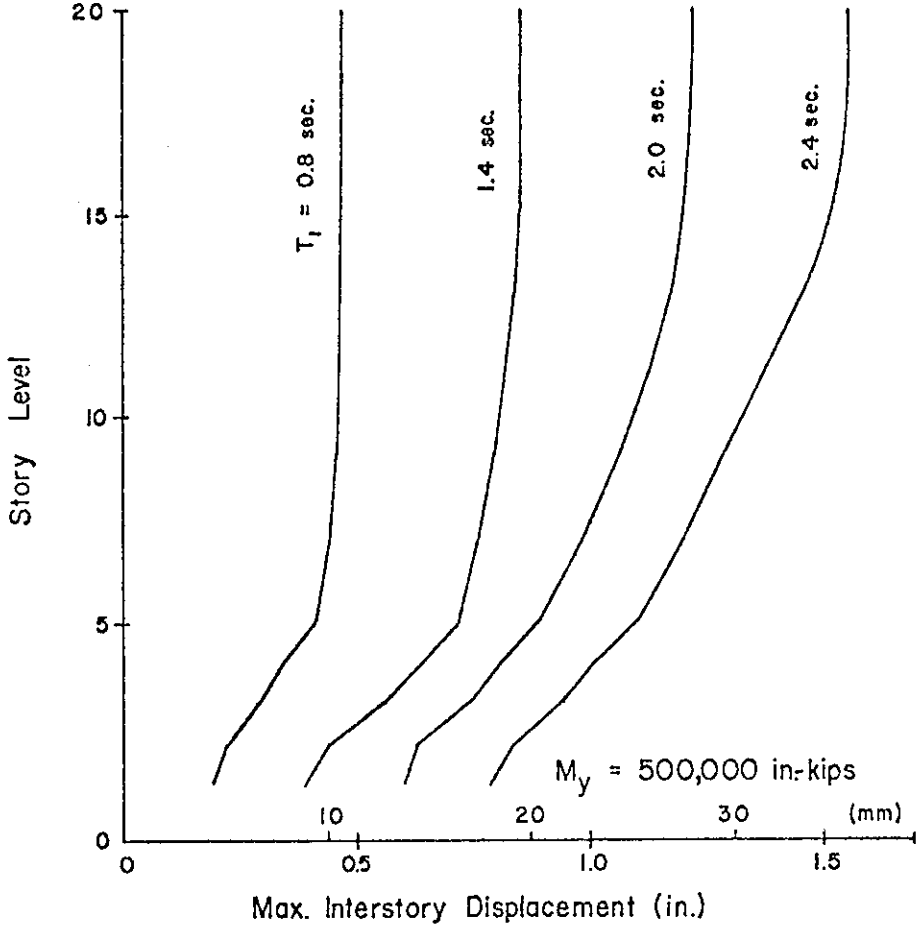

(b)

Fig. 38 Effect of Fundamental Period of Vibration, T_1

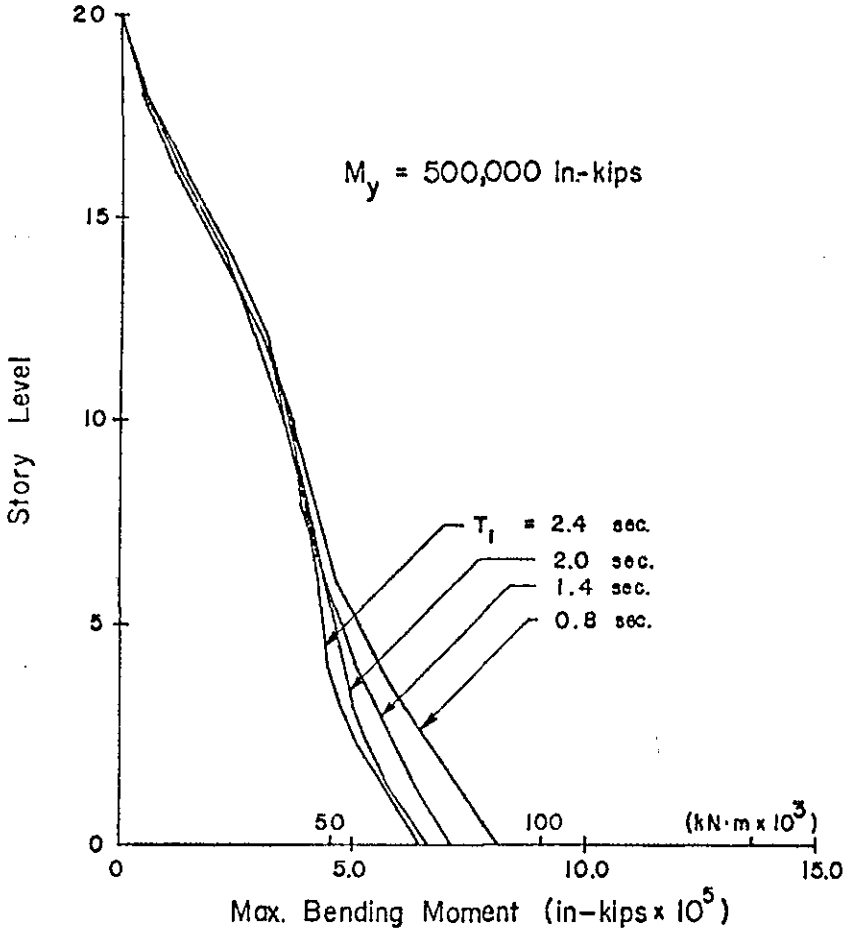

(c)

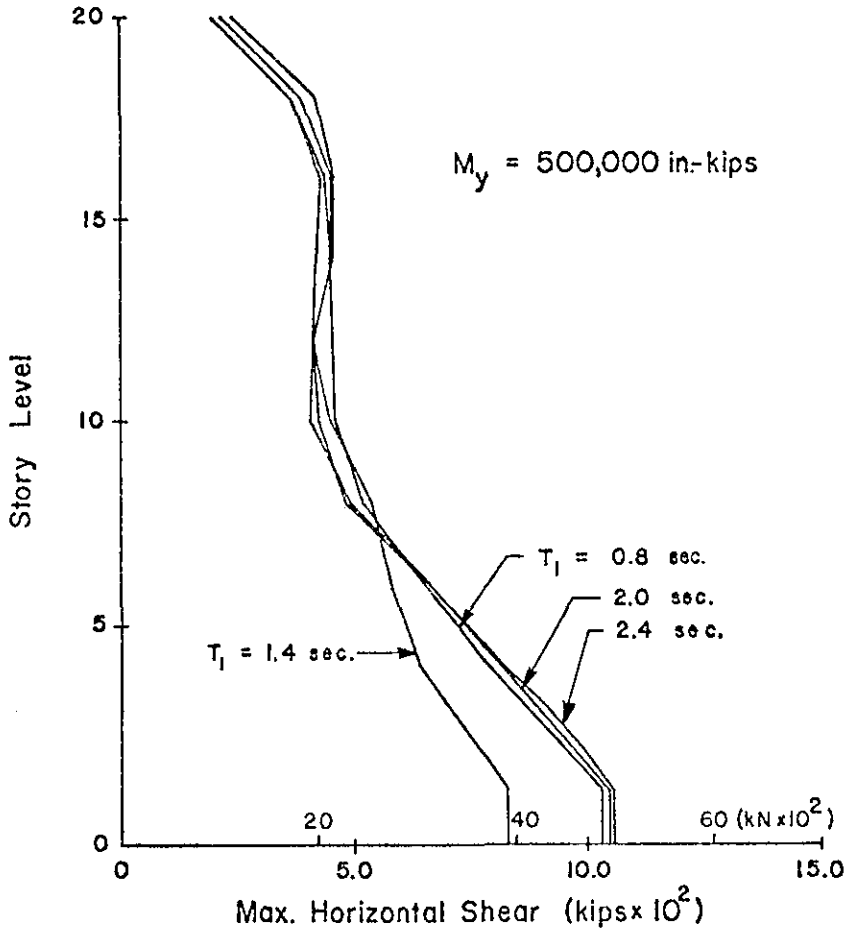

(d)

Fig. 38 (cont'd.) Effect of Fundamental Period of Vibration, T_1

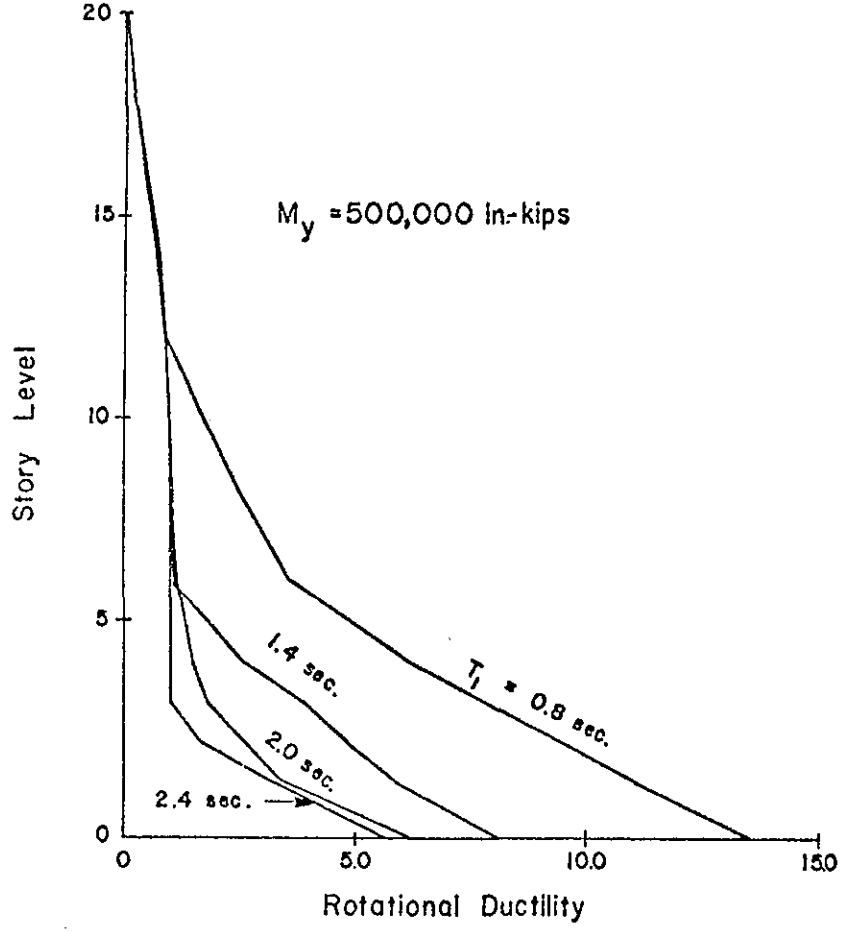

(e)

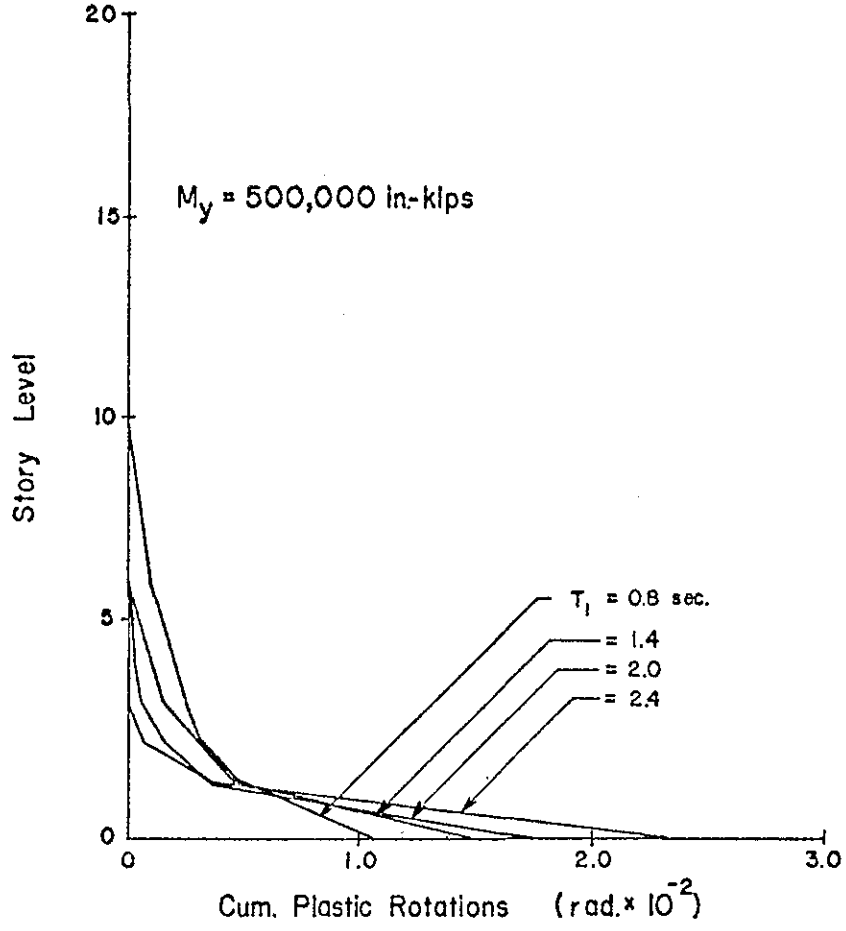

(f)

Fig. 38 (cont'd.) Effect of Fundamental Period of Vibration, T_1

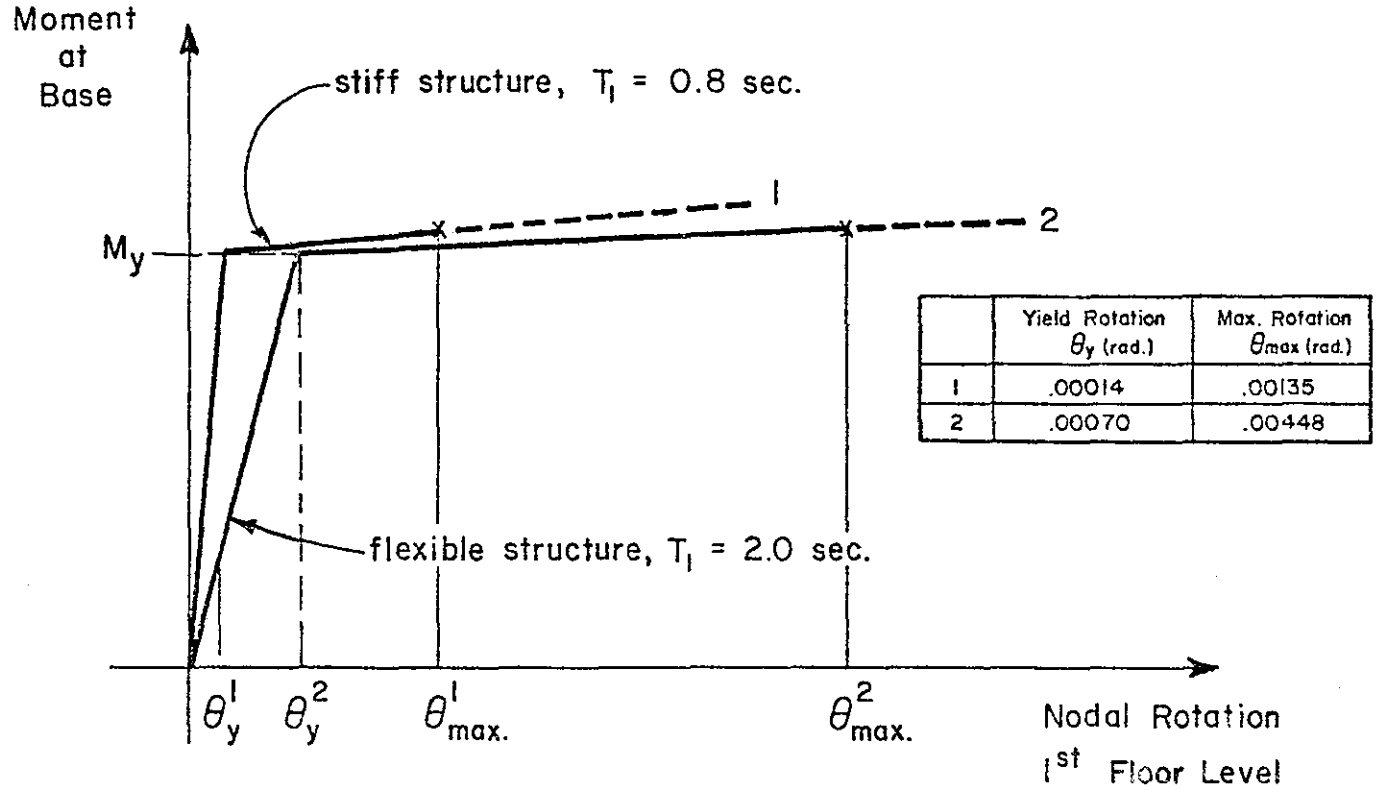

	Yield Rotation θ_y (rad.)	Max. Rotation θ_{max} (rad.)
1	.00014	.00135
2	.00070	.00448

MEASURES OF DEFORMATION

Ductility Ratio vs. Absolute Rotations

$$M_1 = \frac{\theta_{max.}^1}{\theta_y^1} = 9.6$$

$$M_2 = \frac{\theta_{max.}^2}{\theta_y^2} = 6.4$$

but note that:

$$\theta_{max.}^2 = 3.3\ \theta_{max.}^1$$

Fig. 39 Rotational Ductility Ratio versus Maximum Absolute Rotation as Measures of Deformation

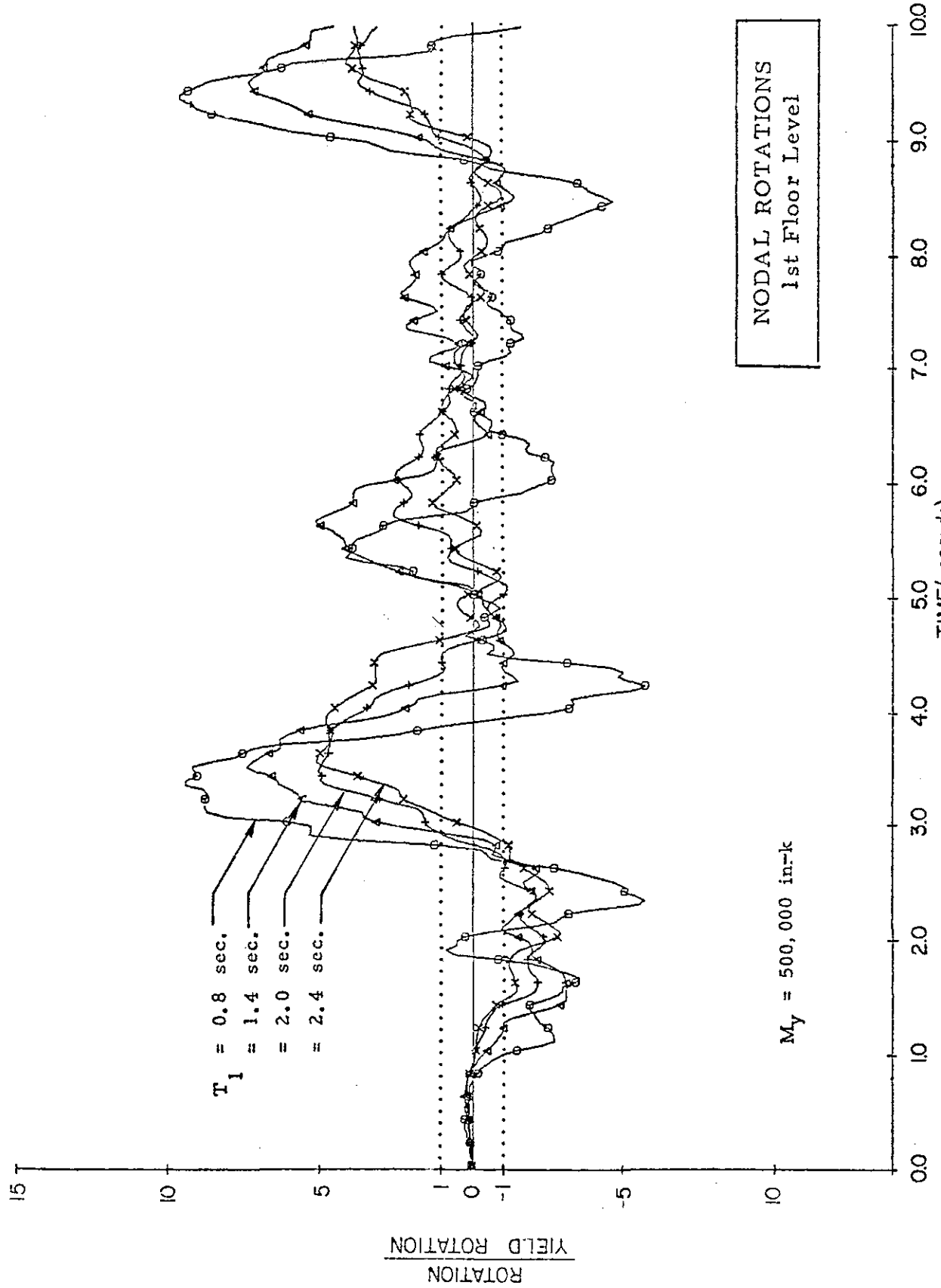

Fig. 40a Normalized Rotations in First Story versus Time for Different Values of Fundamental Period, T_1

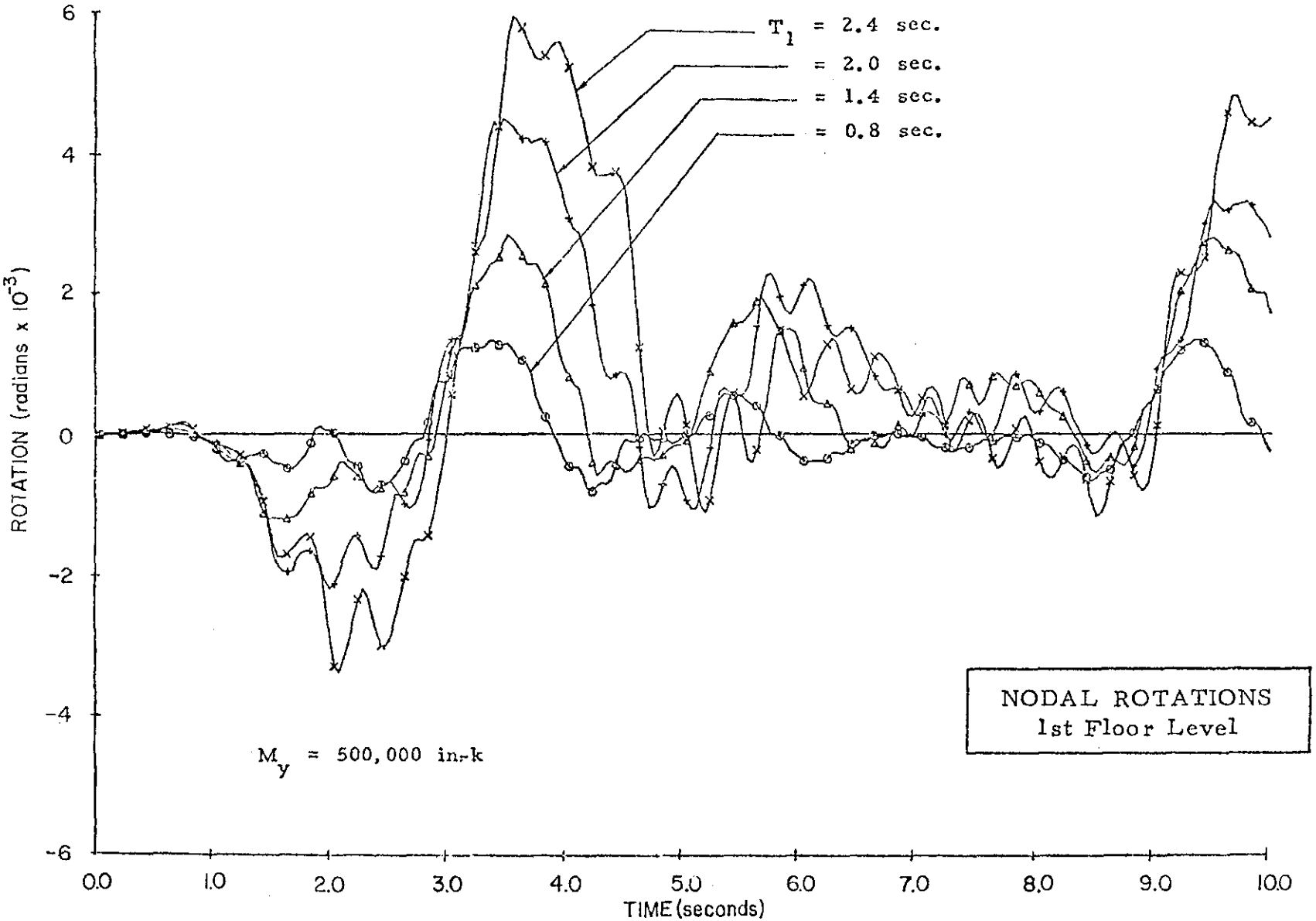

Fig. 40b Actual Values of Rotation in First Story versus Time for Different Values of Fundamental Period, T_1

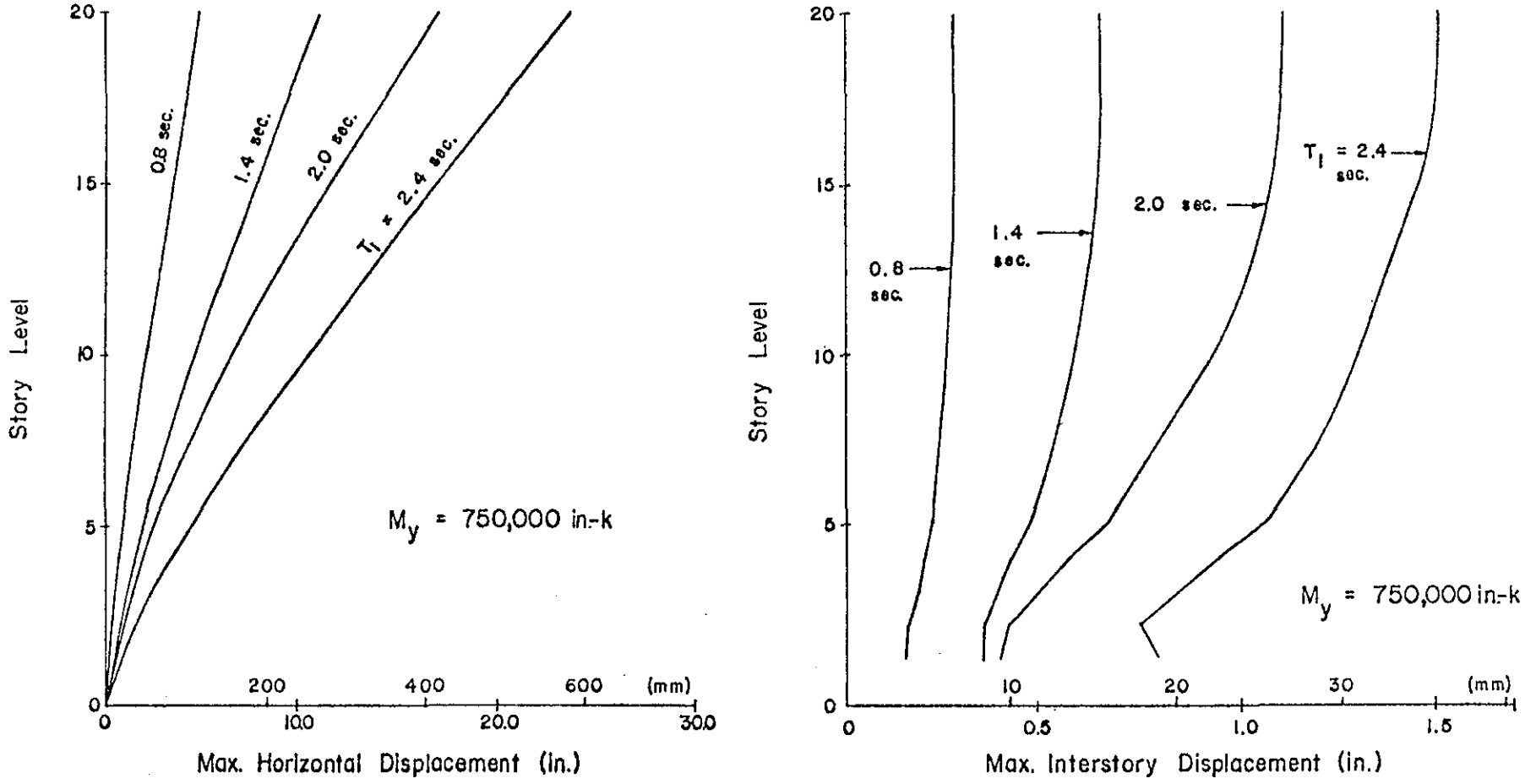

Fig. 41 Effect of Fundamental Period of Vibration, T_1

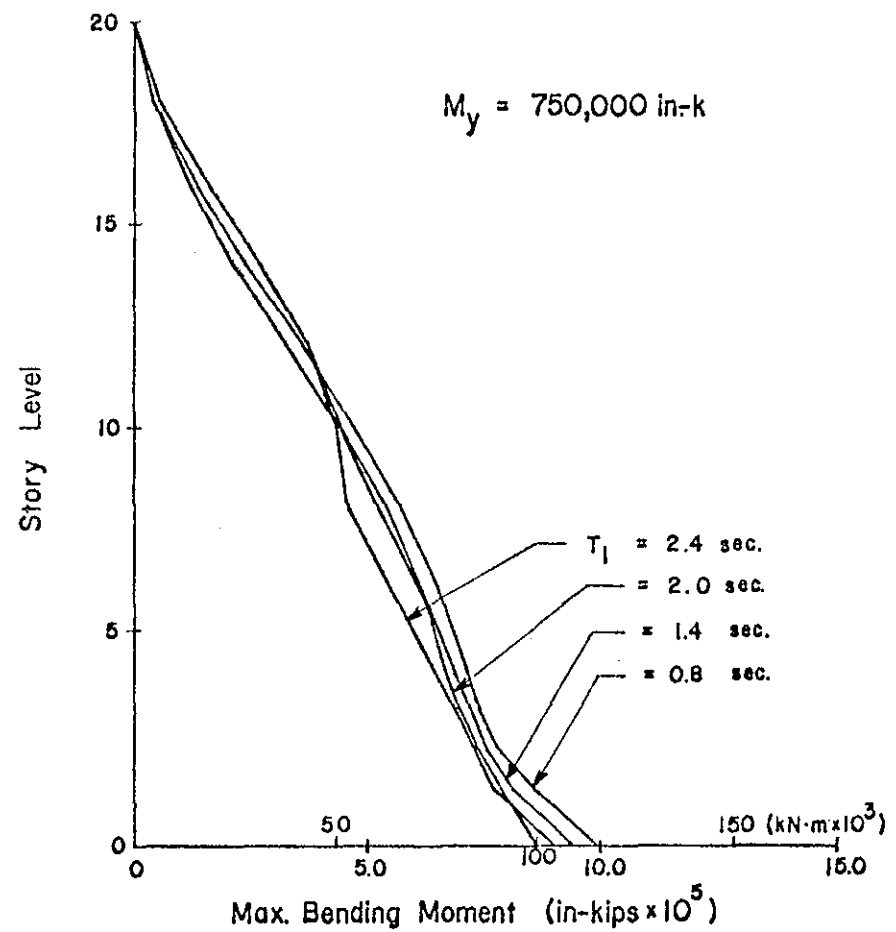

(c)

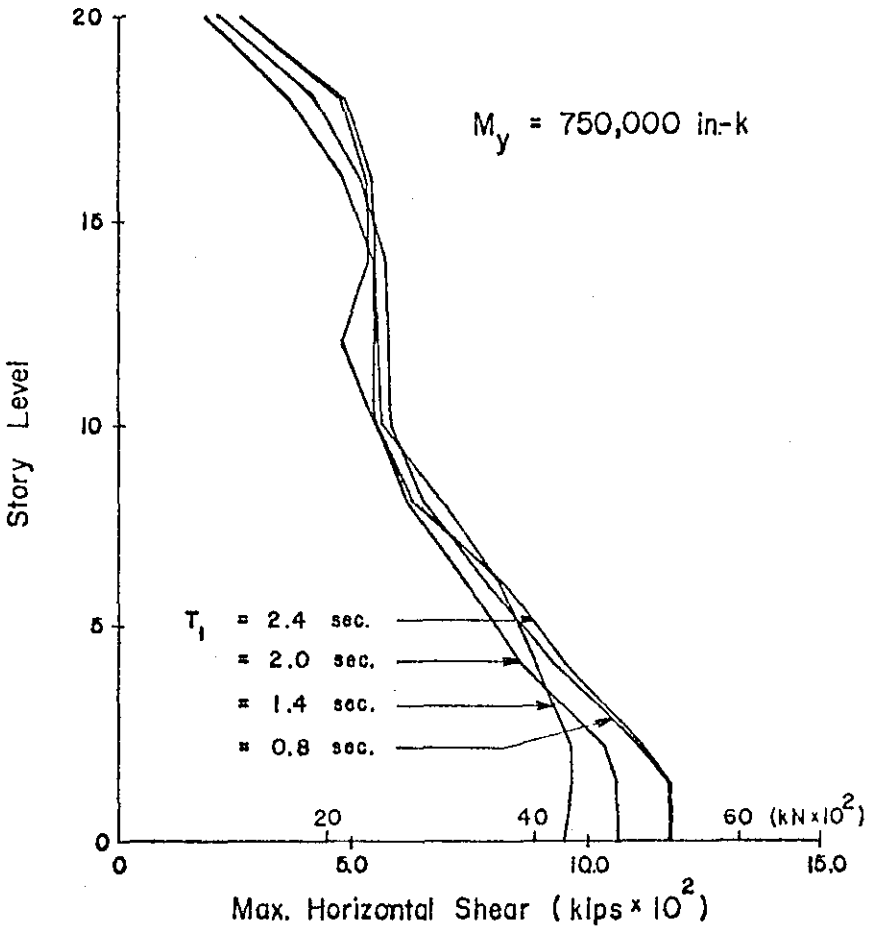

(d)

Fig. 41 (cont'd.) Effect of Fundamental Period of Vibration, T_1

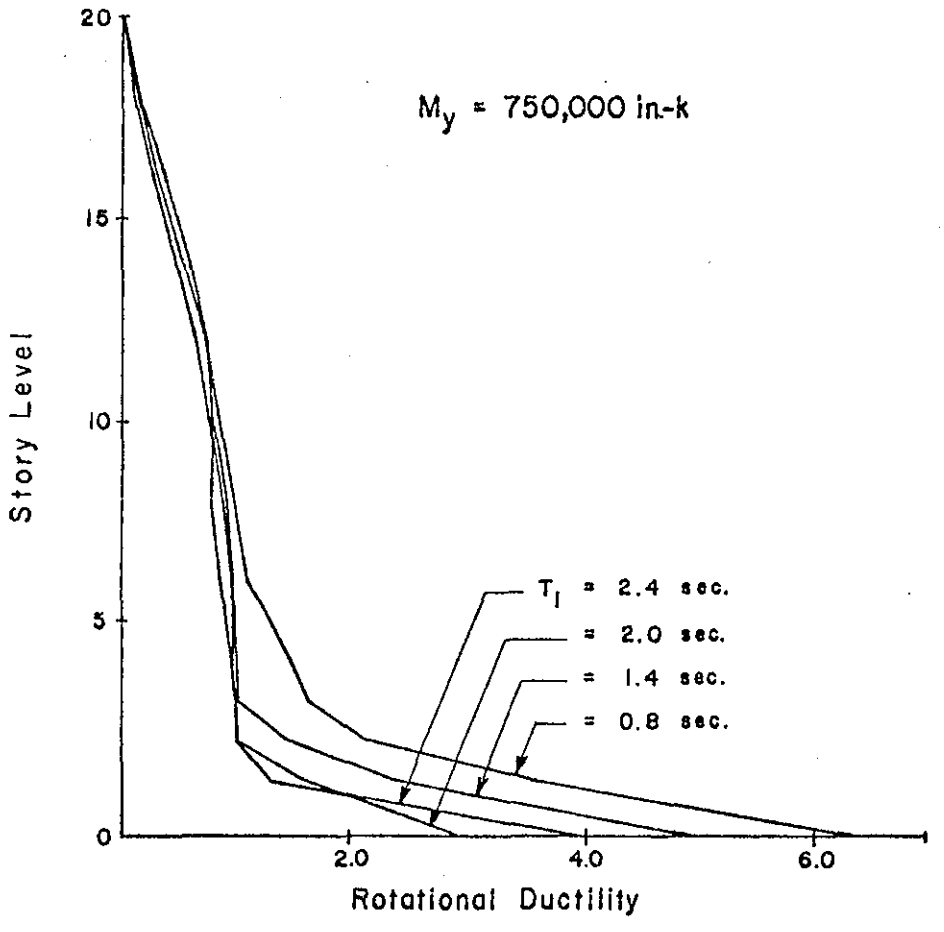

(e)

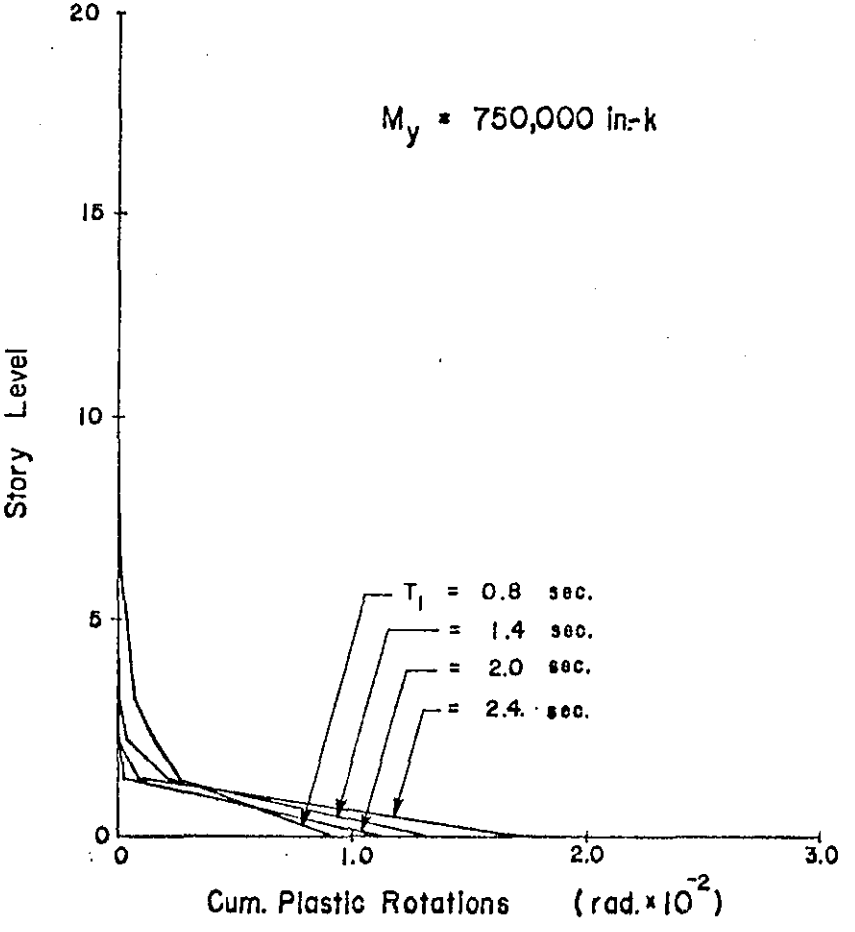

(f)

Fig. 41 (cont'd.) Effect of Fundamental Period of Vibration, T_1

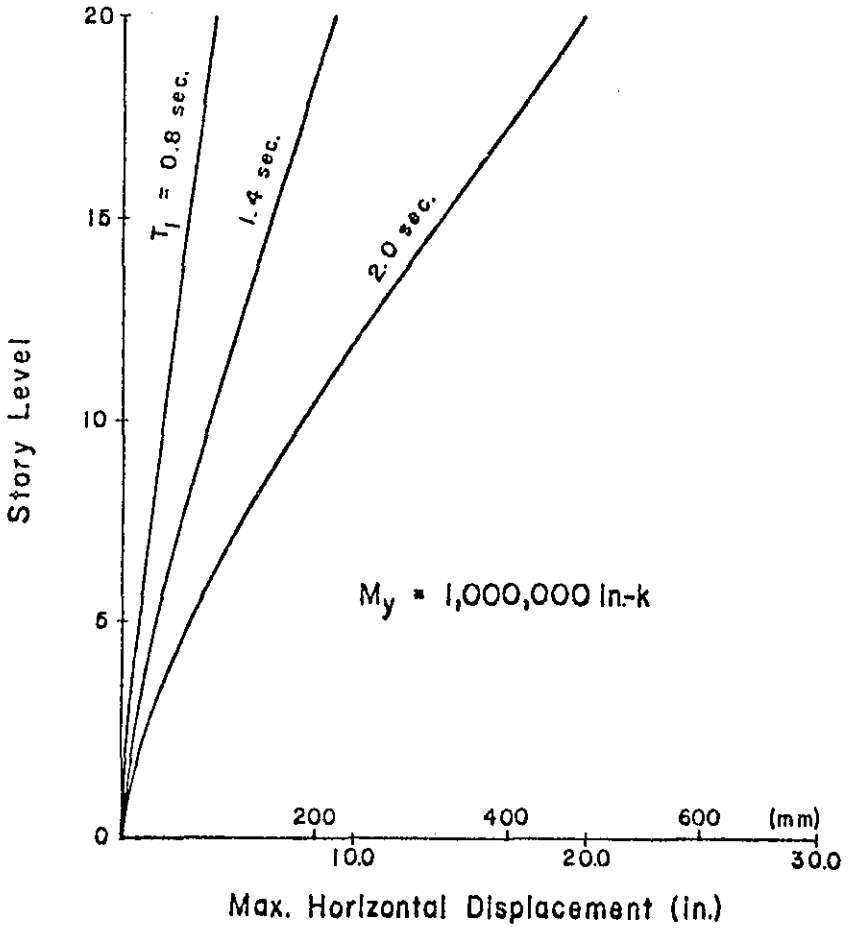

(a)

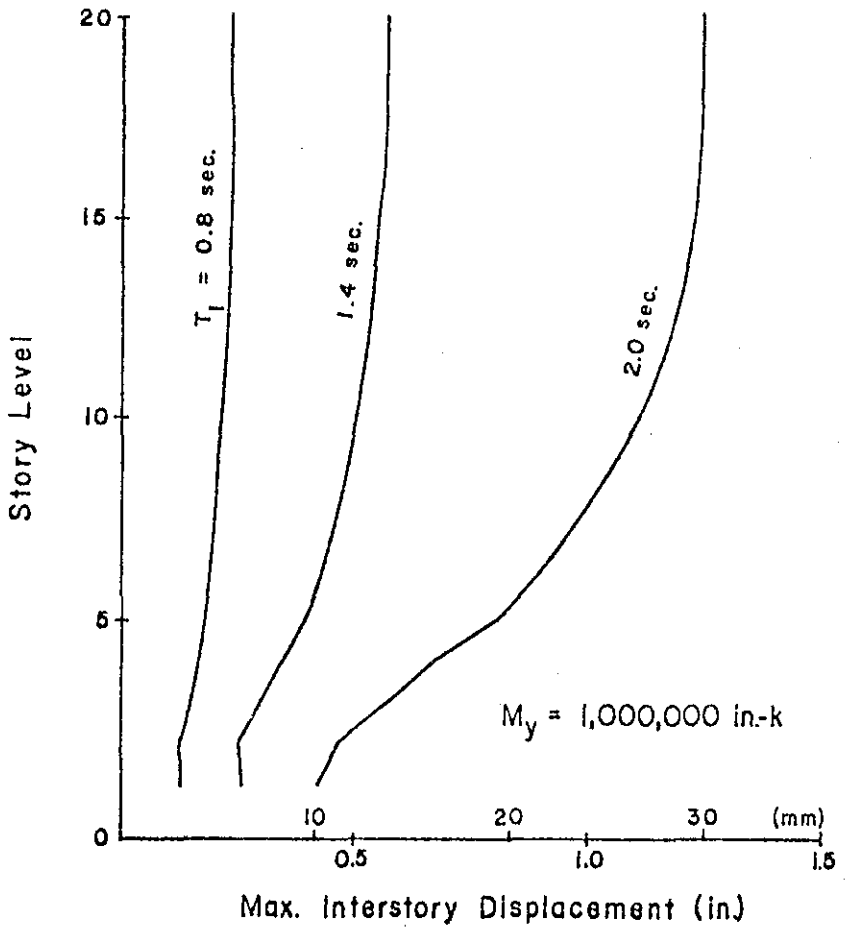

(b)

Fig. 42 Effect of Fundamental Period of Vibration, T_1

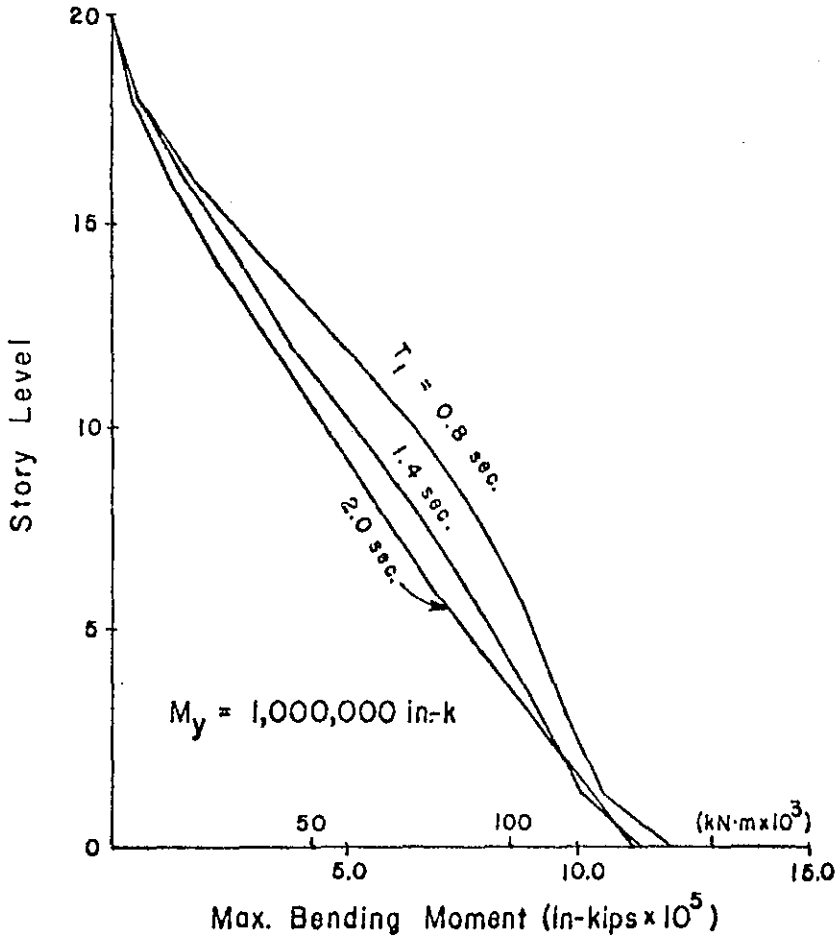

(c)

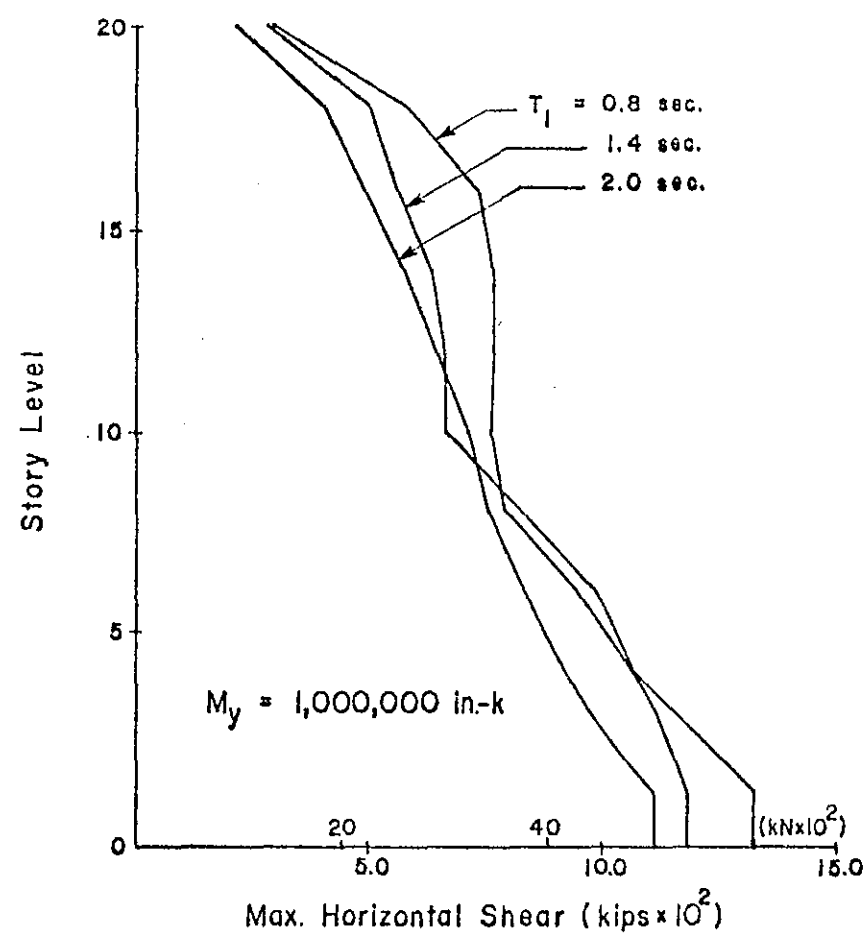

(d)

Fig. 42 (cont'd.) Effect of Fundamental Period of Vibration, T_1

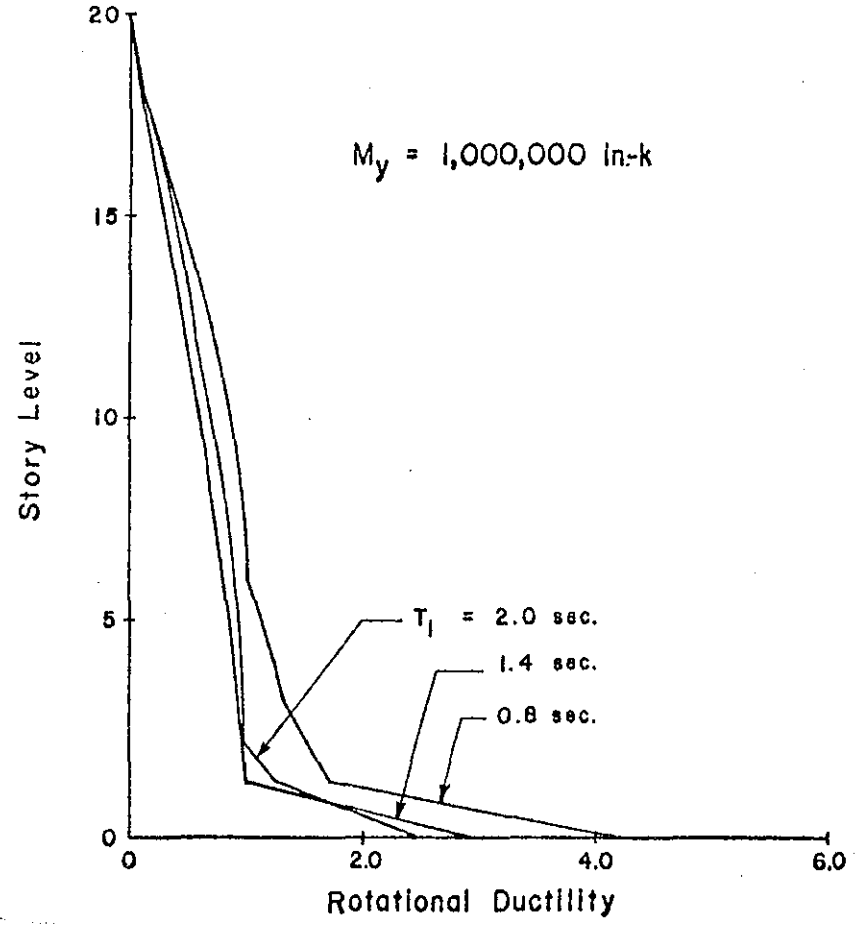

(e)

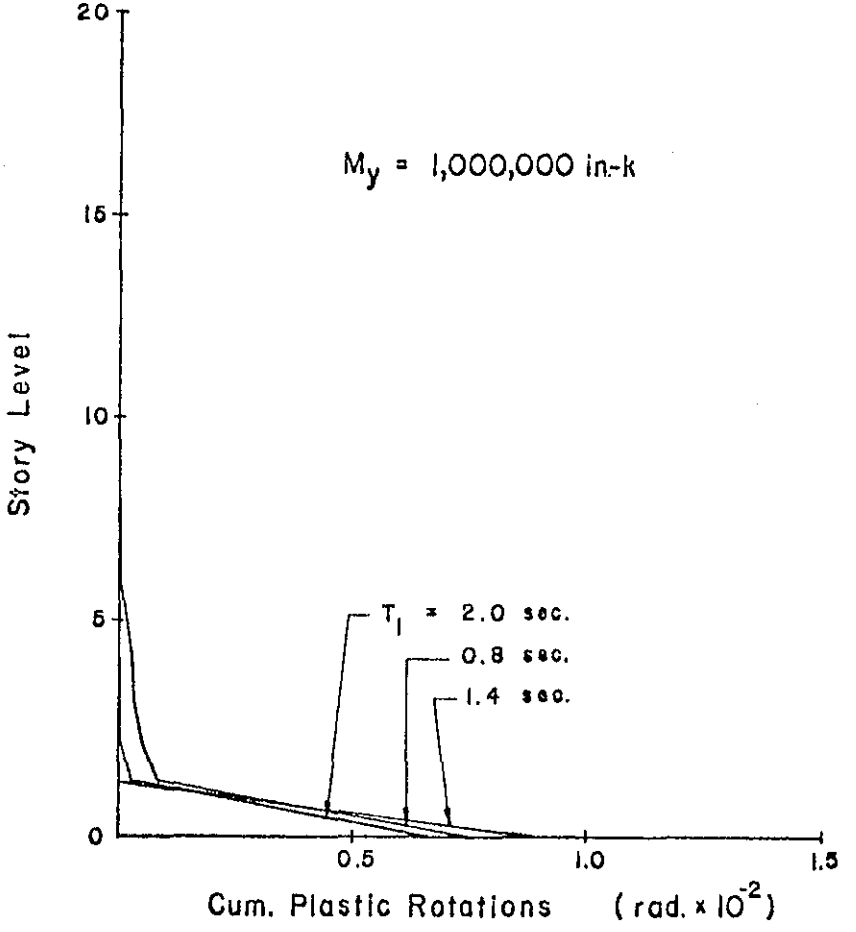

(f)

Fig. 42 (cont'd.) Effect of Fundamental Period of Vibration, T_1

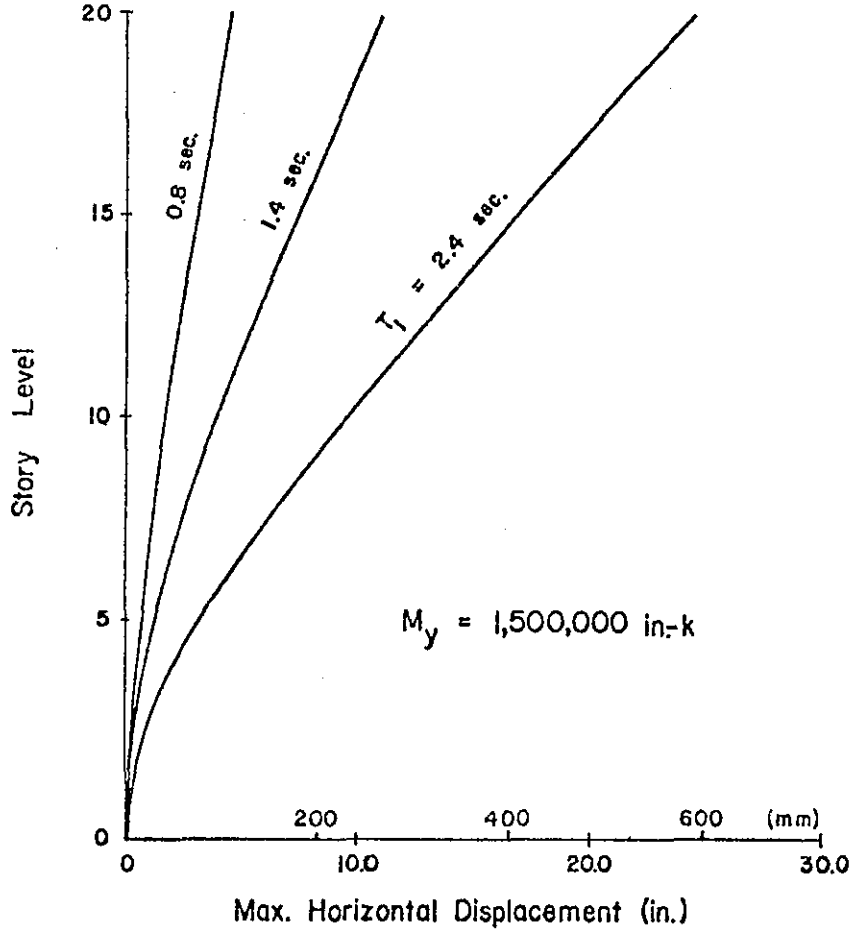

(a)

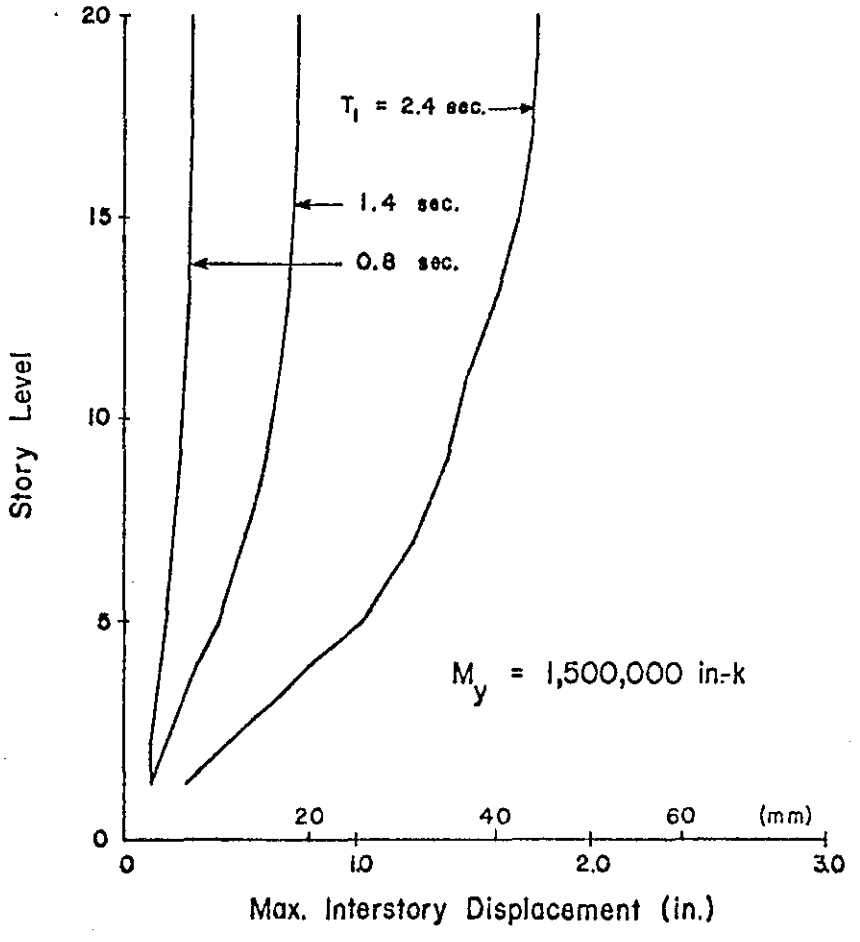

(b)

Fig. 43 Effect of Fundamental Period of Vibration, T_1

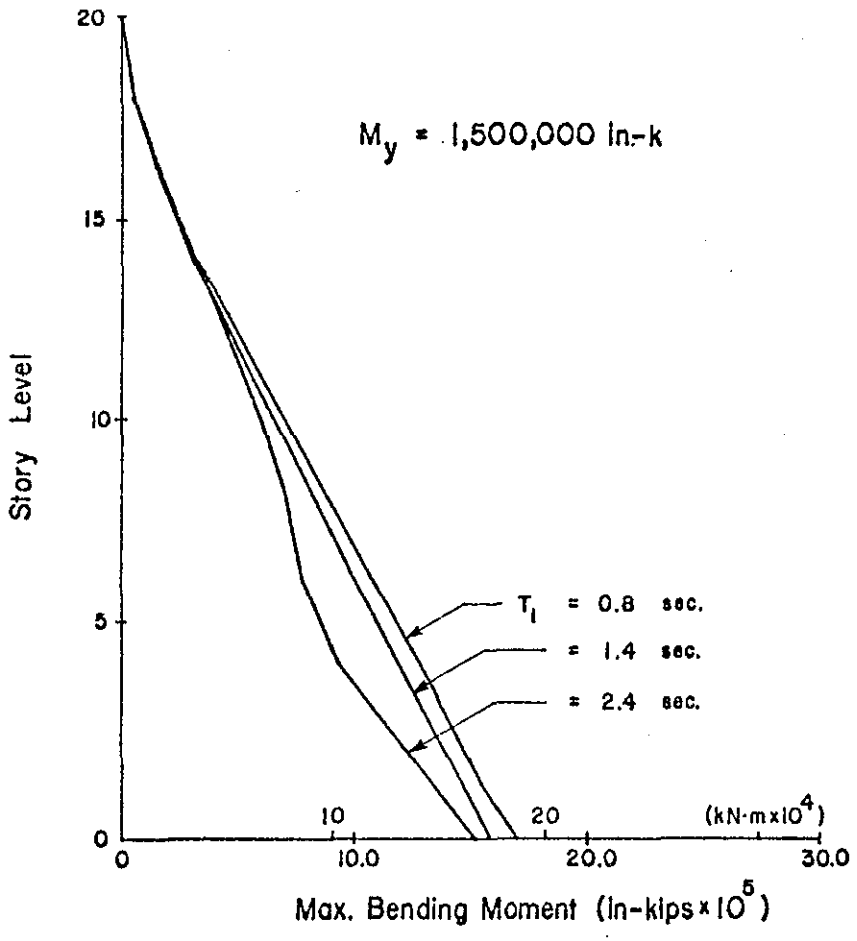

(c)

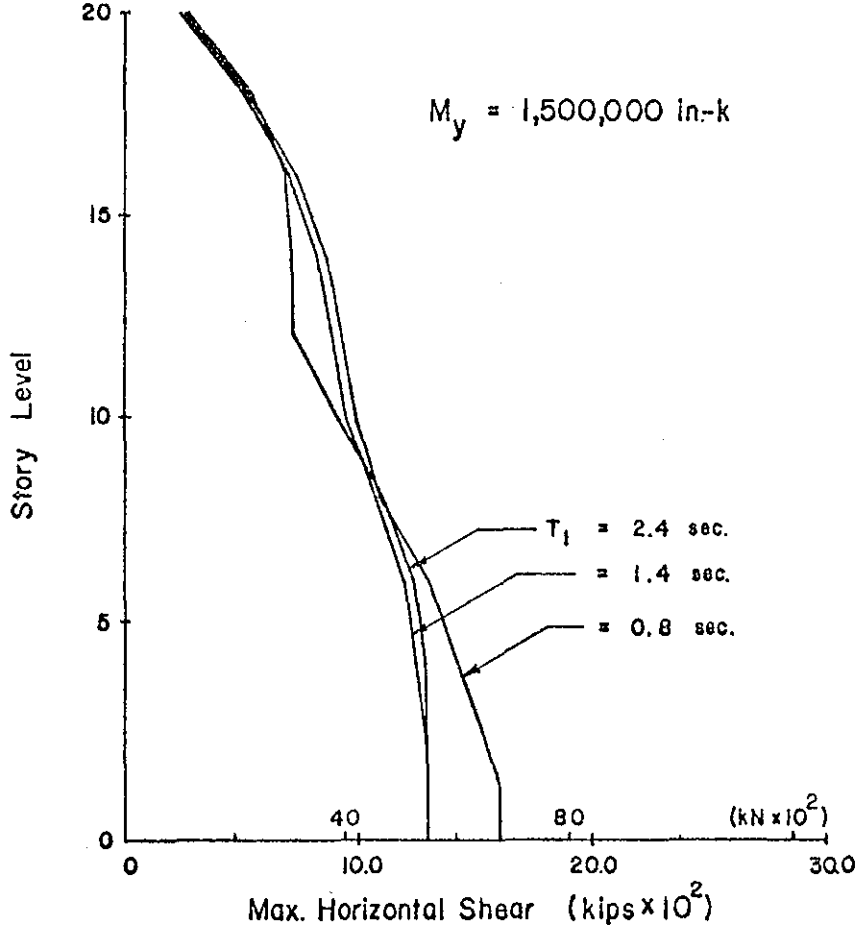

(d)

Fig. 43 (cont'd.) Effect of Fundamental Period of Vibration, T_1

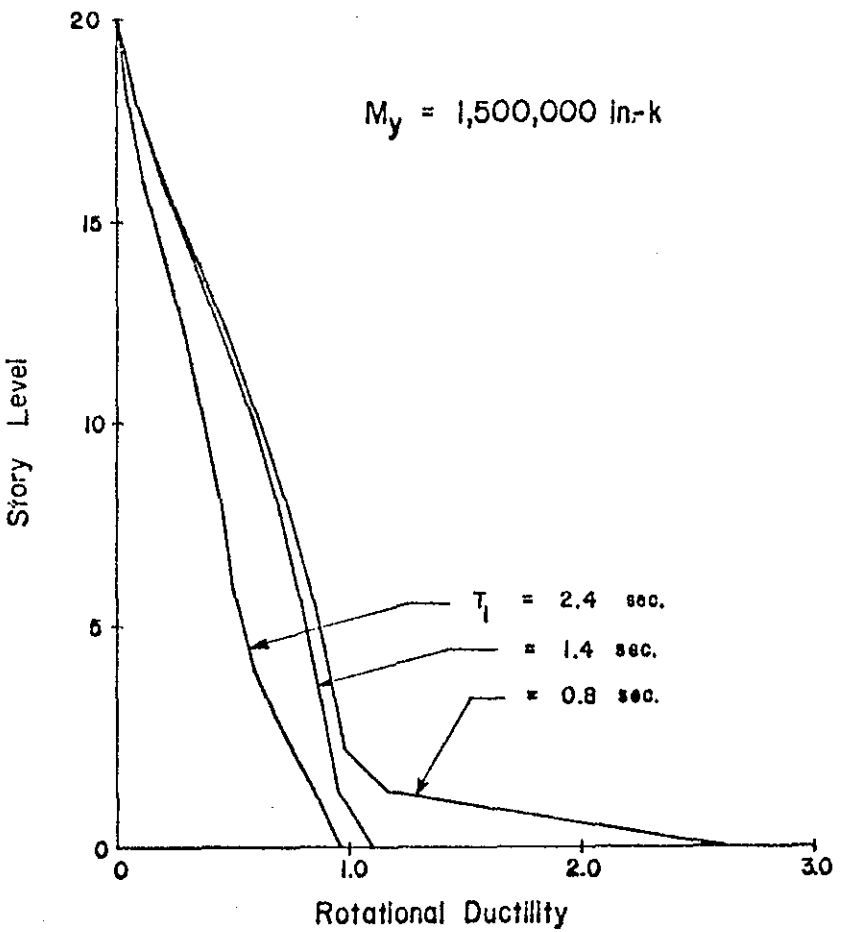

(e)

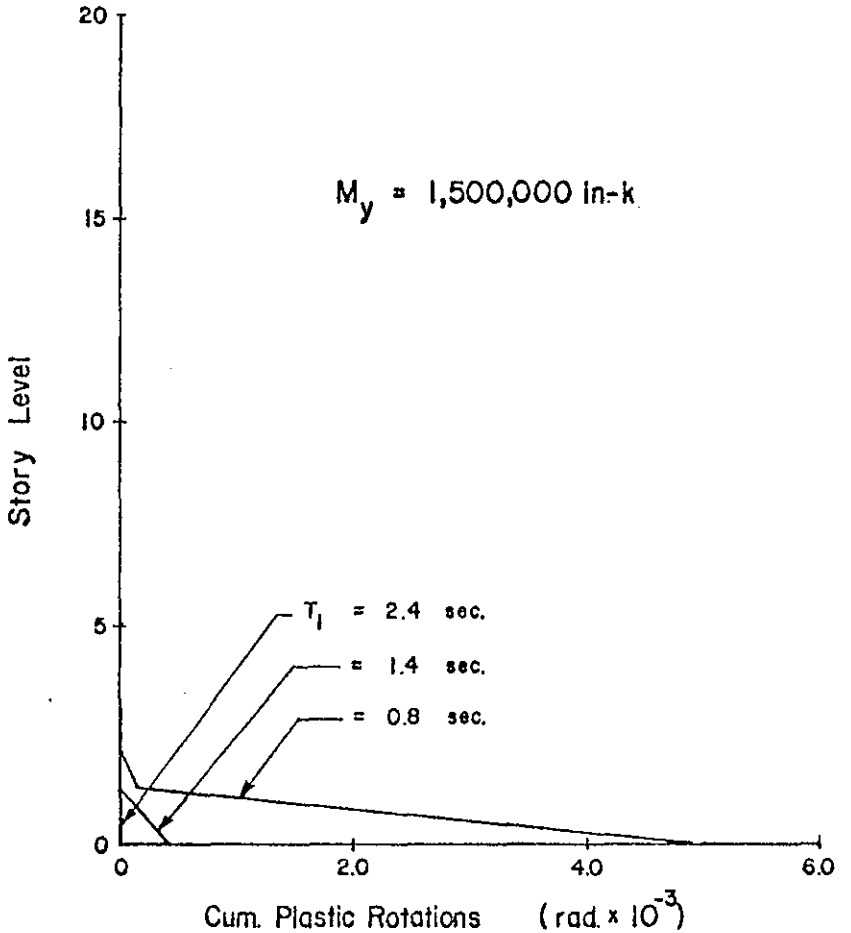

(f)

Fig. 43 (cont'd.) Effect of Fundamental Period of Vibration, T_1

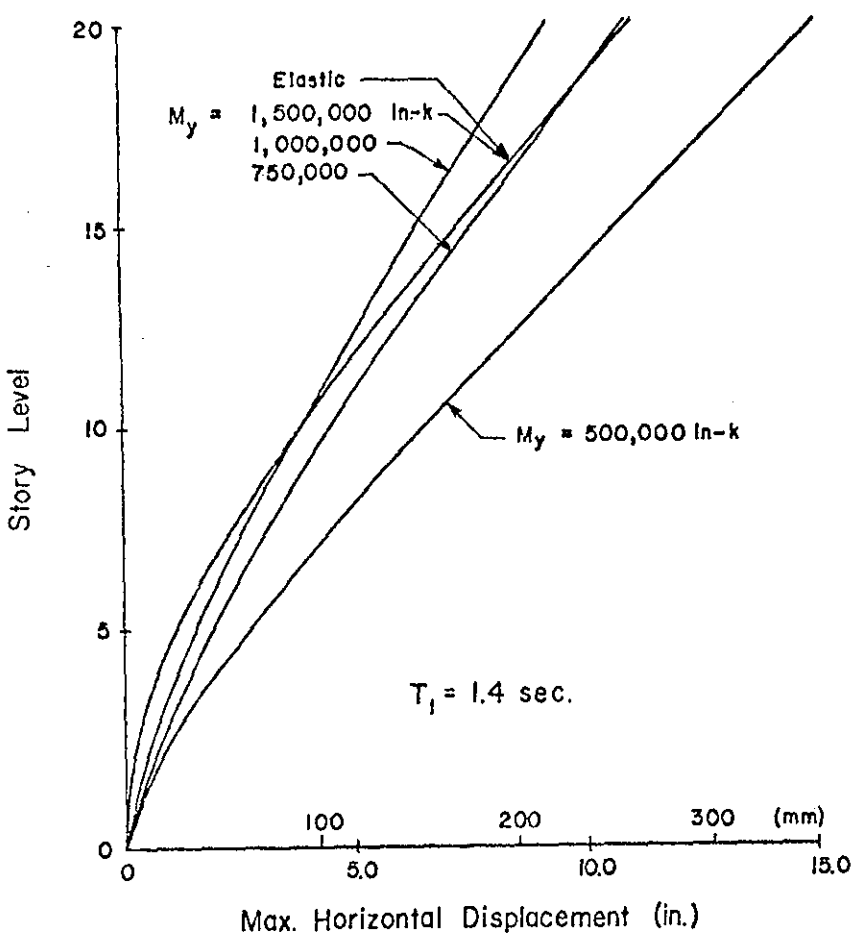

(a)

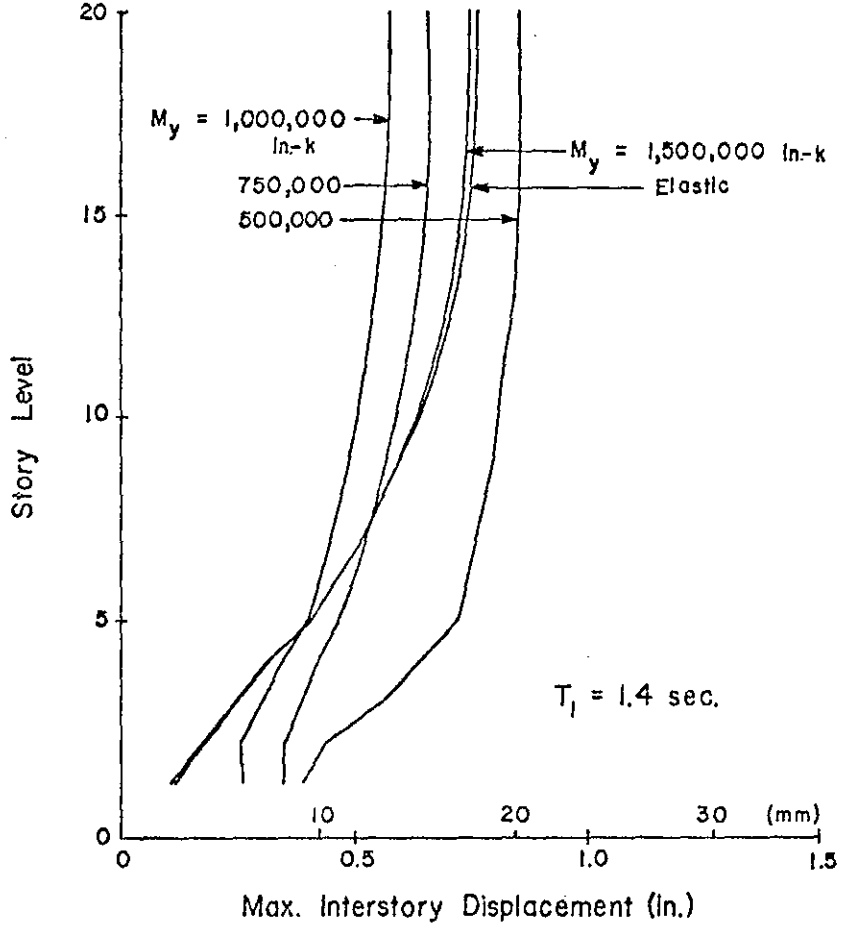

(b)

Fig. 44 Effect of Yield Level, M_y

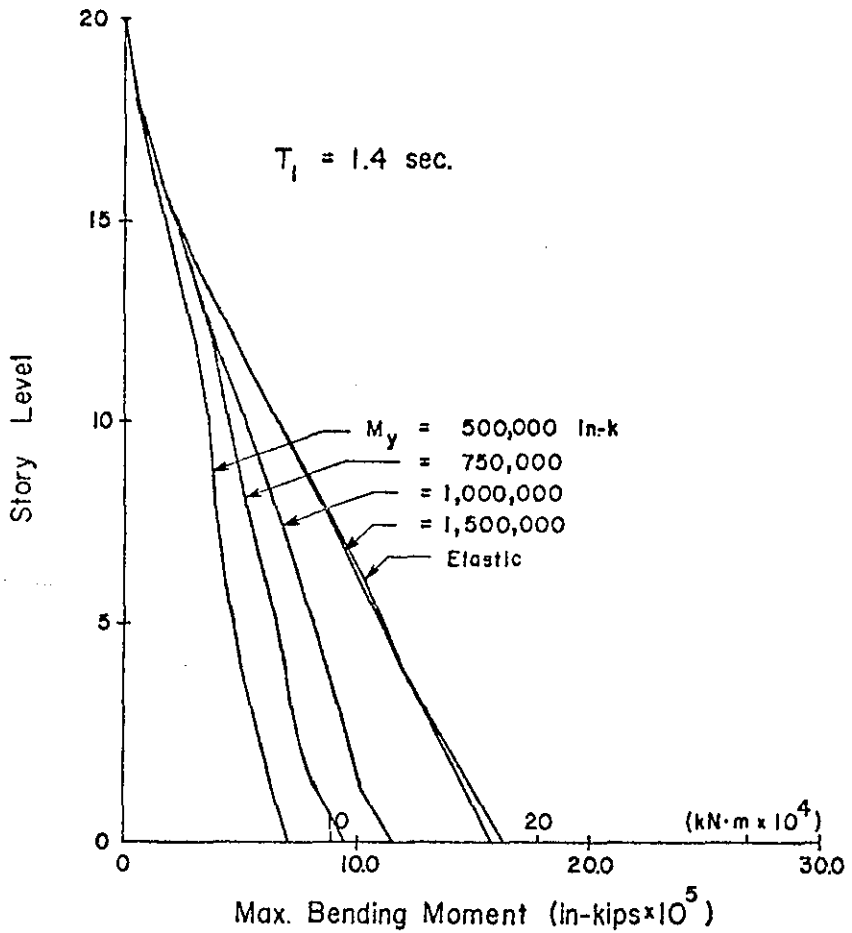

(c)

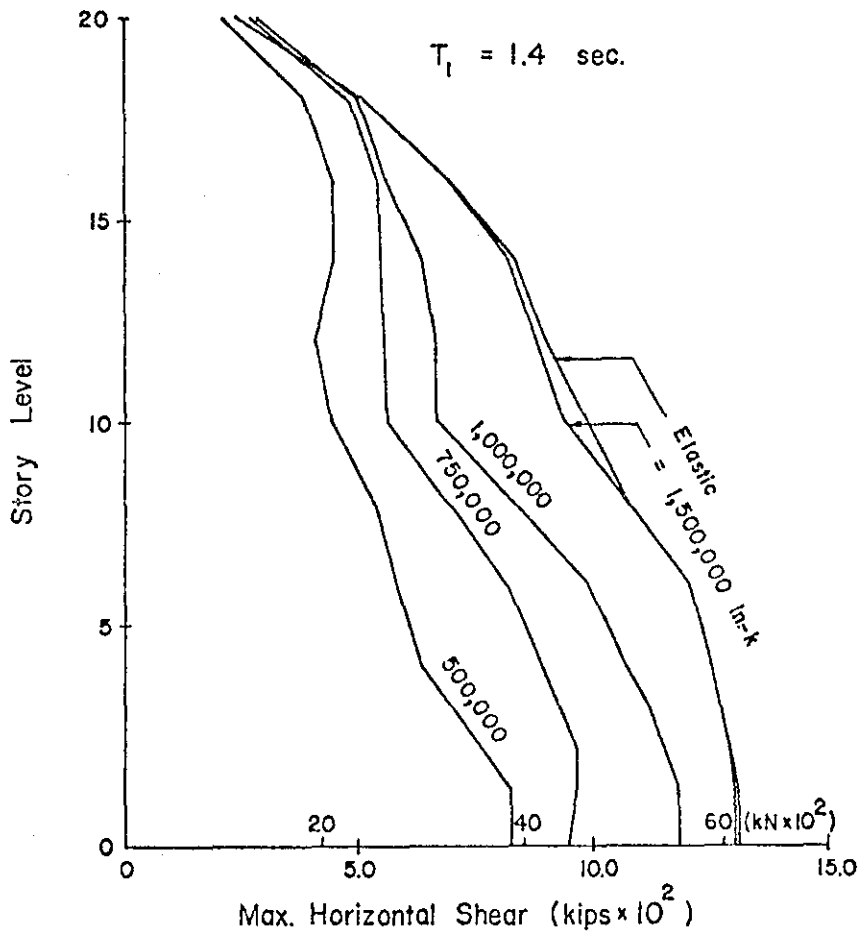

(d)

Fig. 44 (cont'd.) Effect of Yield Level, M_y

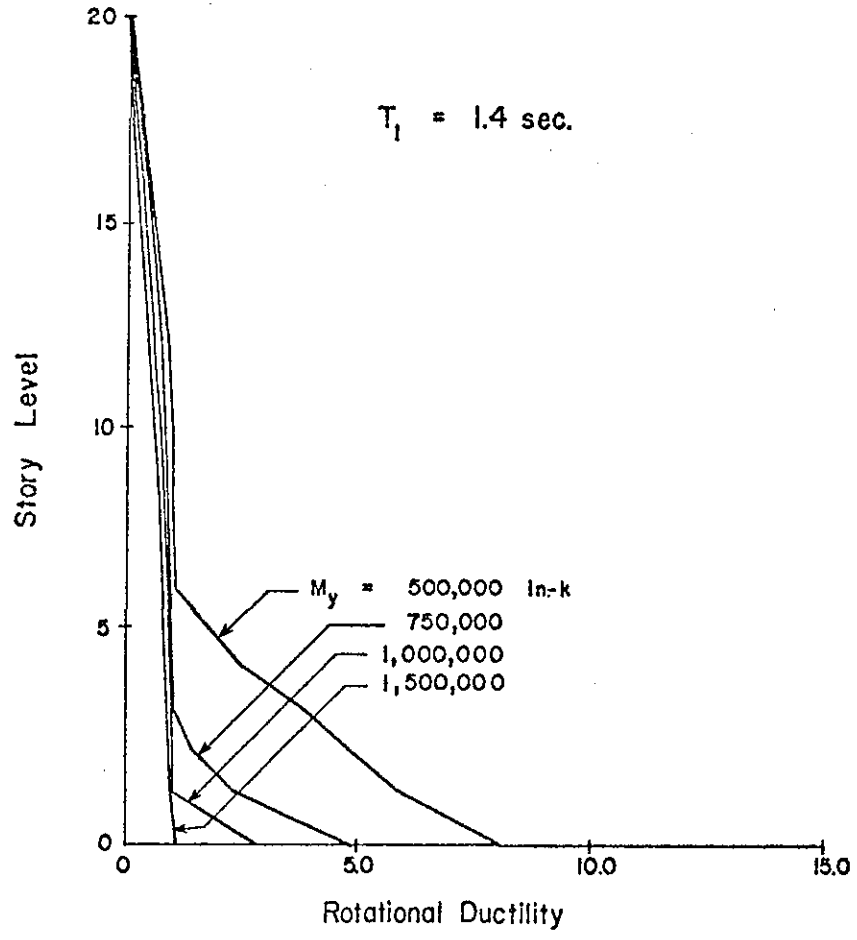

(e)

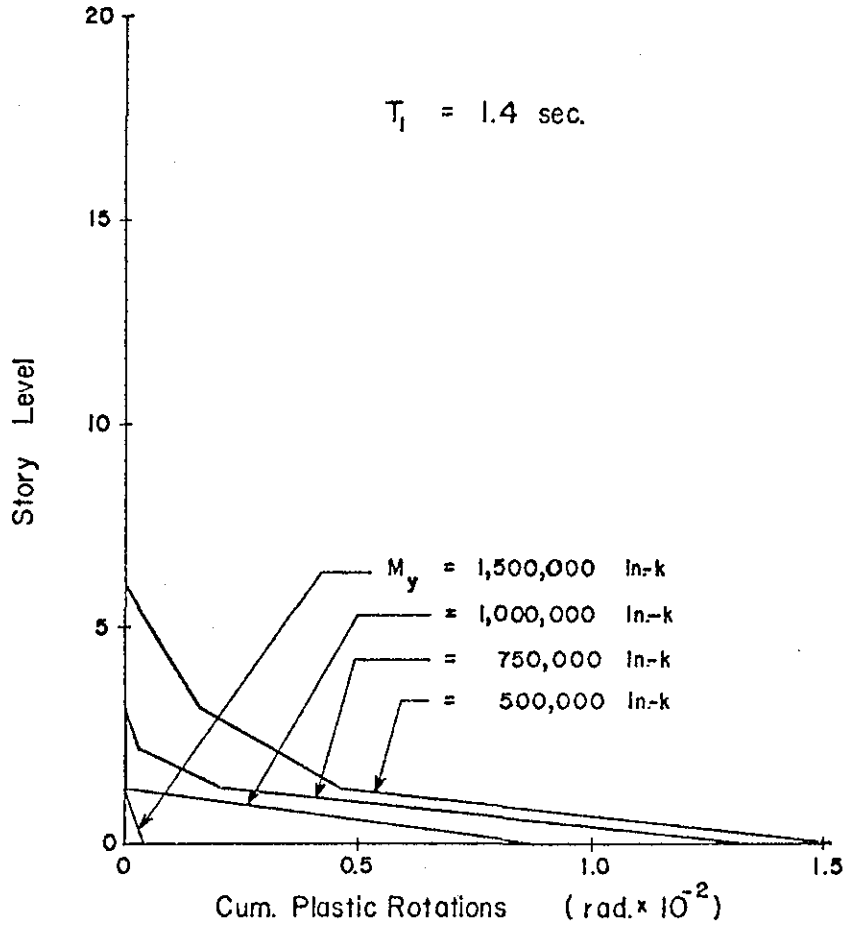

(f)

Fig. 44 (cont'd.) Effect of Yield Level, M_y

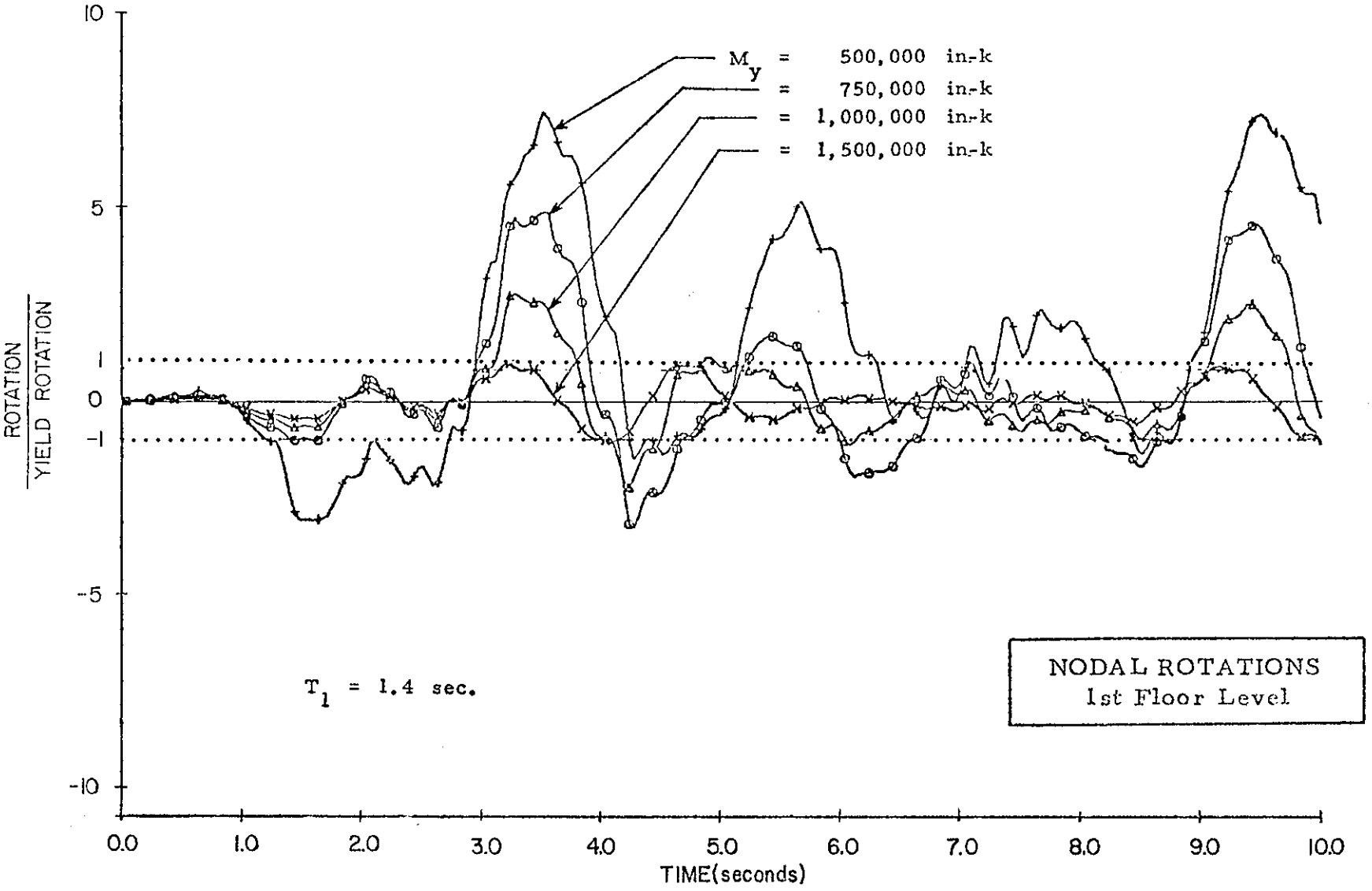

Fig. 45 Rotation in First Story versus Time for Different Values of Yield Level, M_y

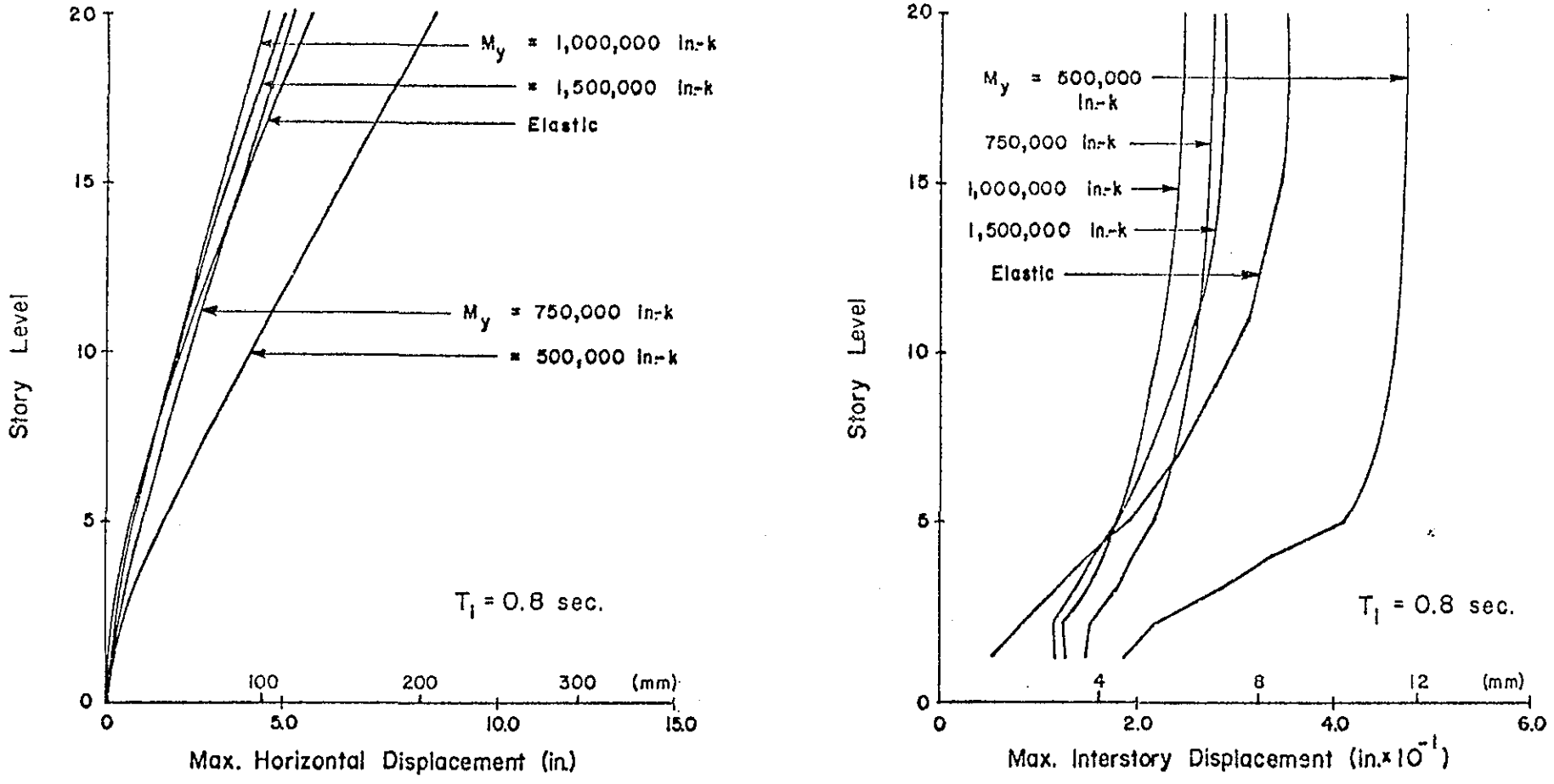

Fig. 46 Effect of Yield Level, M_y

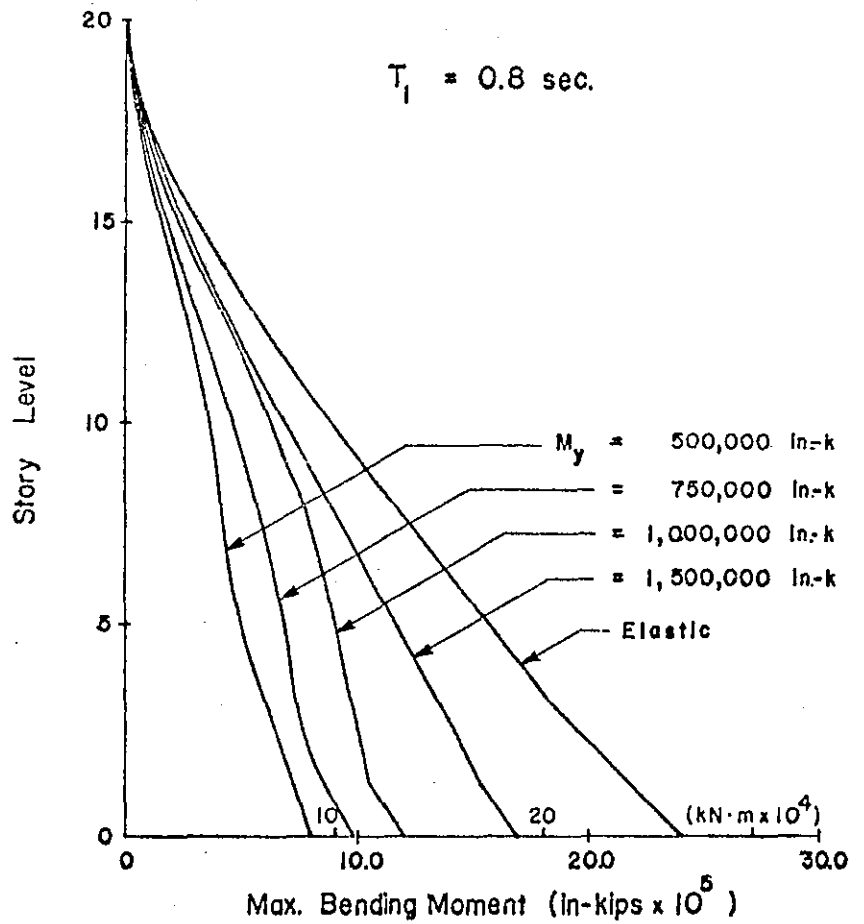

(c)

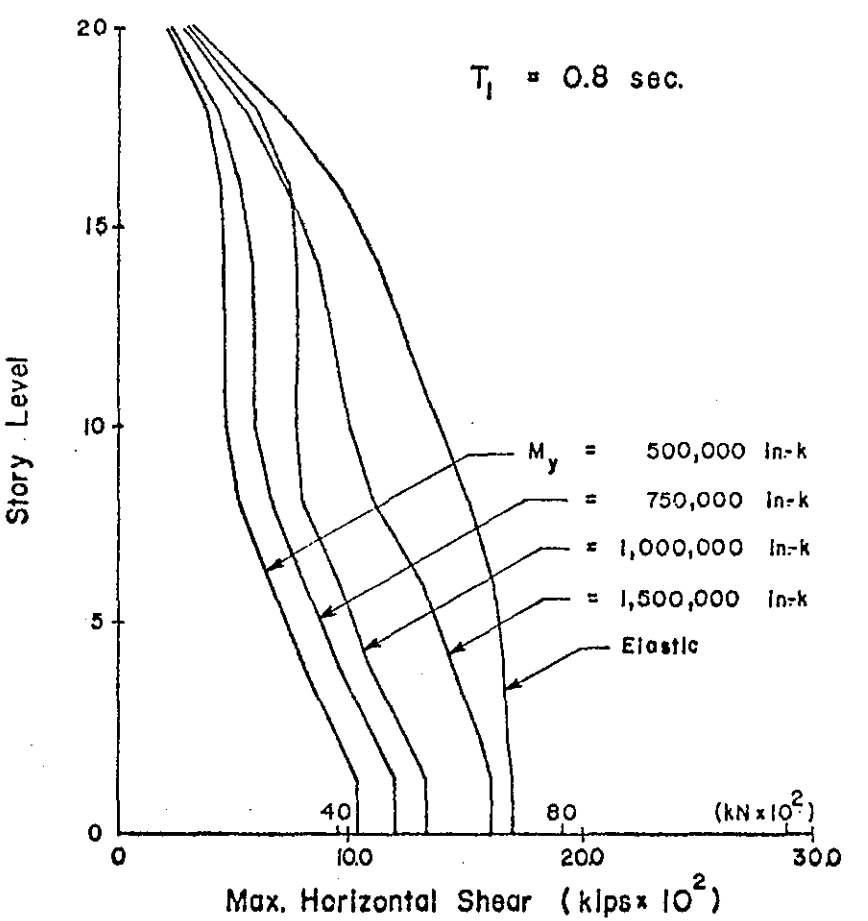

(d)

Fig. 46 (cont'd.) Effect of Yield Level, M_y

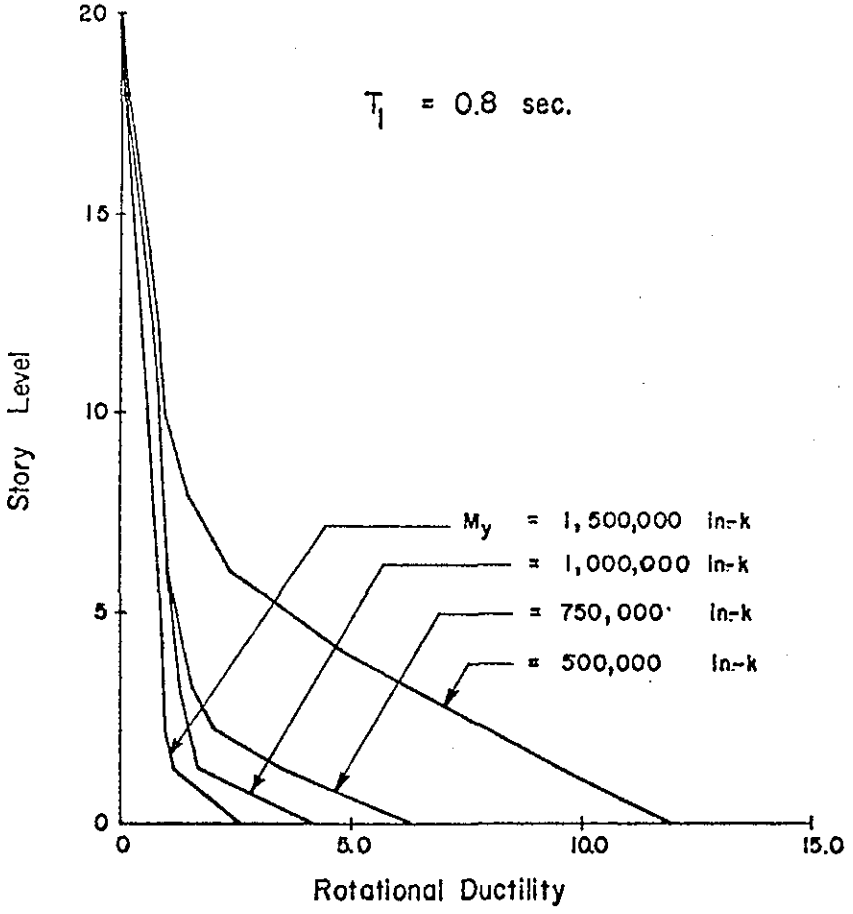

(e)

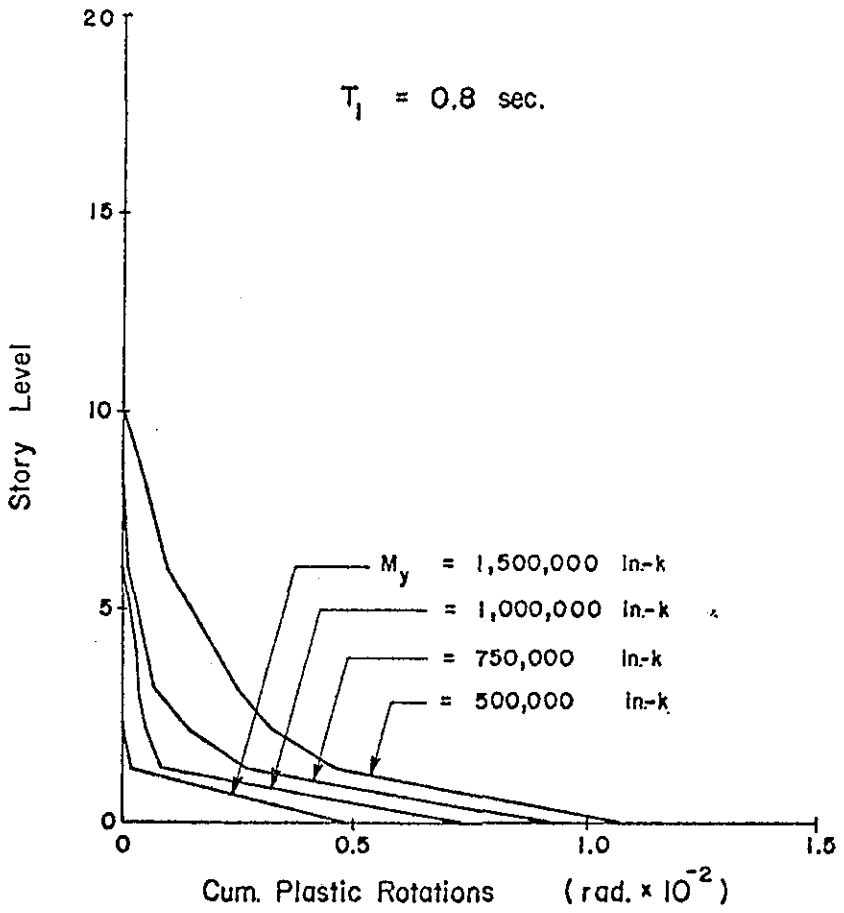

(f)

Fig. 46 (cont'd.) Effect of Yield Level, M_y

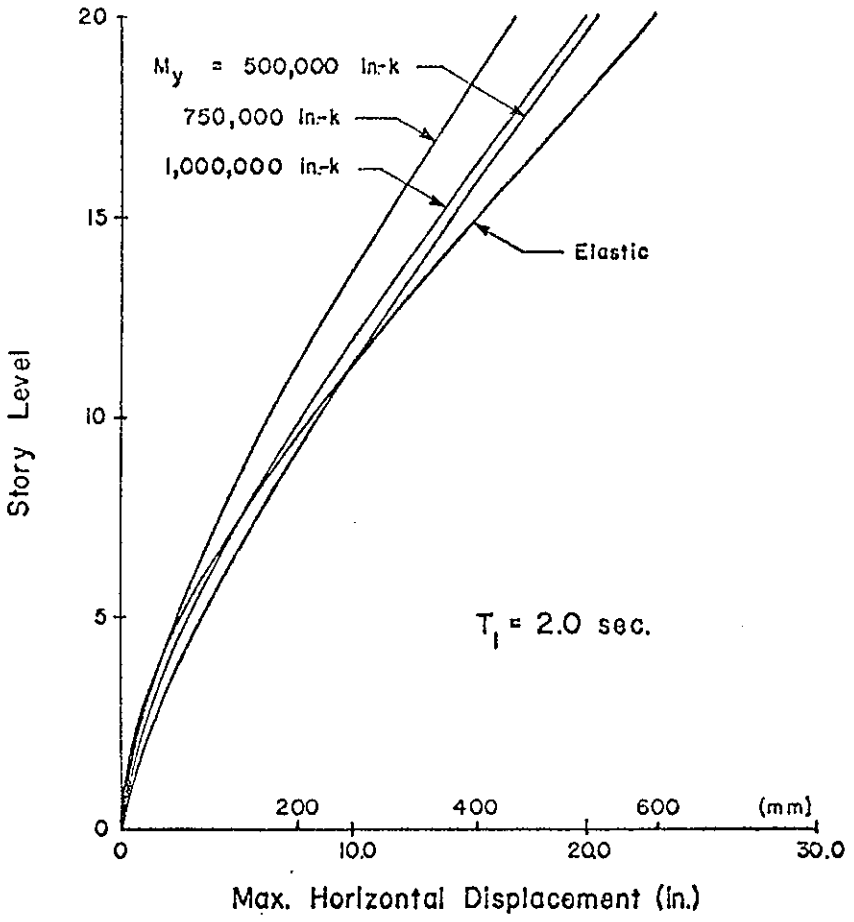

(a)

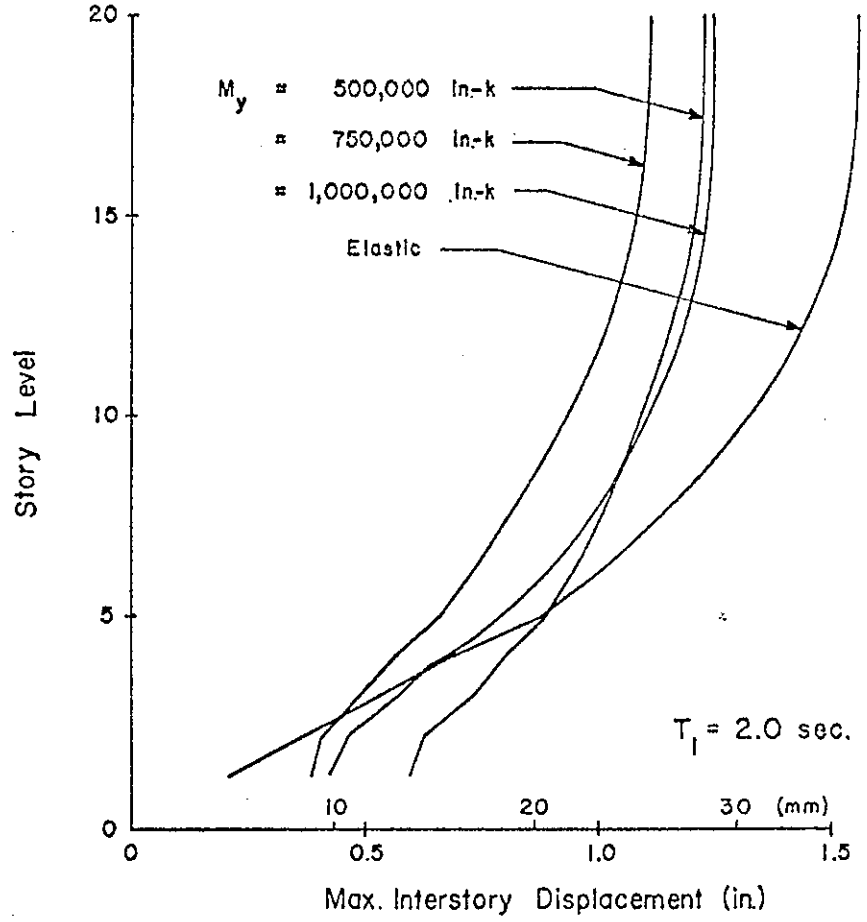

(b)

Fig. 47 Effect of Yield Level, M_y

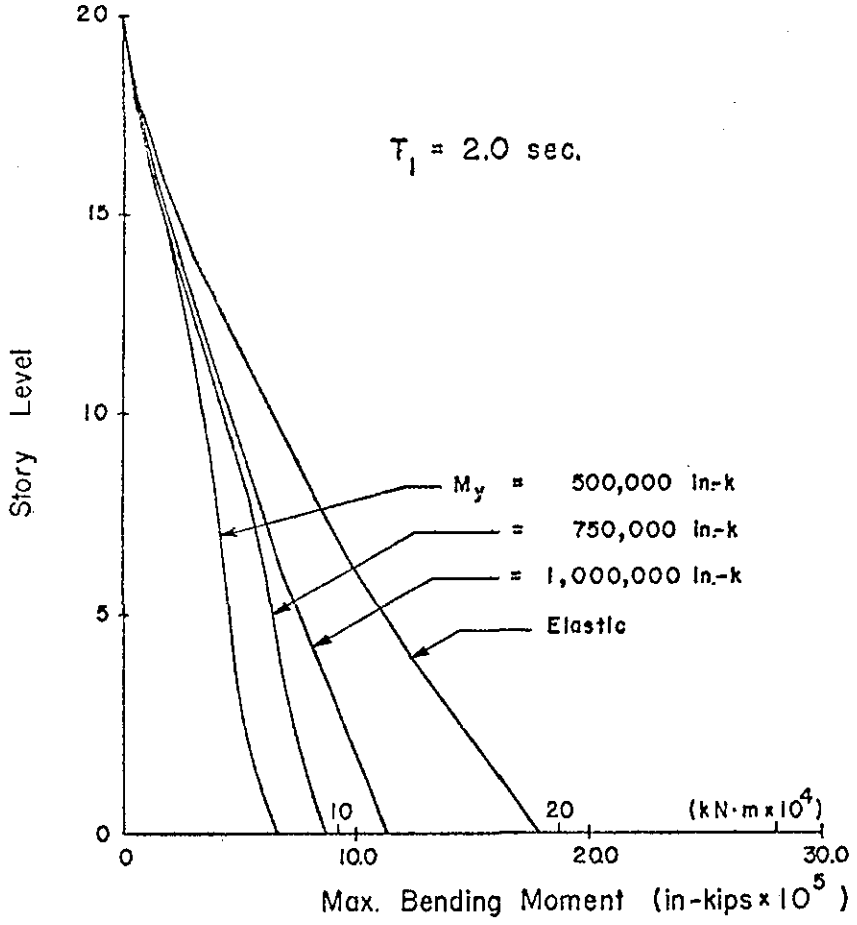

(c)

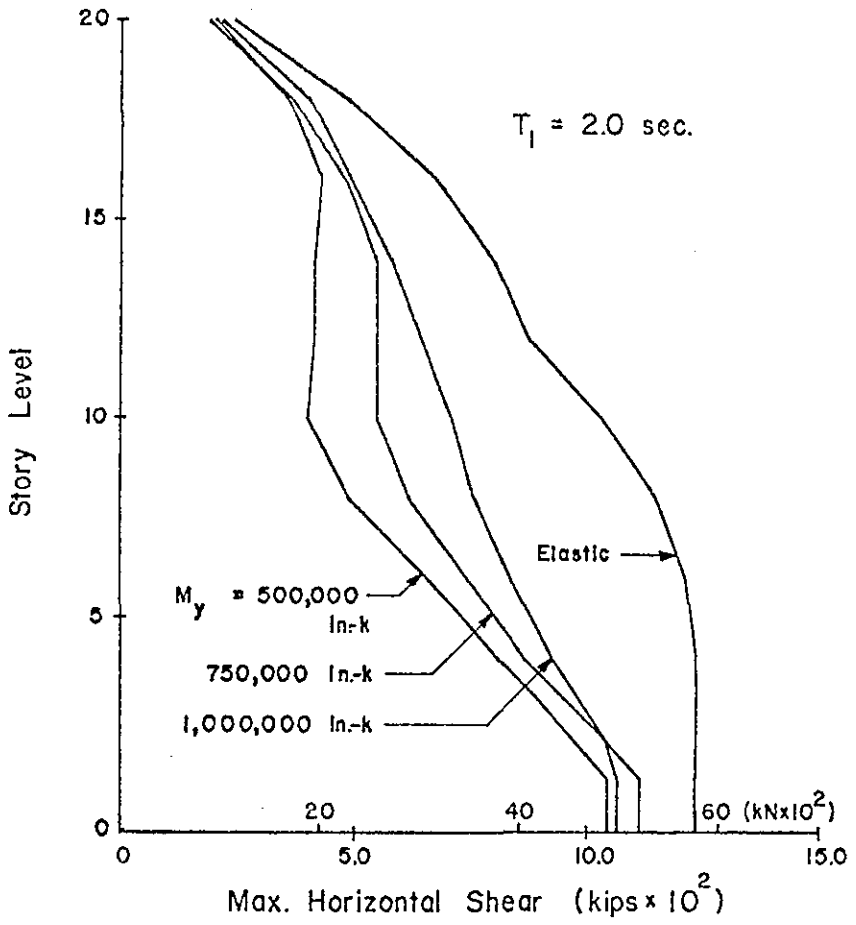

(d)

Fig. 47 (cont'd.) Effect of Yield Level, M_y

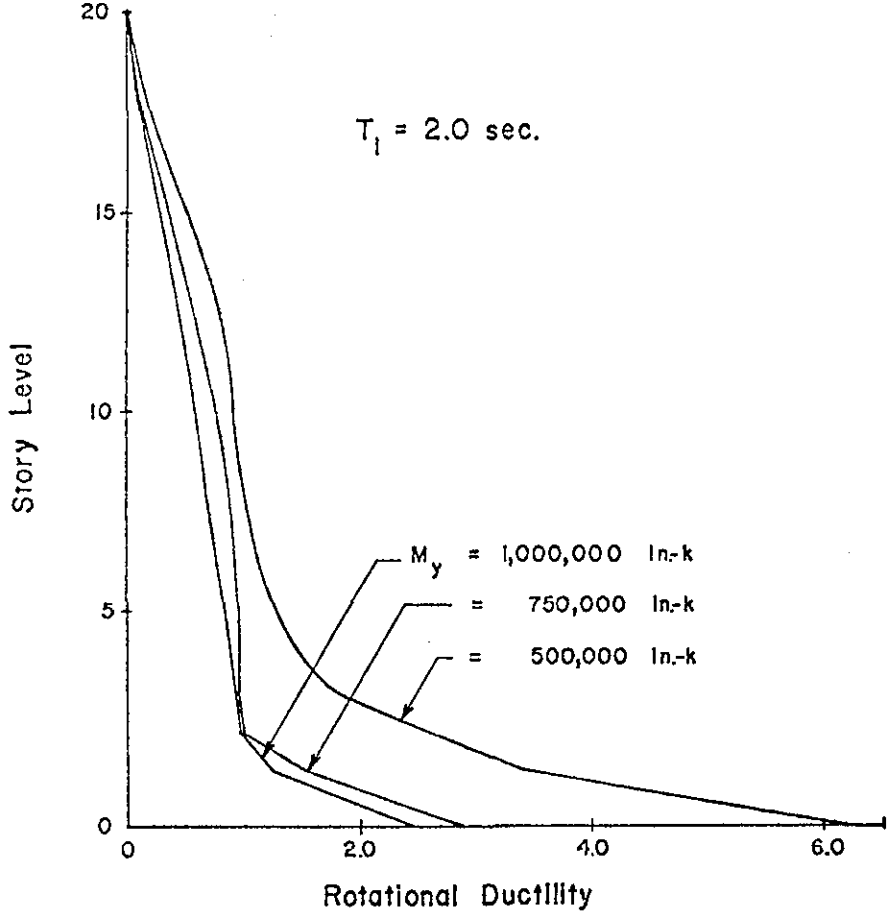

(e)

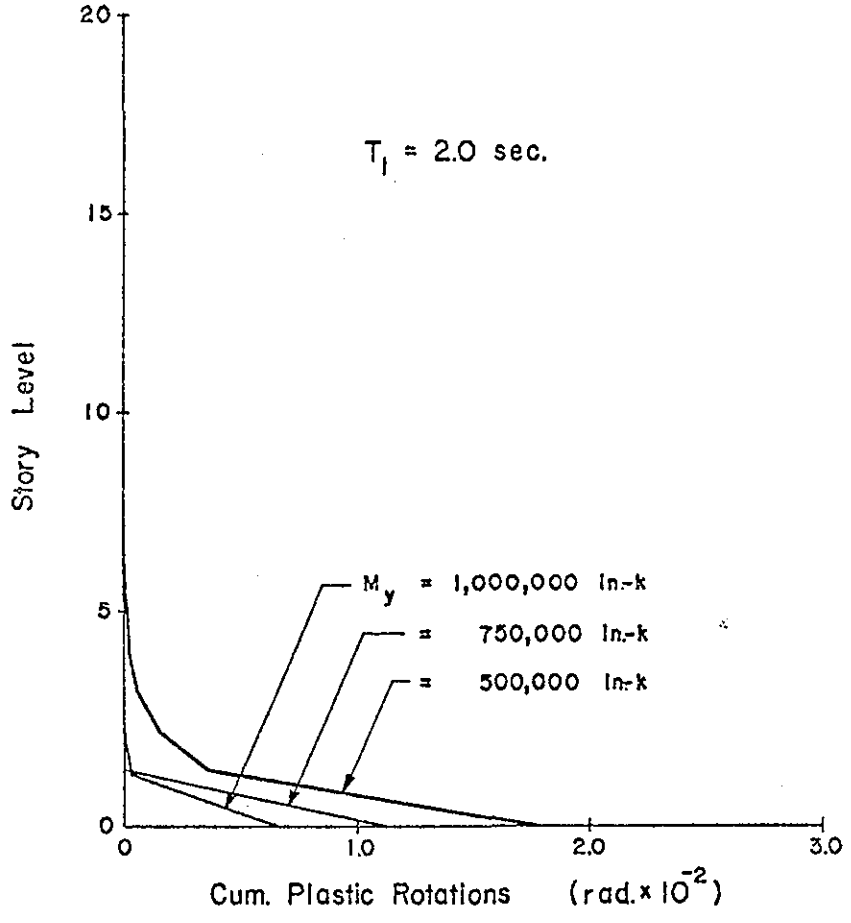

(f)

Fig. 47 (cont'd.) Effect of Yield Level M_y

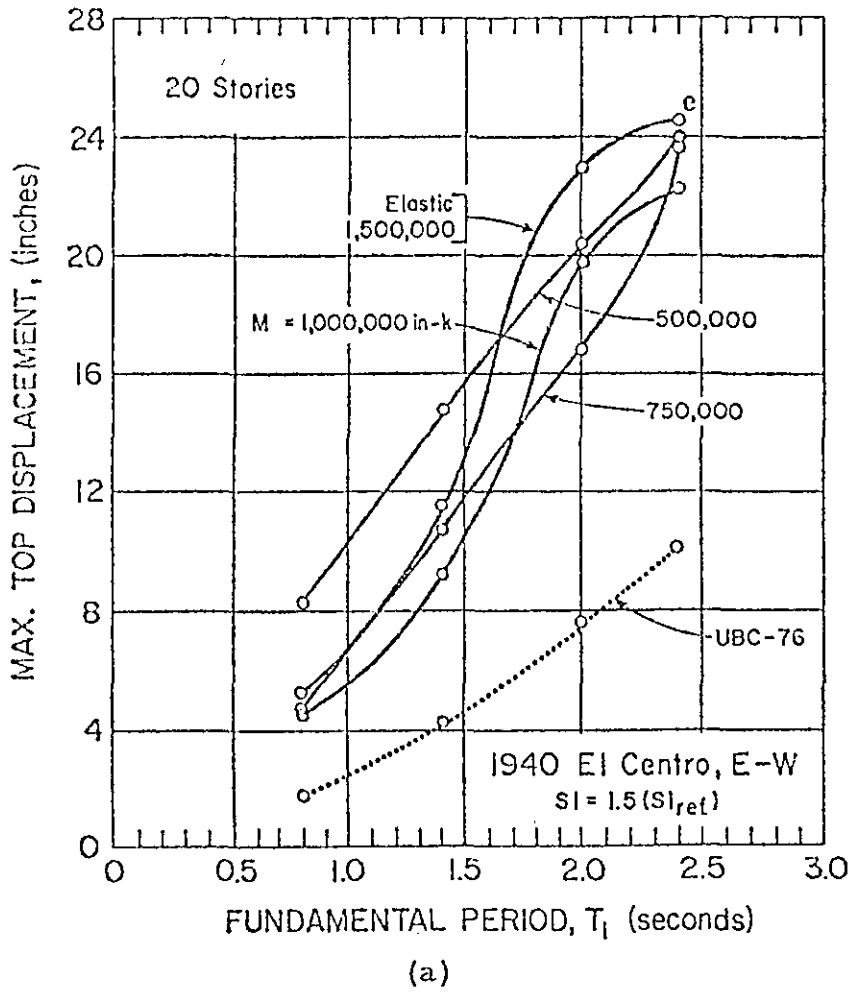

(a)

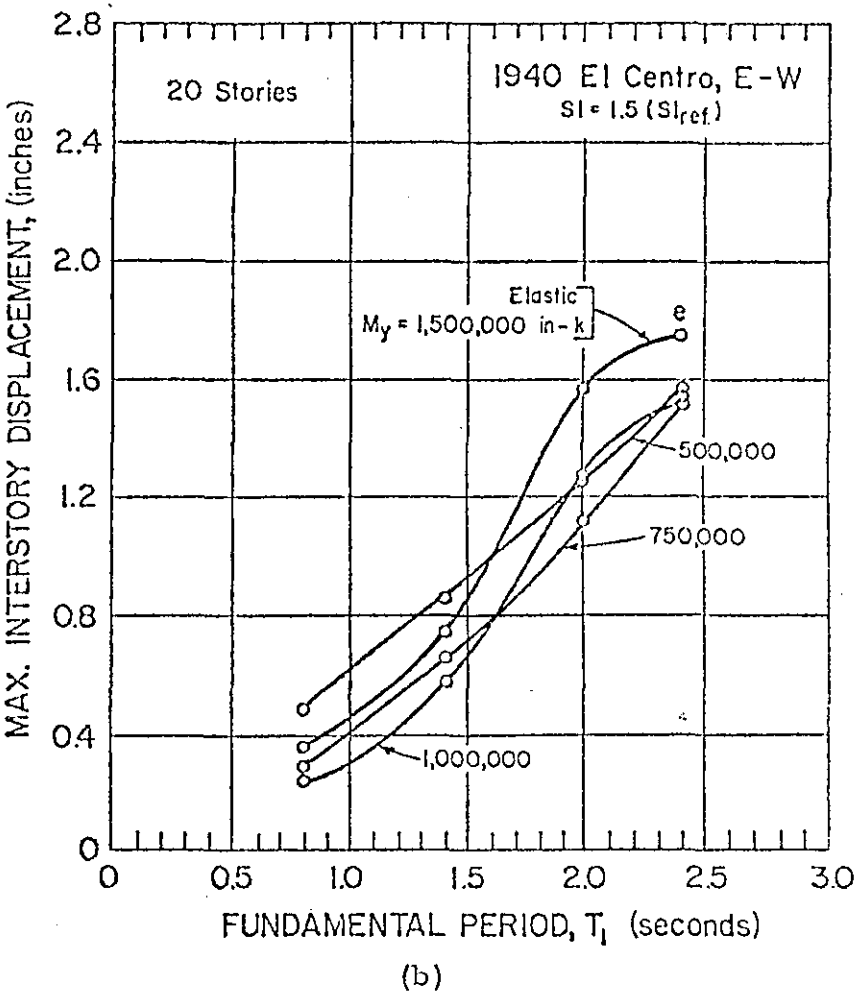

(b)

Fig. 48 Interactive Effects of Fundamental Period, T_1, and Yield Level, M_y, on Maximum Response

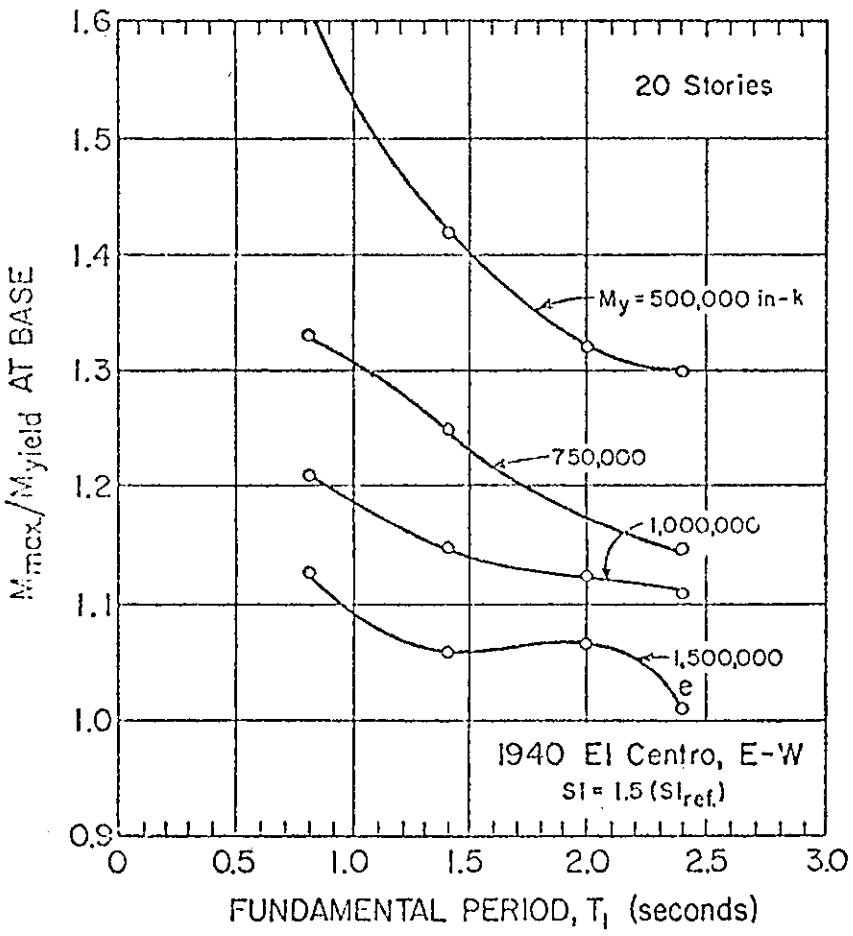

(c)

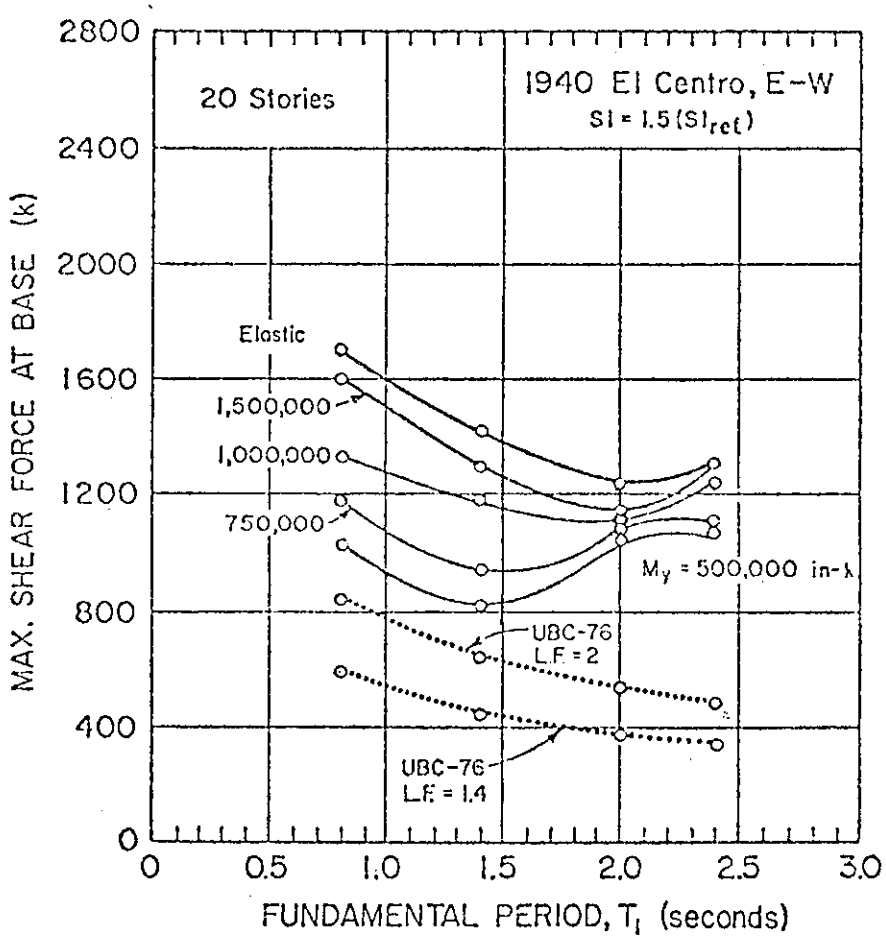

(d)

Fig. 48 (Cont'd.) Interactive Effects of Fundamental Period, T_1, and Yield Level, M_y on Maximum Response

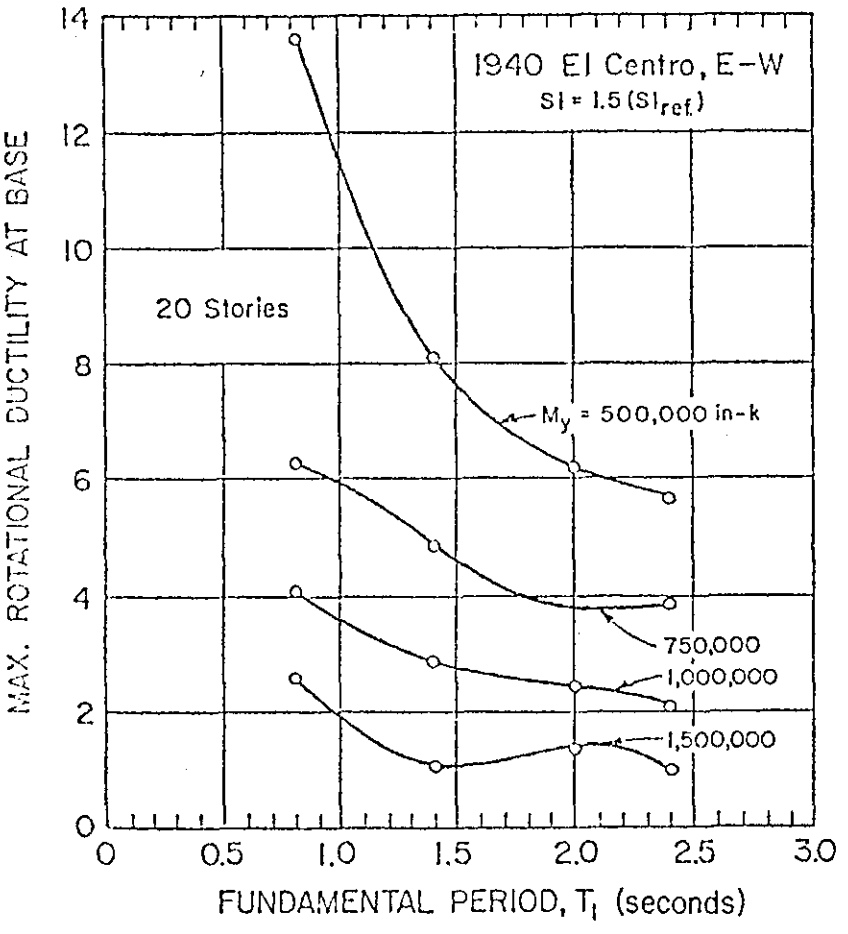

(e)

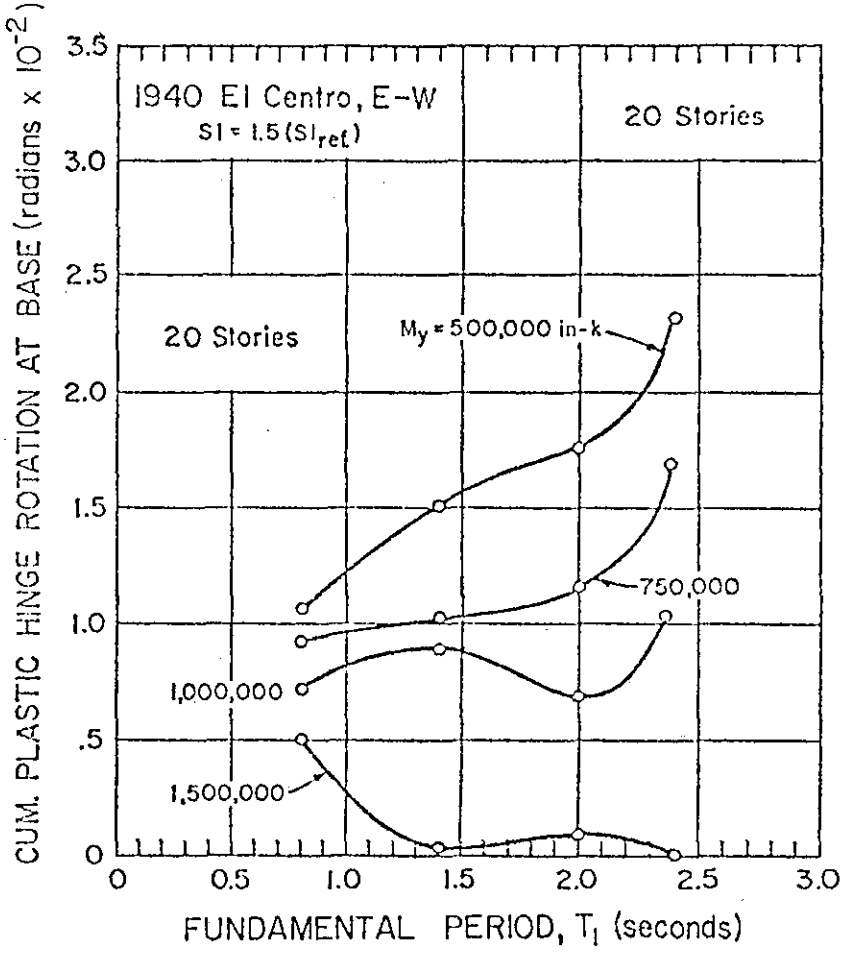

(f)

Fig. 48 (Cont'd.) Interactive Effects of Fundamental Period, T_1, and Yield Level, M_y, on Maximum Response

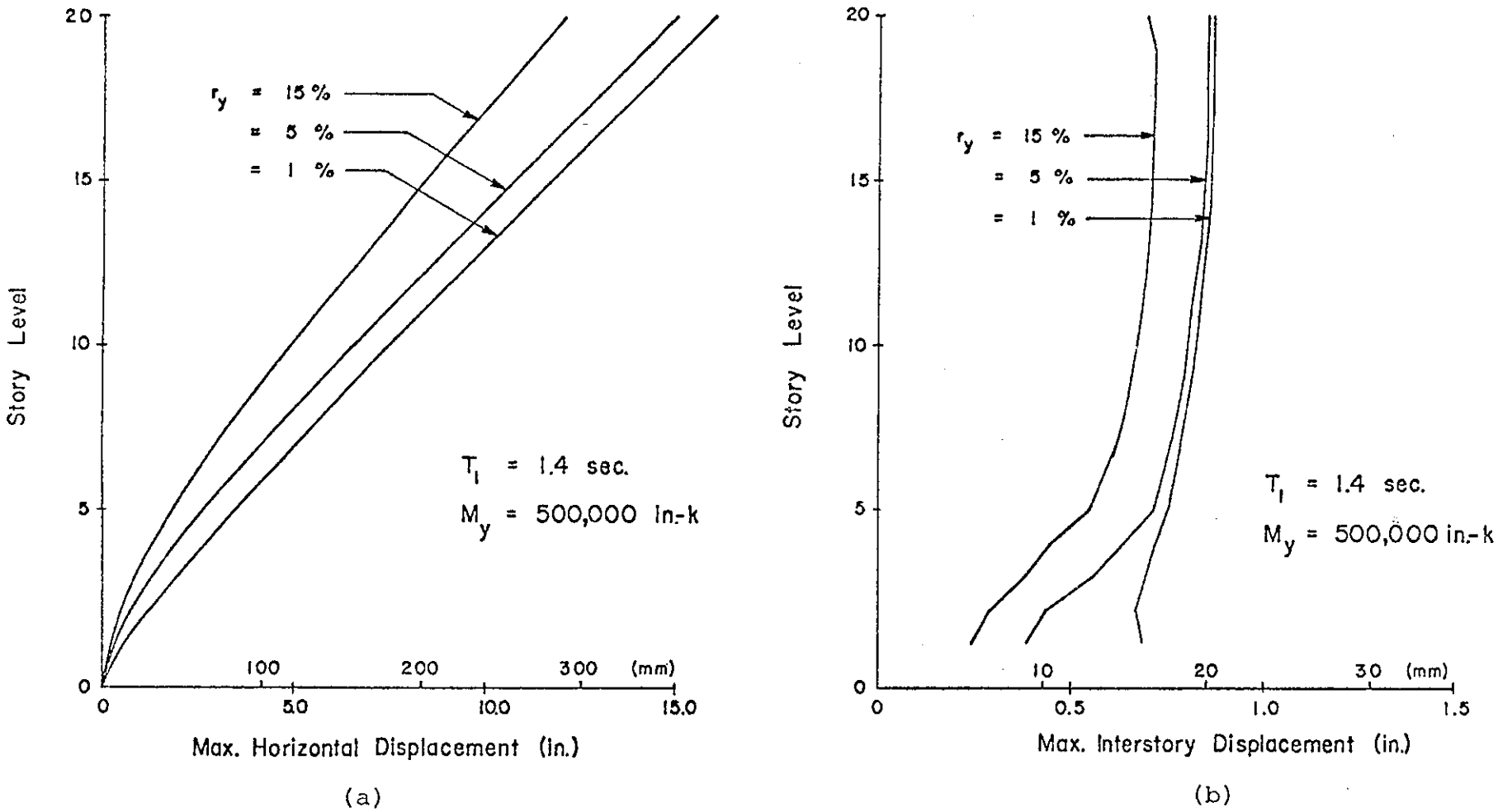

Fig. 49 Effect of Slope of Post-Yield Branch of Moment-Rotation Curve

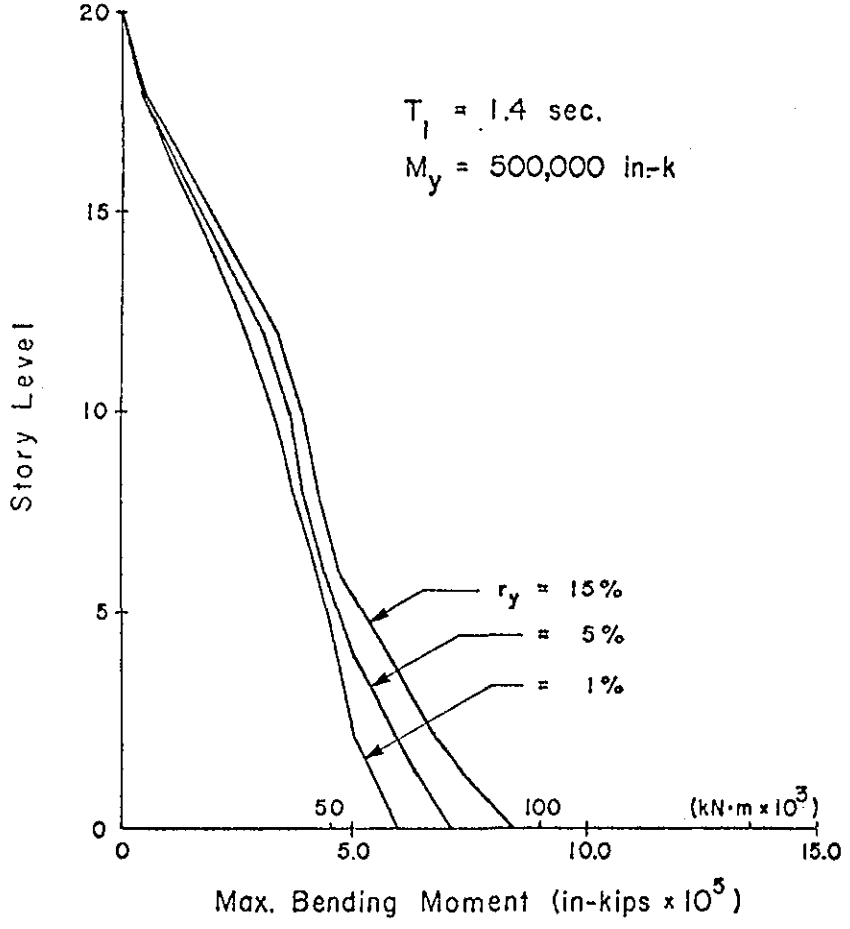

(c)

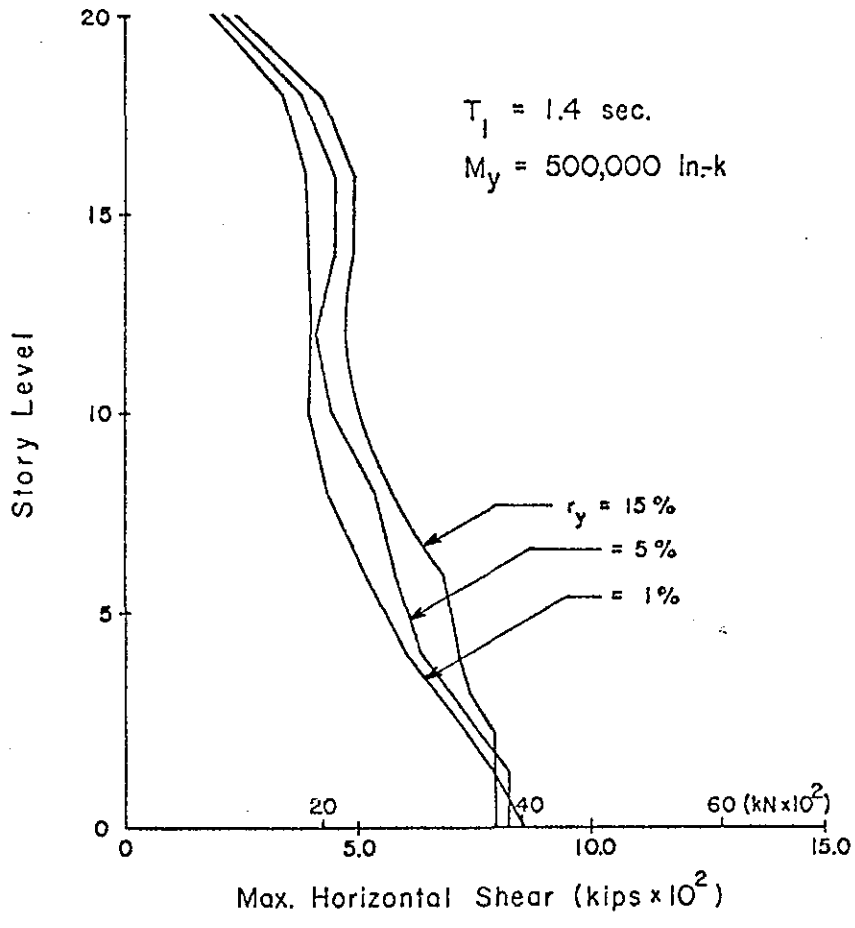

(d)

Fig. 49 (cont'd.) Effect of Slope of Post-Yield Branch of Moment-Rotation Curve

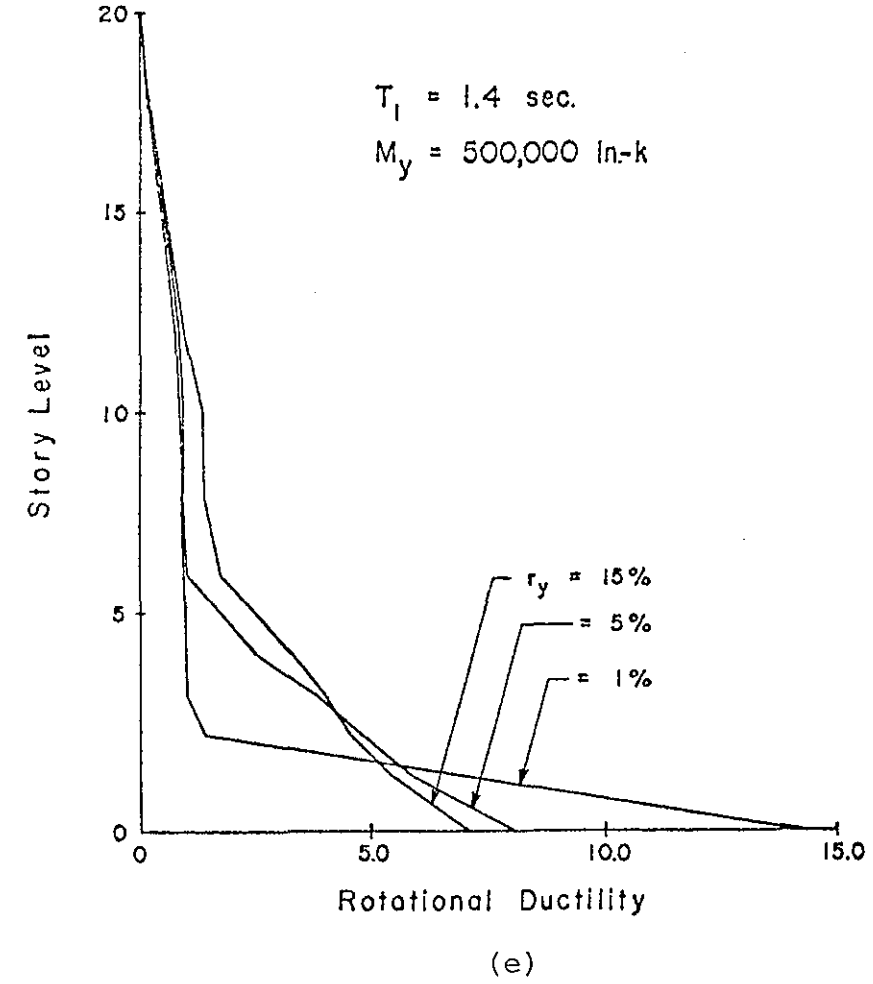

(e)

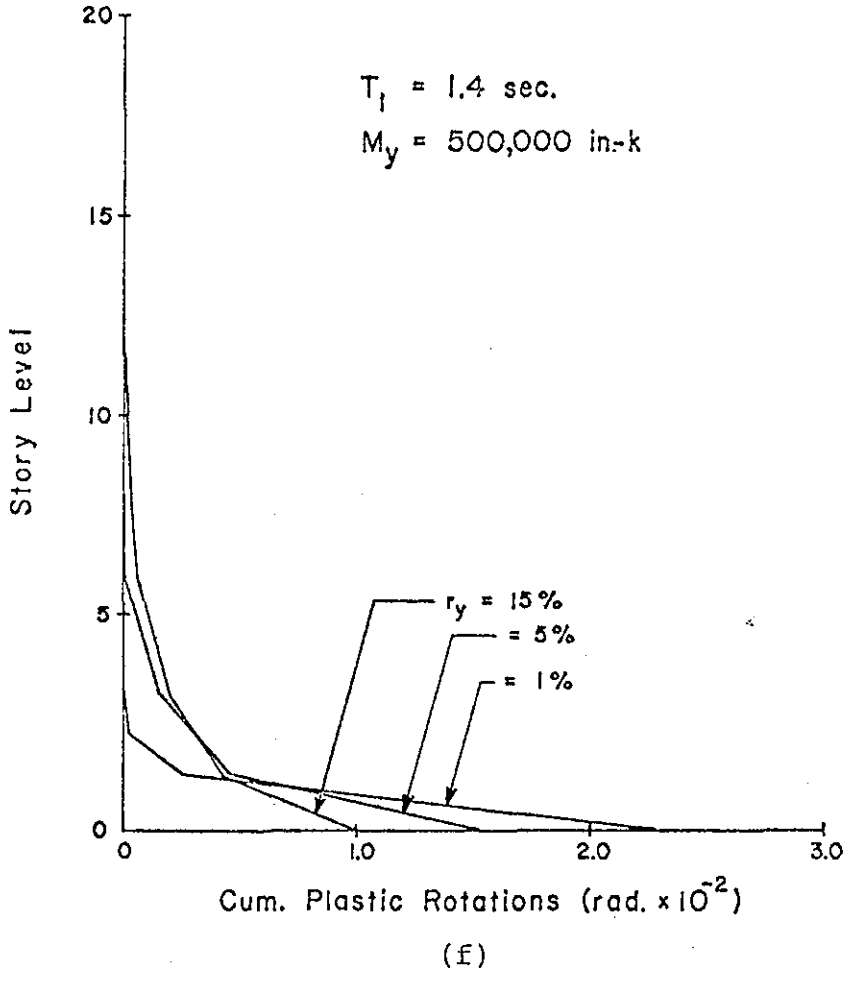

(f)

Fig. 49 (cont'd.) Effect of Slope of Post-Yield Branch of Moment-Rotation Curve

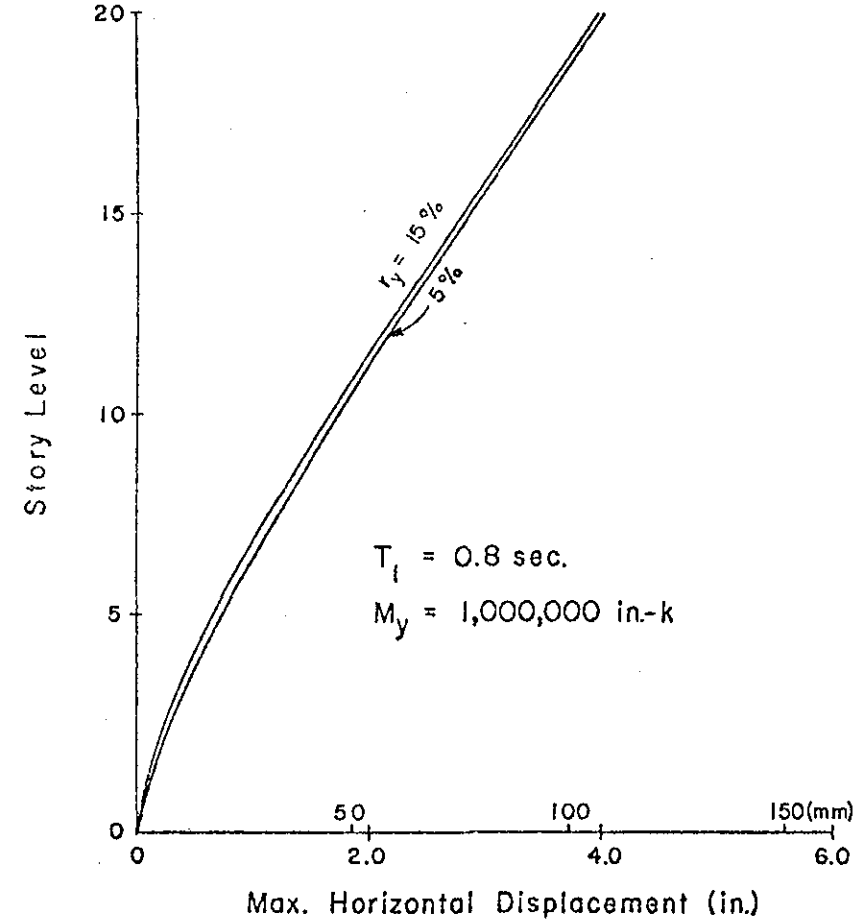

(a)

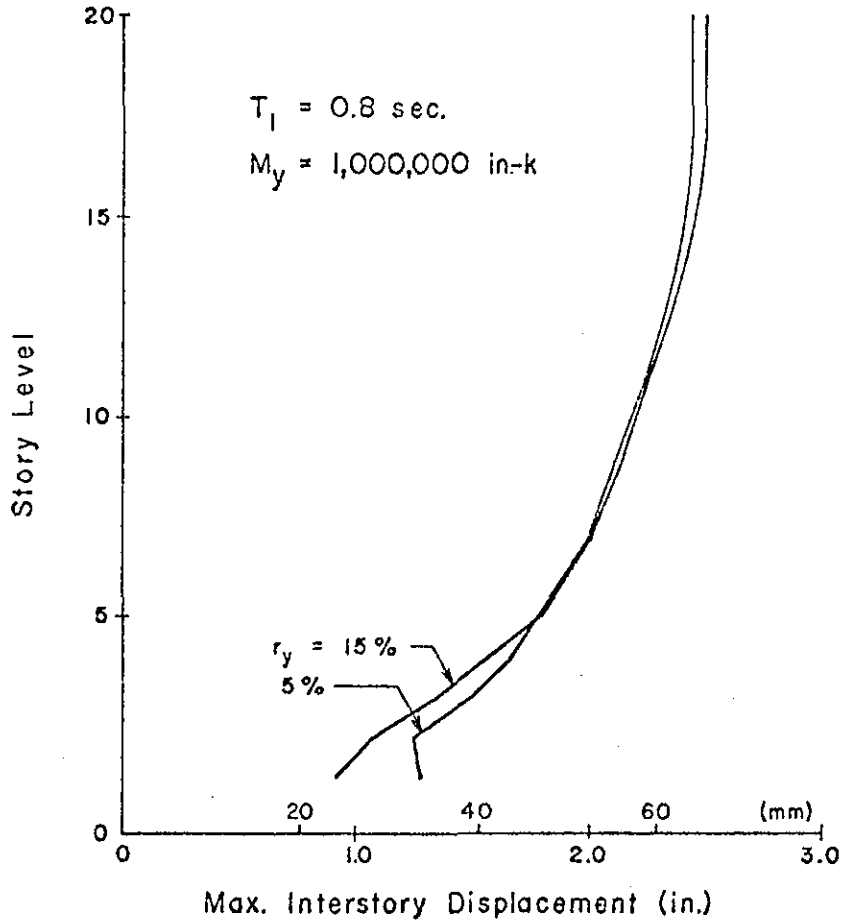

(b)

Fig. 50 Effect of Slope of Post-Yield Branch of Moment-Rotation Curve

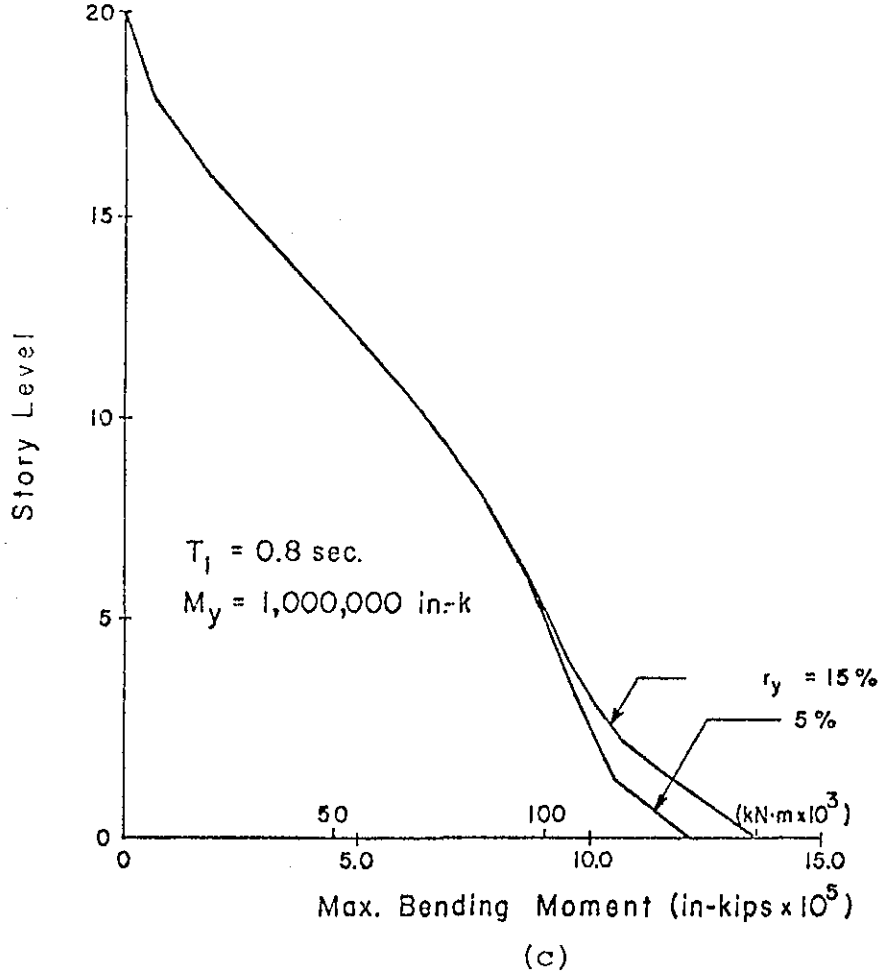

(c)

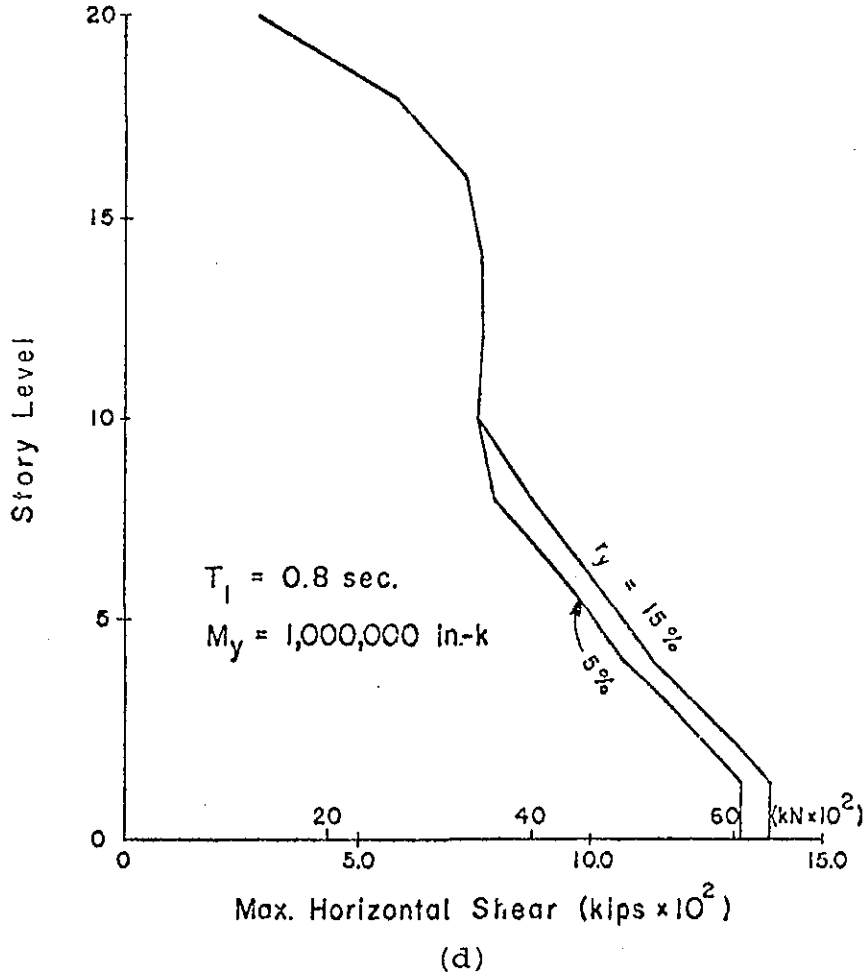

(d)

Fig. 50 (Cont'd.) Effect of Slope of Post-Yield Branch of Moment-Rotation Curve

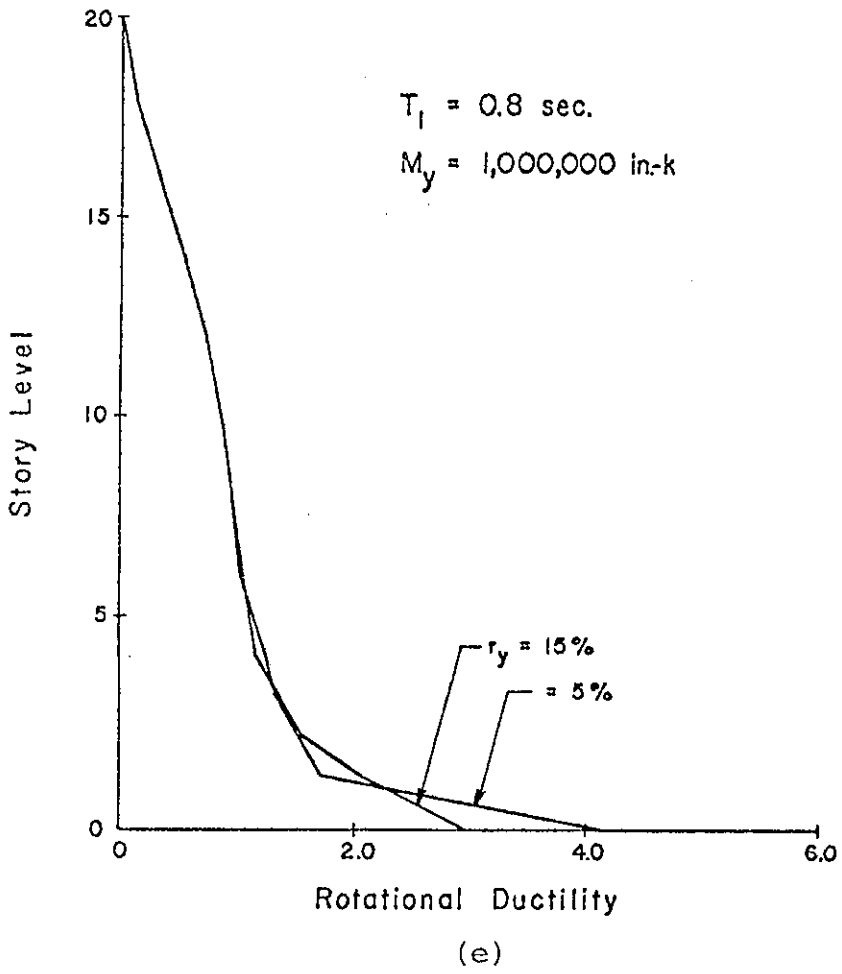

(e)

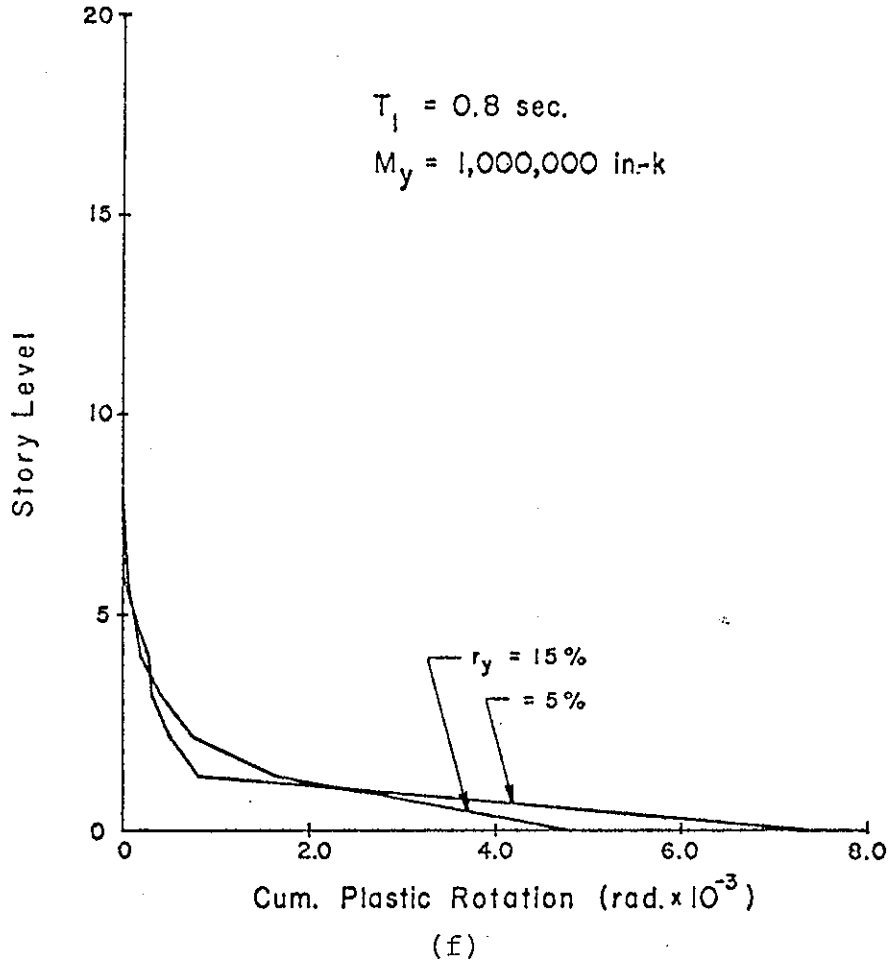

(f)

Fig. 50 (cont'd.) Effect of Slope of Post-Yield Branch of Moment-Rotation Curve

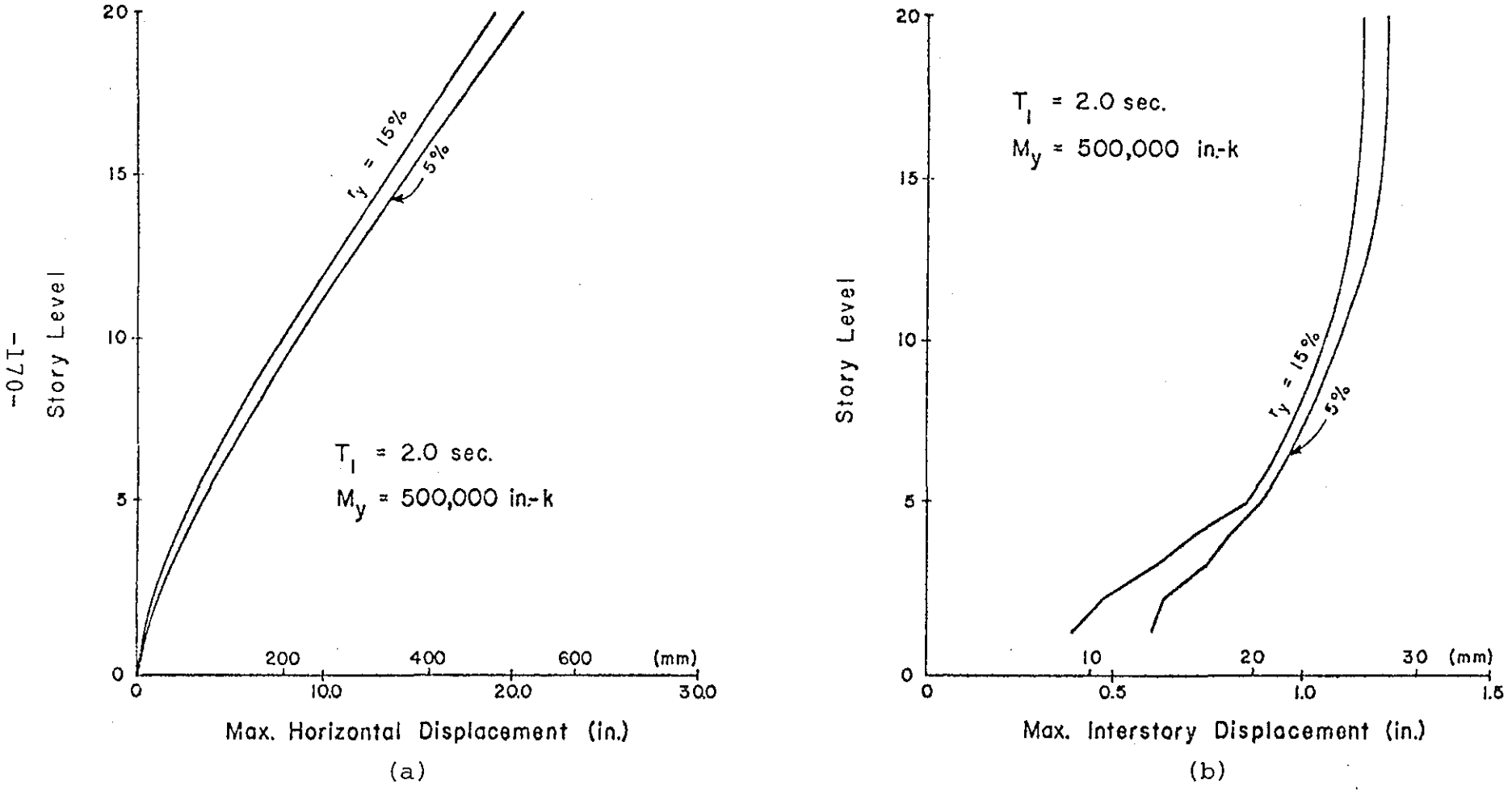

Fig. 51 Effect of Slope of Post-Yield Branch of Moment-Rotation Curve

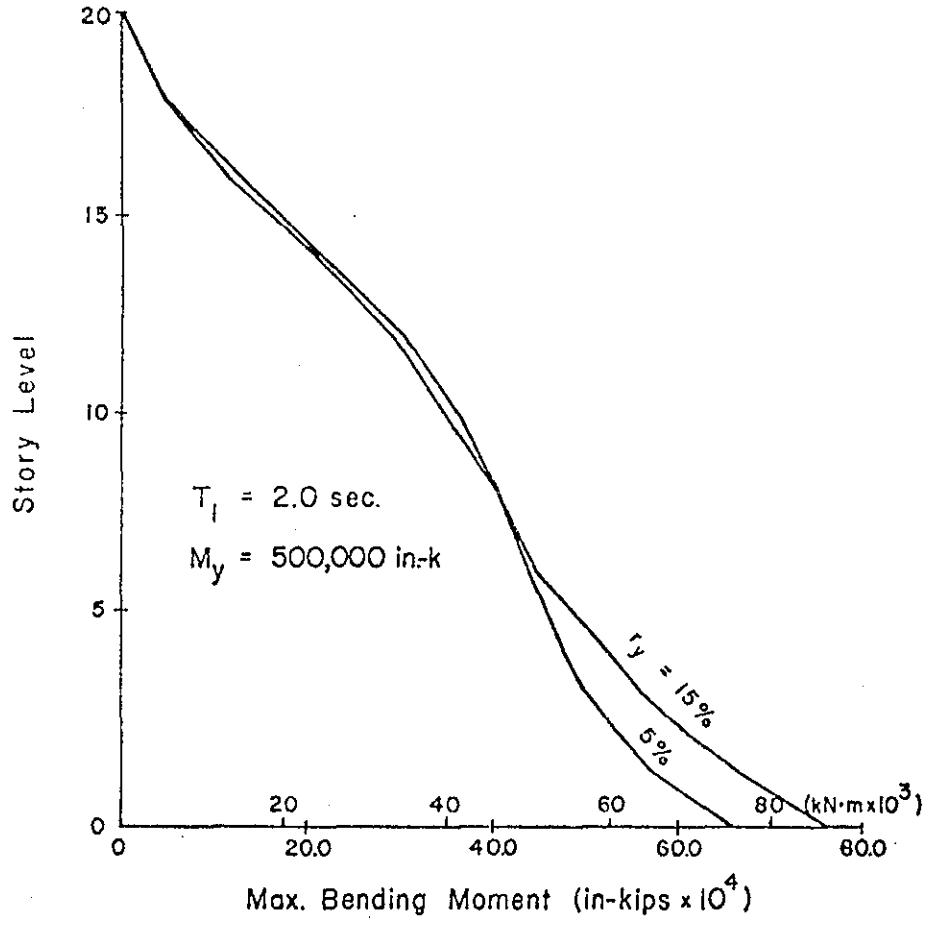

(c)

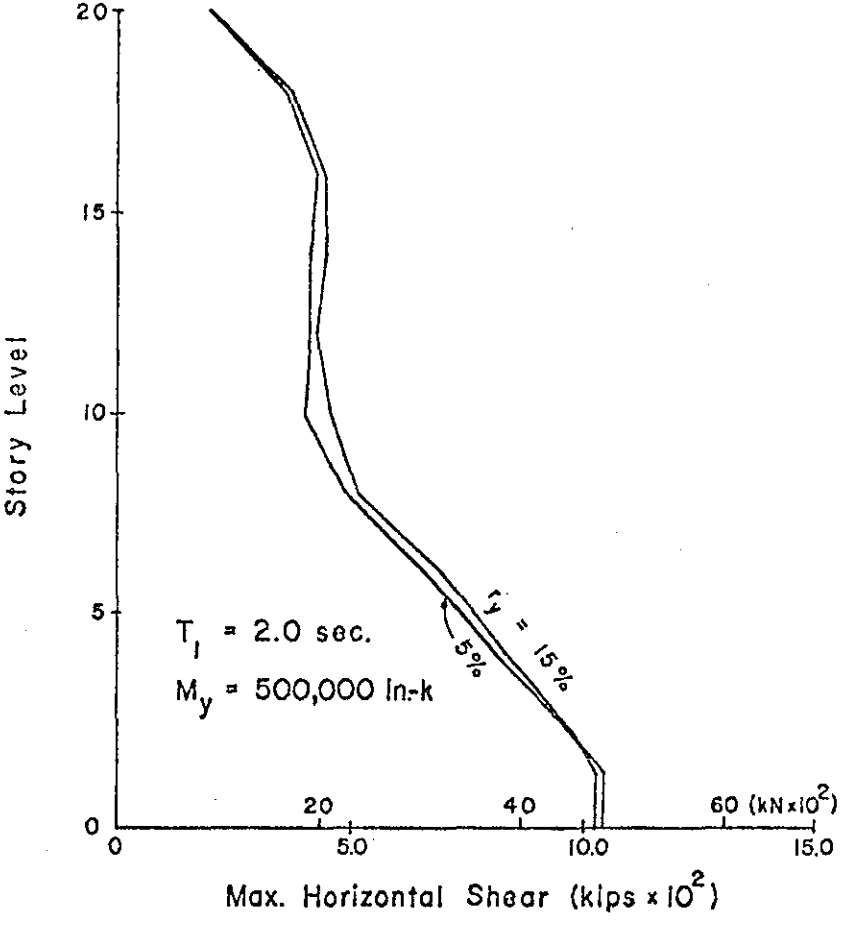

(d)

Fig. 51 (Cont'd.) Effect of Slope of Post-Yield Branch of Moment-Rotation Curve

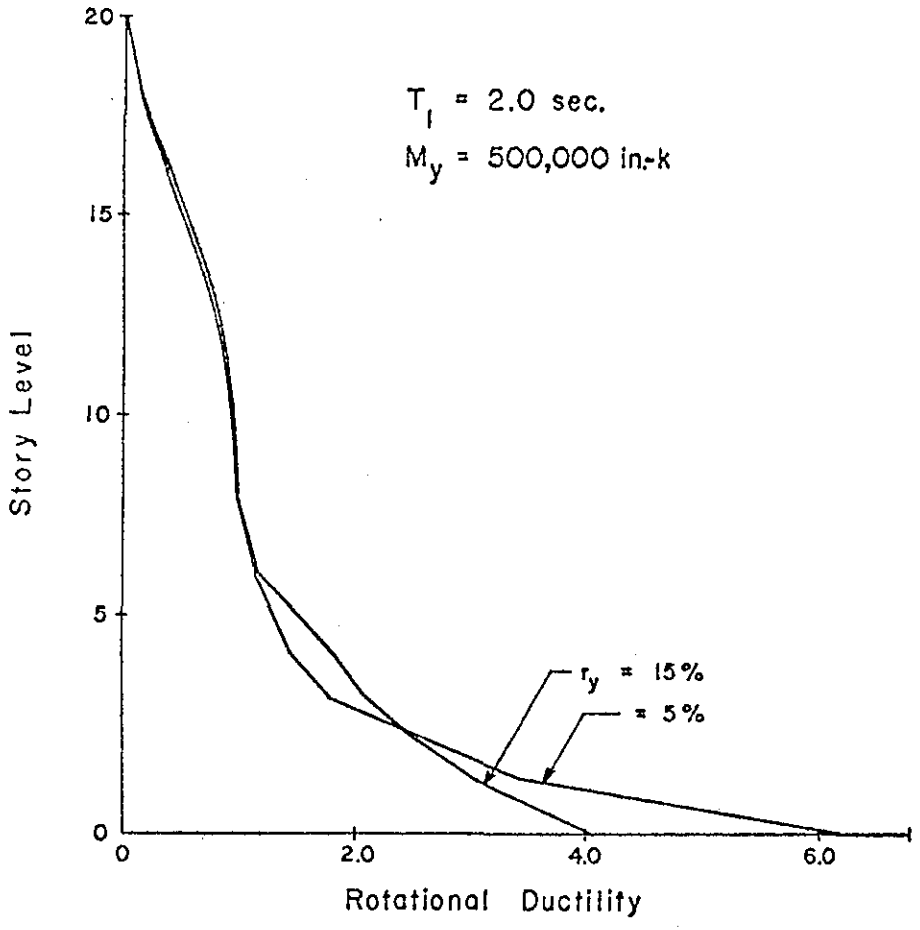

(e)

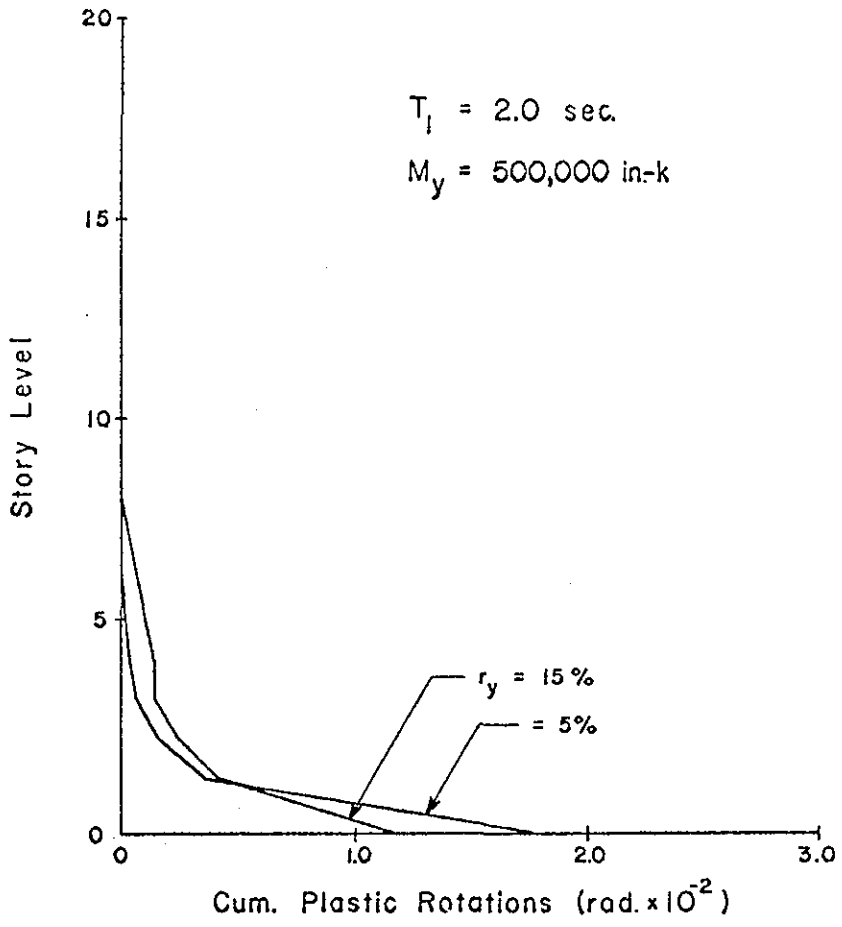

(f)

Fig. 51 (cont'd.) Effect of Slope of Post-Yield Branch of Moment-Rotation Curve

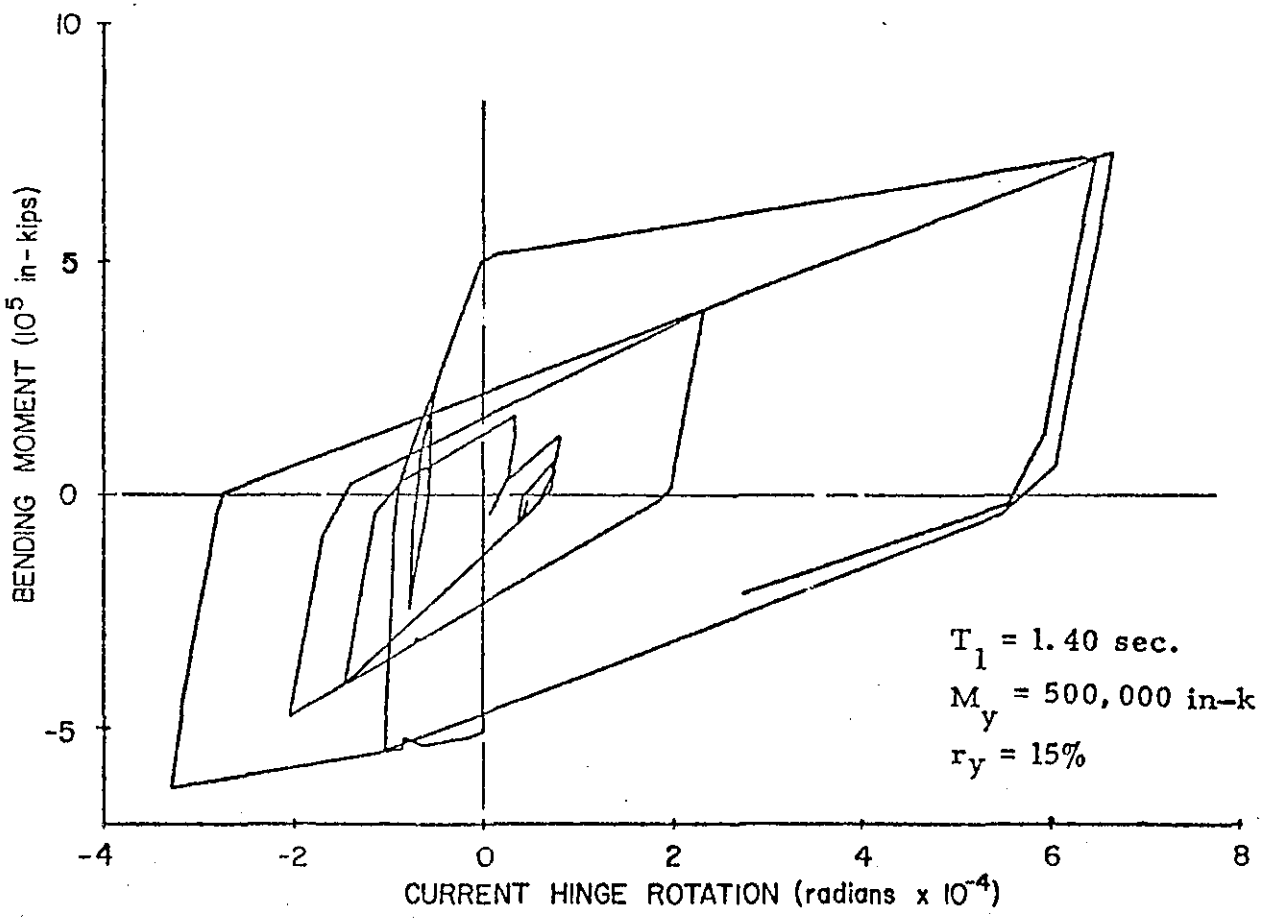

Fig. 52 Moment-Rotation Loop for First Story Hinge

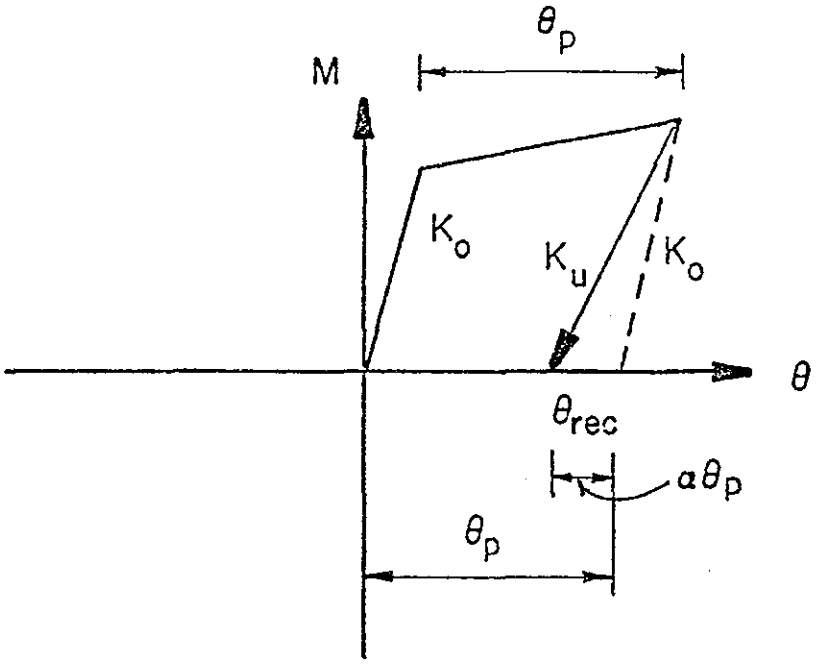

(a) unloading stiffness

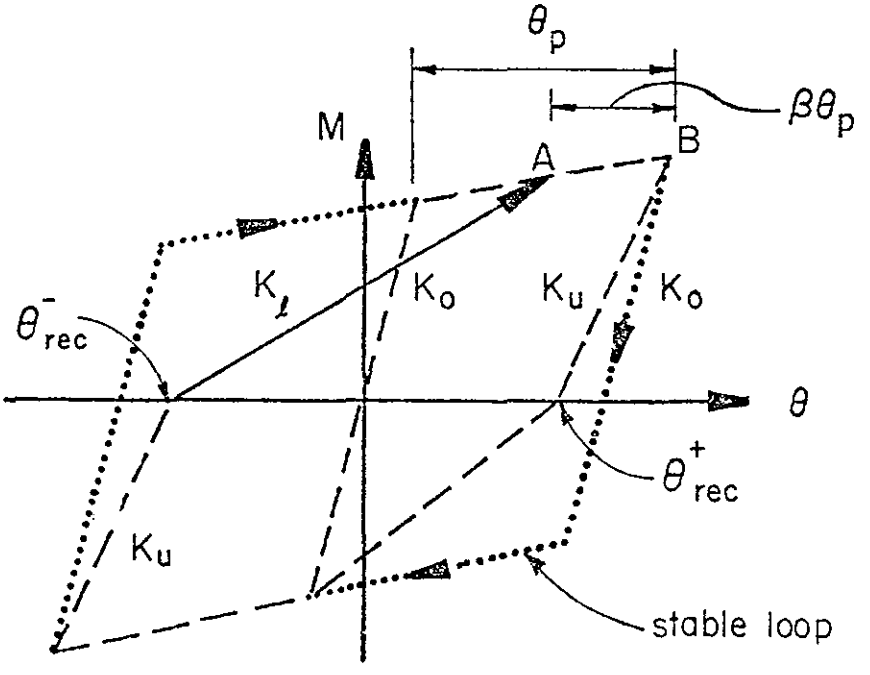

(b) reloading stiffness

Fig. 53 Takeda Model Parameters α and β

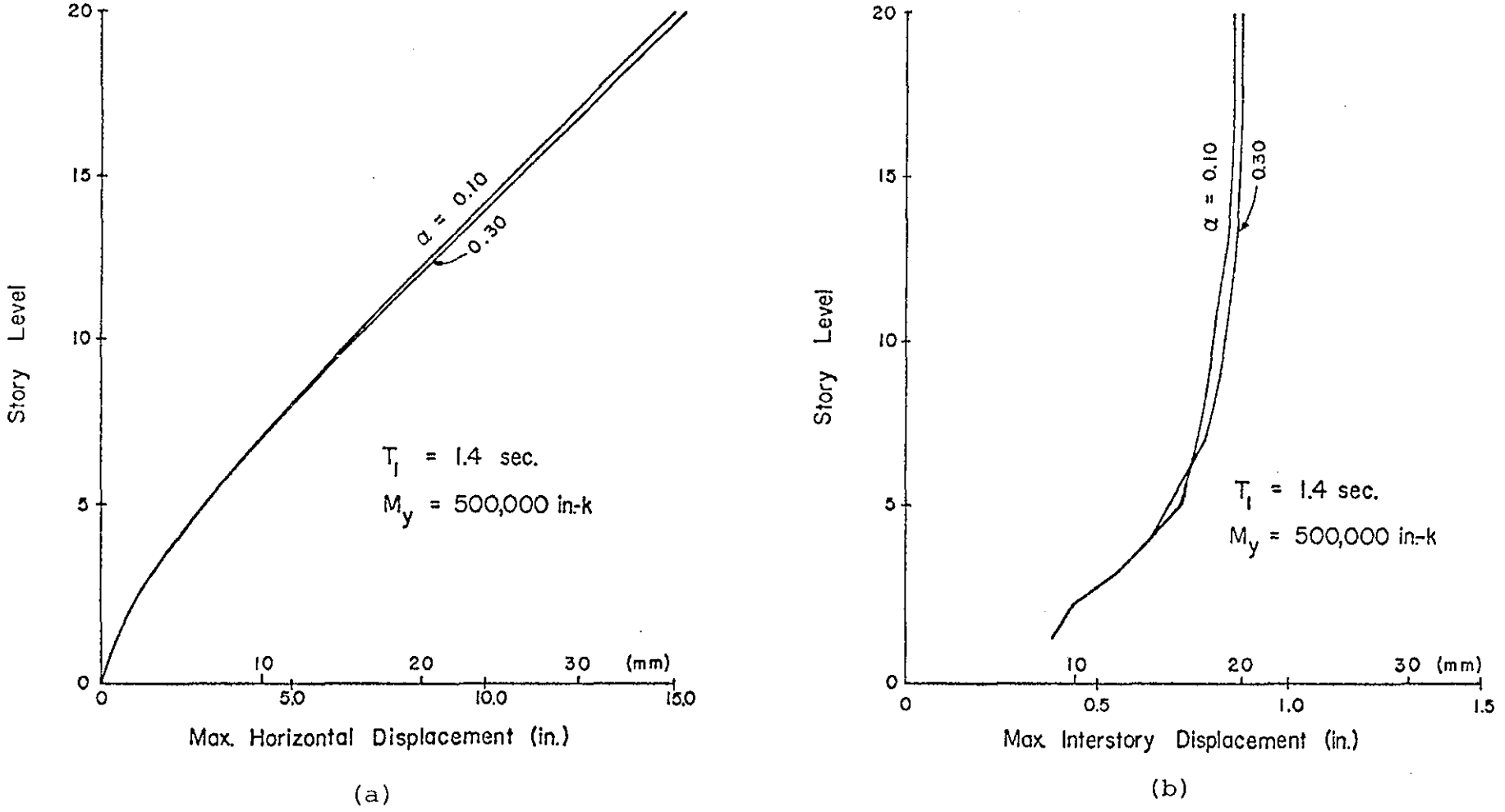

Fig. 54 Effect of Plastic Hinge M-θ Hysteretic Loop Unloading Parameters α

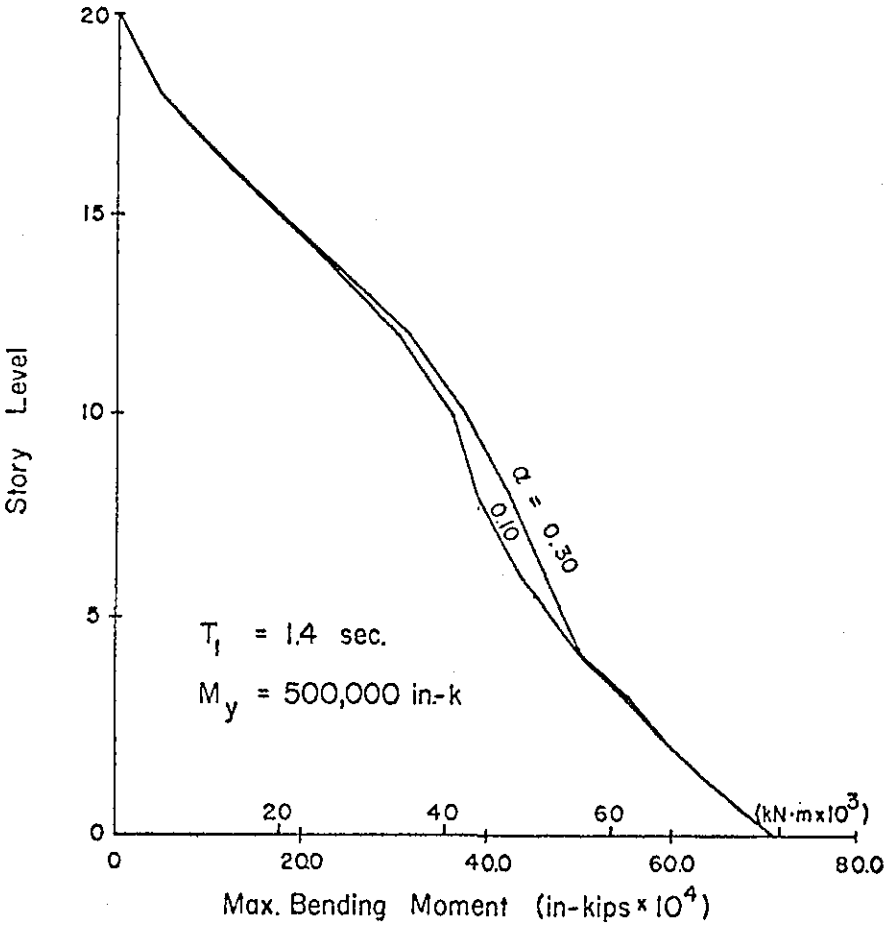

(c)

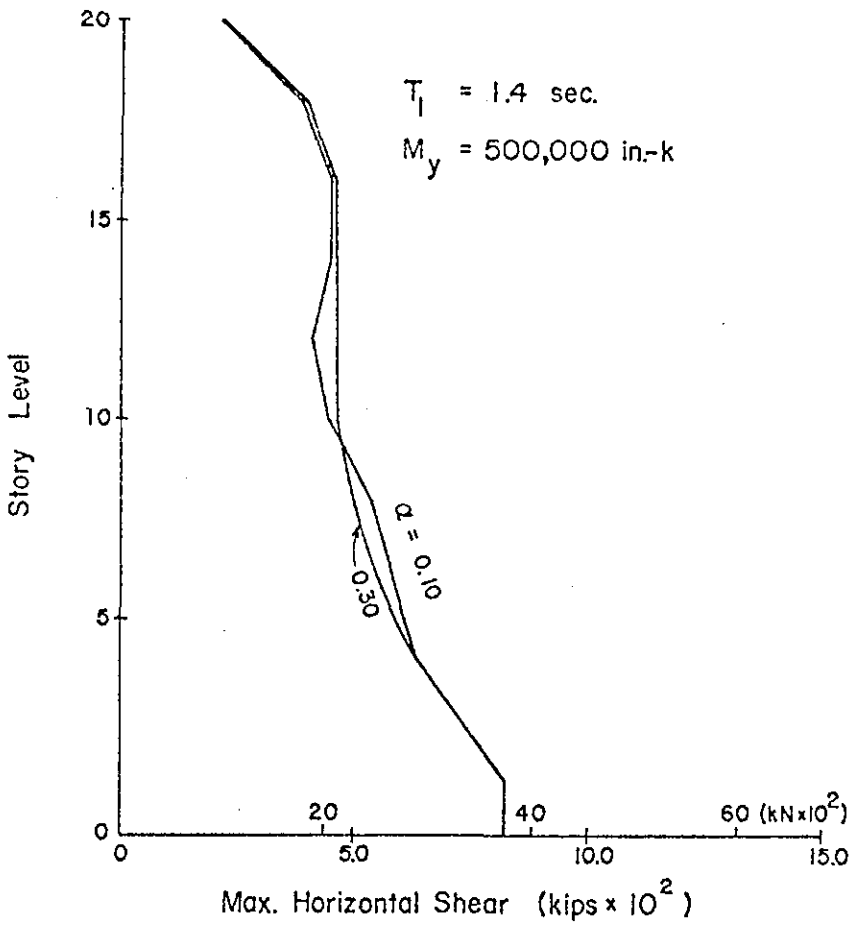

(d)

Fig. 54 (cont'd.) Effect of Plastic Hinge M-θ Hysteretic Loop Unloading Parameters α

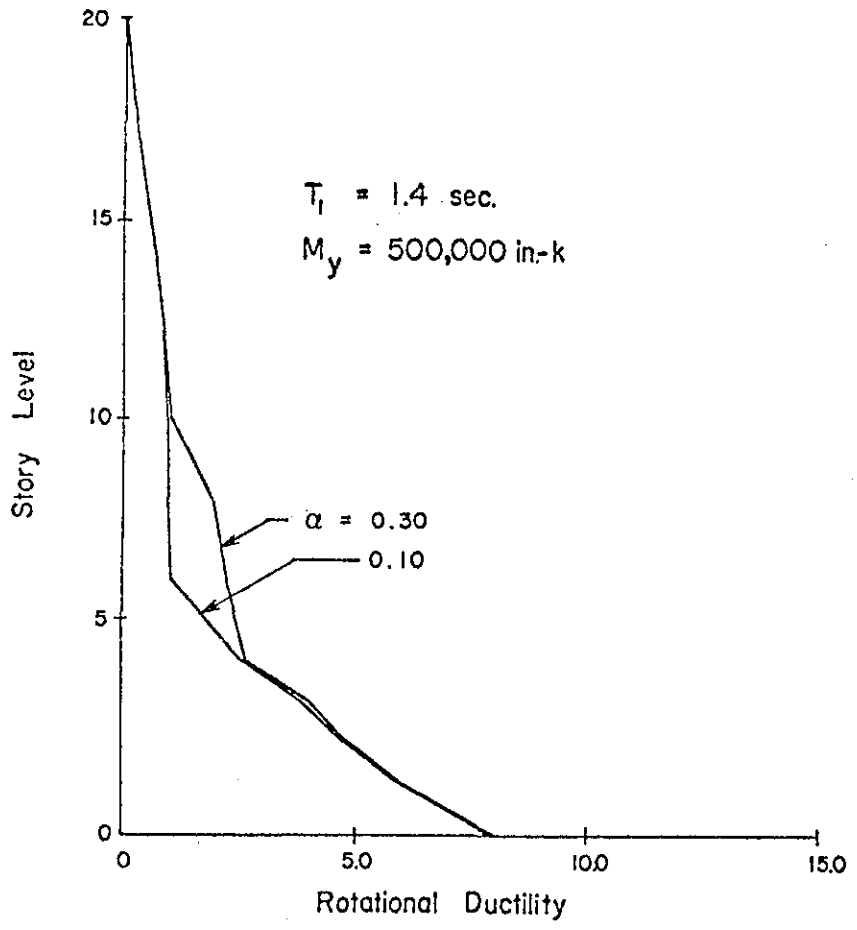

(e)

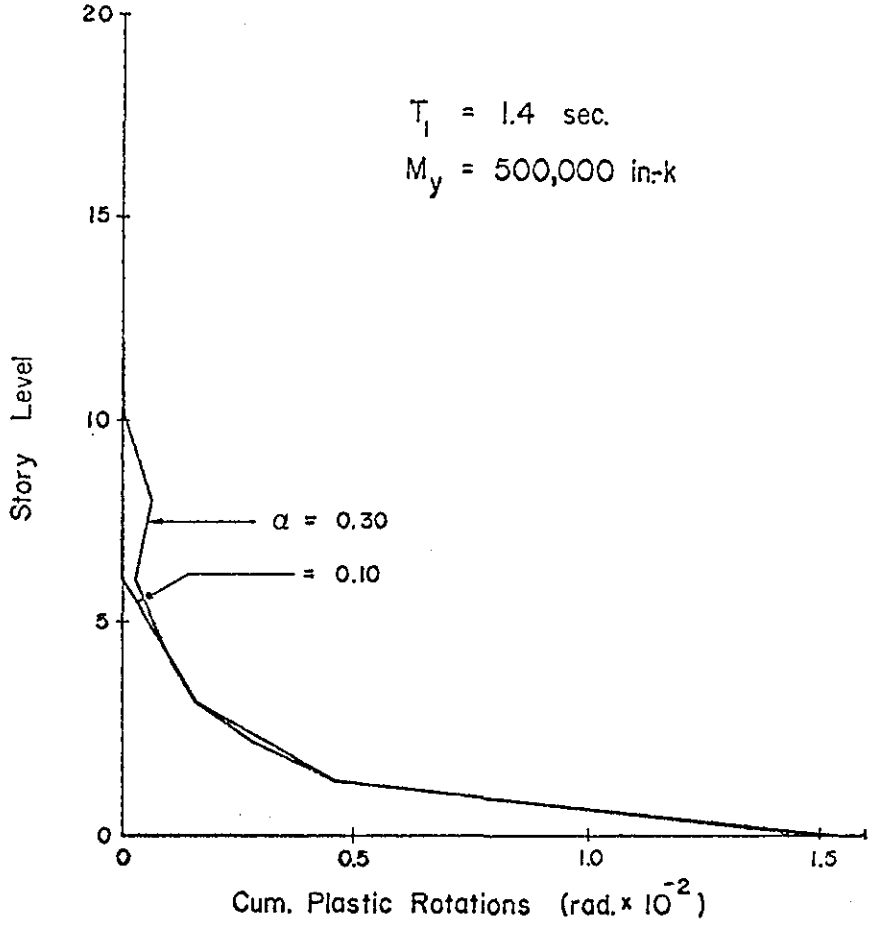

(f)

Fig. 54(cont'd.) Effect of Plastic Hinge M-θ Hysteretic Loop Unloading Parameters α

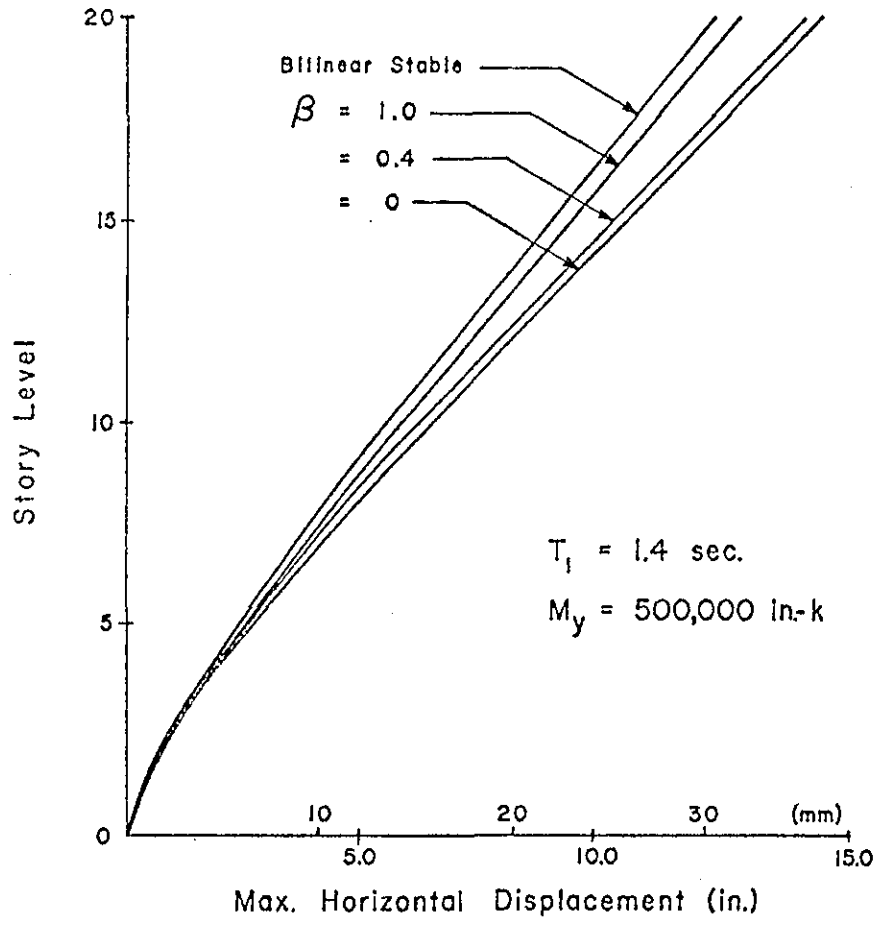

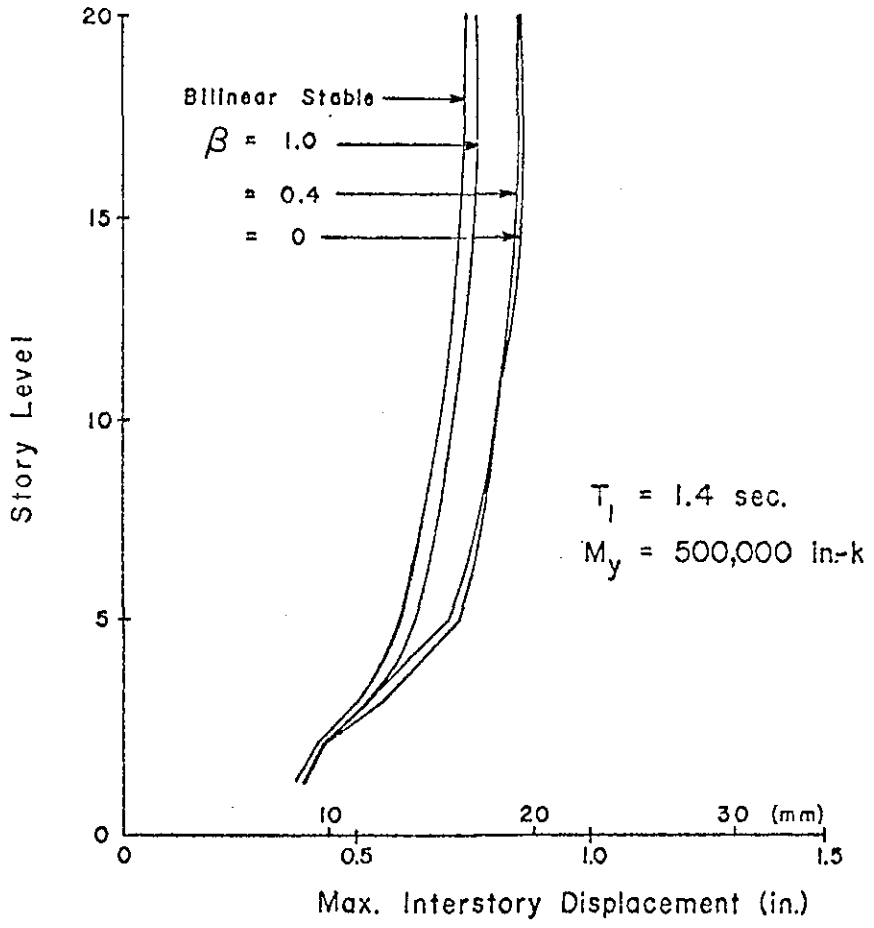

Fig. 55 Effect of Plastic Hinge M-θ Hysteretic Loop Reloading Parameter β

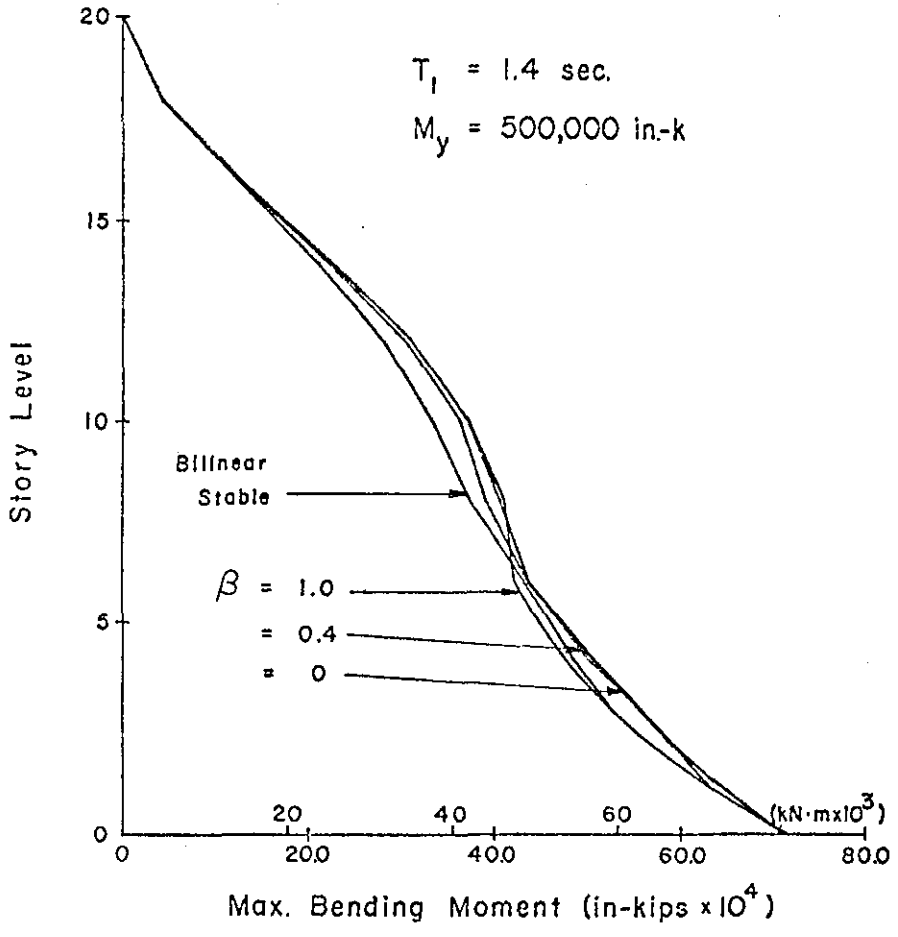

(c)

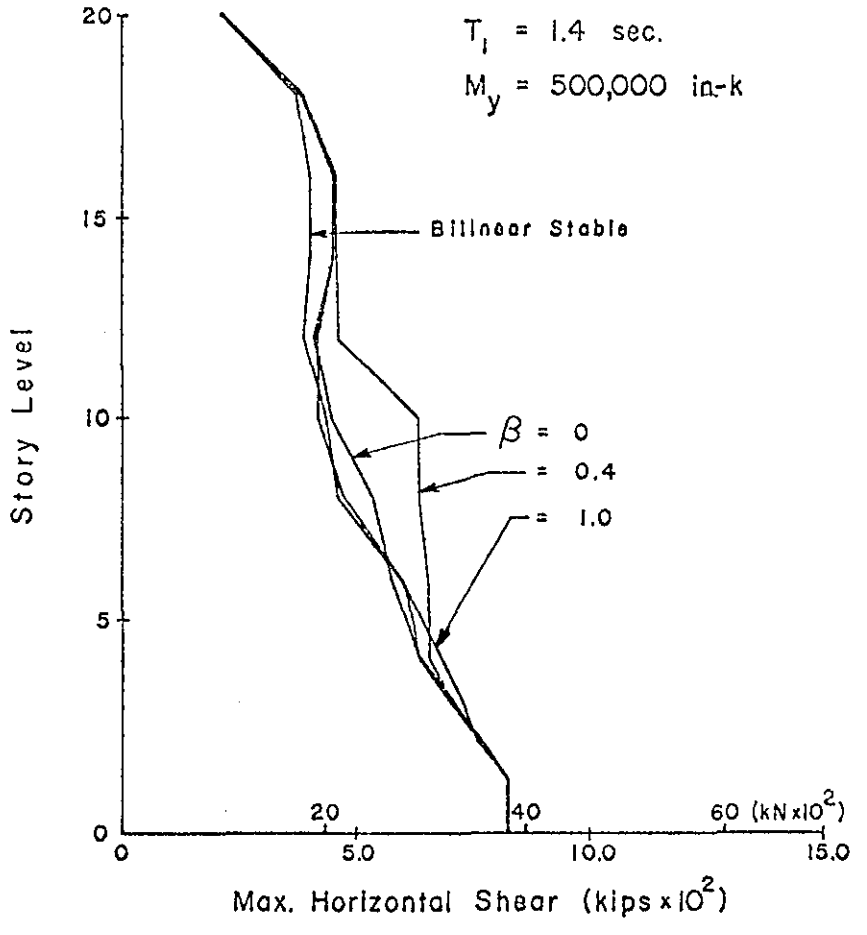

(d)

Fig. 55 (cont'd.) Effect of Plastic Hinge M-θ Hysteretic Loop Reloading Parameter β

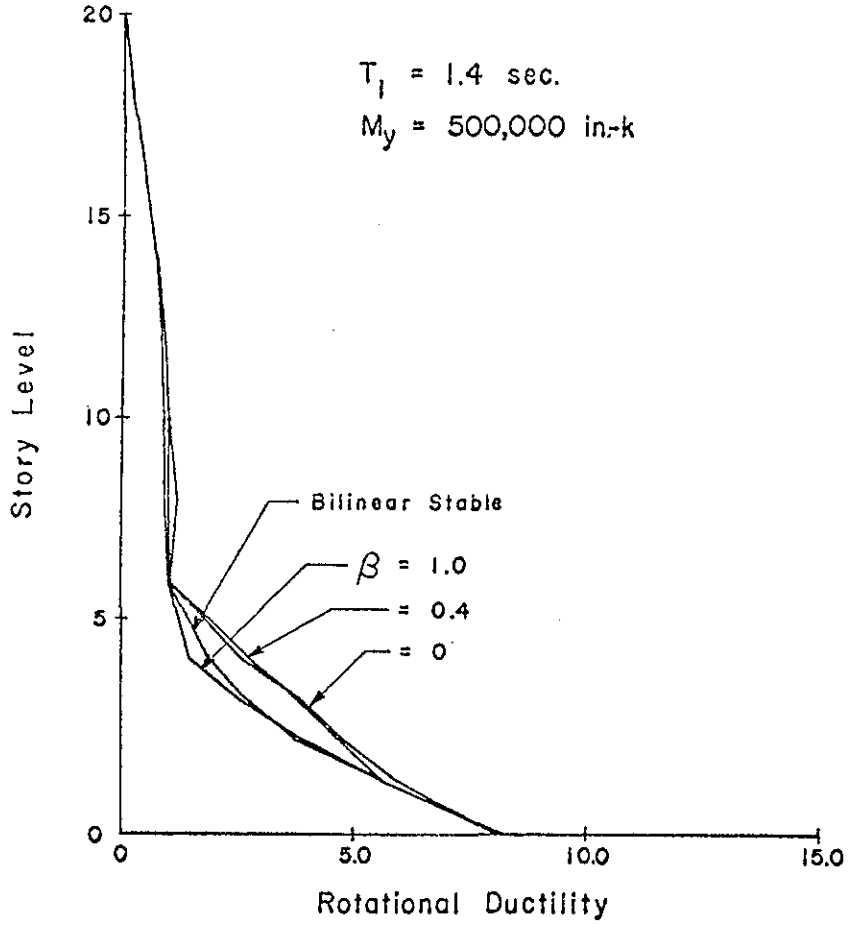

(e)

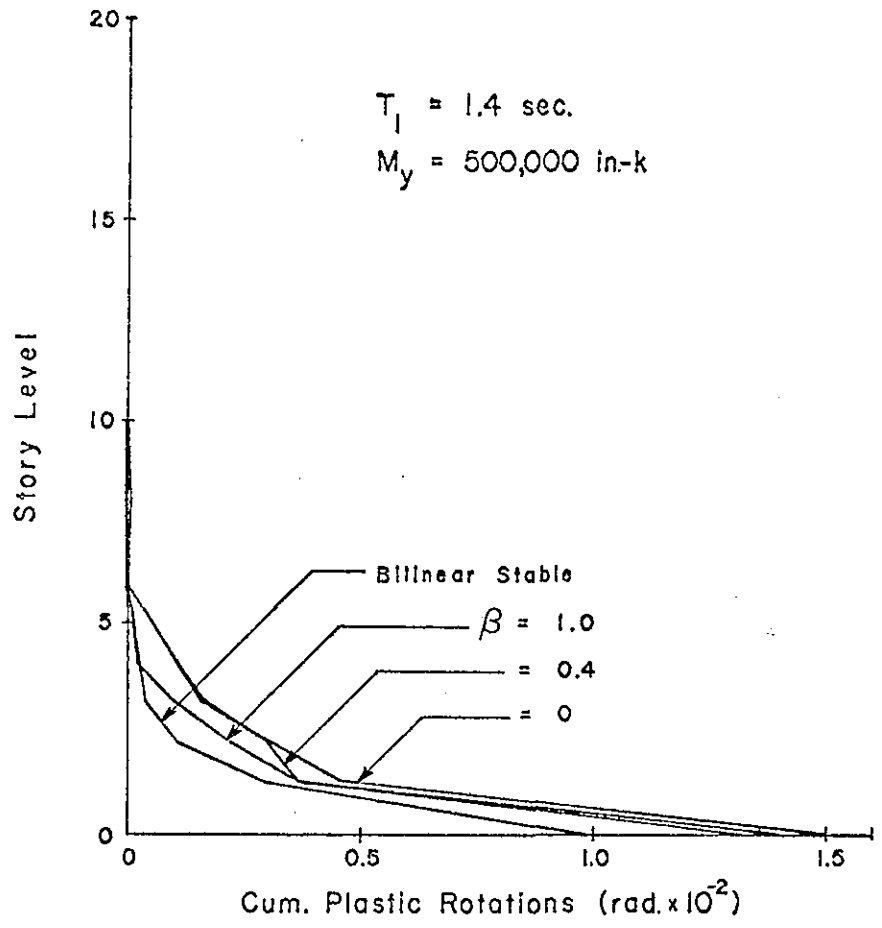

(f)

Fig. 55 (cont'd.) Effect of Plastic Hinge M-θ Hysteretic Loop Reloading Parameter β

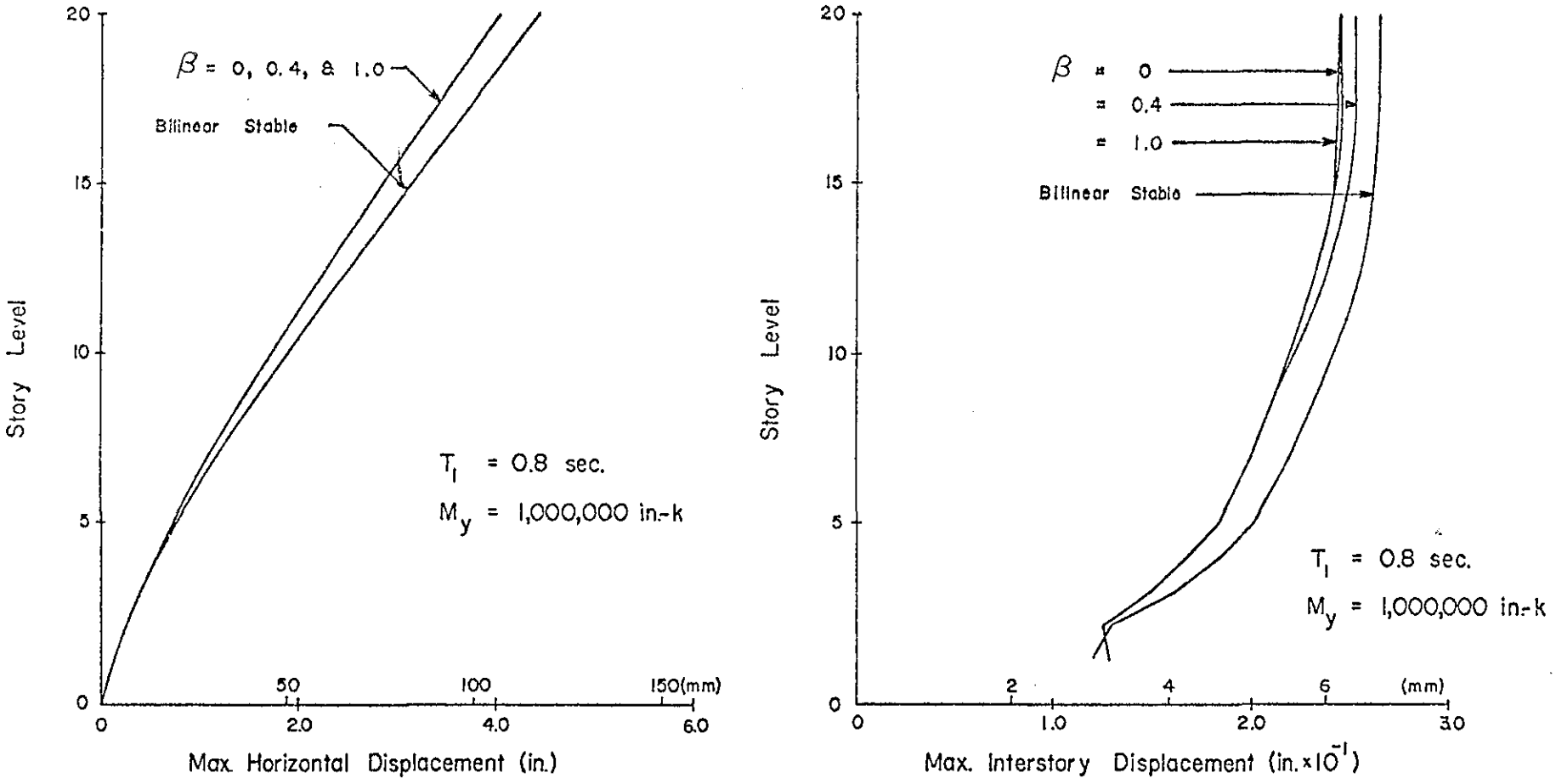

(a) (b)

Fig. 56 Effect of Plastic Hinge M-θ Hysteretic Loop Reloading Parameter β

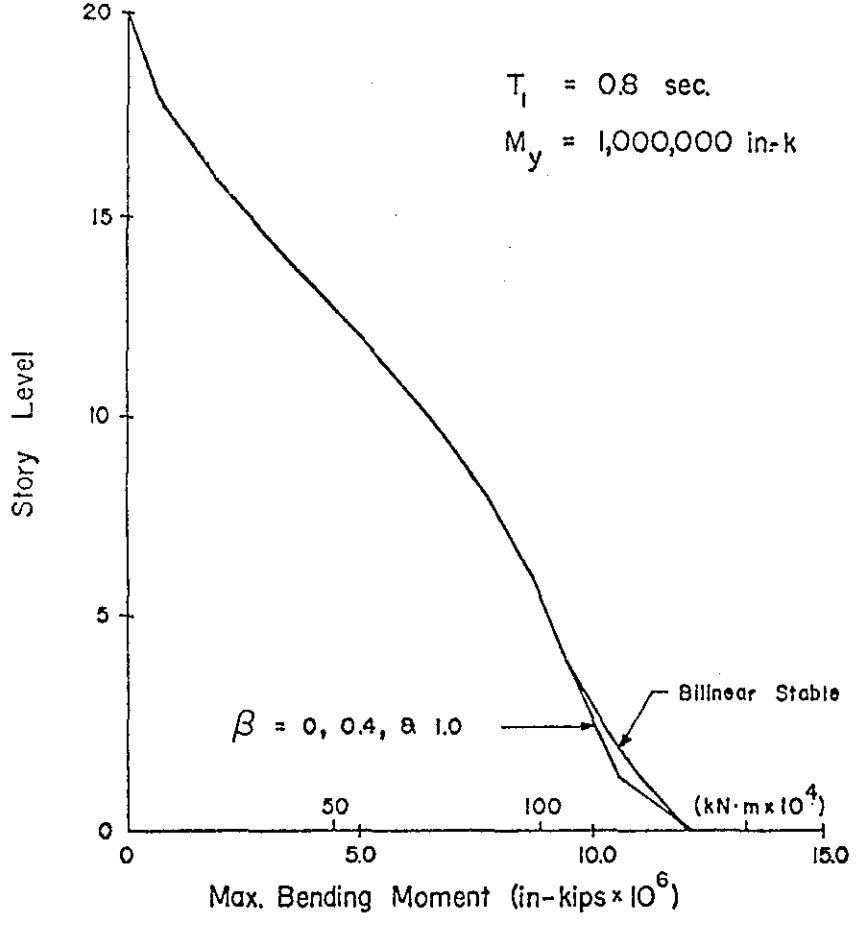

(c)

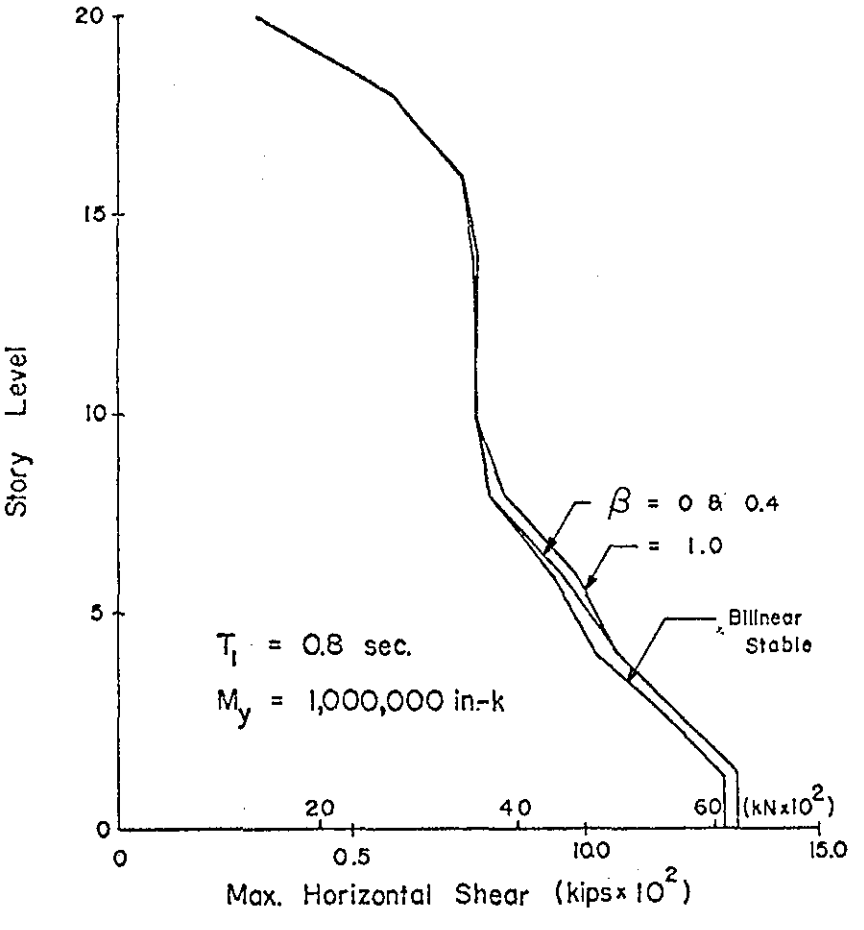

(d)

Fig. 56 (cont'd.) Effect of Plastic Hinge M-θ Hysteretic Loop Reloading Parameter β

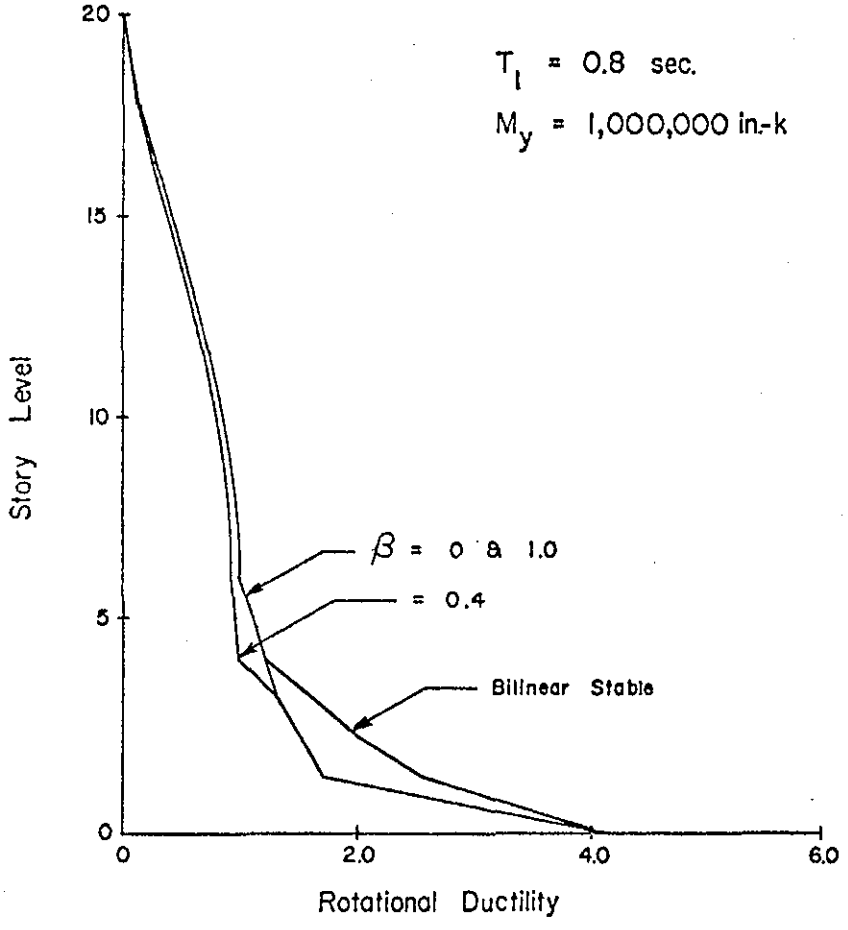

(e)

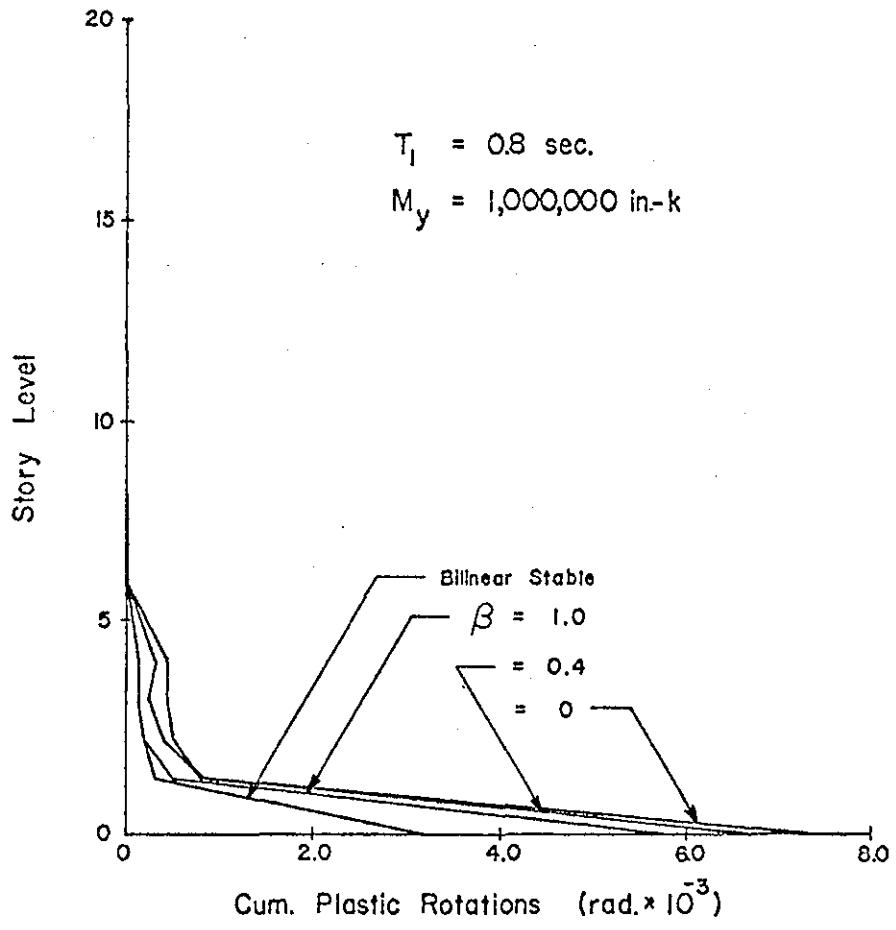

(f)

Fig. 56 (cont'd.) Effect of Plastic Hinge M-θ Hysteretic Loop Reloading Parameter β

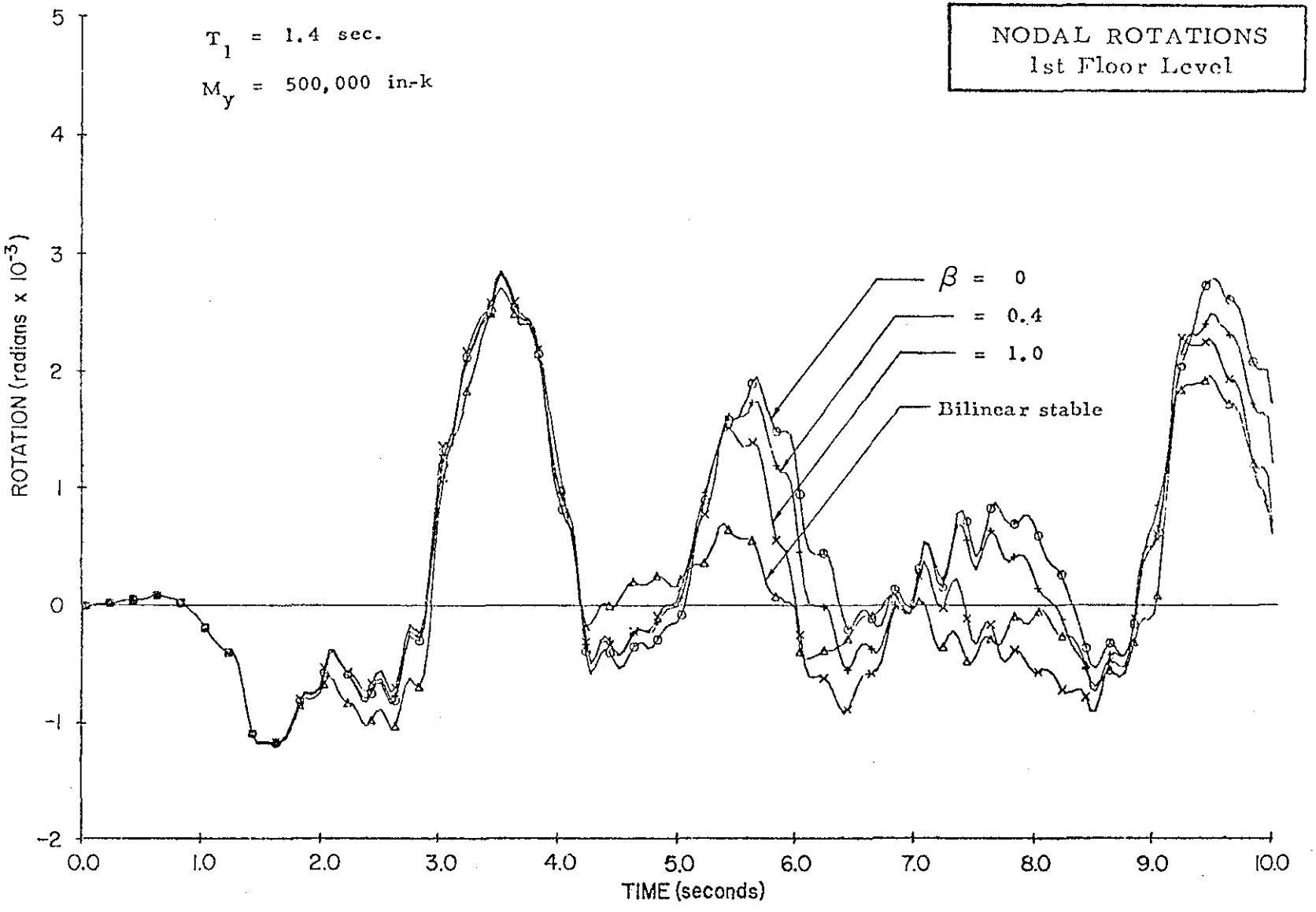

Fig. 57 Rotation in First Story versus Time for Different Values of the Plastic Hinge M-θ Hysteretic Loop Reloading Parameter β

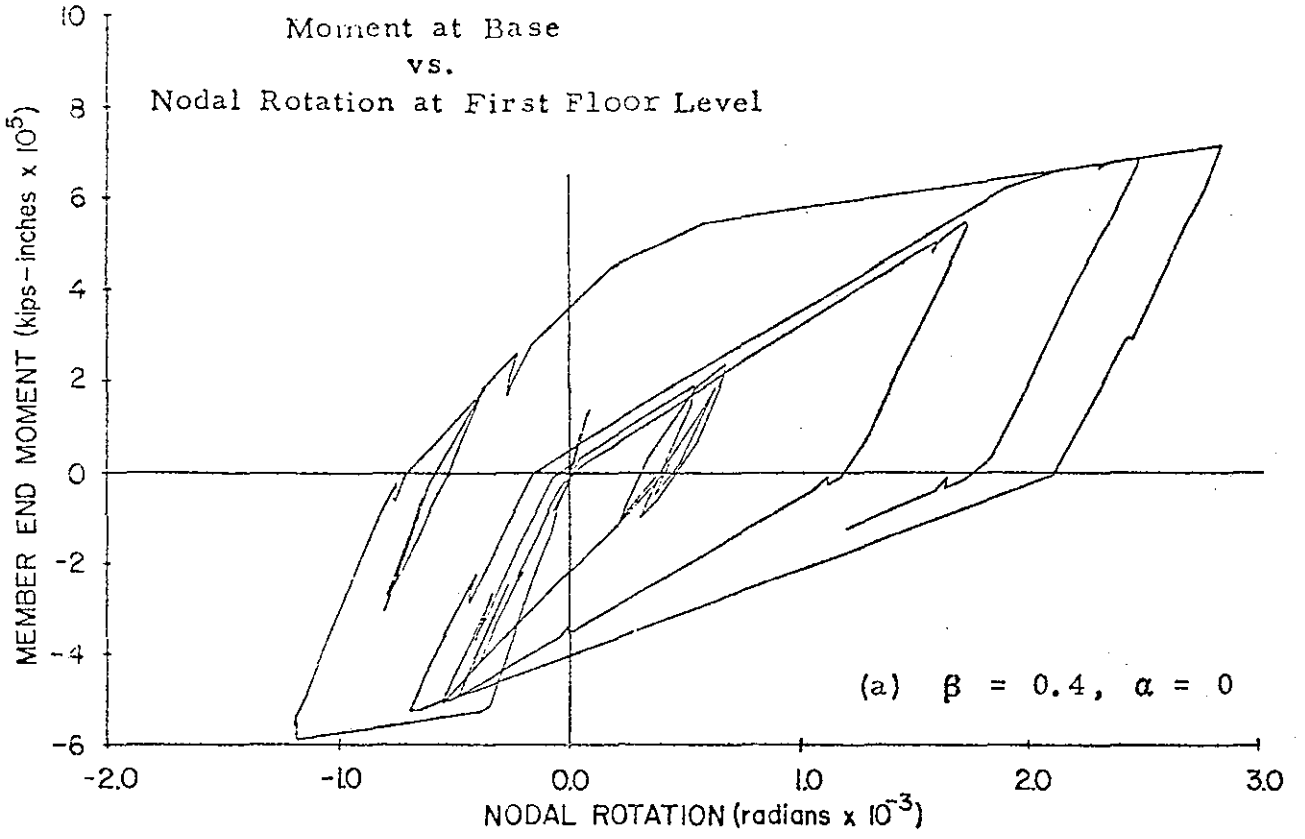

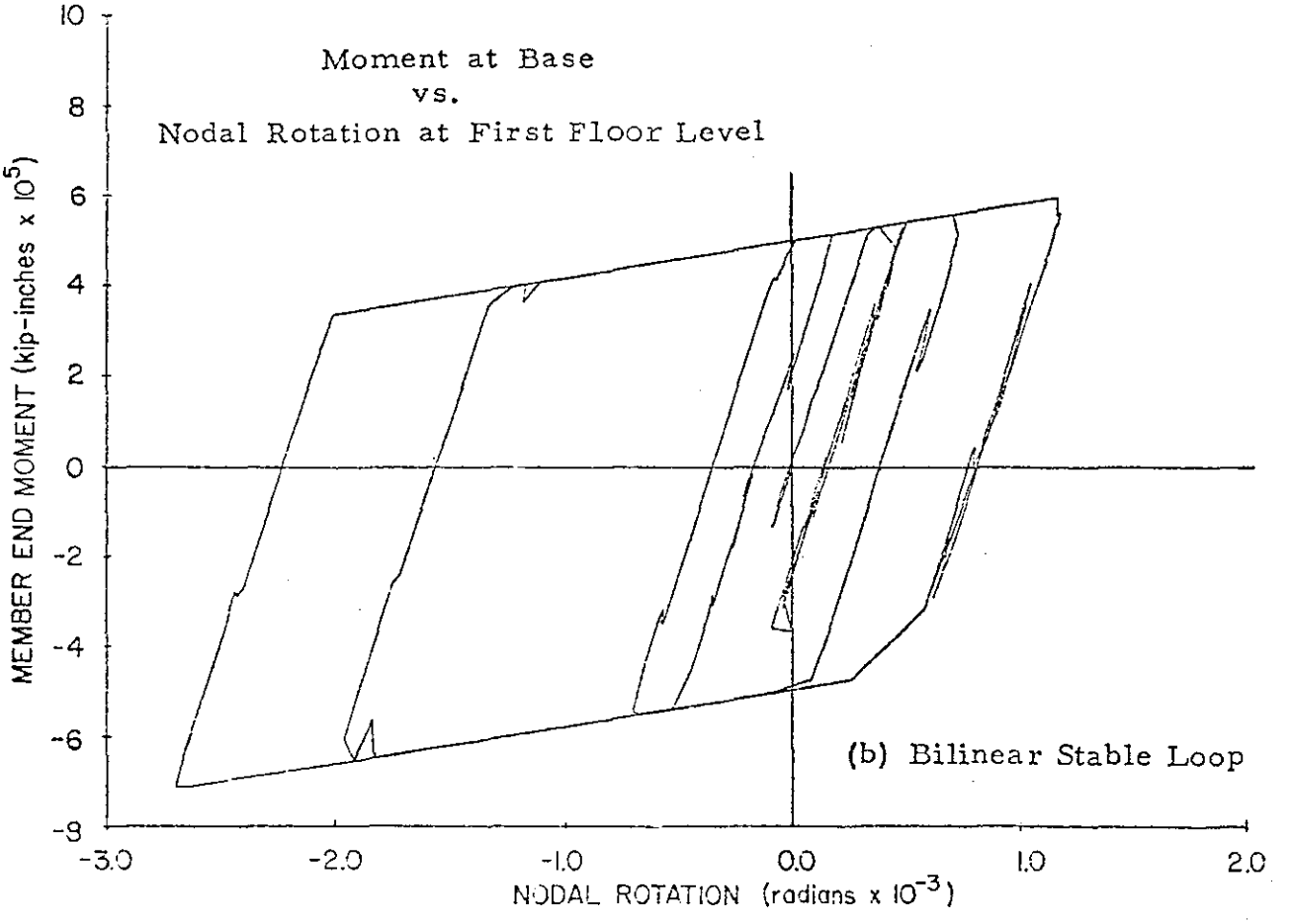

Fig. 58 Moment at base versus Nodal Rotation at First Story Level for Different M-θ Curve Characteristics

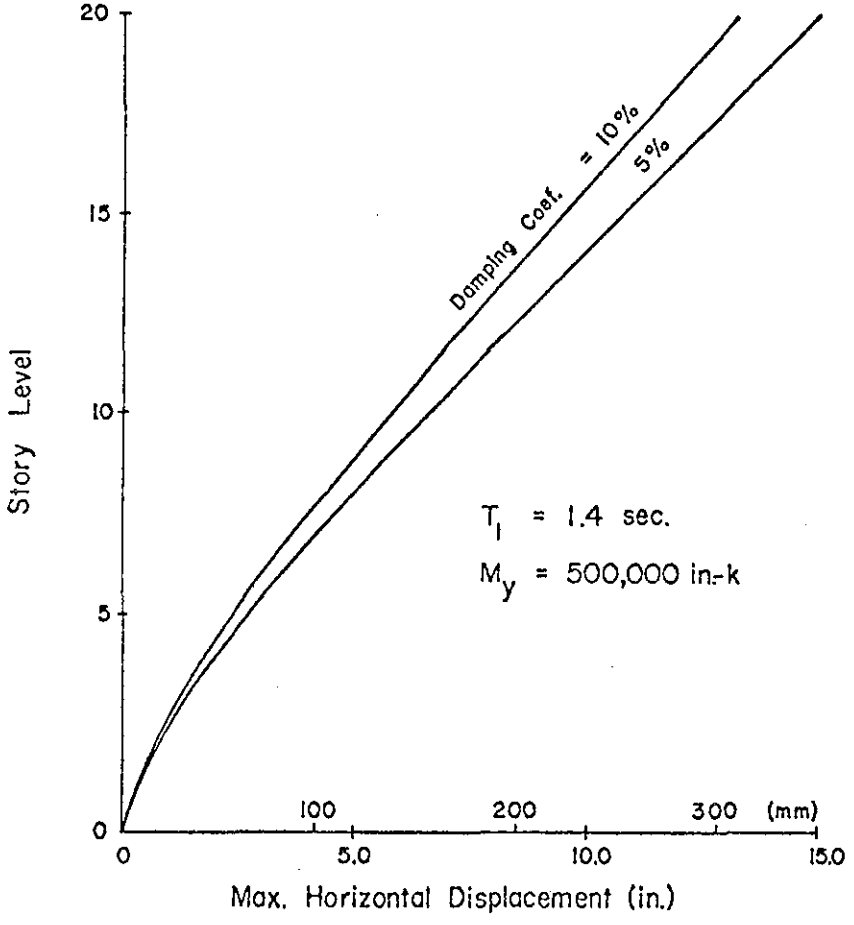

(a)

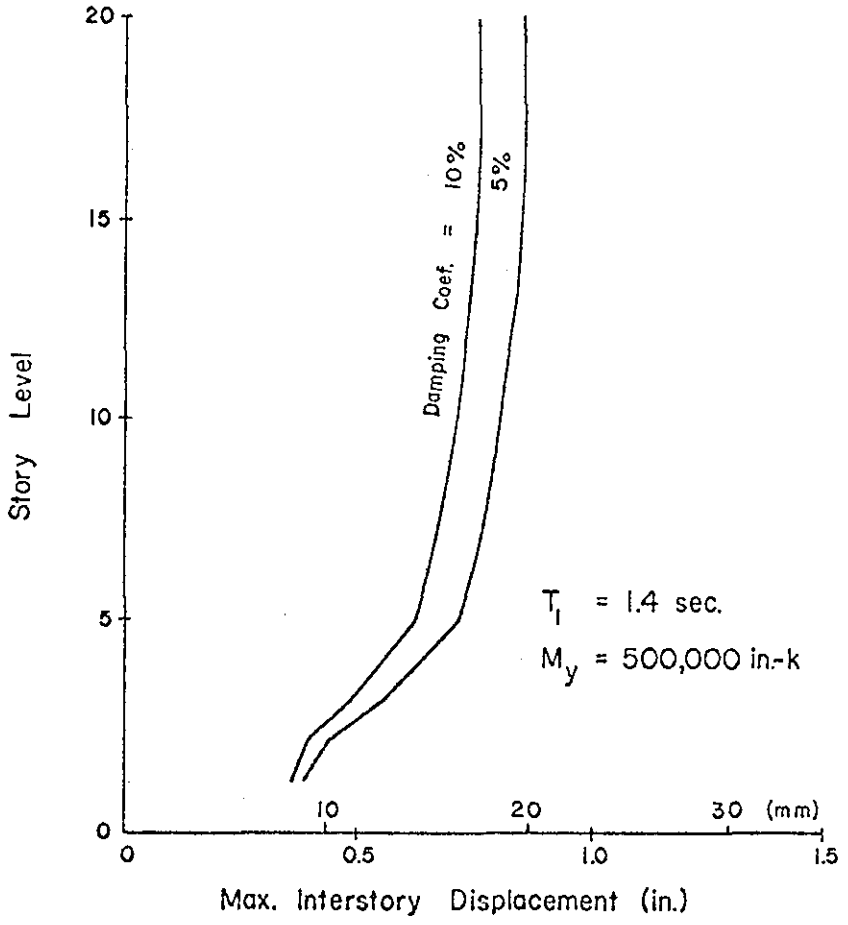

(b)

Fig. 59 Effect of Damping

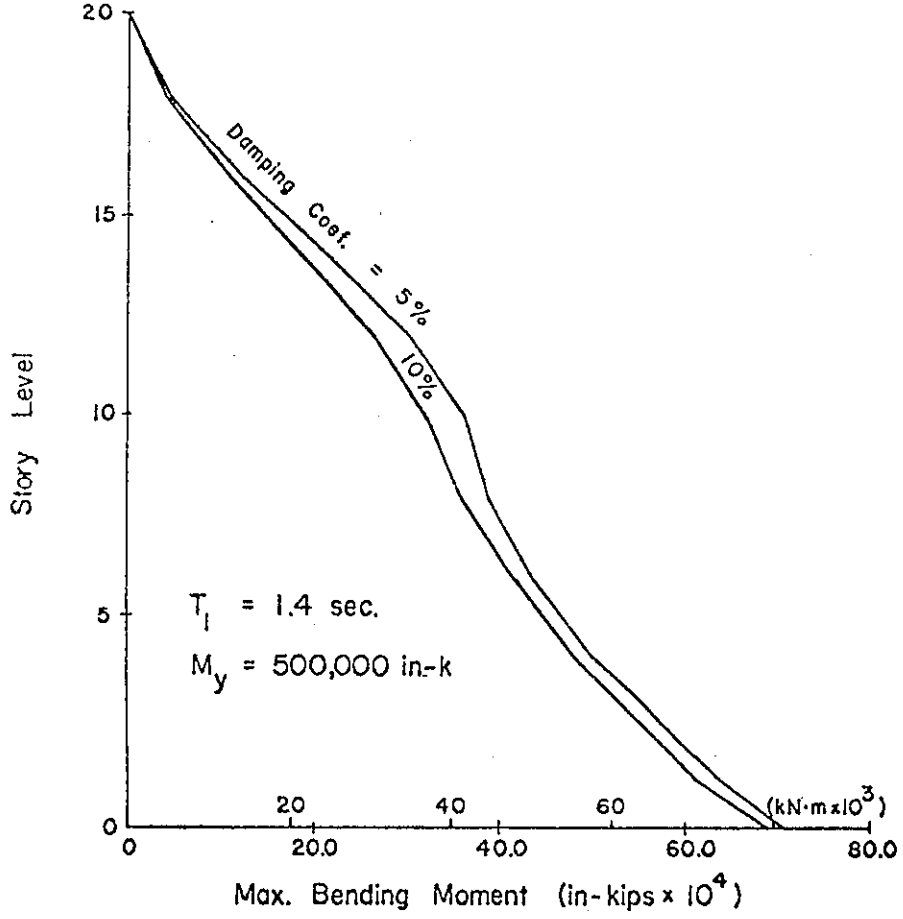

(c)

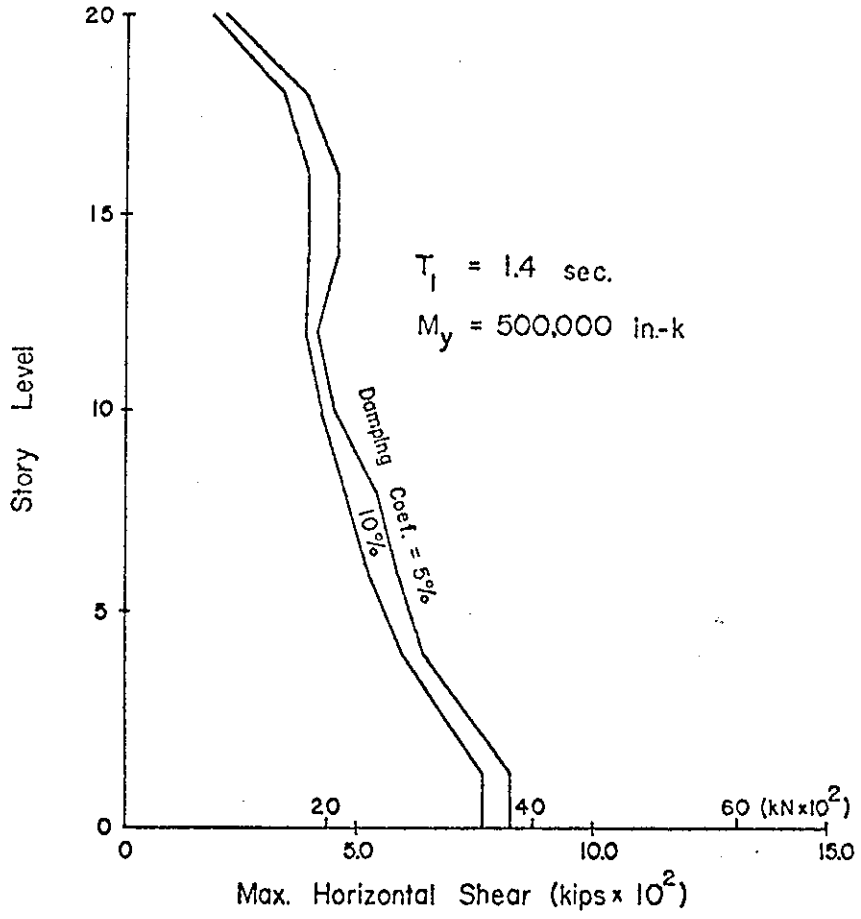

(d)

Fig. 59 (cont'd.) Effect of Damping

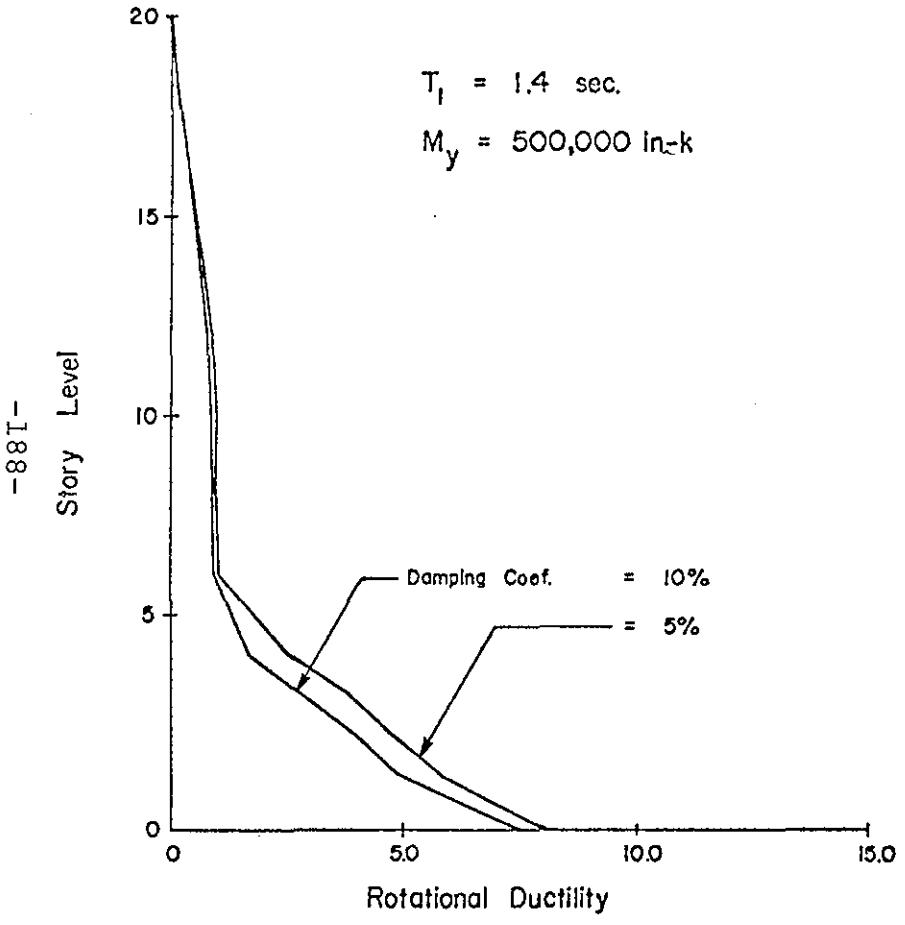

(e)

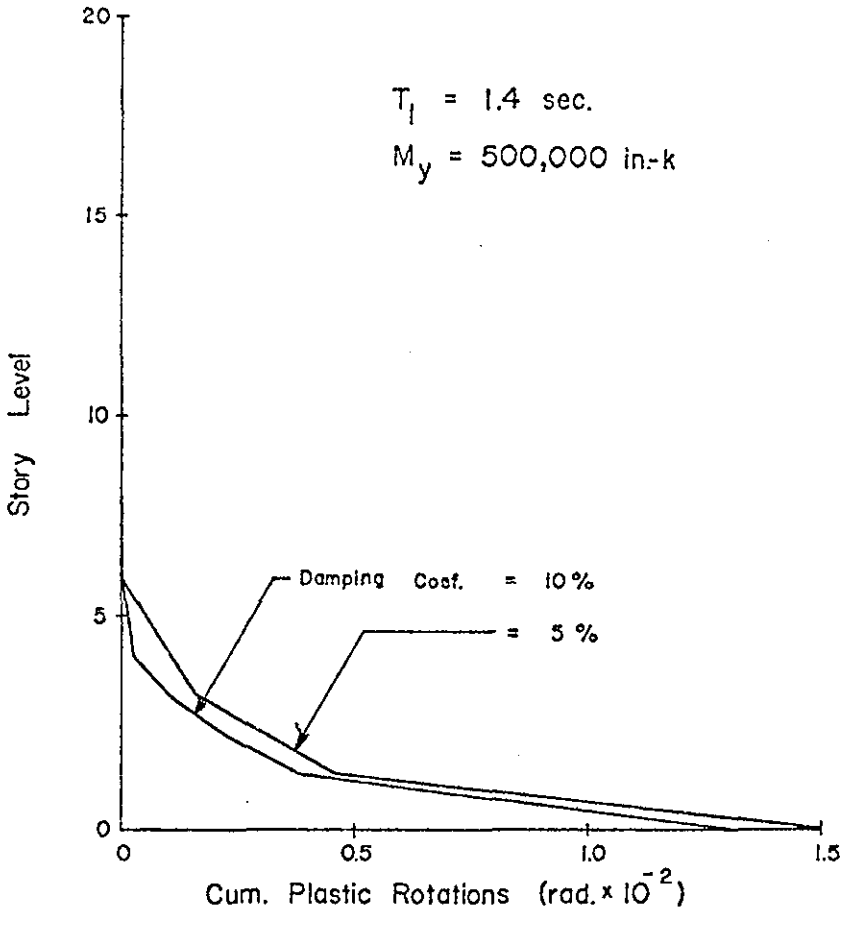

(f)

Fig. 59 (cont'd.) Effect of Damping

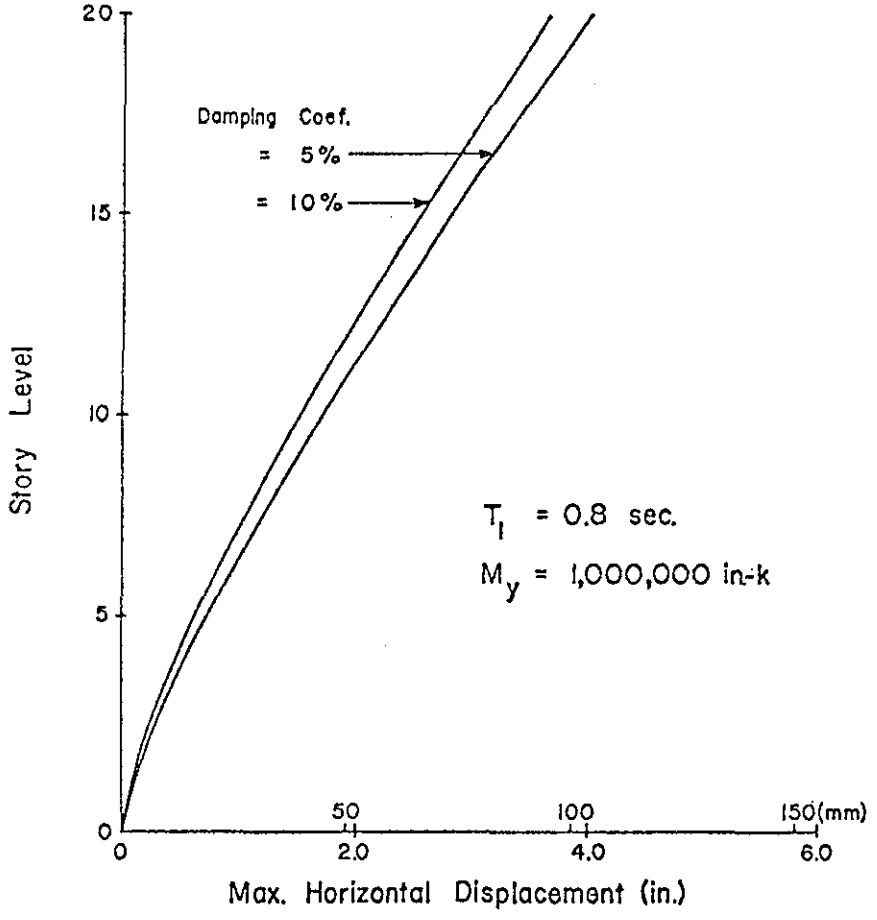

(a)

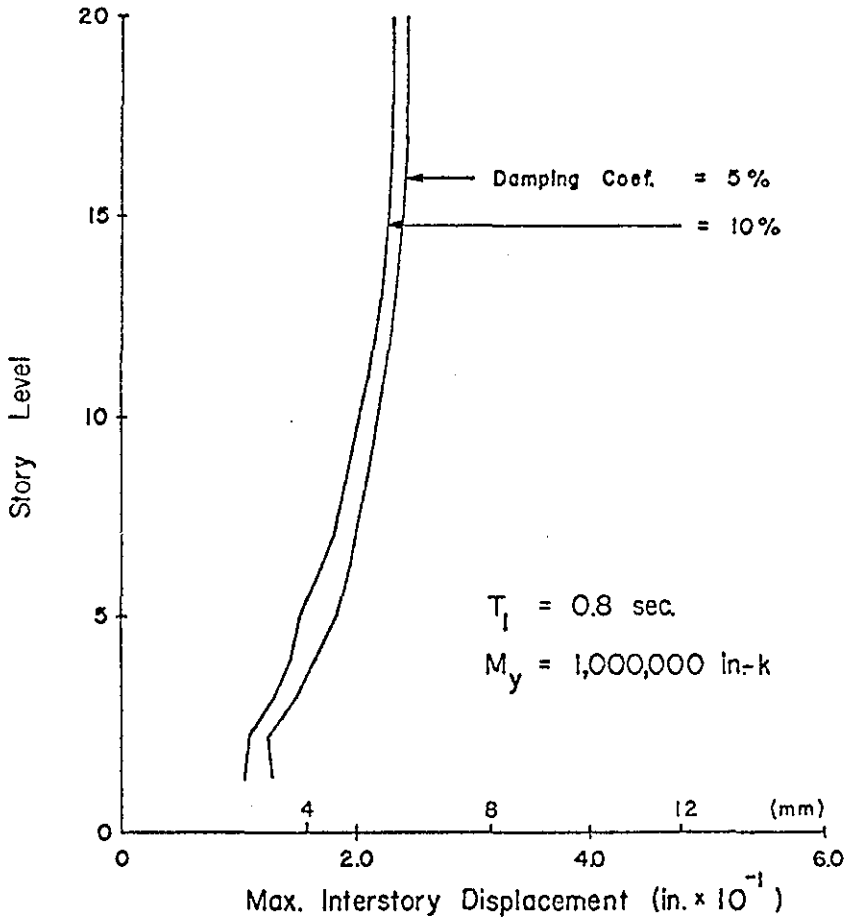

(b)

Fig. 60 Effect of Damping

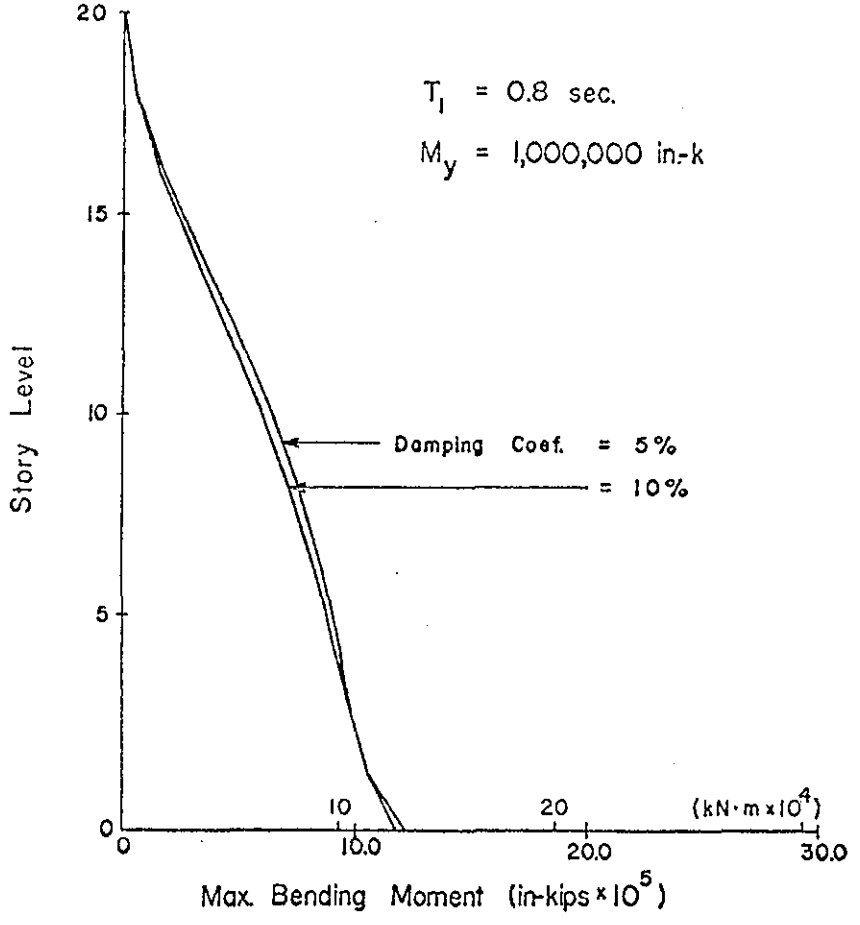

(c)

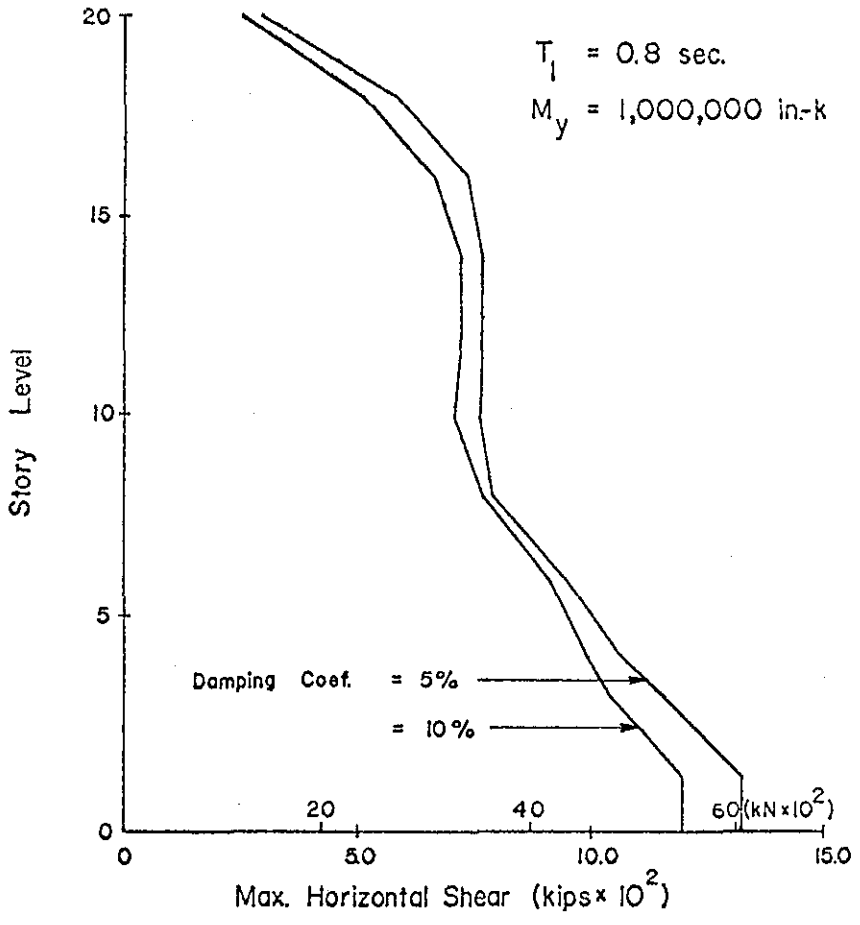

(d)

Fig. 60 (cont'd.) Effect of Damping

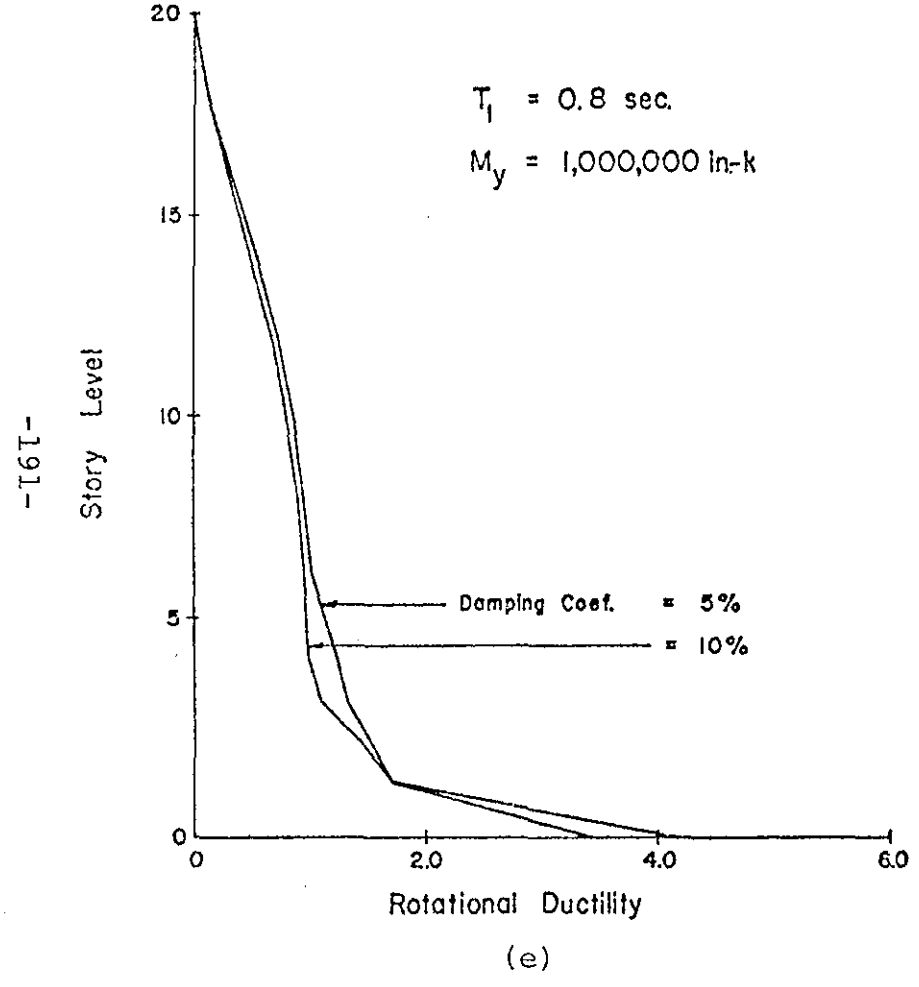

(e)

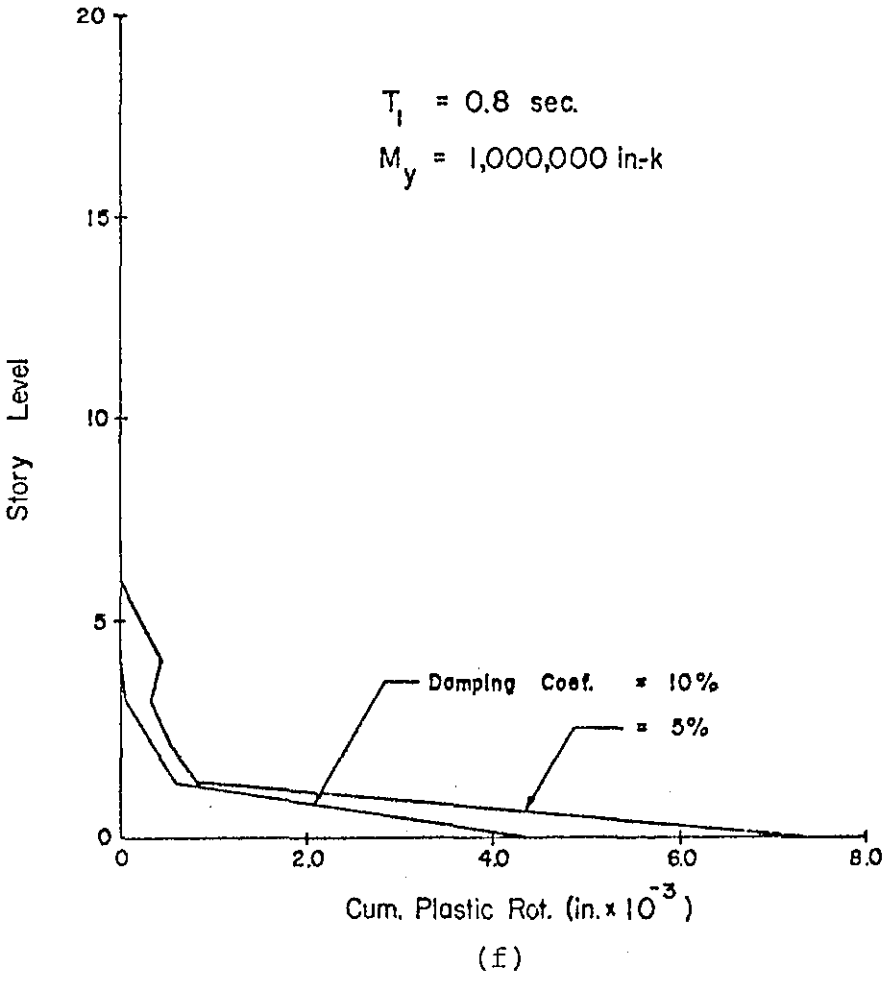

(f)

Fig. 60 (Cont'd.) Effect of Damping

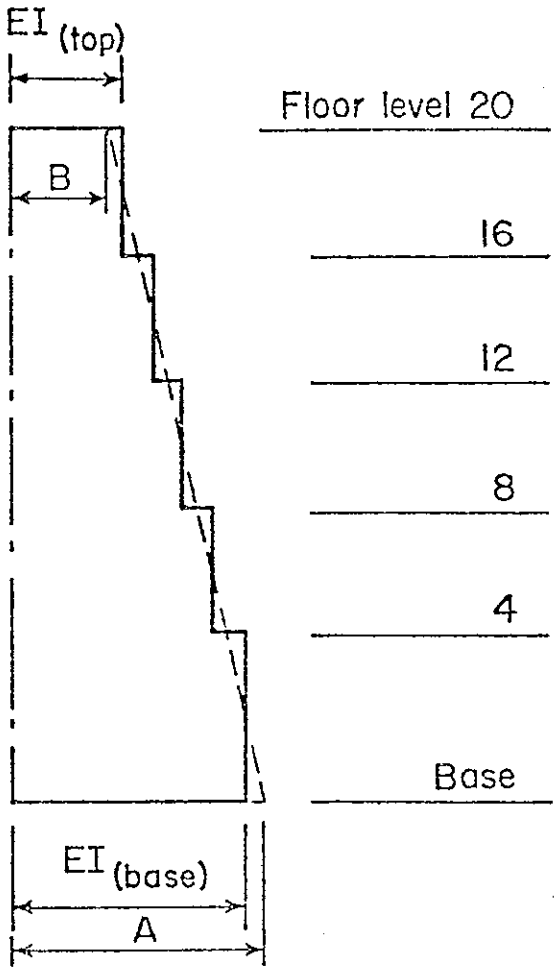

Fig. 61 Stiffness Taper

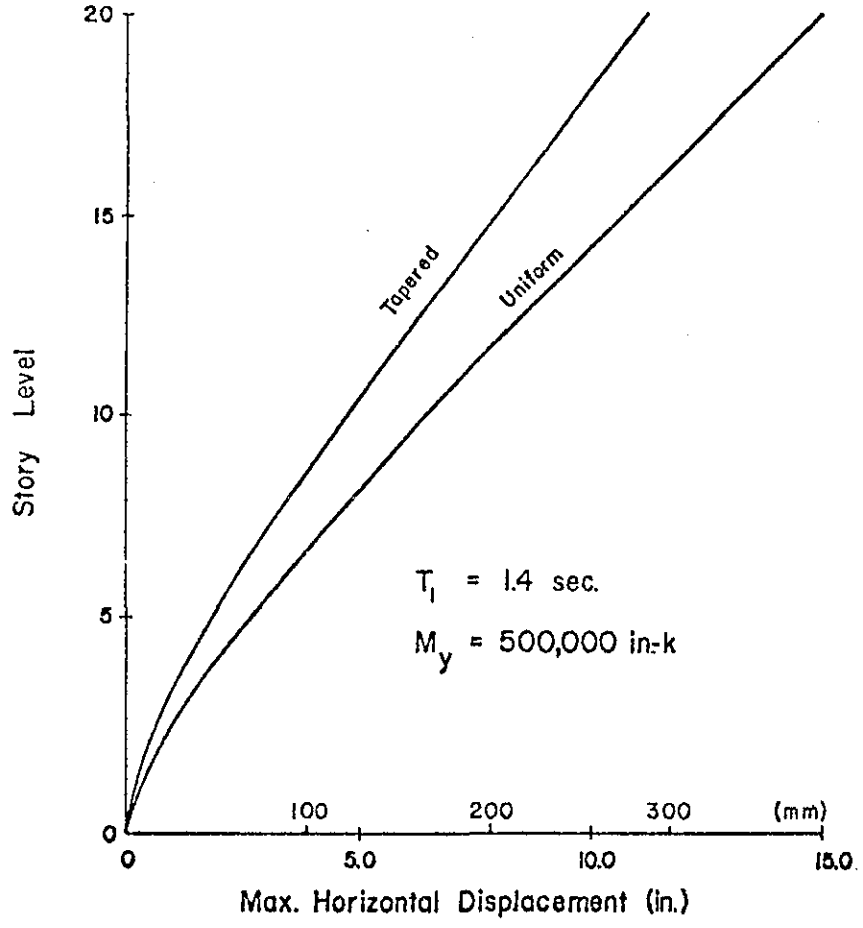

(a)

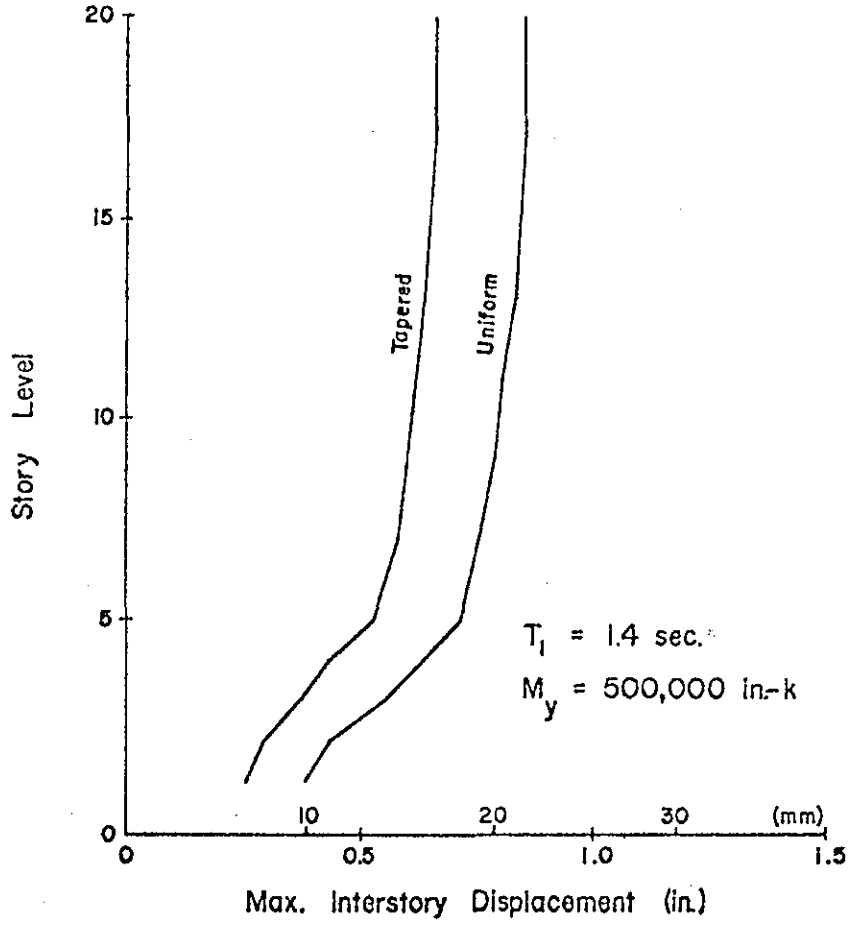

(b)

Fig. 62 Effect of Stiffness Taper

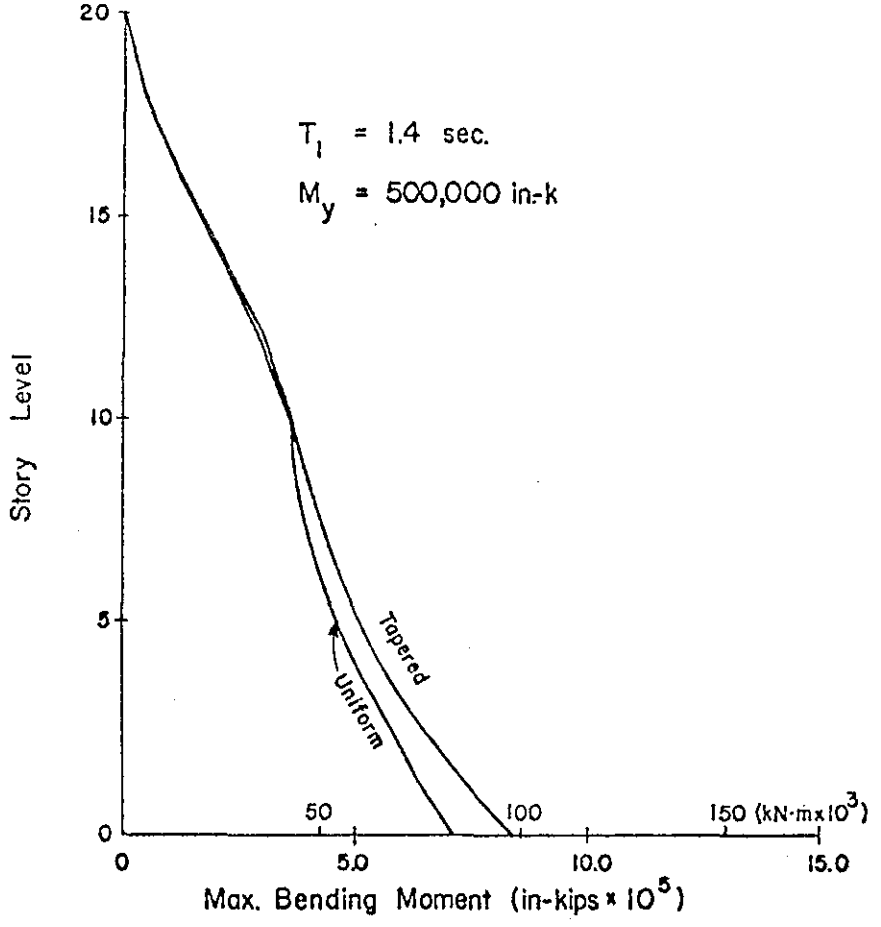

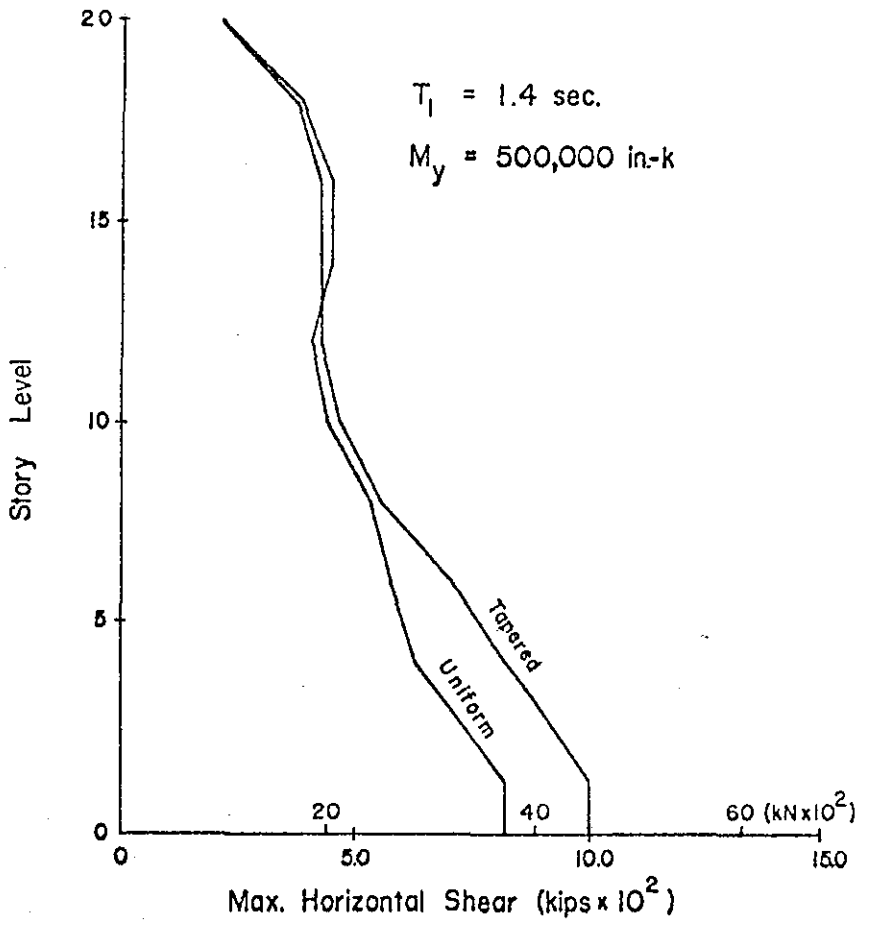

Fig. 62 (cont'd.) Effect of Stiffness Taper

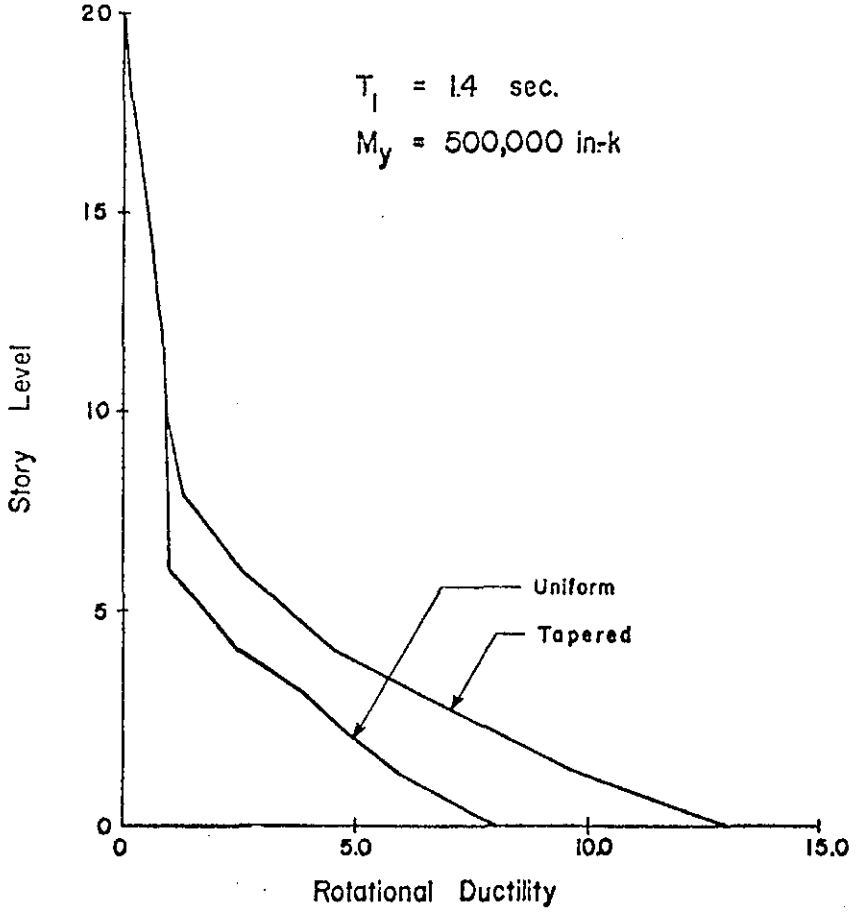

(e)

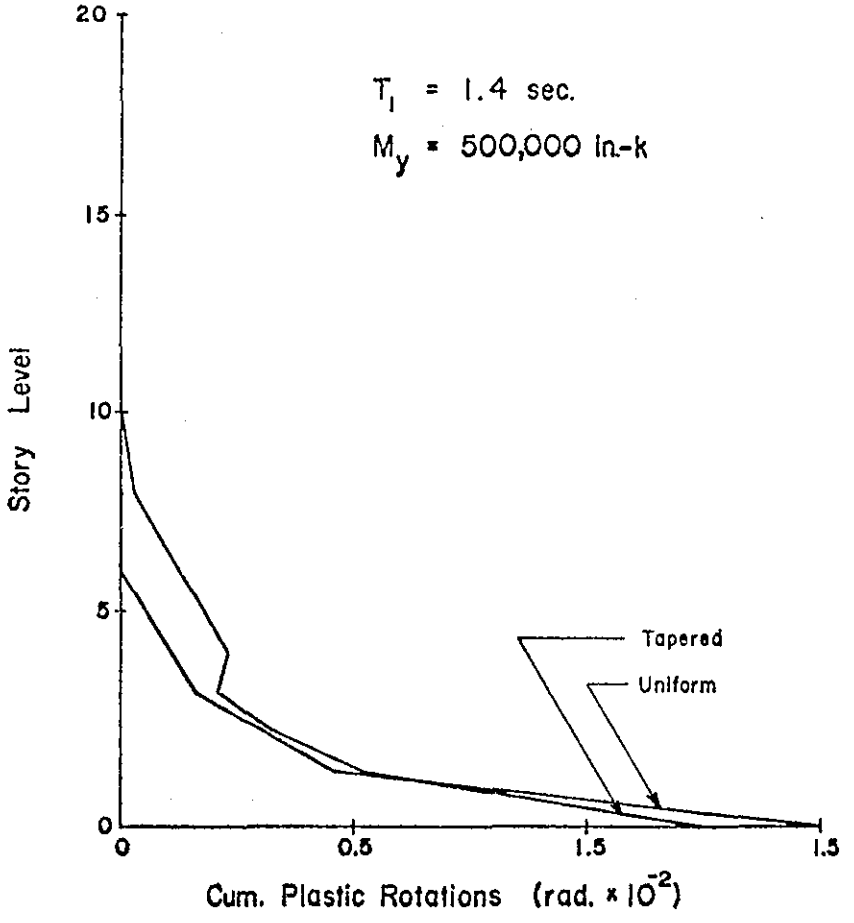

(f)

Fig. 62 (cont'd.) Effect of Stiffness Taper

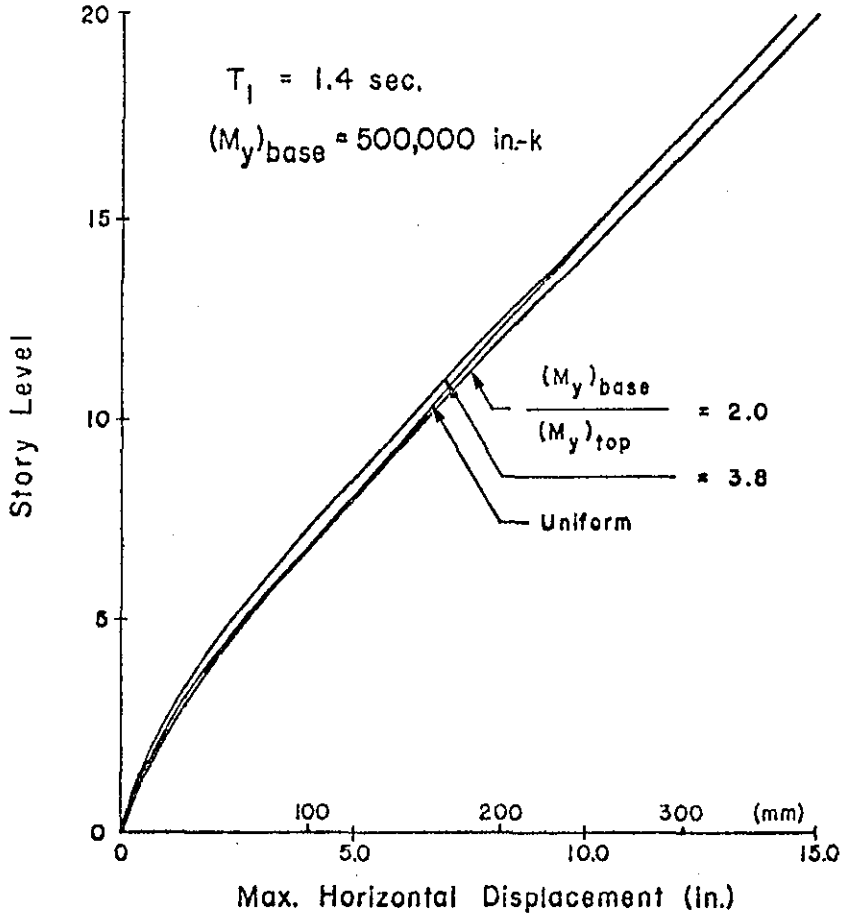

(a)

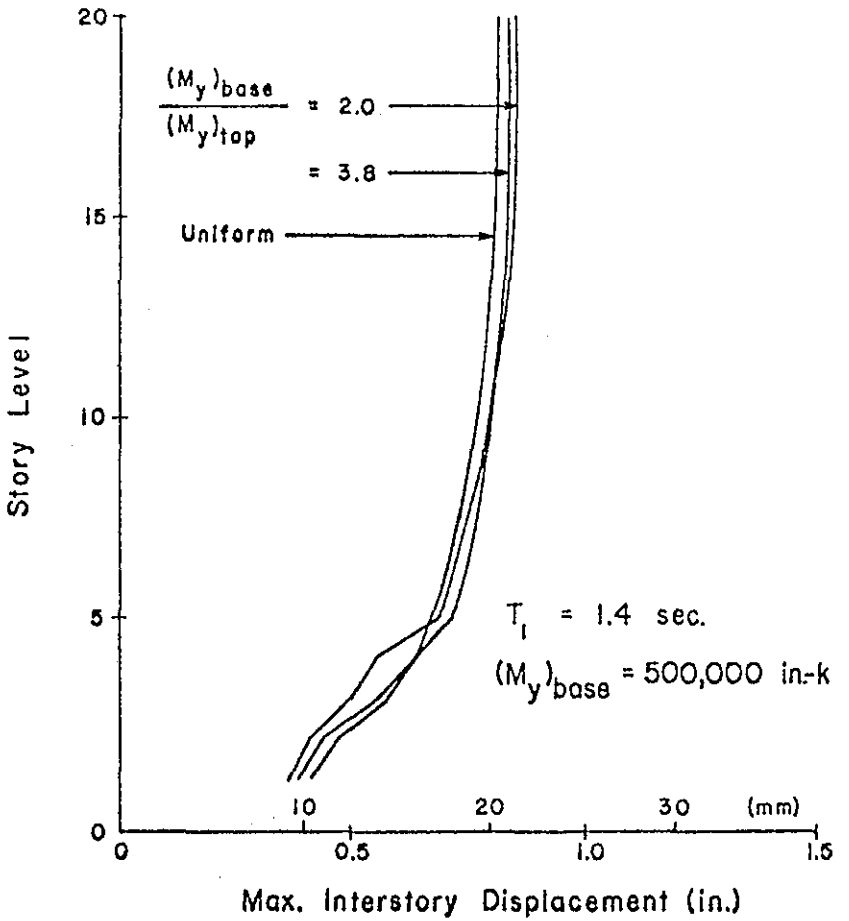

(b)

Fig. 63 Effect of Strength Taper

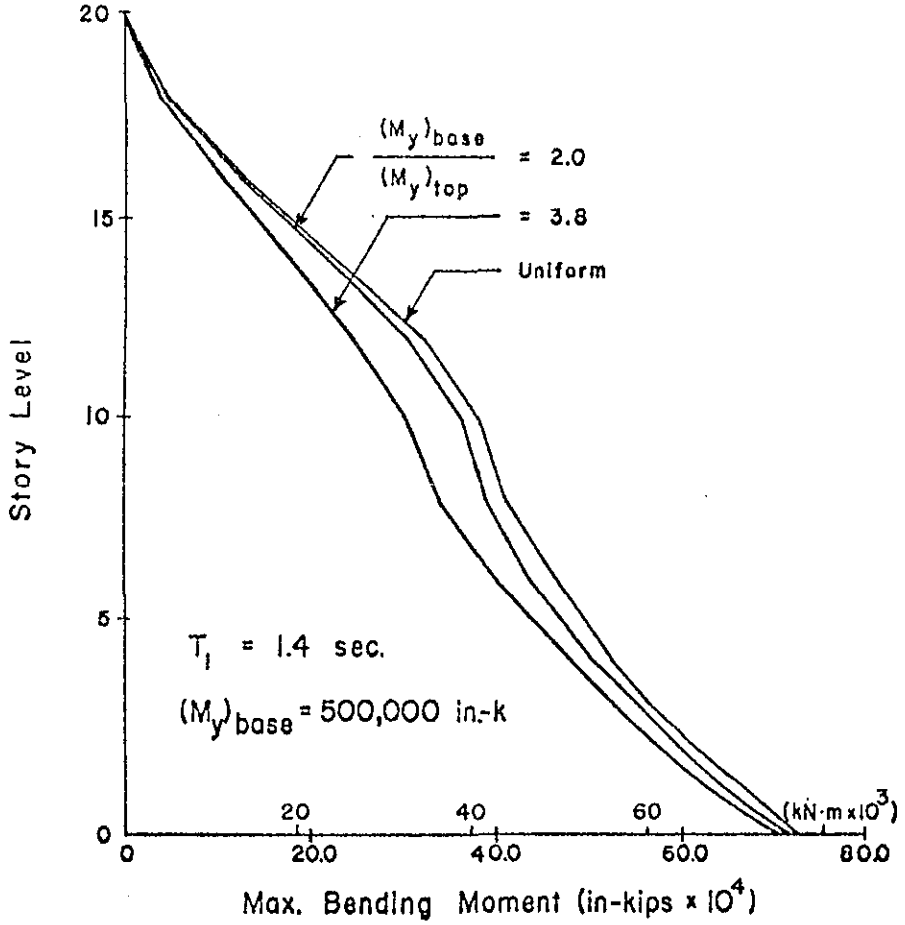

(c)

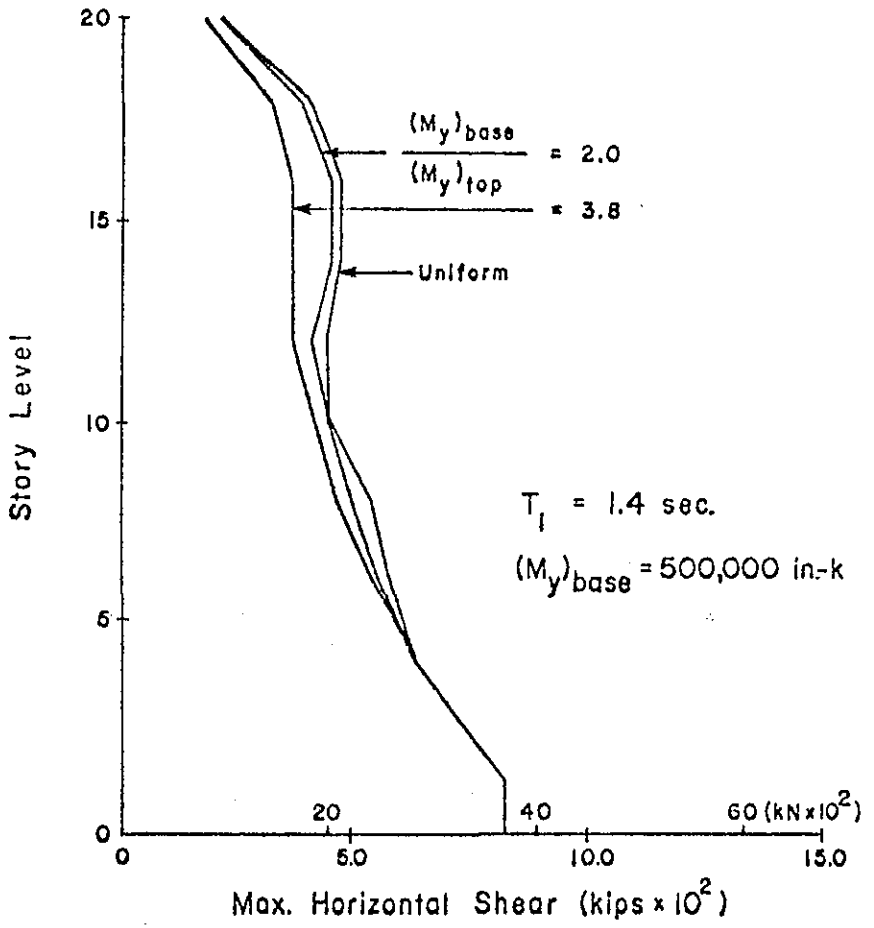

(d)

Fig. 63 (cont'd.) Effect of Strength Taper

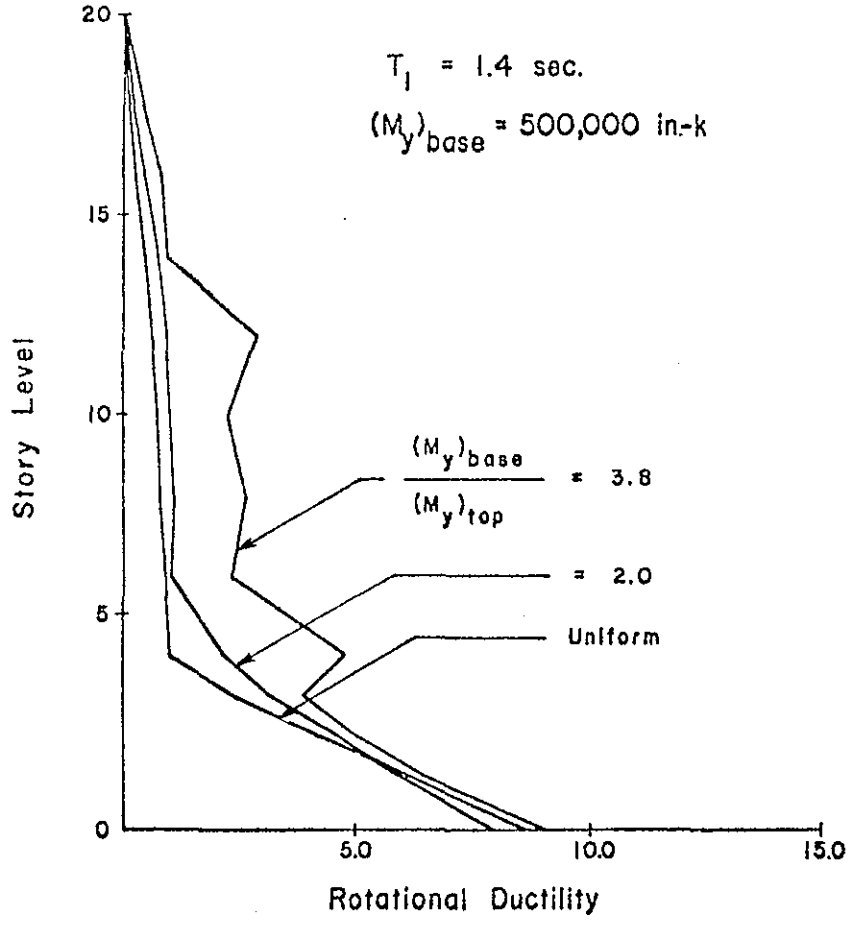

(e)

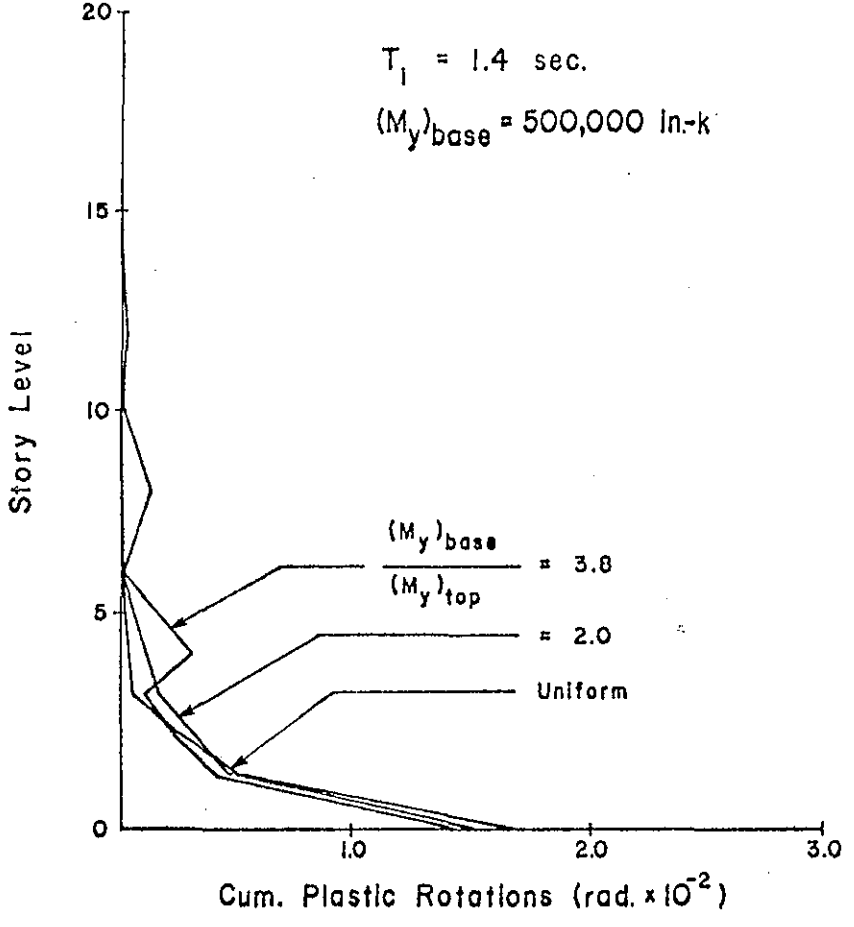

(f)

Fig. 63 (cont'd.) Effect of Strength Taper

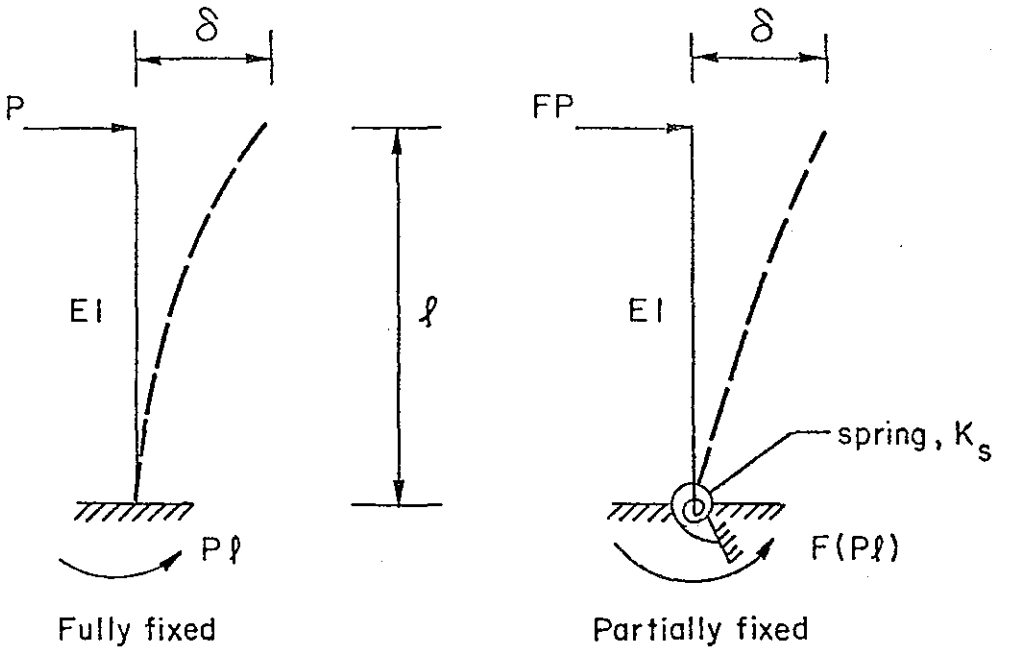

Fig. 64 Definition of Base Fixity Factor, F

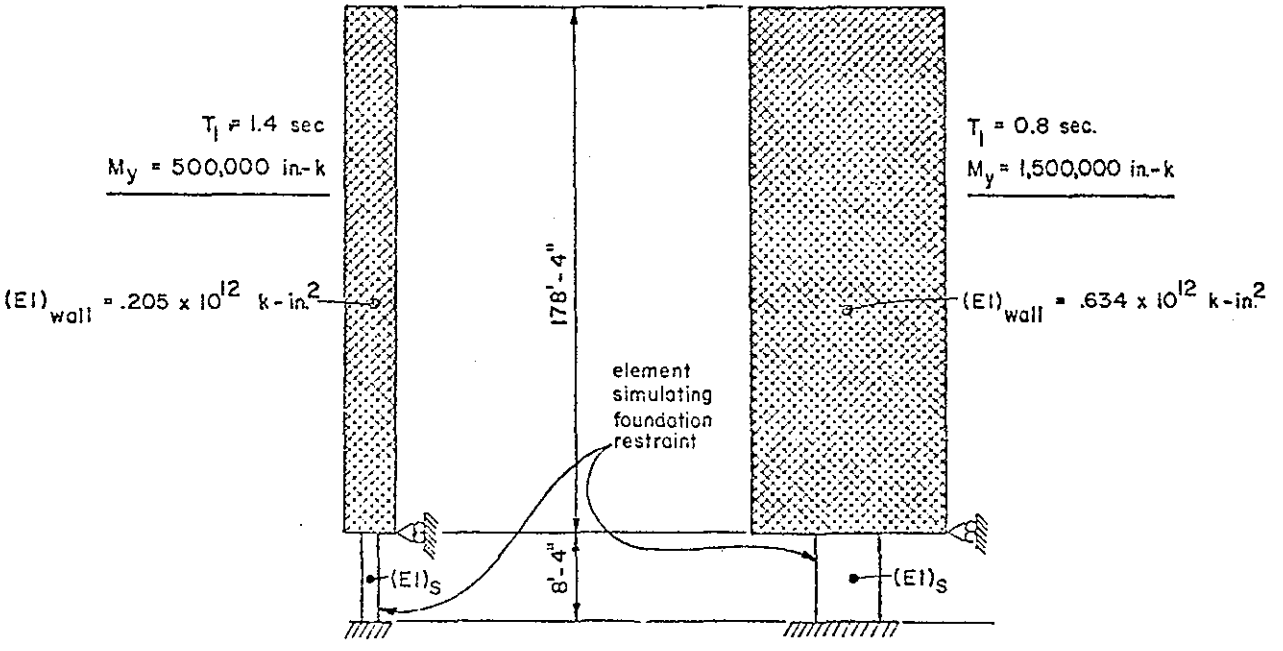

Base Fixity (%)	$(EI)_S$ k-in^2	T_1 (sec.)
100	∞	1.40
75	.31 x 10^{11}	1.43
50	.104 x 10^{11}	1.52

Base Fixity (%)	$(EI)_S$	T_1 (sec.)
100	∞	0.80
75	.96 x 10^{11}	0.83
50	.32 x 10^{11}	0.88

Fig. 65 Models Used in Study of Effect of Base Fixity Condition

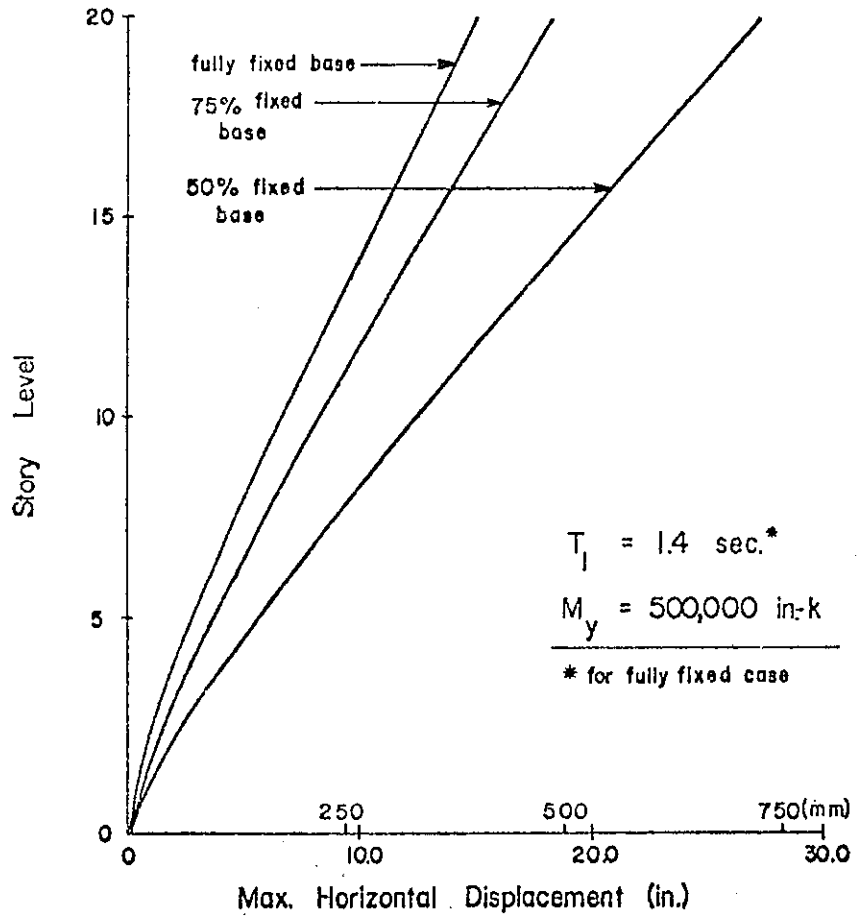

(a)

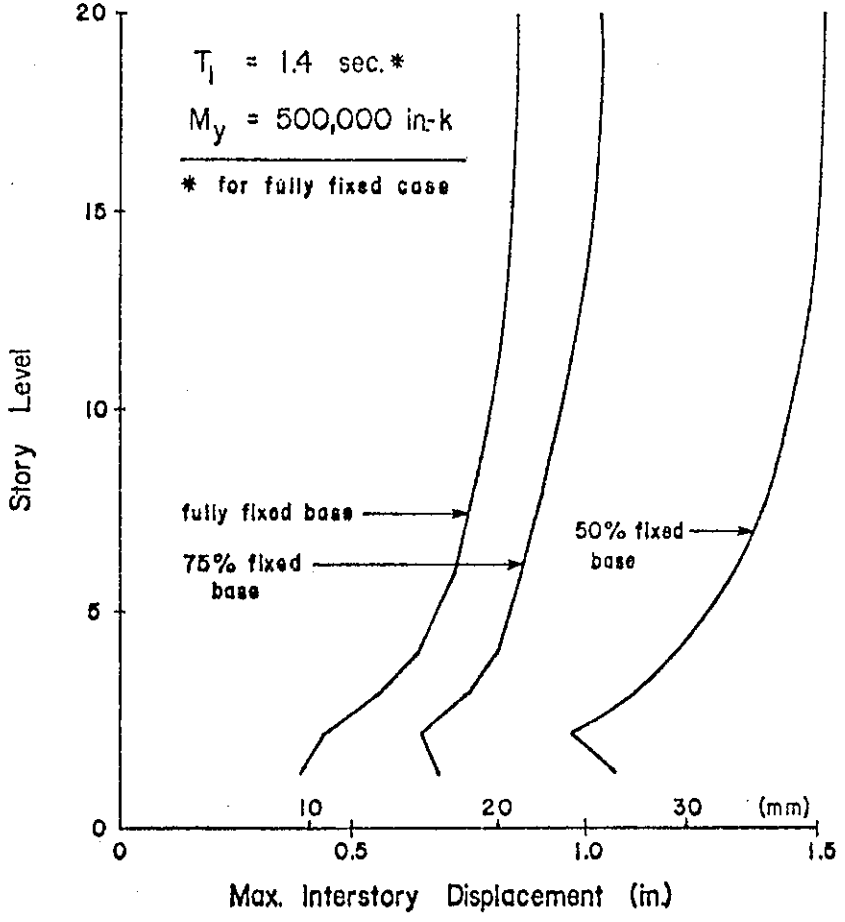

(b)

Fig. 66 Effect of Base Fixity Condition

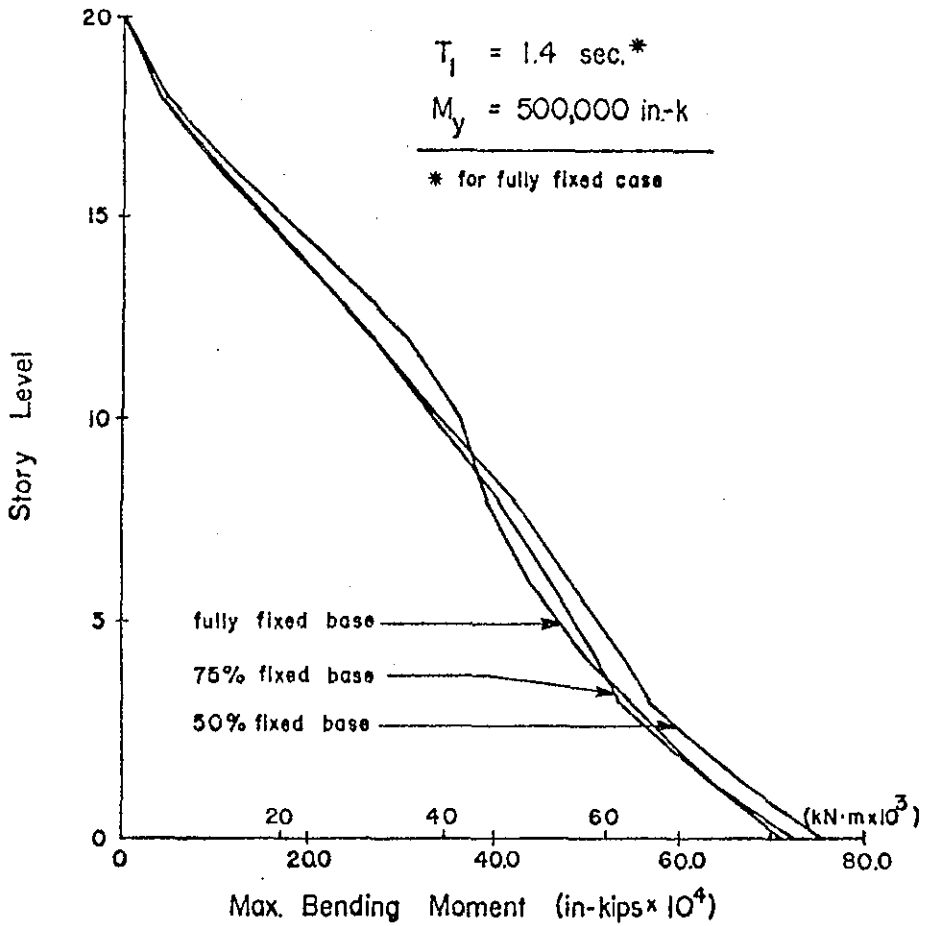

(c)

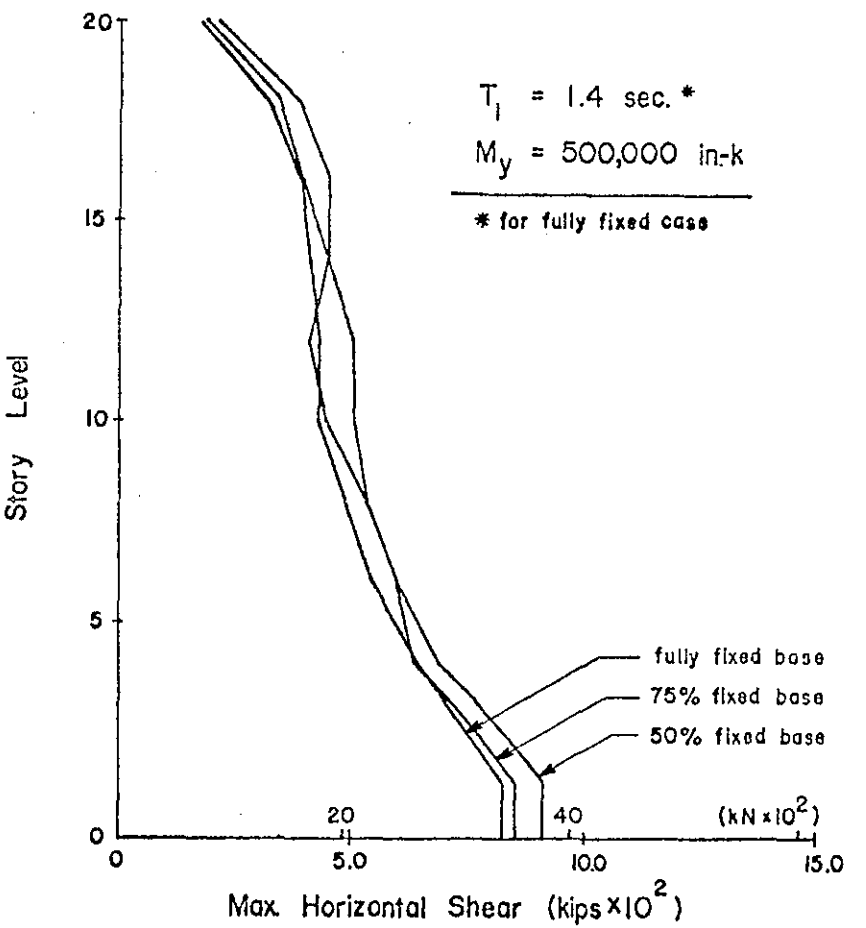

(d)

Fig. 66 (cont'd.) Effect of Base Fixity Condition

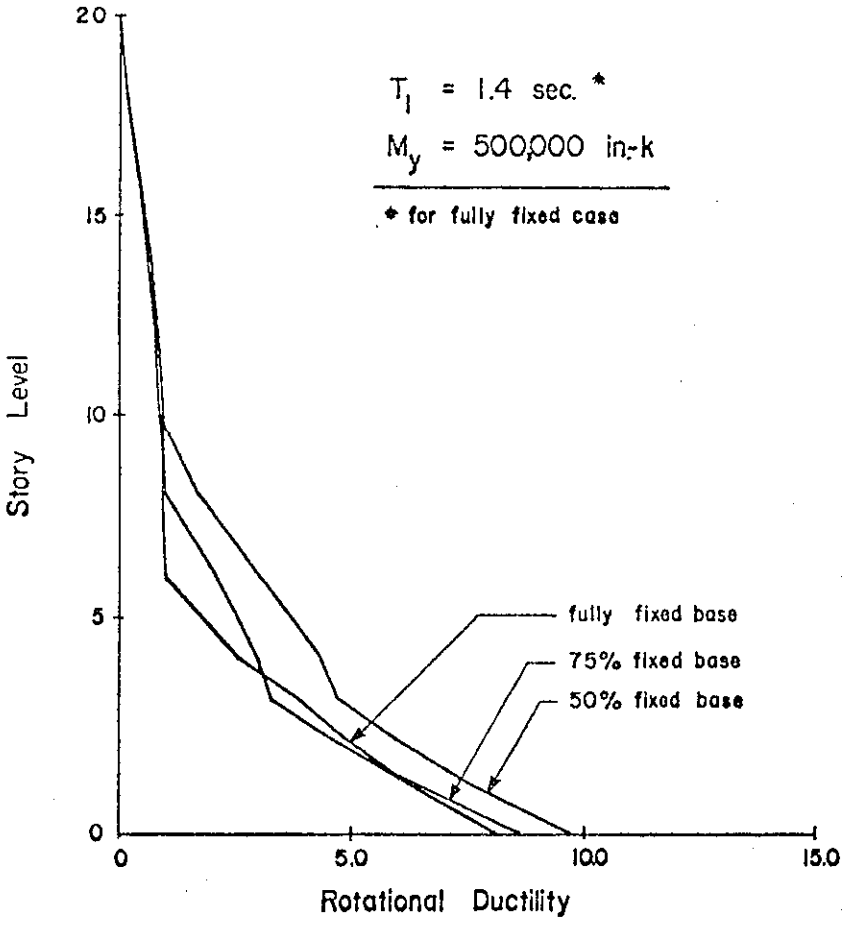

(e)

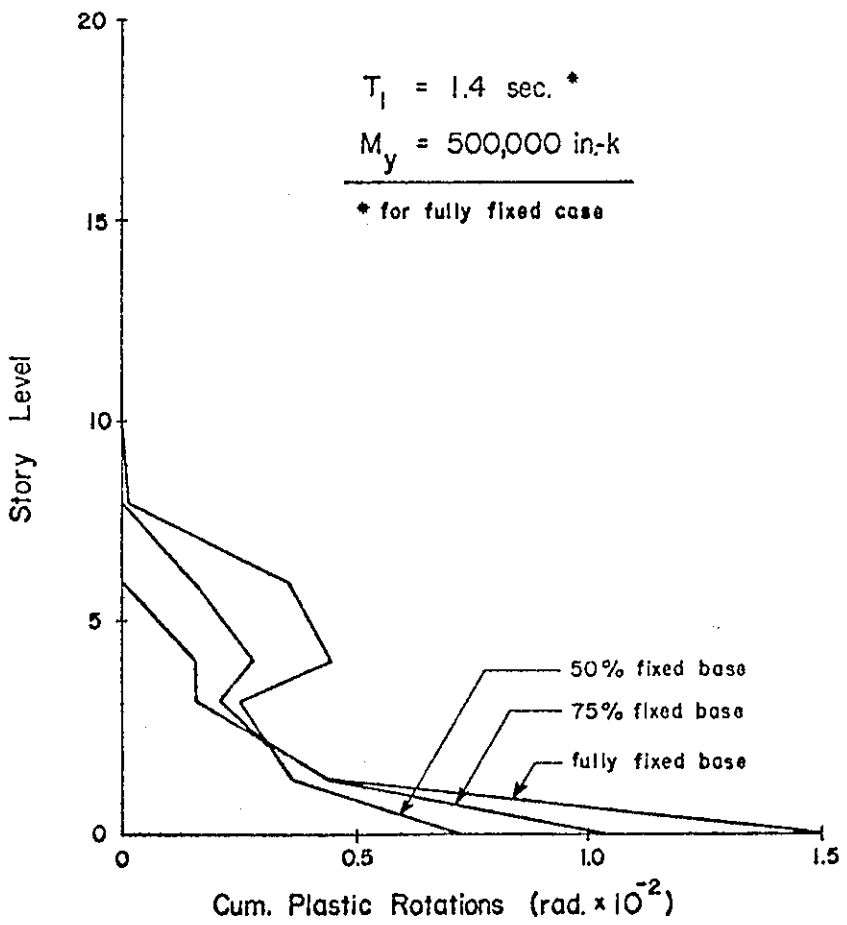

(f)

Fig. 66 (cont'd.) Effect of Base Fixity Condition

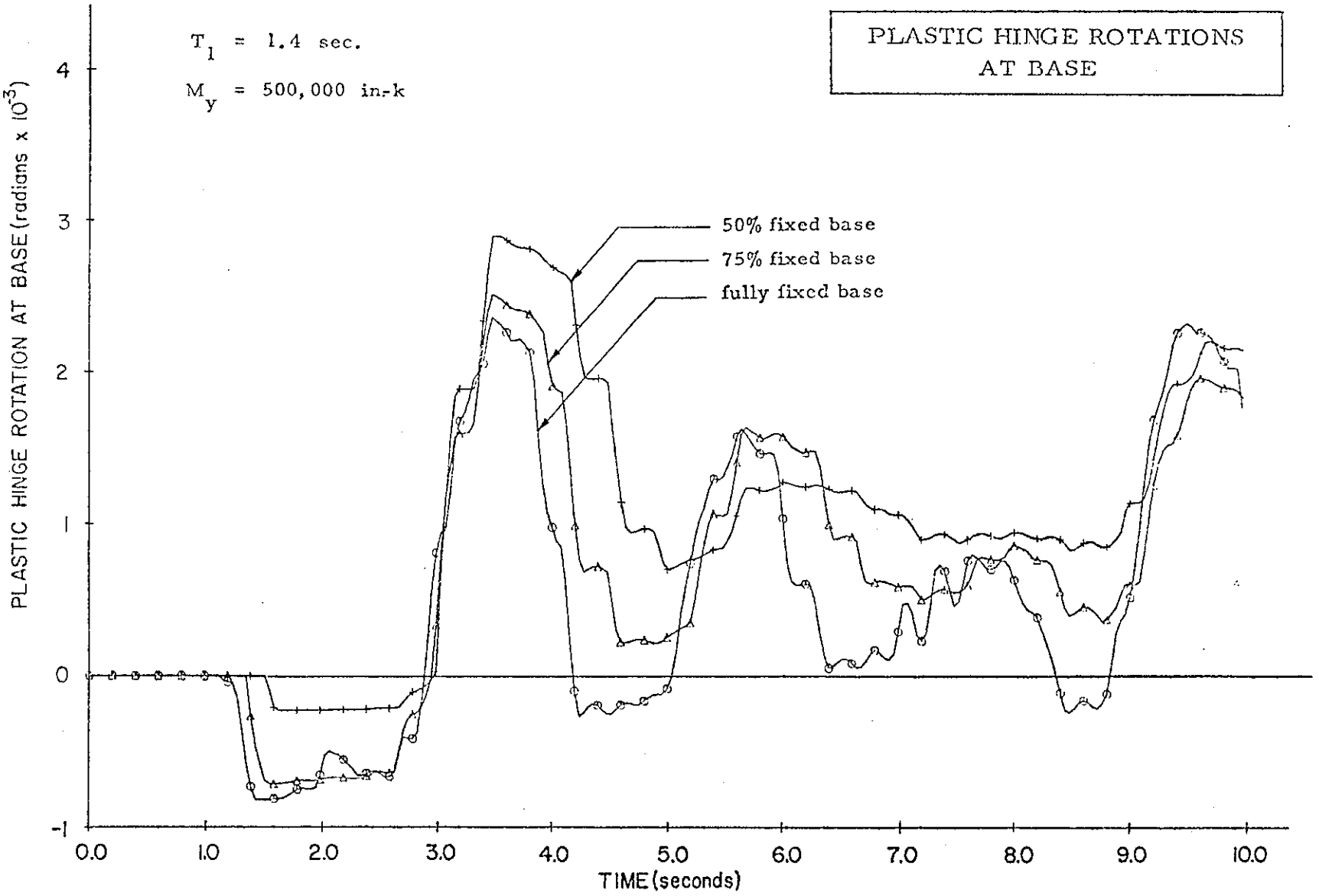

Fig. 67 Plastic Hinge Rotations at Base versus Time for Different Degrees of Base Fixity

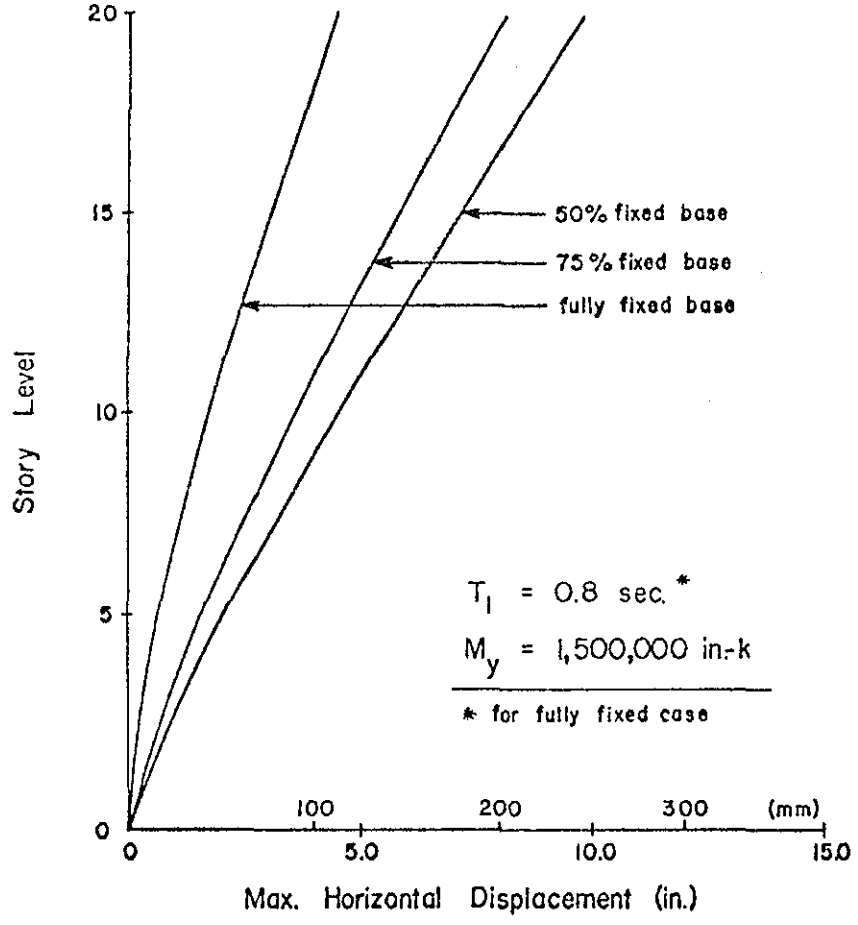

(a)

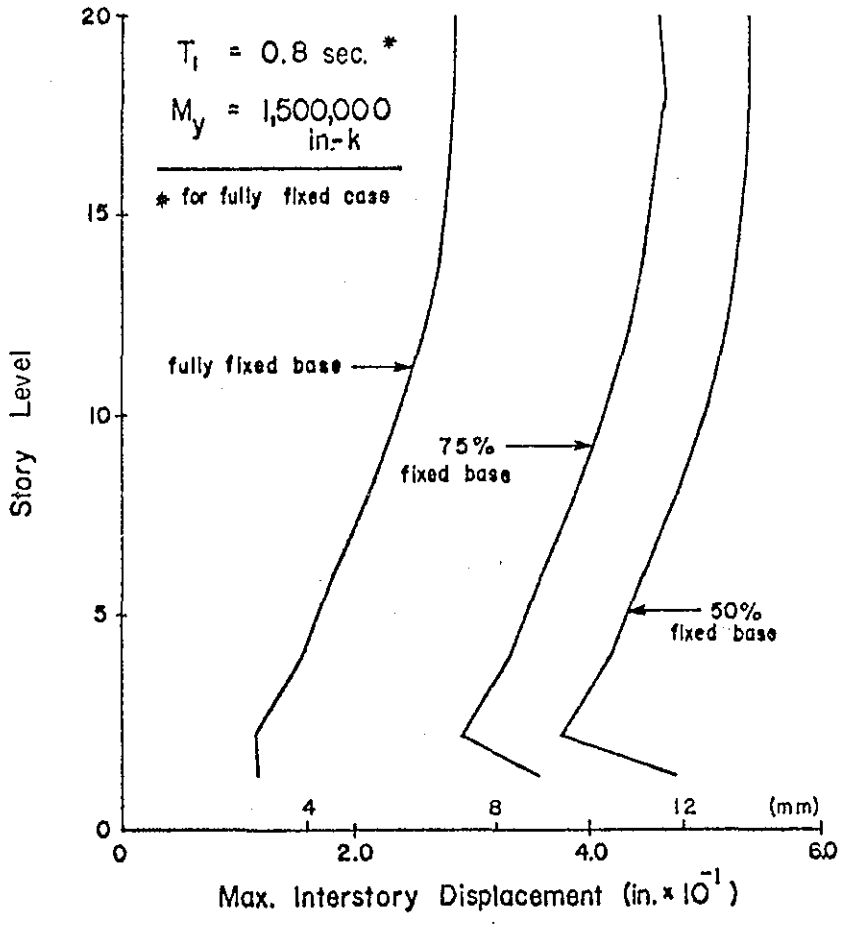

(b)

Fig. 68 Effect of Base Fixity Condition

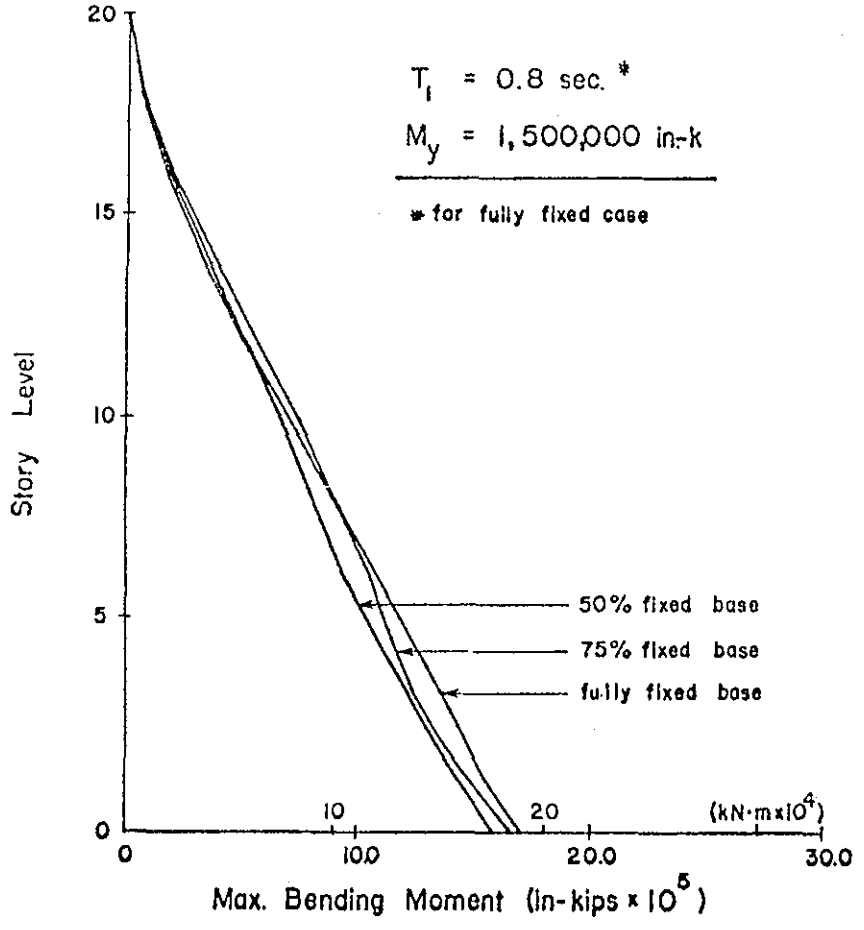

(c)

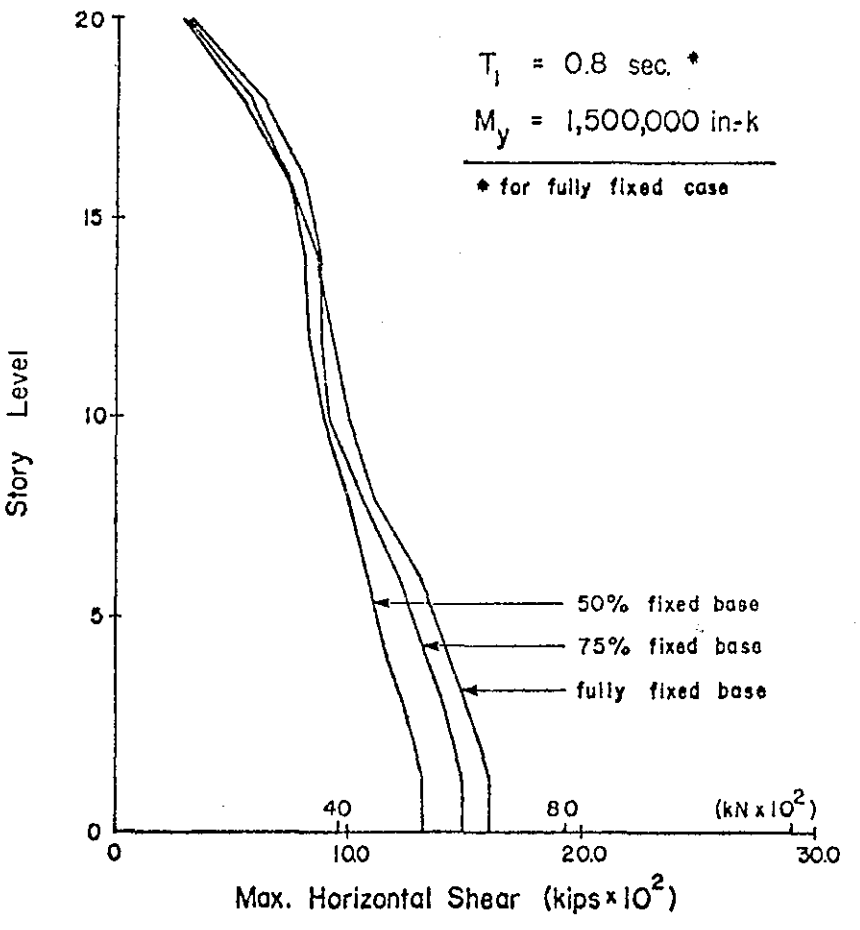

(d)

Fig. 68 (cont'd.) Effect of Base Fixity Condition

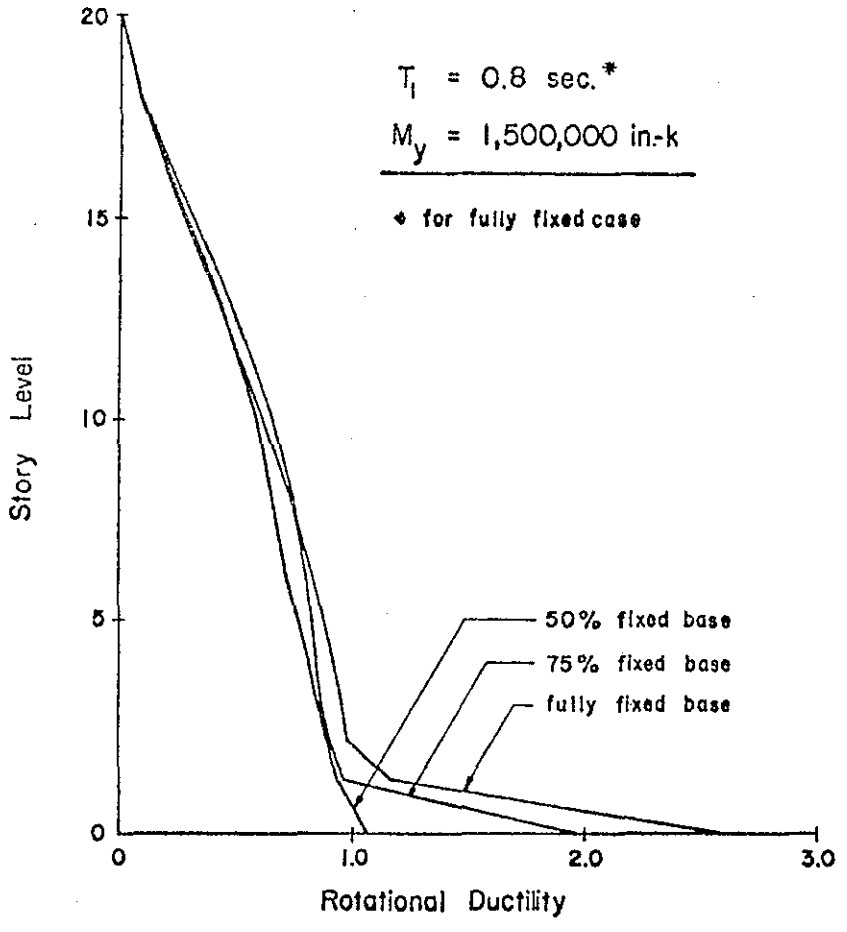

(e)

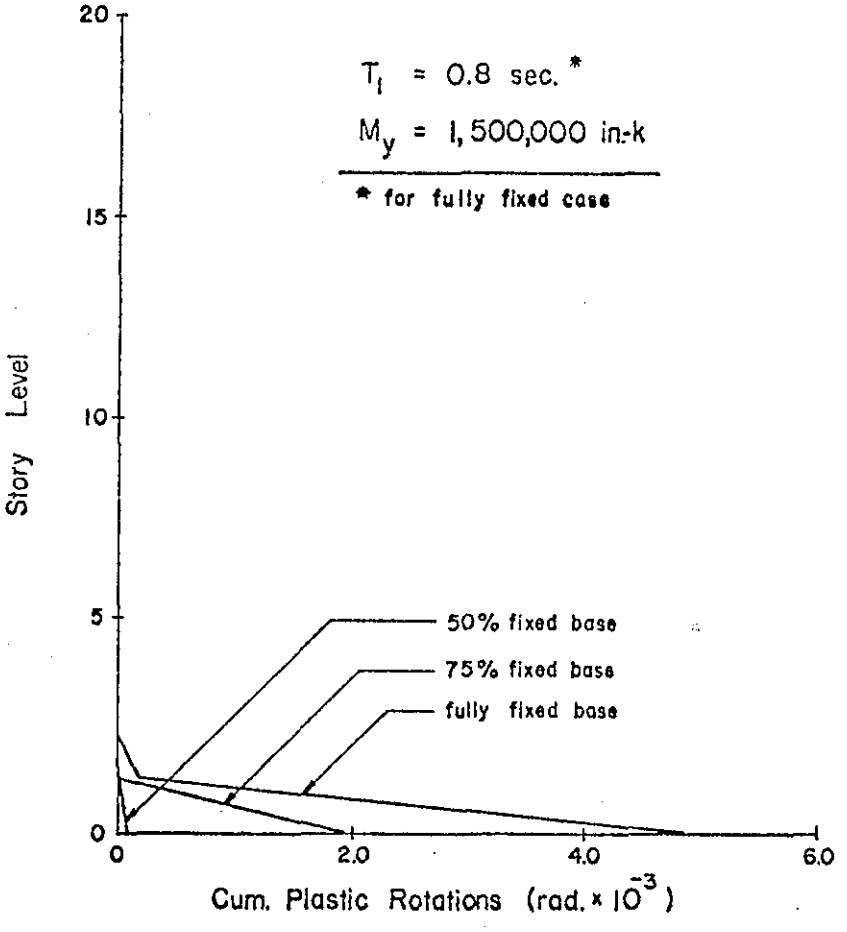

(f)

Fig. 68 (cont'd.) Effect of Base Fixity Condition

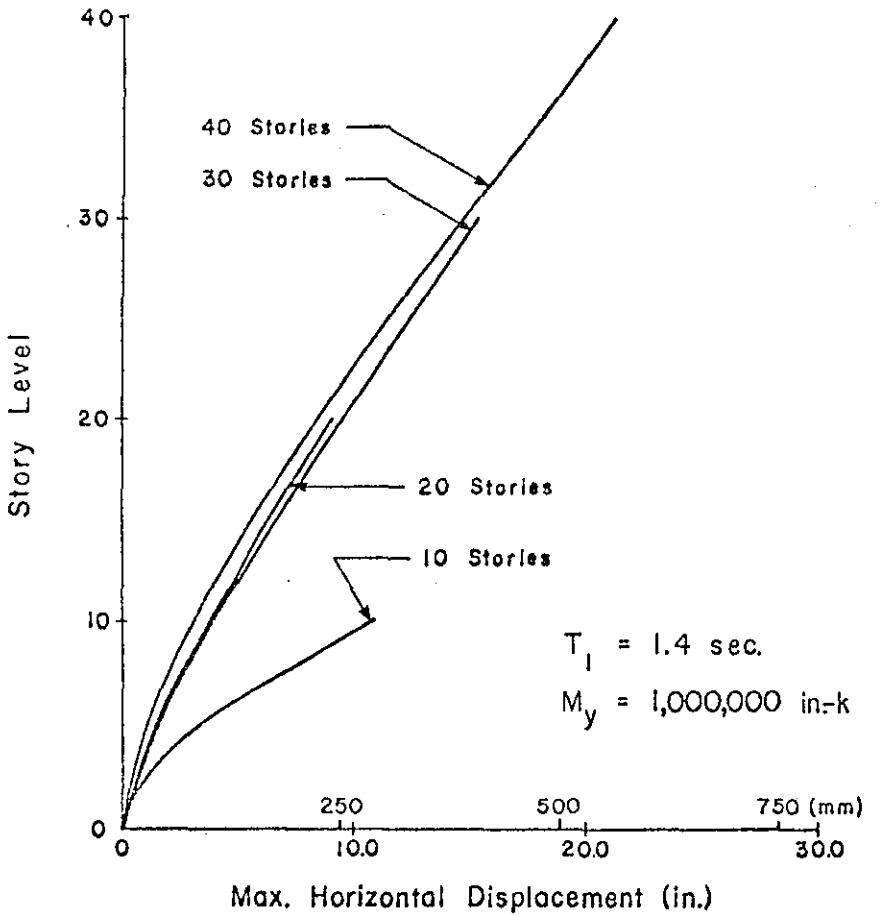

(a)

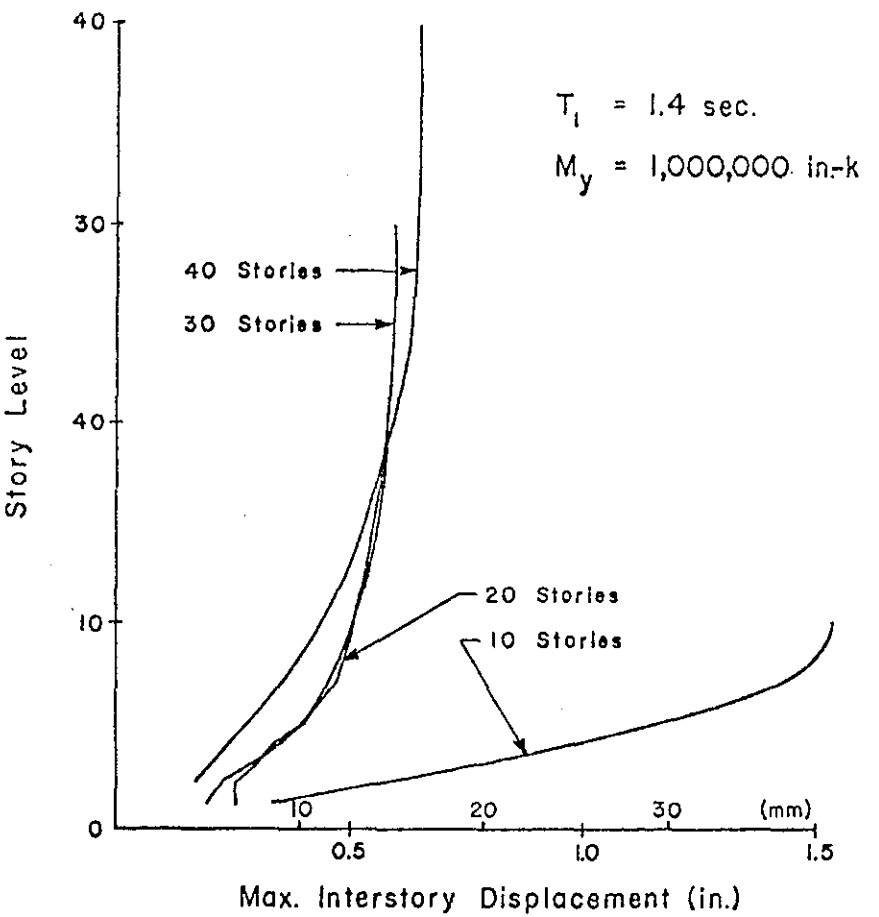

(b)

Fig. 69 Effect of Number of Stories

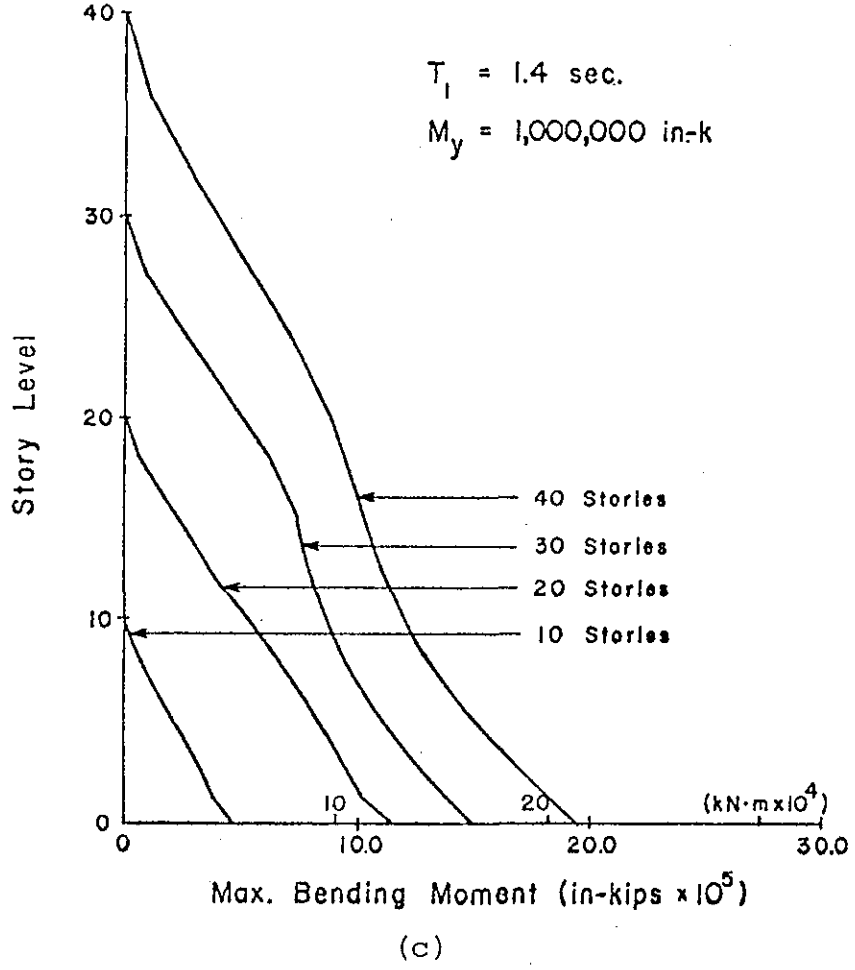

(c)

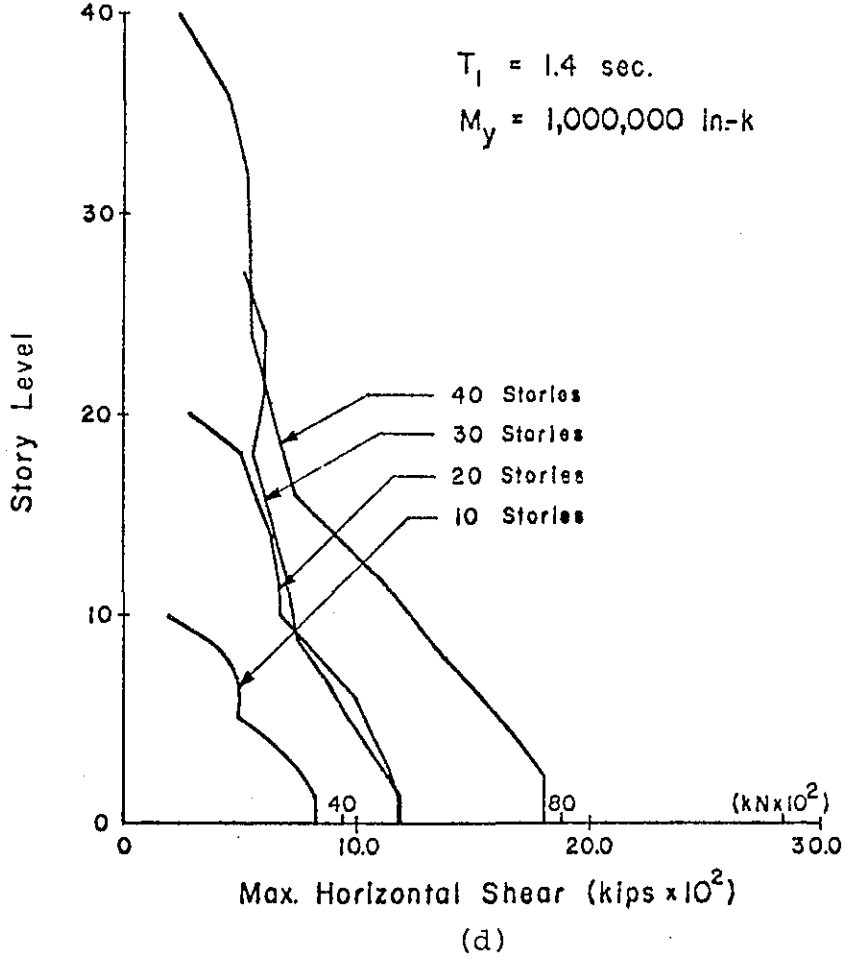

(d)

Fig. 69 (cont'd.) Effect of Number of Stories

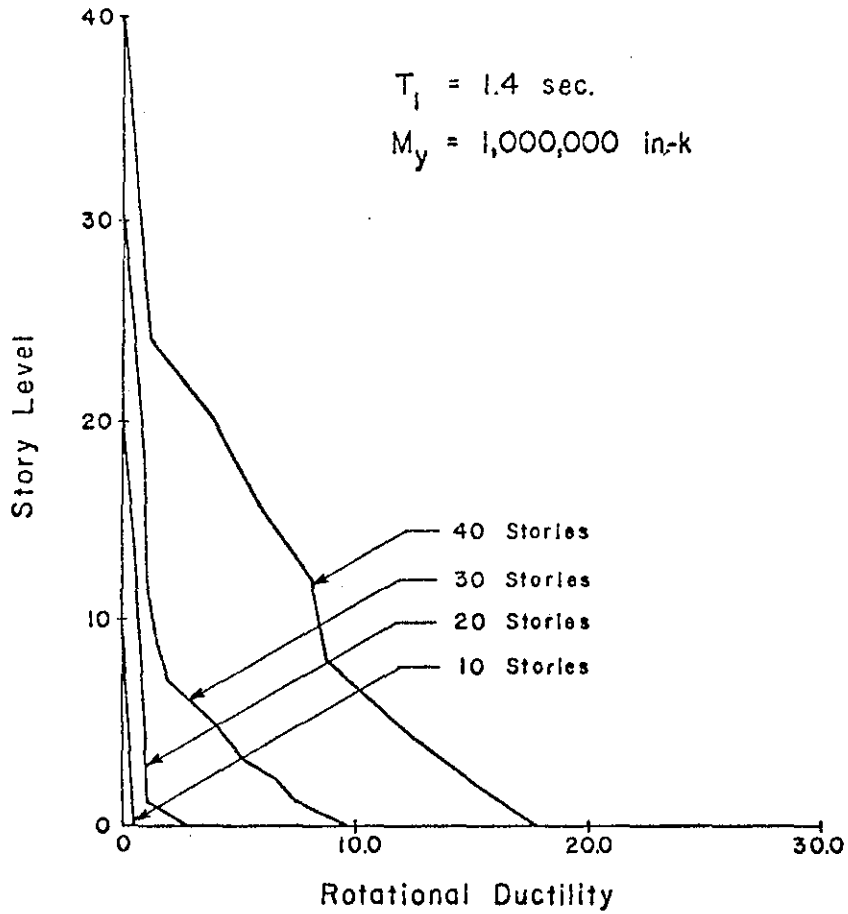

(e)

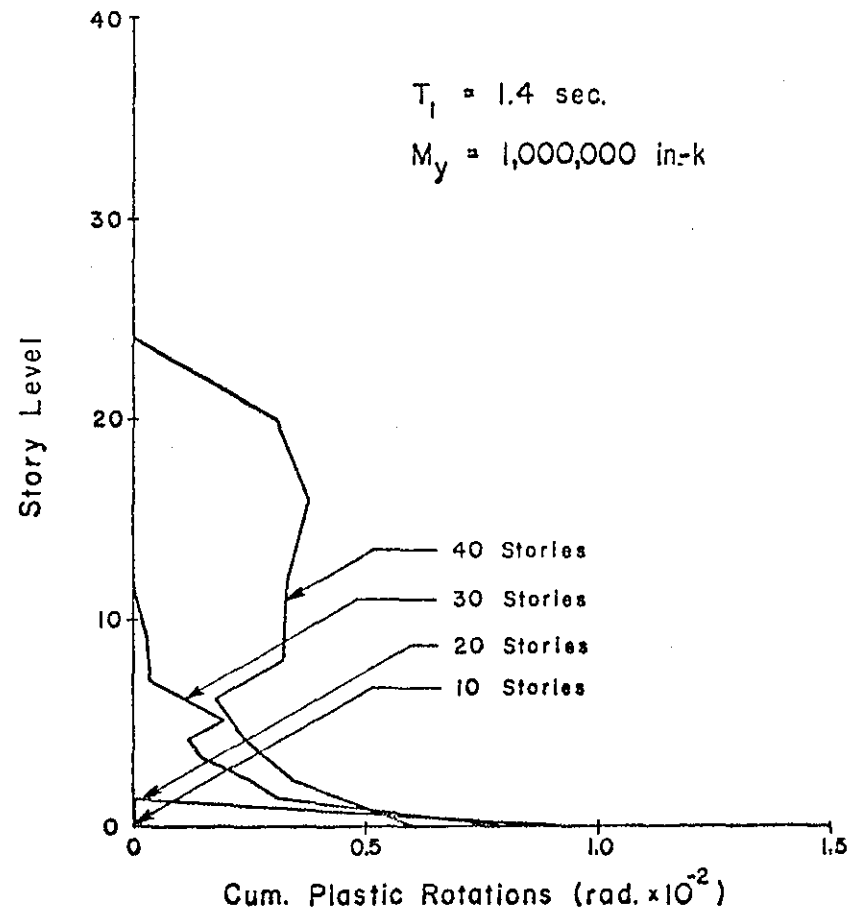

(f)

Fig. 69 (cont'd.) Effect of Number of Stories

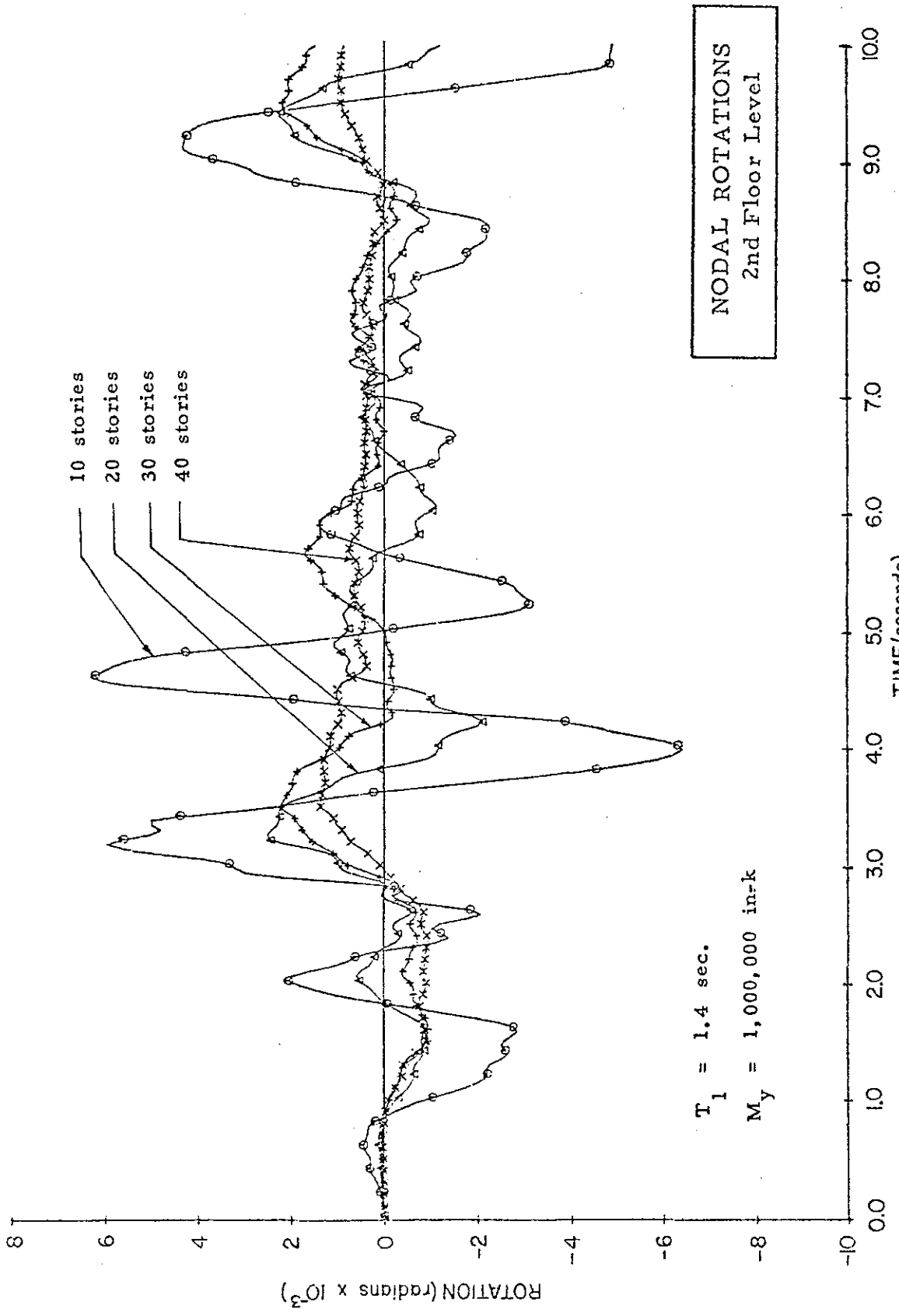

Fig. 70 Nodal Rotations at Second Story Level versus Time for Different Heights of Structure

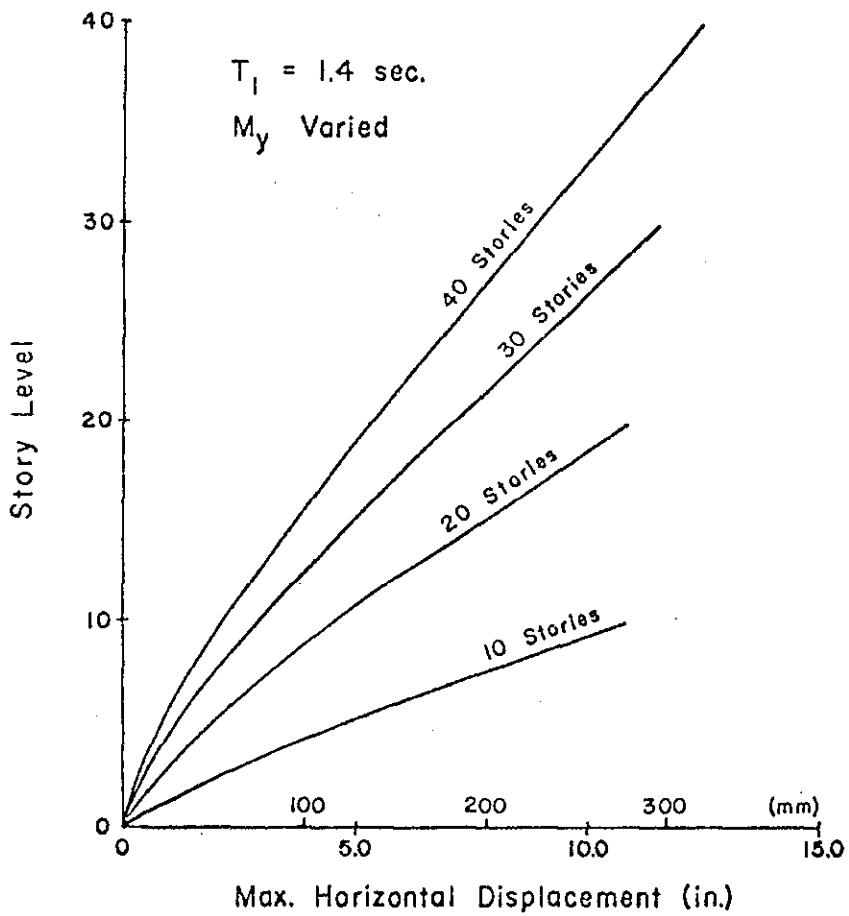

(a)

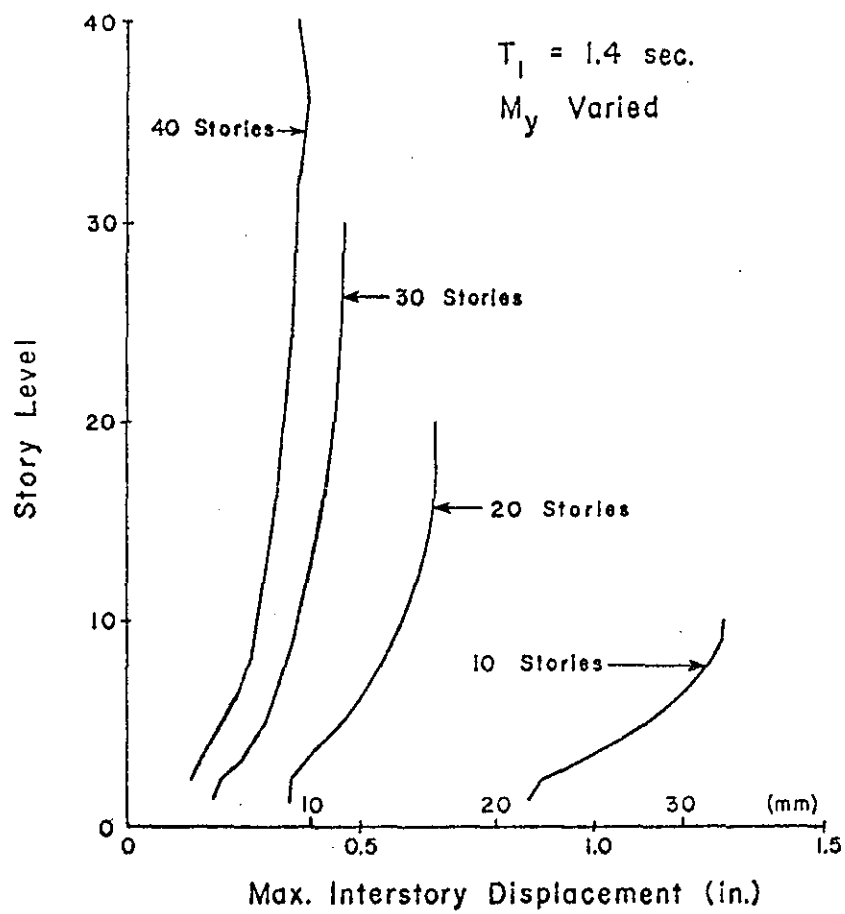

(b)

Fig. 71 Effect of Number of Stories

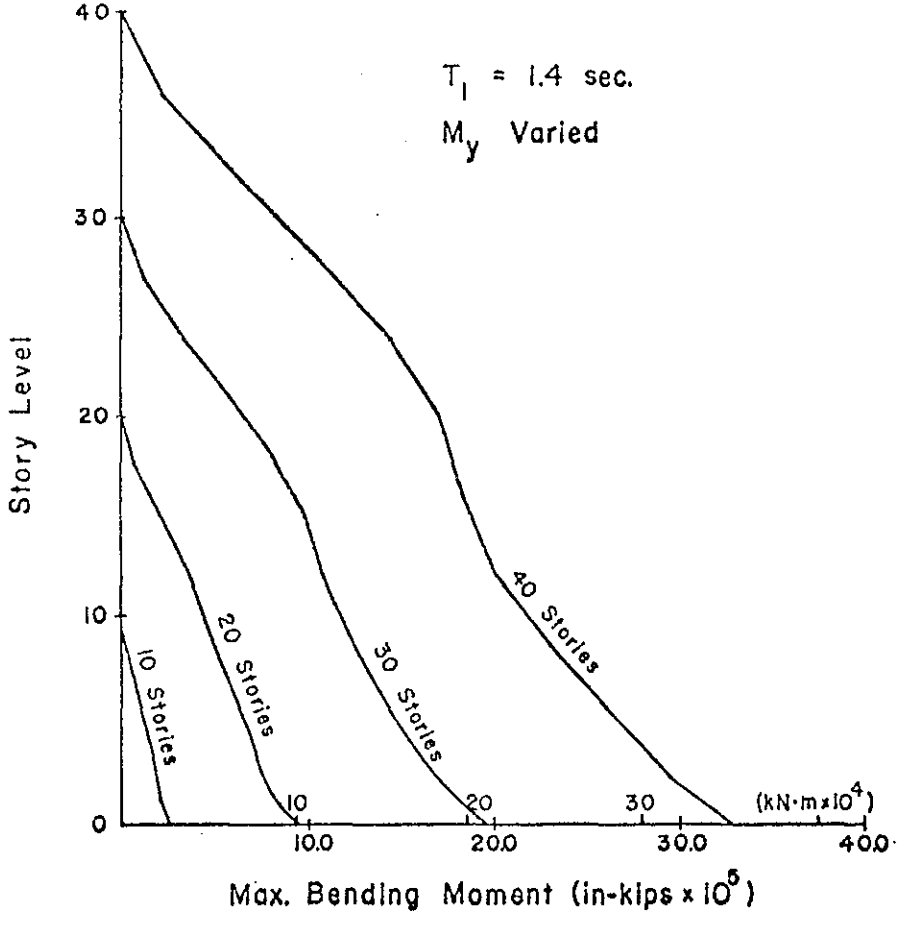

(c)

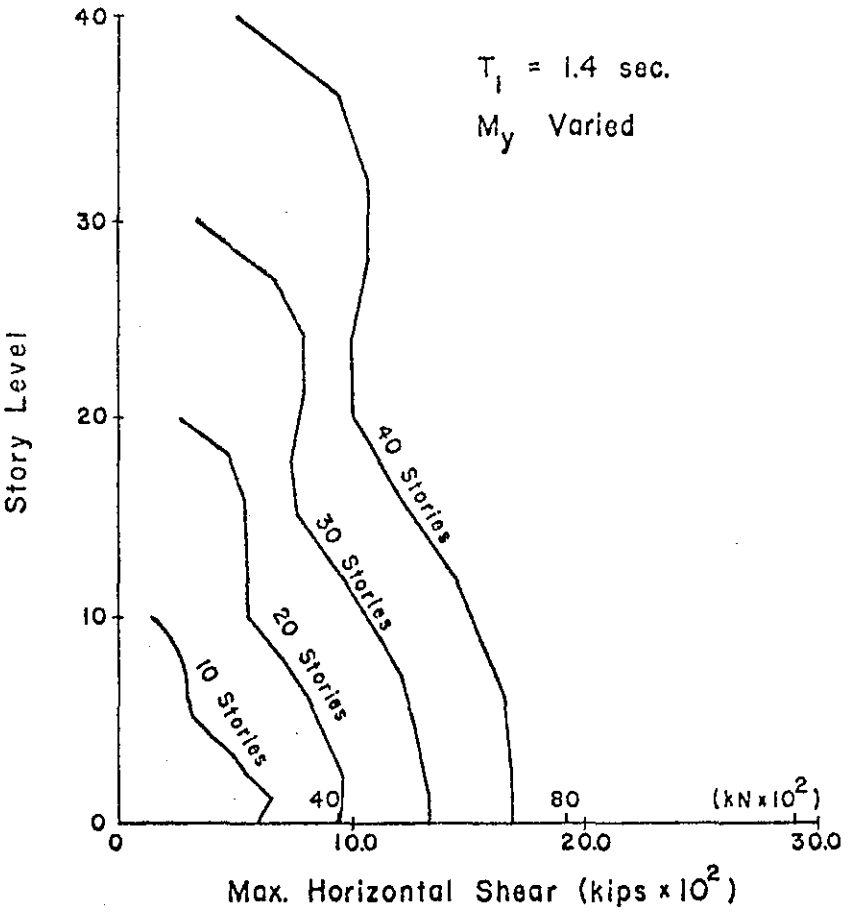

(d)

Fig. 71 (cont'd.) Effect of Number of Stories

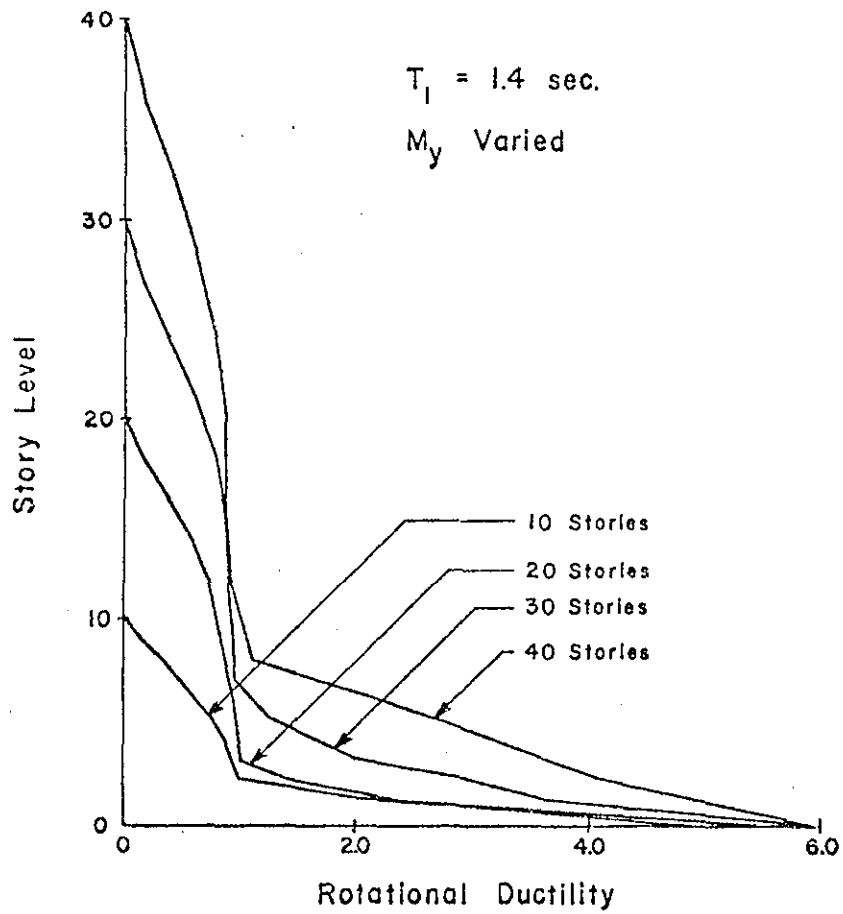

(e)

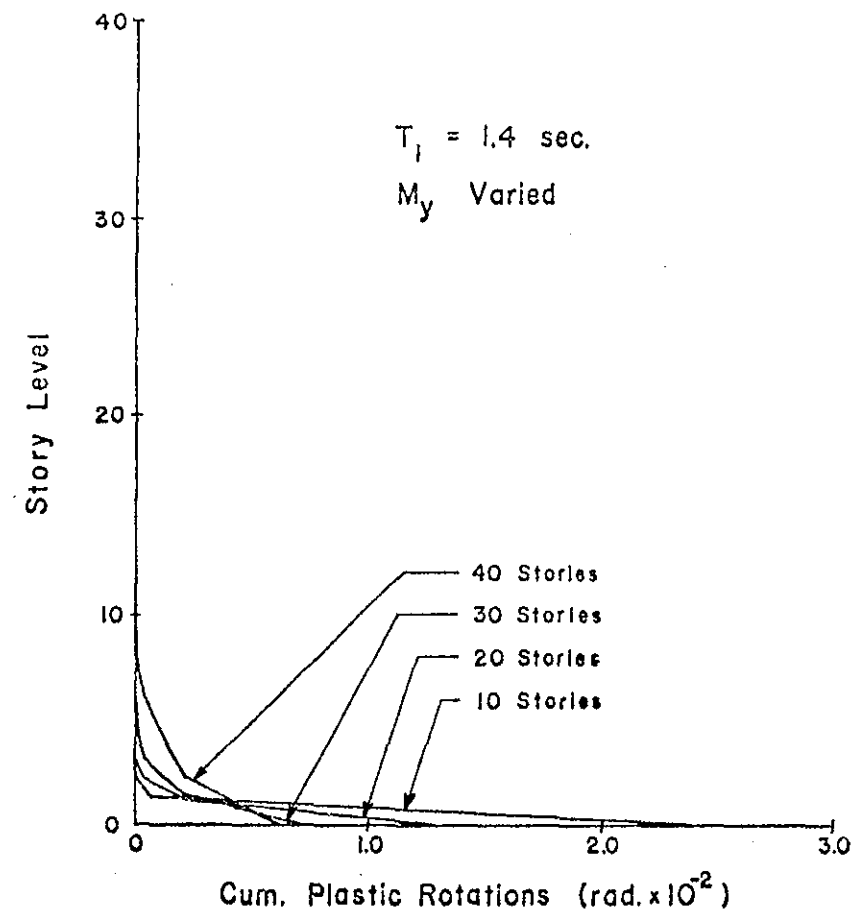

(f)

Fig. 71 (cont'd.) Effect of Number of Stories

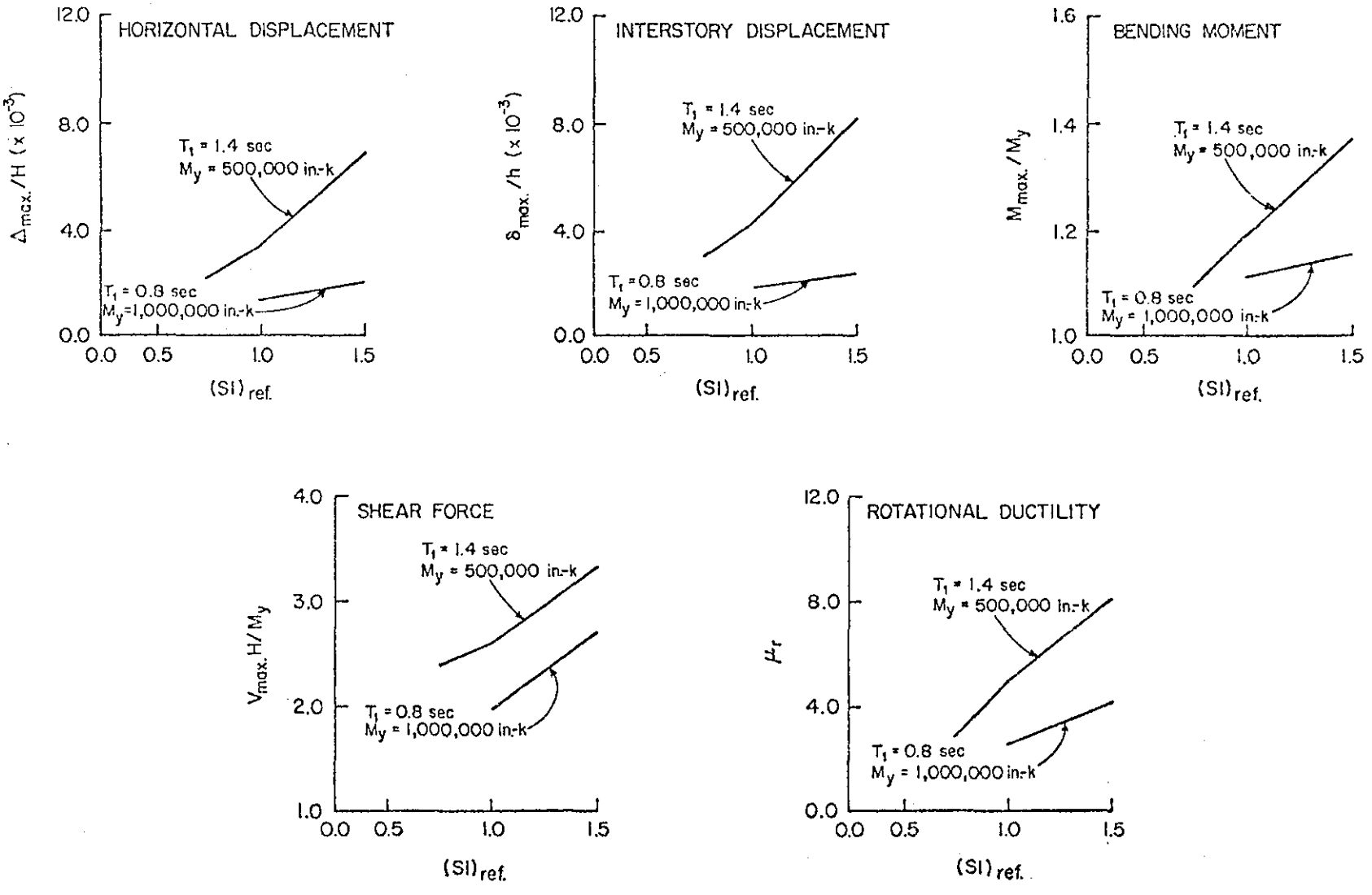

Fig. 72 Summary: Effect of Ground Motion Intensity

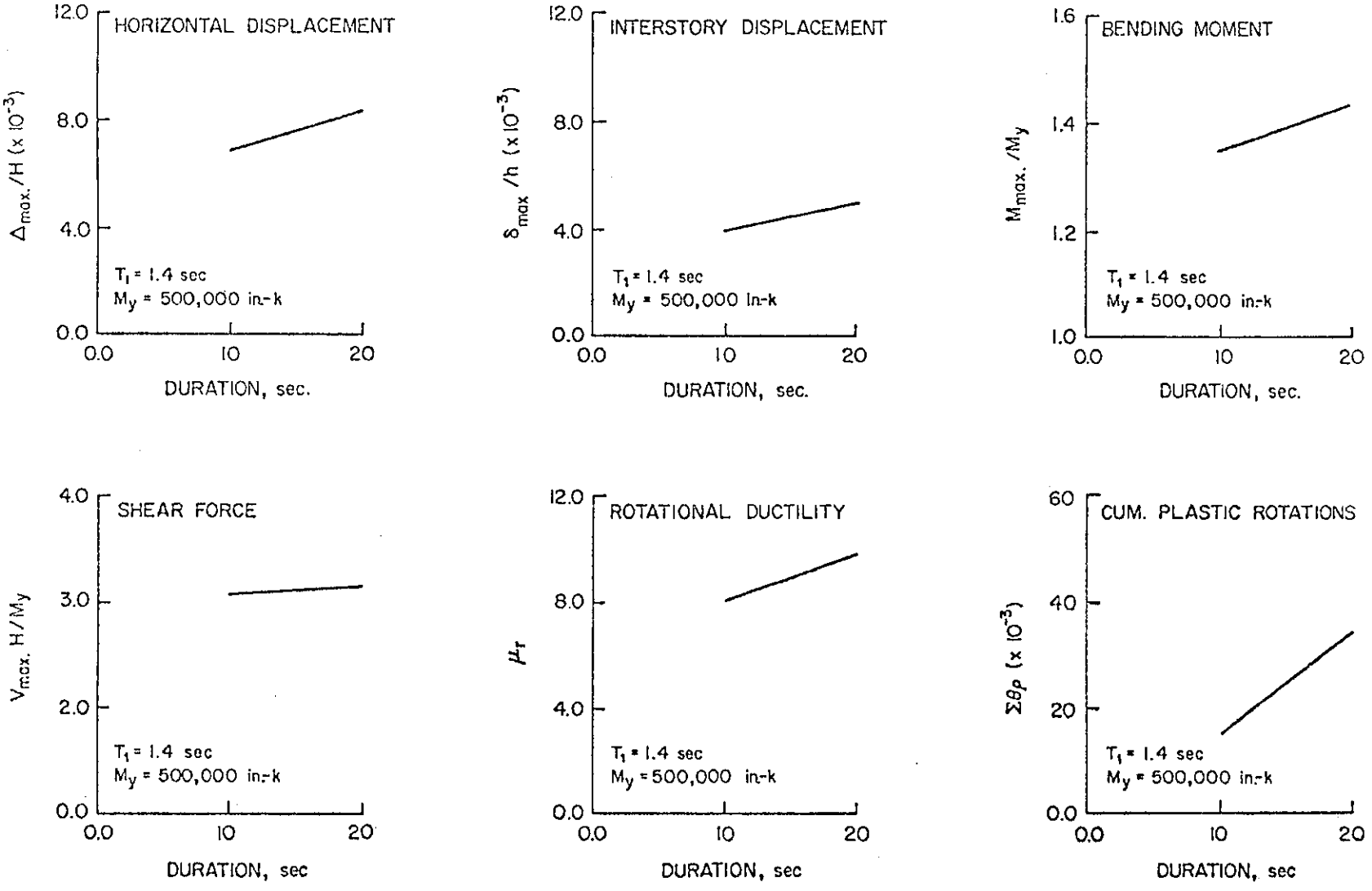

Fig. 73 Summary: Effect of Duration of Ground Motion

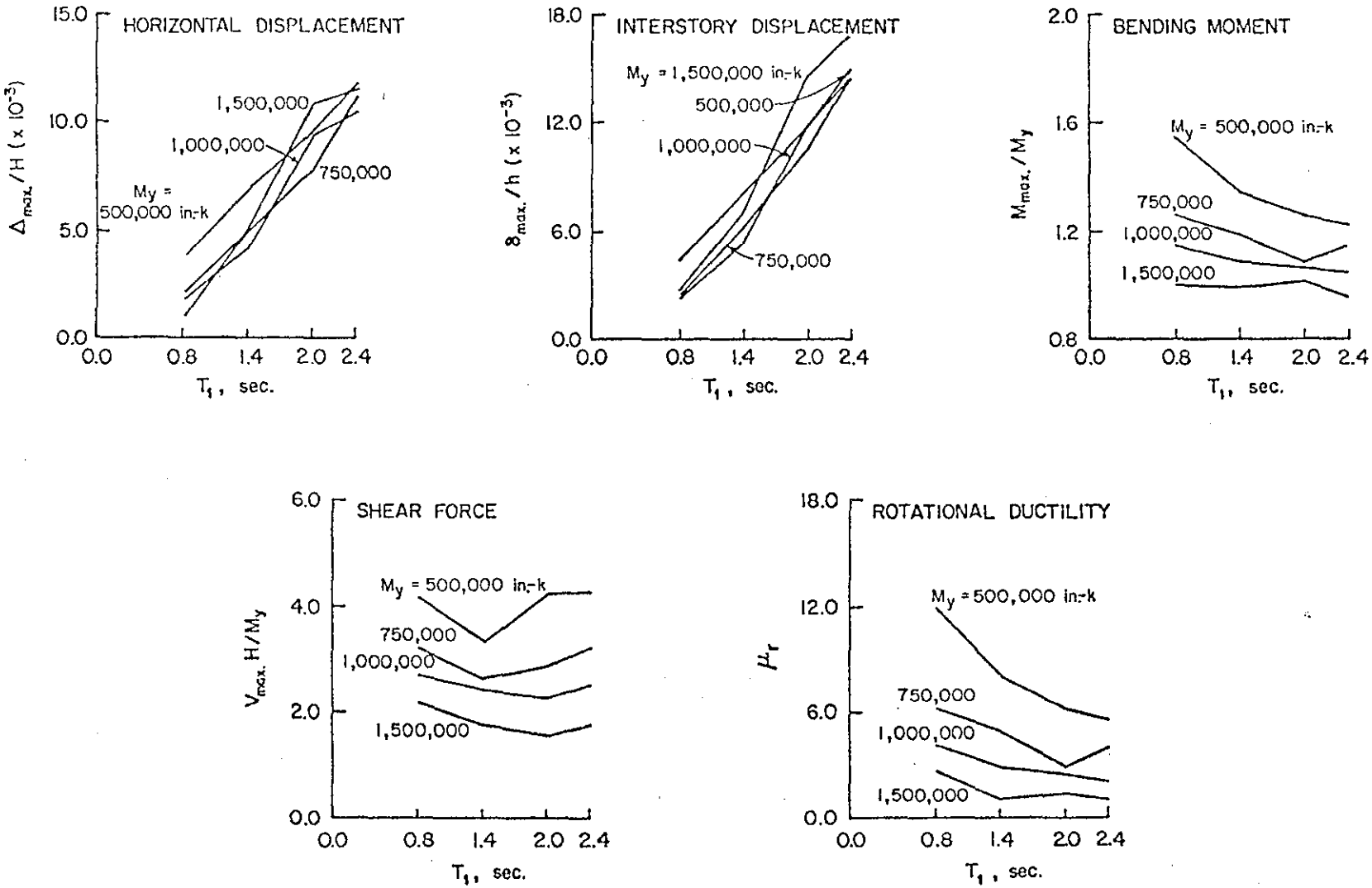

Fig. 74 Summary: Effect of Fundamental Period of Vibration, T_1

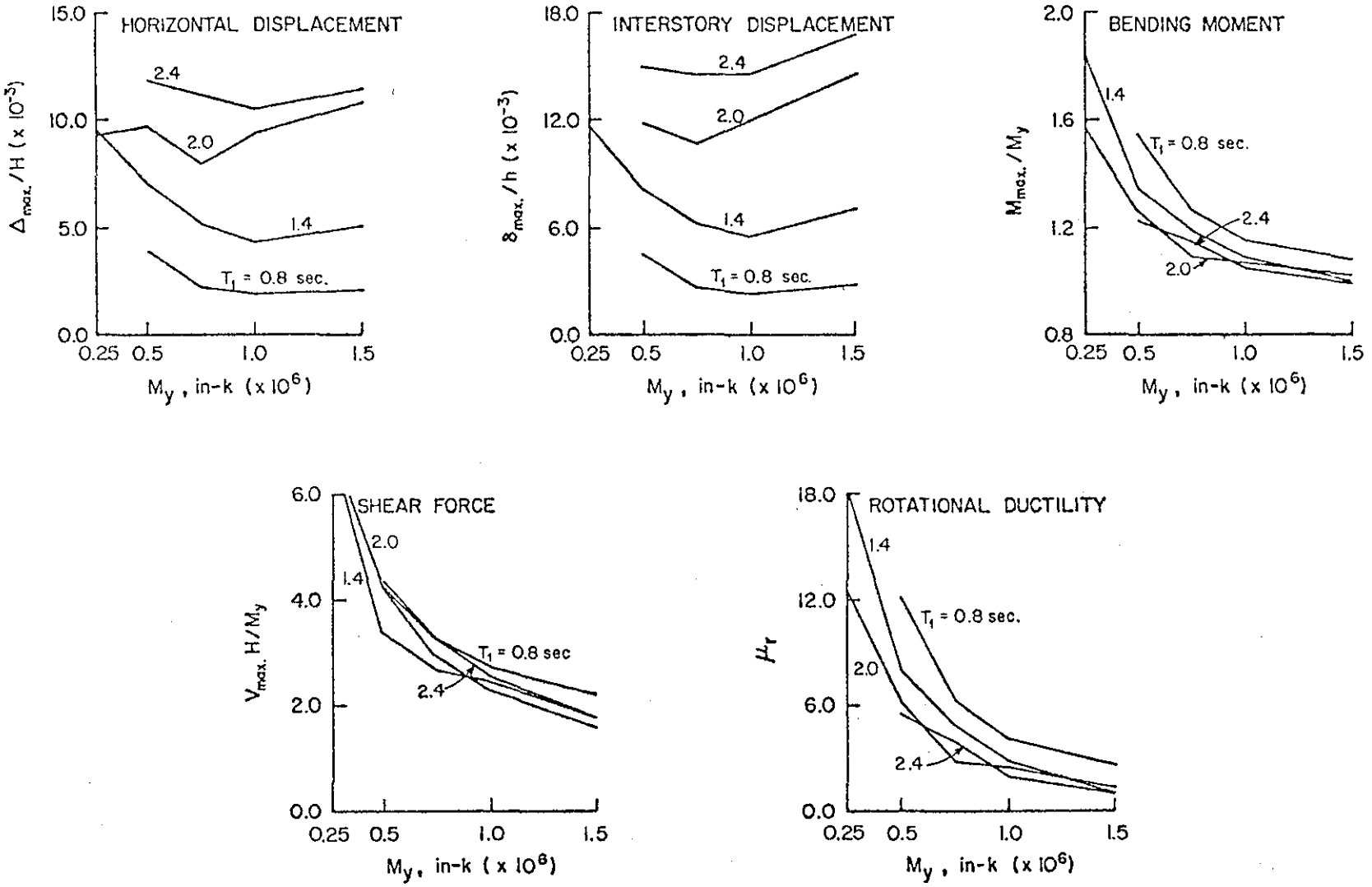

Fig. 75 Summary: Effect of Yield Level in Flexure, M_y

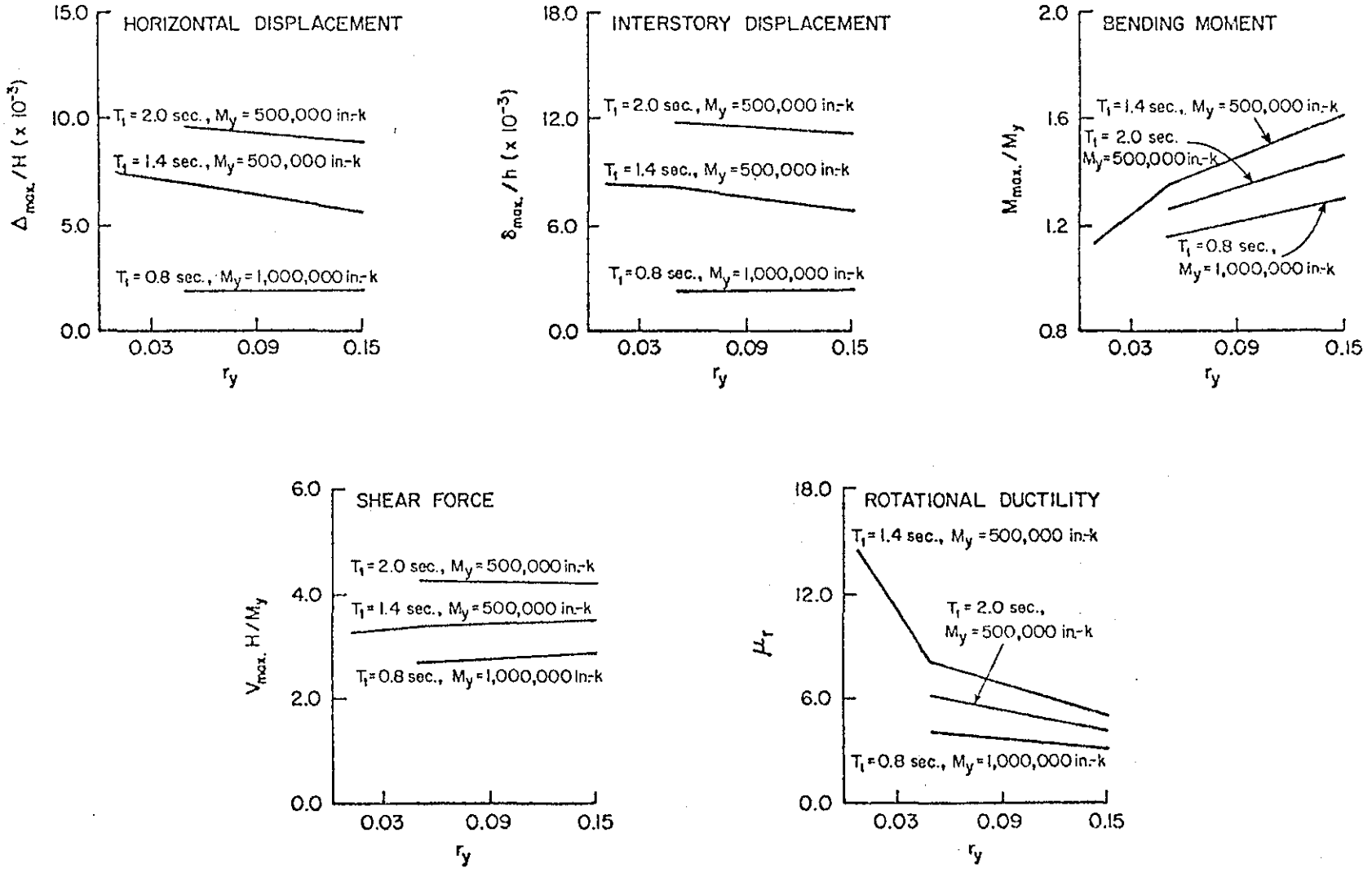

Fig. 76 Summary: Effect of Yield Stiffness Ratio, r_y

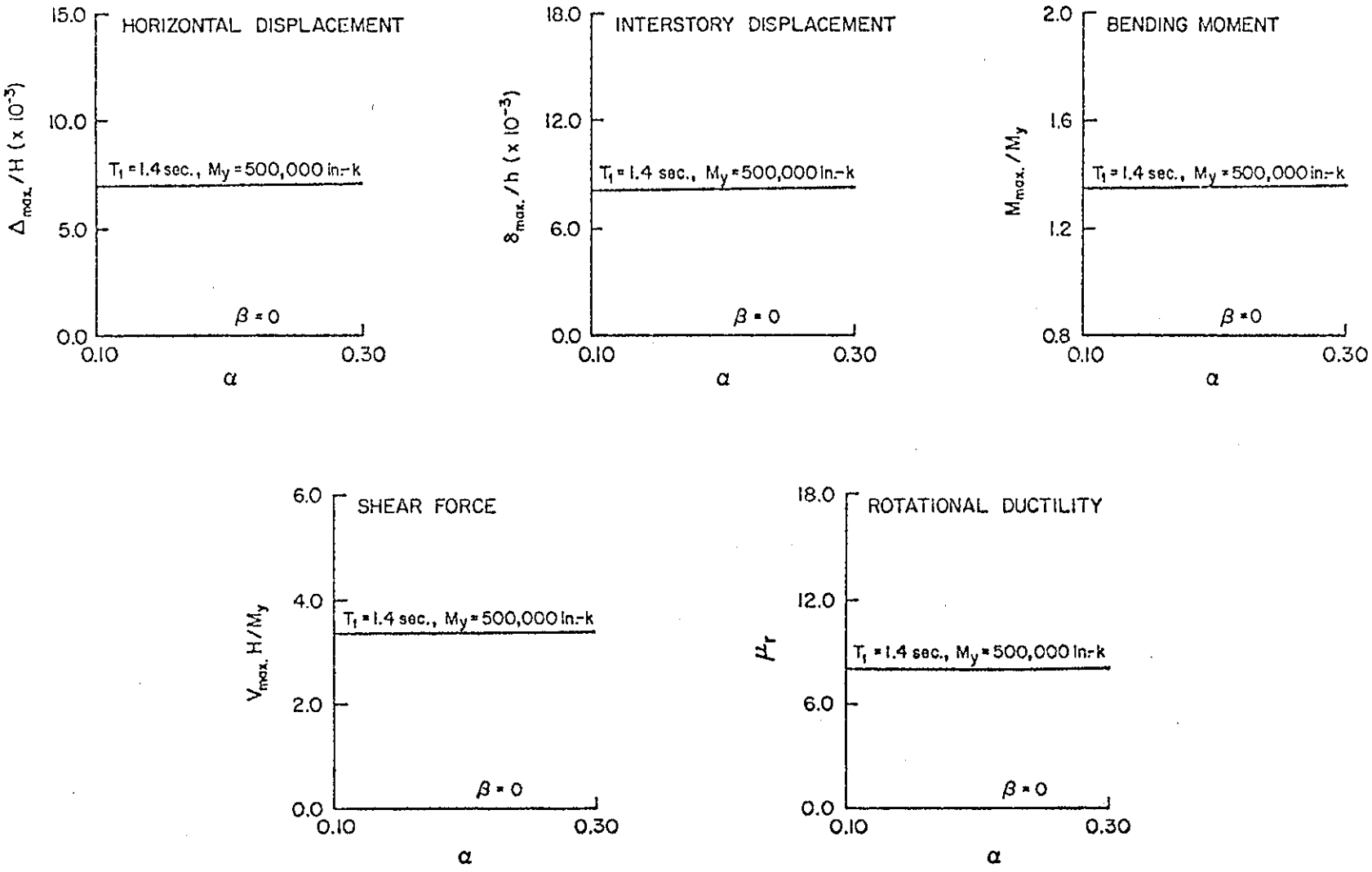

Fig. 77 Summary: Effect of M-θ Loop Unloading Parameter α

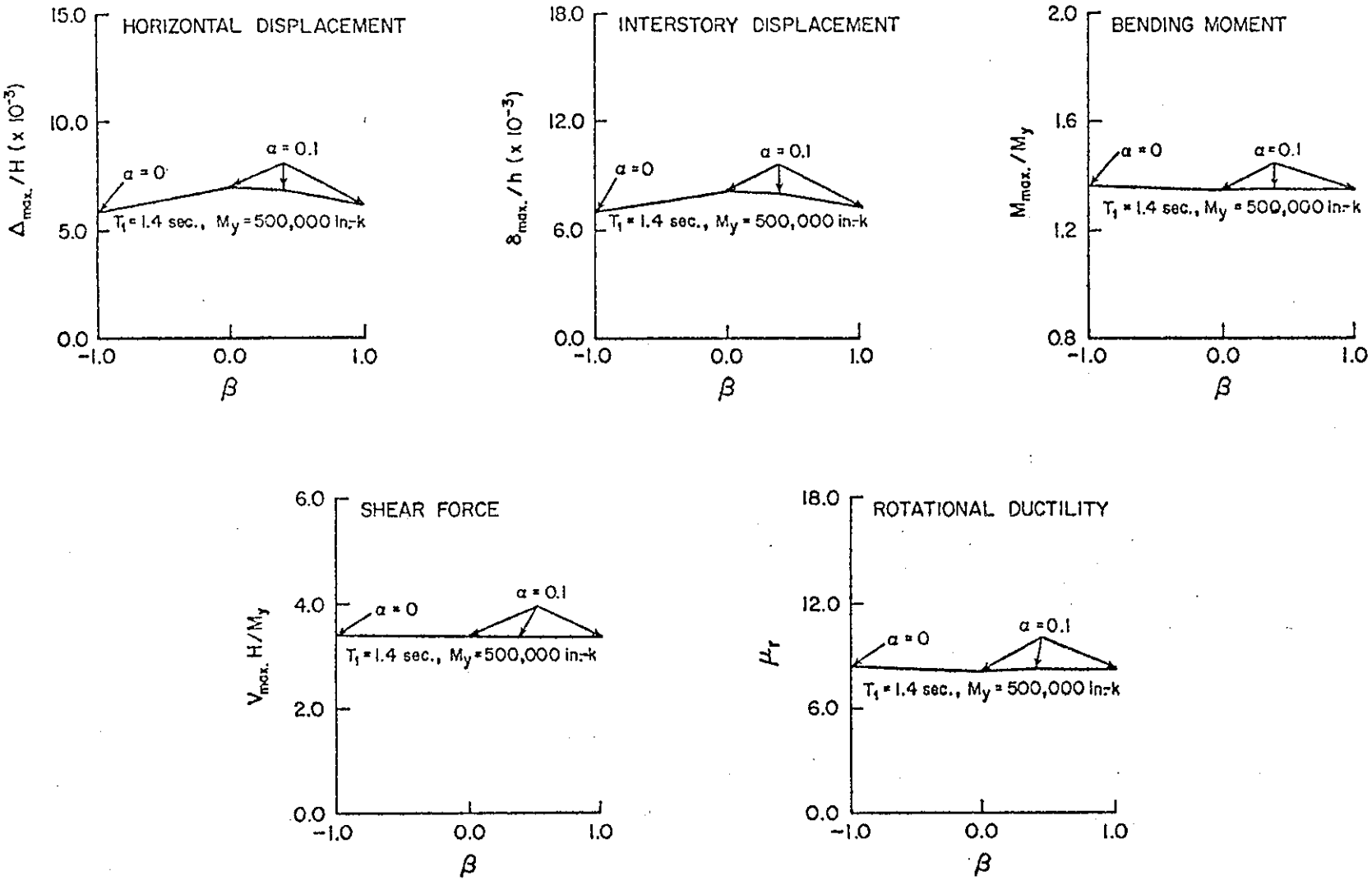

Fig. 78 Summary: Effect of M-θ Loop Reloading Parameter β

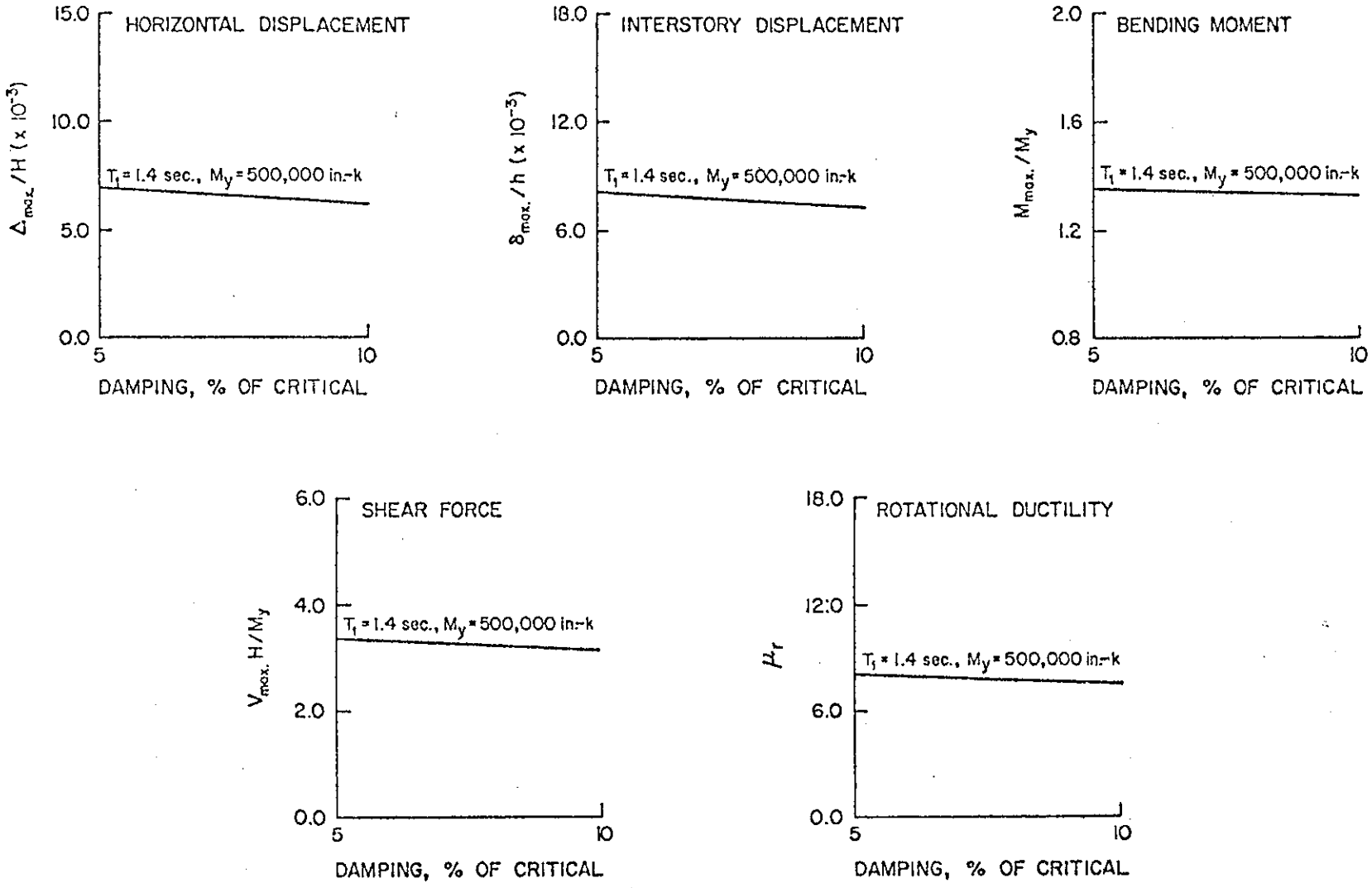

Fig. 79 Summary: Effect of Viscous Damping

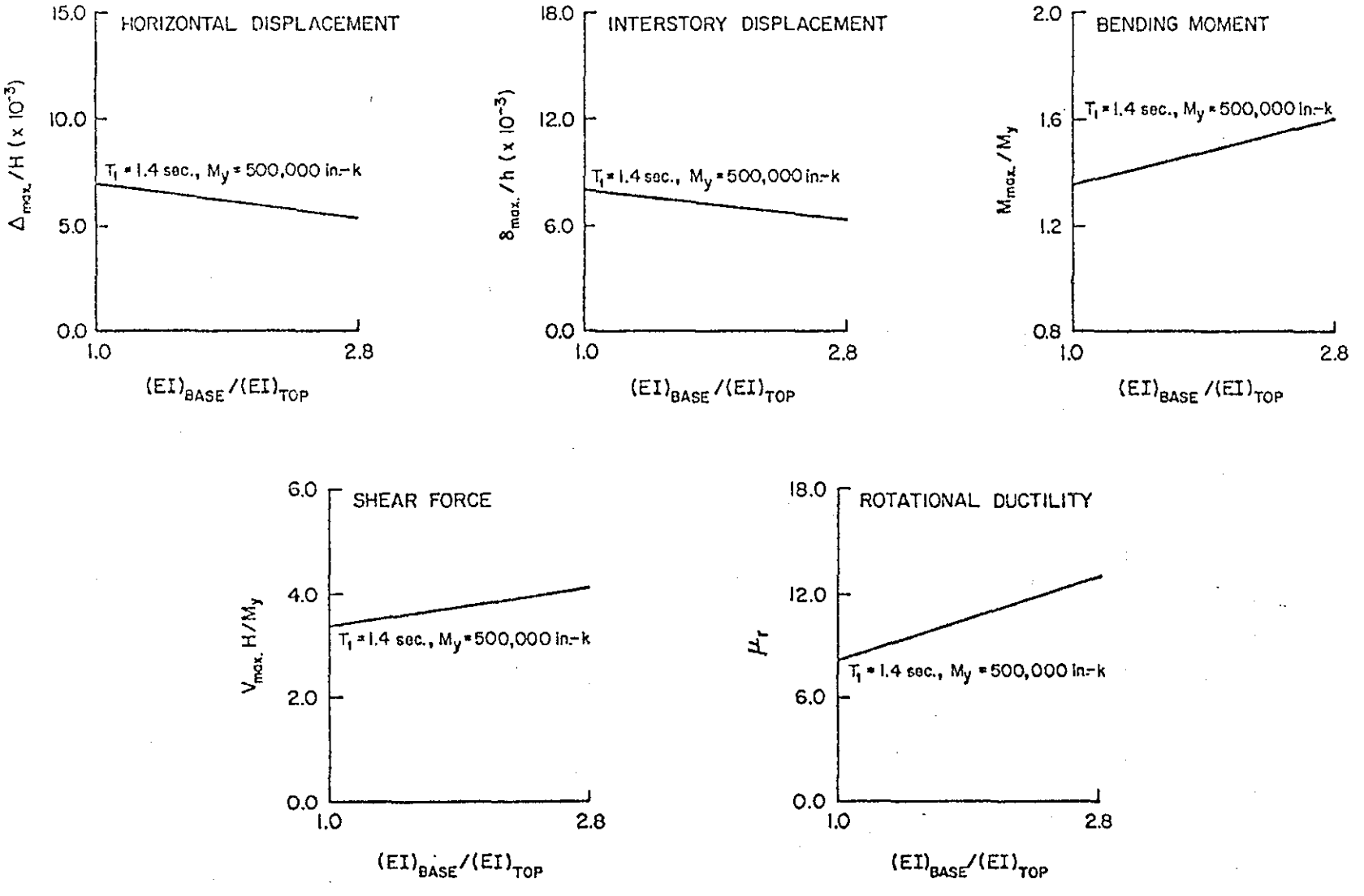

Fig. 80 Summary: Effect of Stiffness Taper Along Height of Wall

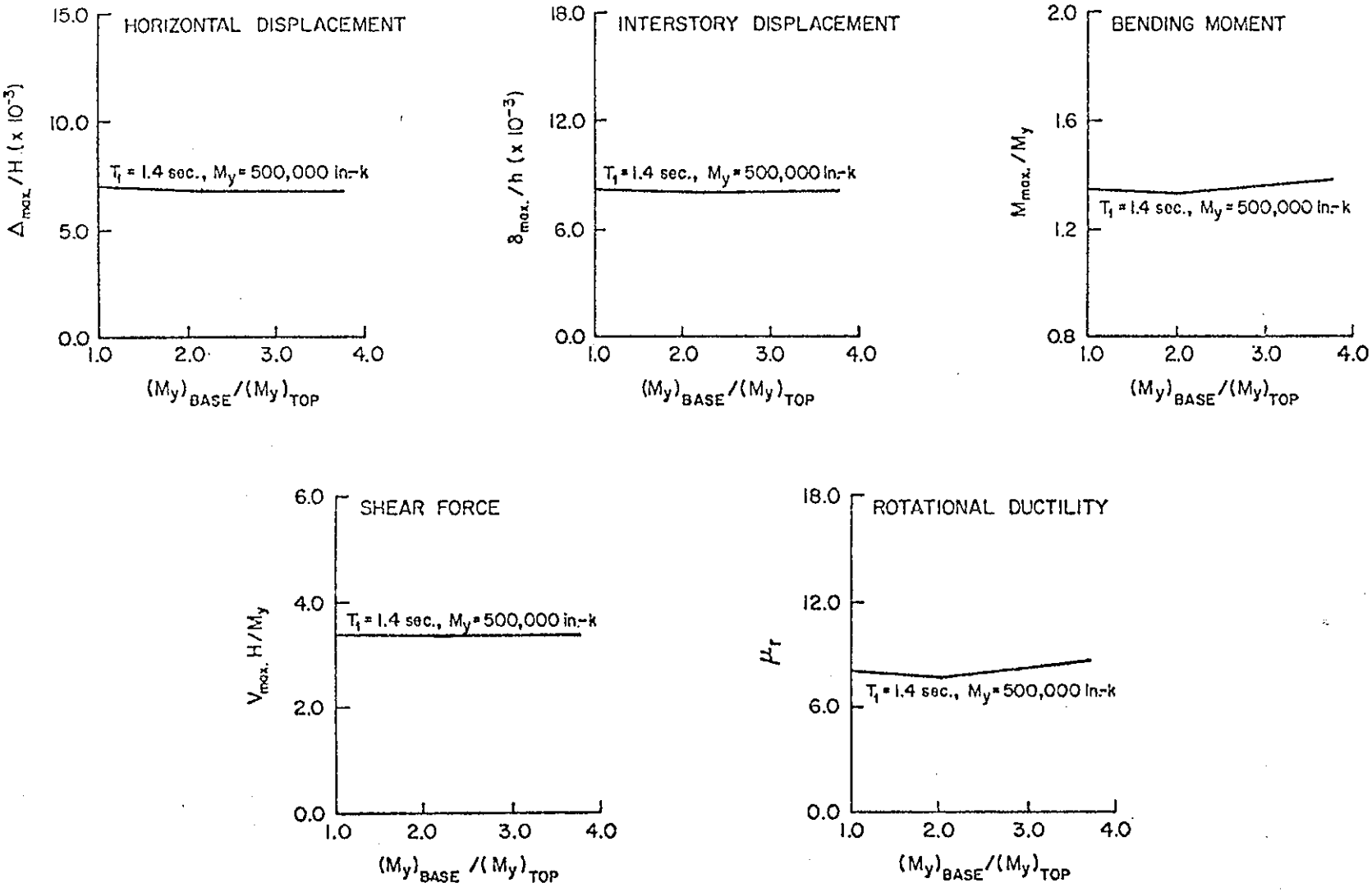

Fig. 81 Summary: Effect of Strength Taper Along Height of Wall

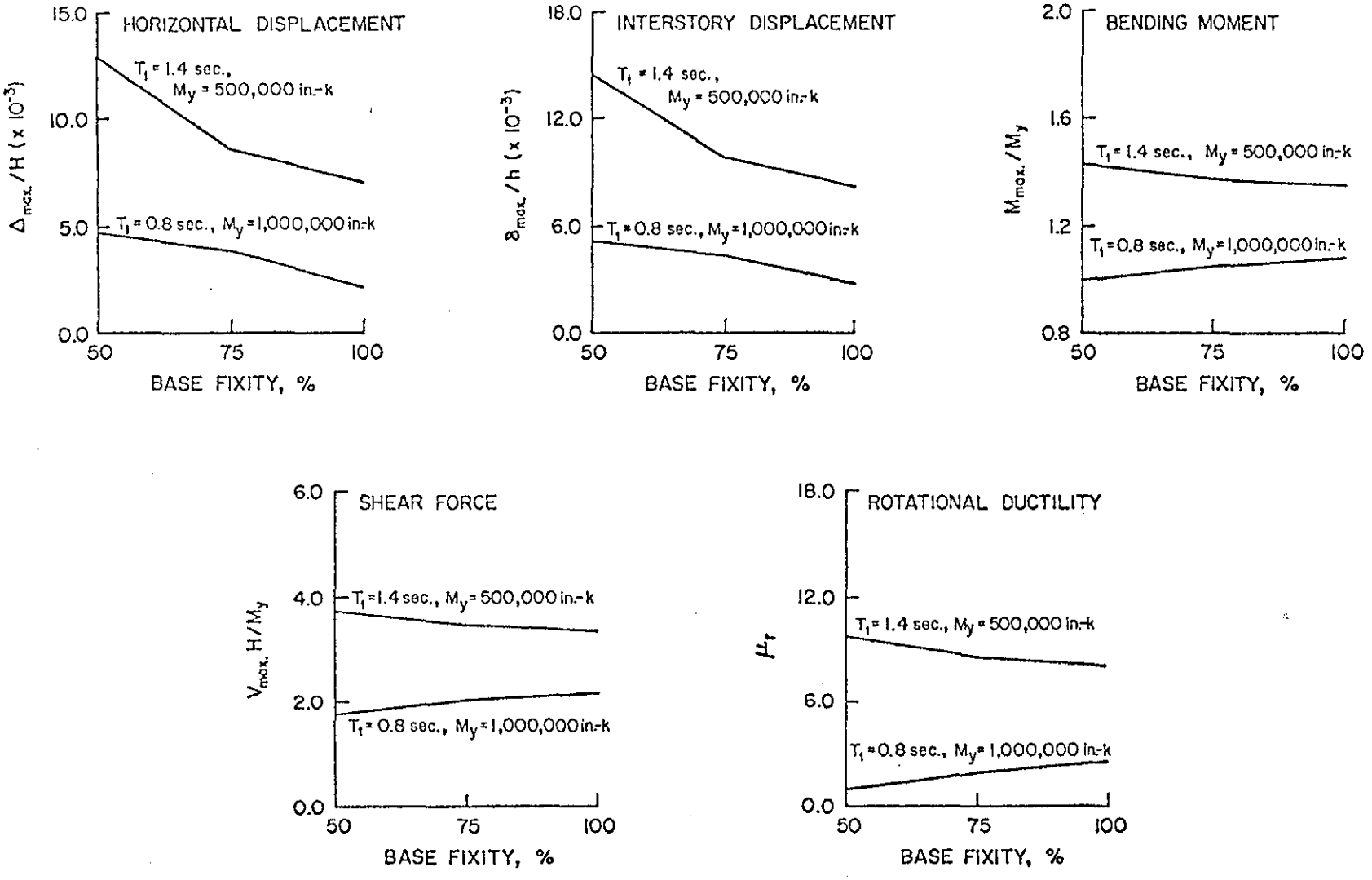

Fig. 82 Summary: Effect of Base Fixity Condition

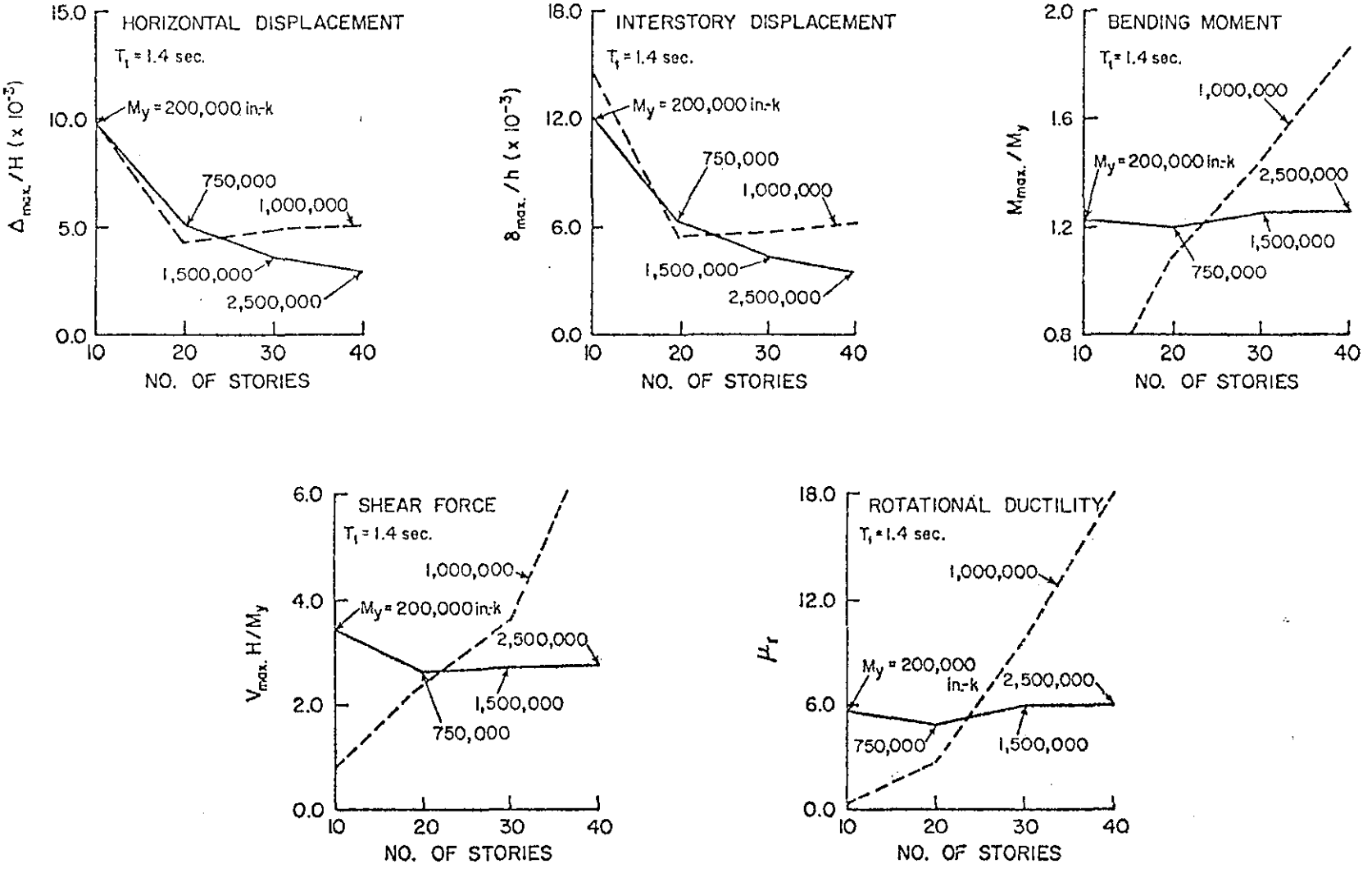

Fig. 83 Summary: Effect of Number of Stories (Wall Height)

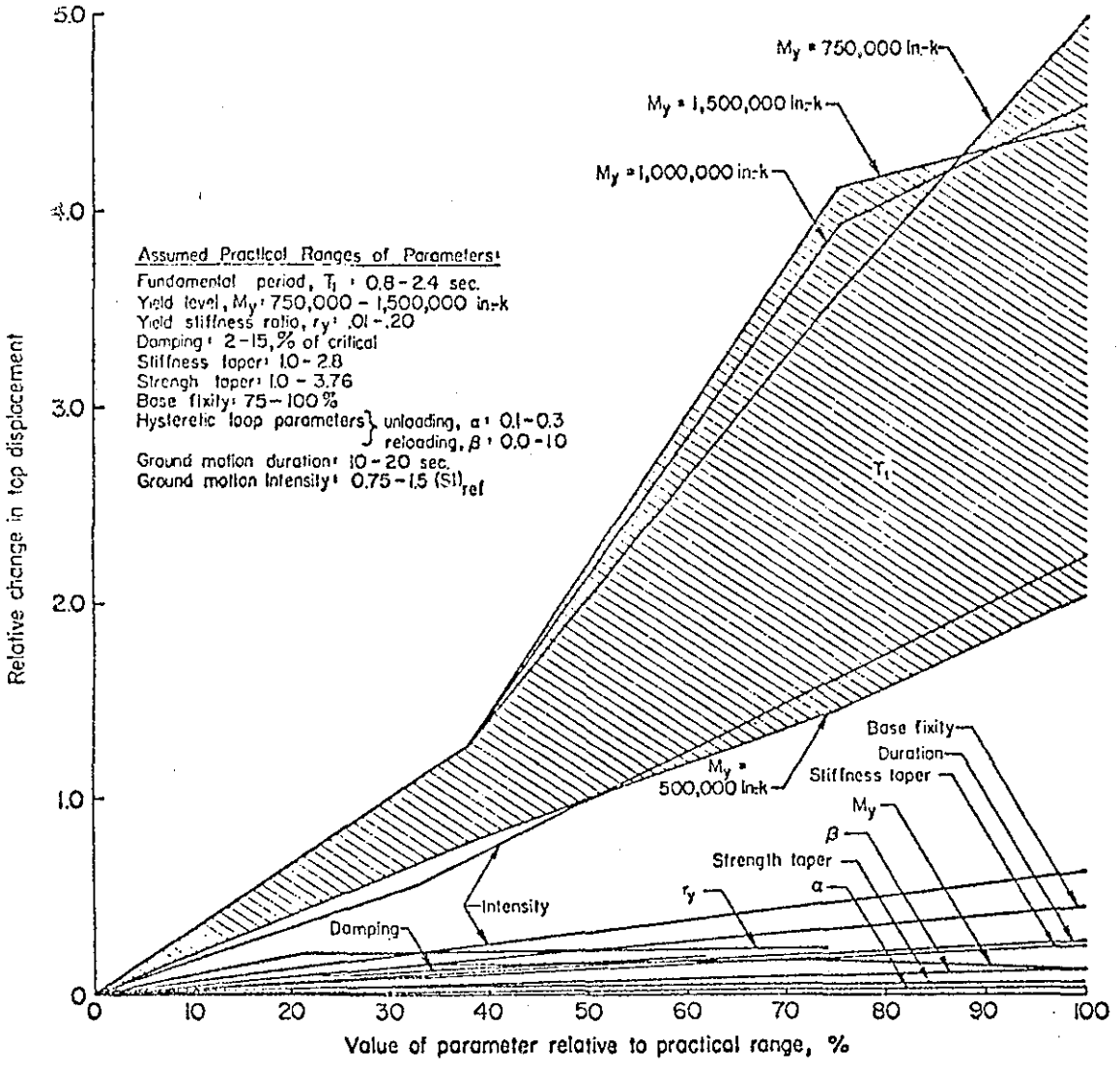

Fig. 84 Relative Effects of Different Parameters on Maximum Top Displacement

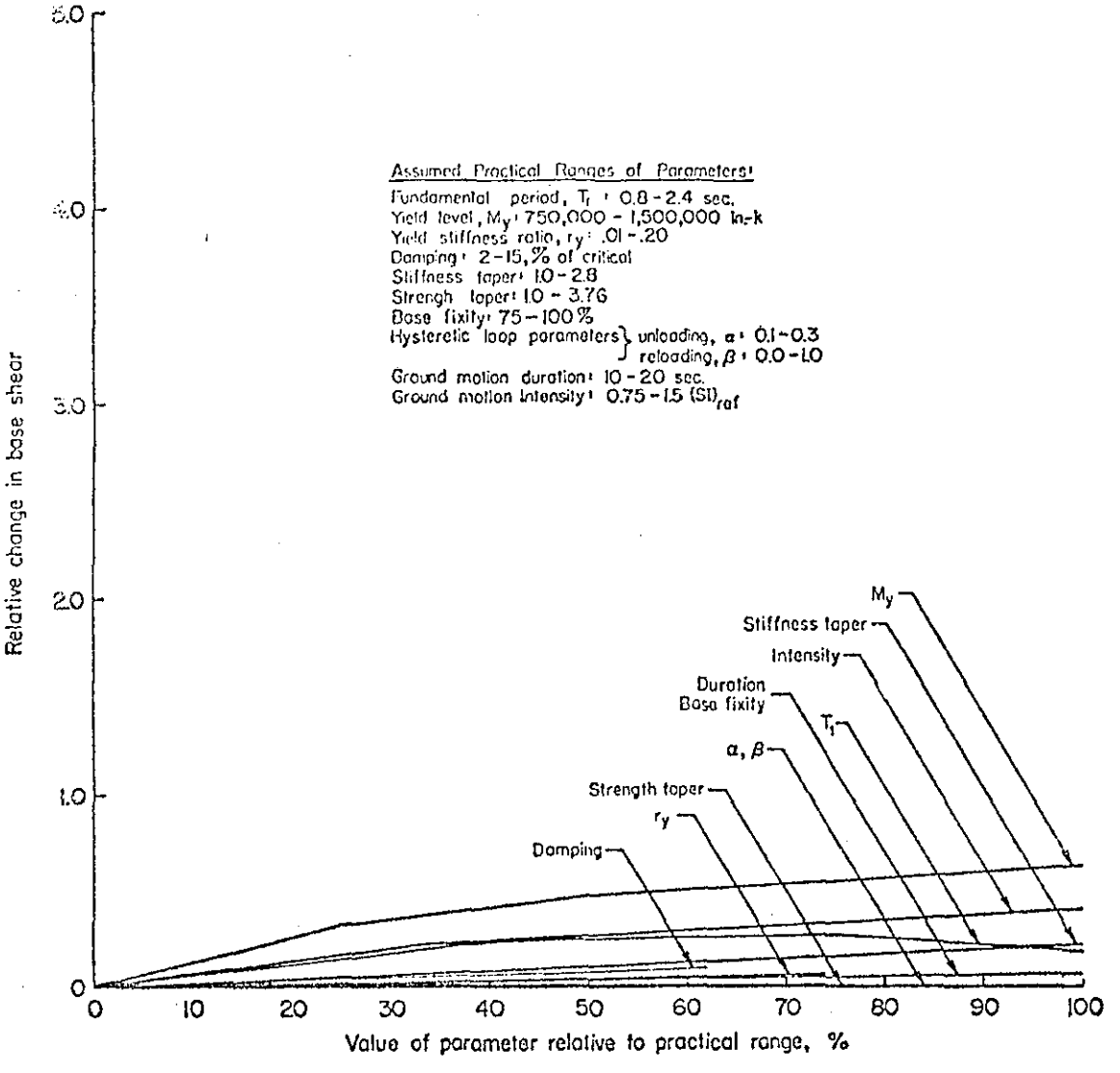

Fig. 85 Relative Effects of Different Parameters on Maximum Base Shear

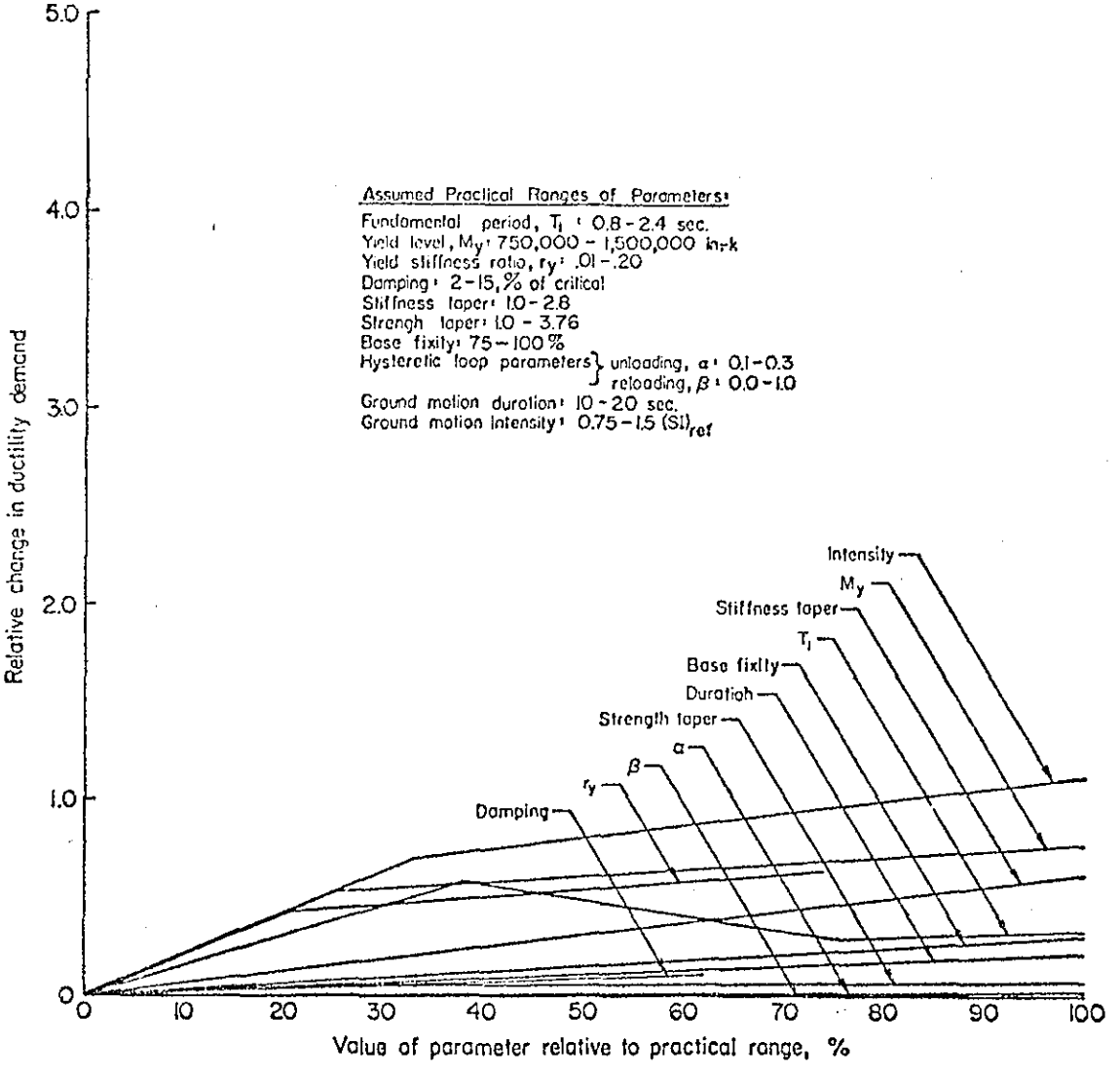

Fig. 86 Relative Effects of Different Parameters on Rotational Ductility Demand